LONG ISLAND UNIVERSITY
SCIENCE ENGINEERING RESEARCH GROUP
C.W. POST CENTER
GREENVALE, NEW YORK 11548

CO-INVESTIGATOR REPORT

NASA APOLLO 9 S065 EXPERIMENT MULTISPECTRAL TERRAIN PHOTOGRAPHY

Edward Yost

with

Robert Anderson
Sondra Wenderoth

Prepared for the Earth Resources Division, Manned Spacecraft Center, National Aeronautics and Space Administration under contract NAS9-9341.

NASA CR108562

LONG ISLAND UNIVERSITY
SCIENCE ENGINEERING RESEARCH GROUP

Technical Report SERG TR-13
15 January 1970

ABSTRACT

A three part quantiative study of multispectral photography of the earth obtained from the S065 experiment carried aboard Apollo 9 has been performed.

Part 1:

An analysis of the multispectral camera array, which consisted of four 70mm Hasselbald cameras aligned in a common rack and attached to the Apollo command module window, showed that there existed: (a) sufficient spectral separation of each band, (b) balance of photographic exposure, and(c) relative spatial accuracy to allow additive color analysis of the imagery to be performed. This analysis indicated that there was a small amount of photographic response to red-infrared radiation in the green band. A photographic reprocessing technique was developed for use in conjunction with additive color viewing of the S065 multispectral photography in order to give good chromatic image signatures. This photographic reprocessing technique utilized an internegative step to increase the density range and gamma while decreasing the minimum density of the positive transparencies.

Part 2:

A quantitative colorimetric study of additive color renditions of the S065 space multispectral imagery and the underflight multiband photography using the Long Island University additive color viewer showed:

1) Agricultural land use catagories of vegetation, soil, and water could be identified 100 per cent of the time with good statistical reliability,

2) crop type was found to be related to multispectral image color 67 per cent of the time on the basis of a post facto knowledge of ground truth,

3) a comparison of the information content of multispectral additive color and subtractive color infrared film based on the capability to chromatically identify vegetation types showed that multispectral color space photographs were significantly superior to color infrared films,

4) a comparison of space and underflight multispectral photography showed that per cent ground cover is quantitatively related to image color, implying that ground resolution is an important factor in the ability to correctly classify crop types using space imagery,

5) upper layer and bottom effect in coastal waters of the Colorado River estuary were quantitatively imaged in the green and red band respectively. No information relating to the water depth was found to be exhibited in the infrared spectral band,

6) a comparison of similar images on infrared color film and on additive color renditions of S065 photographs indicated that multiband additive color presentations had at least 10 times greater capability in discriminating subtle water detail. Extreme care was used in reprocessing black-and-white photography to insure that water detail was not an artifact of the photographic process,

7) a photographic density slicing process was applied to multispectral imagery. This photographic technique is capable of uniquely separating agricultural vegetation from all other image detail. The results demonstrate the feasibility of semi-automatic vegetation mapping from space multispectral photographs,

8) an isoluminous (constant brightness) photographic technique was applied to the underflight multispectral color photography demonstrating the ability to correct for image color changes due to differential illumination of terrain slopes.

Part 3:

Spectroradiometric measurements of incident solar radiation and radiation reflected by the Willcox Playa were made and related to the S065 multispectral photography taken at the same time. Computer analysis of the spectral data indicated that it is possible to obtain a quantitative relationship of "spectral brightness" of terrain objects and multiband photographic exposure. This analysis indicated that it is feasible to obtain quantitative relationships between the per cent directional reflectance of terrestial objects in order to predict filter characteristics for optimum image formation from space sensors.

TABLE OF CONTENTS

SECTION | TITLE | PAGE

PREFACE

Most modern scientific endeavors are team activities of a great number of people. The S065 Multispectral Terrain Photographic Experiment is no exception. The three astronauts who flew in the Apollo 9 spacecraft and took the photography, James Mc Divott, James Scott, and Russ Schweichert, were the spaceborne hands of a team of scientists at the Manned Spacecraft Center who were making real time and decisions as to areas best photographed while the spacecraft was in orbit. At the operational control center for the experiment, Dr. John Dornbach, Assistant Chief of the Earth Resources Division, served as Project Scientist along with Dr. Paul Lowman, of the NASA Goddard Spacecraft Center, who was Principal Investigator for the experiment.

The S065 multispectral photographic equipment was incorporated in the Apollo 9 flight on very short notice through the vigorous support of Leonard Jaffee and his staff at NASA headquarters. Chief of the Earth Resources Program, Robert Piland, had the basic responsibility in getting the multispectral camera system aboard the spacecraft, seeing that the experiment was performed, and coordinating the subsequent data reduction and scientific investigations that were carried out. Alan Grandfield, Project Engineer for the experiment, performed an outstanding job in designing the multispectral camera system on very short notice, performing the necessary logistics in getting it aboard the spacecraft and in briefing the Apollo 9 astronauts on the

use of the equipment.

In addition to the author, three other co-investigators for the experiment are performing complementary studies. Dr. Philip Slater of the University of Arizona, Dr. Robert Colwell, University of California at Berkeley, and Mr. Herbert Tidemann of the NASA Manned Spacecraft Center.

Personnel of the University of Michigan, in conjunction with the United States Department of Agriculture, obtained and made available significant ground truth in the Imperial Valley area during the experiment. It is a pleasure to acknowledge the assistance of all these individuals and organizations as well as the Department of the Interior and the Naval Oceanographic Office for the information supplied during the data reduction phase reported herein.

SECTION 1

INTRODUCTION AND SUMMARY

The S065 experiment, "Multispectral Terrain Photography", was surprisingly successful. At a minimum expense and in a short period of time, with great effort the first multispectral space photographic experiment was flown on Apollo 9. From a scientific standpoint, the results have been impressive. It is the purpose of this report to present some of these results.

For purposes of exposition, this document has been divided into three parts. The first part consists of three sections which deal with a quantitative analysis of the multispectral camera array, additive color methods of data reduction and the photographic techniques used to reprocess the imagery. The second part of this co-investigator's report is devoted to an analysis of the results of the experiment, particular attention being given to associating measurable image characteristics with quantitative ground truth. This second part also deals with newer methods for the extraction of information from multispectral photography such as density slicing and isoluminous techniques. The problem of the measurement of spectral radiation and the effects of the spectral distribution and intensity of reflected radiation on multispectral image quality is treated in the final part of this document.

The S065 Multiband Camera

The S065 multispectral photographic experiment provided the

scientific community with the first simultaneous satellite photography of the earth's surface in three distinct spectral bands. These spectral bands cover the visible and near infrared part of the electromagnetic spectrum. The photography consists of four sets of photographs of identical surface locations, all of which were taken simultaneously. This set of four spectral photographs, three black-and-white and one color infrared, is tabularized below.

Band (NASA designation)	Film and filter	Mean wavelength of sensitivity	Nominal bandpass
A	Infrared Ektachrome, SO-180, Photar 15	Green, red, and infrared	Total sensitivity of all dye layers, 510 to 900 millimicrons
B	Panchromatic-X, type 3400, Photar 58	525 millimicrons, green	460 to 610 millimicrons
C	Infrared Aerographic type SO-246, Photar 89B	800 millimicrons, infrared	700 to 900 millimicrons
D	Panchromatic-X, type 3400, Photar 25A	645 millimicrons, red	580 to 700 millimicrons

FIGURE 1: BASIC PARAMETERS OF THE SO65 MULTIBAND CAMERA ARRAY

The multispectral camera array used to take SO65 photography consisted of four Hasselblad cameras arranged in a single fixture and fired by a common intervalometer. This instrument was affixed to the Apollo 9 Command Module hatch window during flight by the astronauts. Vertical photography was obtained by orienting the entire spacecraft in order to place the optical axes of the camera array at the nadar point. By

use of the flight attitude indicator, the astronaut piloting the spacecraft was able to maintain verticality of the spacecraft hatch window with respect to the earth while in orbit.

Photographs were taken during five passes over North America between March 8 and March 12, 1969. Complete sets numbering 127 simultaneous four camera exposures were obtained. Photography was taken over the southwestern United States (south of 34° North Latitude) northwestern Mexico, the south central and southeastern United States, southern Mexico, and the Carribean Atlantic region between Trinidad and the Cape Verde Islands.

The arrangement of four Hasselblad cameras, in the common frame and affixed to the interior of the Apollo 9 Command Module hatch window, proved to be a plausible way to obtain multispectral space photography. Three of the four S065 photographs taken on black-and-white film with appropriate film-filter combinations resulted in photography primarily in the green, red, and infrared bands. Spatial fidelity was sufficient to allow additive color analysis to be performed at a level of spatial resolution comparative to the color infrared photograph in the fourth camera. The exposures were sufficiently well balanced so that by using special photographic processing techniques in the data reduction phase, it was possible to obtain quantitative results of significant scientific interest.

During the period time that the S065 experiment was in orbit, the Long Island University four lens multispectral camera was used to

underfly certain test sites. This multispectral camera provided support photography in approximately the same spectral bands as recorded by the S065 camera in space. These photographs are of considerable use in comparing the relative merits of airborne and spaceborne multispectral photography.

Additive Color Analysis of Multispectral Photography

The primary tool used in data reduction was the additive color viewing technique. The Long Island University multispectral additive color viewer was used for this purpose. This instrument is used for qualitative photographic interpretation as well as to obtain quantified colorimetric measurements. This technique of additive color multispectral photography permits a scientist to select a particular set of bands within the visible near infrared spectrum to obtain imagry and to interpret the results from a single color presentation. It also permits the scientist to alter the color of the presentation and to enhance the particular relationships he may be seeking. Fundamentally, the additive color multispectral data reduction technique allows a scientist to create a color "film" specifically for the purposes of his discipline and interests. In this way the 200 discernable shades of gray in a conventional black-and-white photograph are expanded into 10,000,000 color combinations.

The color of an image which appears on the screen of an additive color viewer depends upon the densities of the positives which are projected. When the three positives have equal densities, and each is

illuminated by an equal energy light source, the image on the screen will be a shade of gray. When the densities in the black-and-white photographs are not equal, the eye will see the composite color in the image. The greatest possible color discrimination is achieved when the densiy lies between zero and unity. Above a density of one, in the Long Island University color viewer, no perceptible color effect will be presented.

The requirements for positives to be used in additive color viewing are: a low base plus fog density, the lowest possible minimum image density to achieve good screen brightness, the density range of areas of interest to be relatively high, the overall image density, density range and gamma of the positives should be matched to each other as closely as possible, subject to the constraint imposed by the log exposure range of each band.

The S065 released positives required photographic reprocessing before they could be used for additive color analysis. A sequence of special reprocessing techniques were developed which allowed a high degree of accuracy to be maintained in producing positives through an internegative step while achieving the necessary photographic characteristics for additive color projection. Analysis of the photometric fidelity was conducted to compare the NASA released positive with the reprocessed positives used for additive color analysis.

Results of The S065 Multispectral Experiment

Four distinct geographical areas in the Southwest were used as

test sites for the evaluation and quantitative analysis of the S065 multispectral imagery. The location of these sites, which are shown in Figure 1, were: Imperial Valley, California; Phoenix, Arizona; Willcox-Fort Huachuca, Arizona and the Colorado River estuary, Mexico.

Agricultural Land Use in The Imperial Valley

The ability to extract agricultural land use classification information from the S065 multispectral photography by making quantitative colorimetric measurements of both additive color and subtractive color film images was established. The Imperial Valley, California was used as the control test site. Not only was excellent ground truth of the area available at the time the Apollo 9 was in orbit, but also this agricultural unit is of great economic significance having a yearly gross value of crop and livestock production in excess of $232,000,000.

Precision photographic techniques were used to reproduce enlargements of the Imperial Valley S065 black-and-white frame number 3799. Enlargements 45 times that of the original S065 photography were utilized for this purpose. The six possible primary color spaces were colorimetrically analyzed. Over two hundred CIE color coordinates were computed from per cent transmission measurements made from reproductions of the additive color viewer screen by using computer programs specifically developed for the purpose. Thirty-three different fields were measured: nine barley fields, nine sugar beet fields, six alfalfa, eight bare soil, and four measurements of surface water.

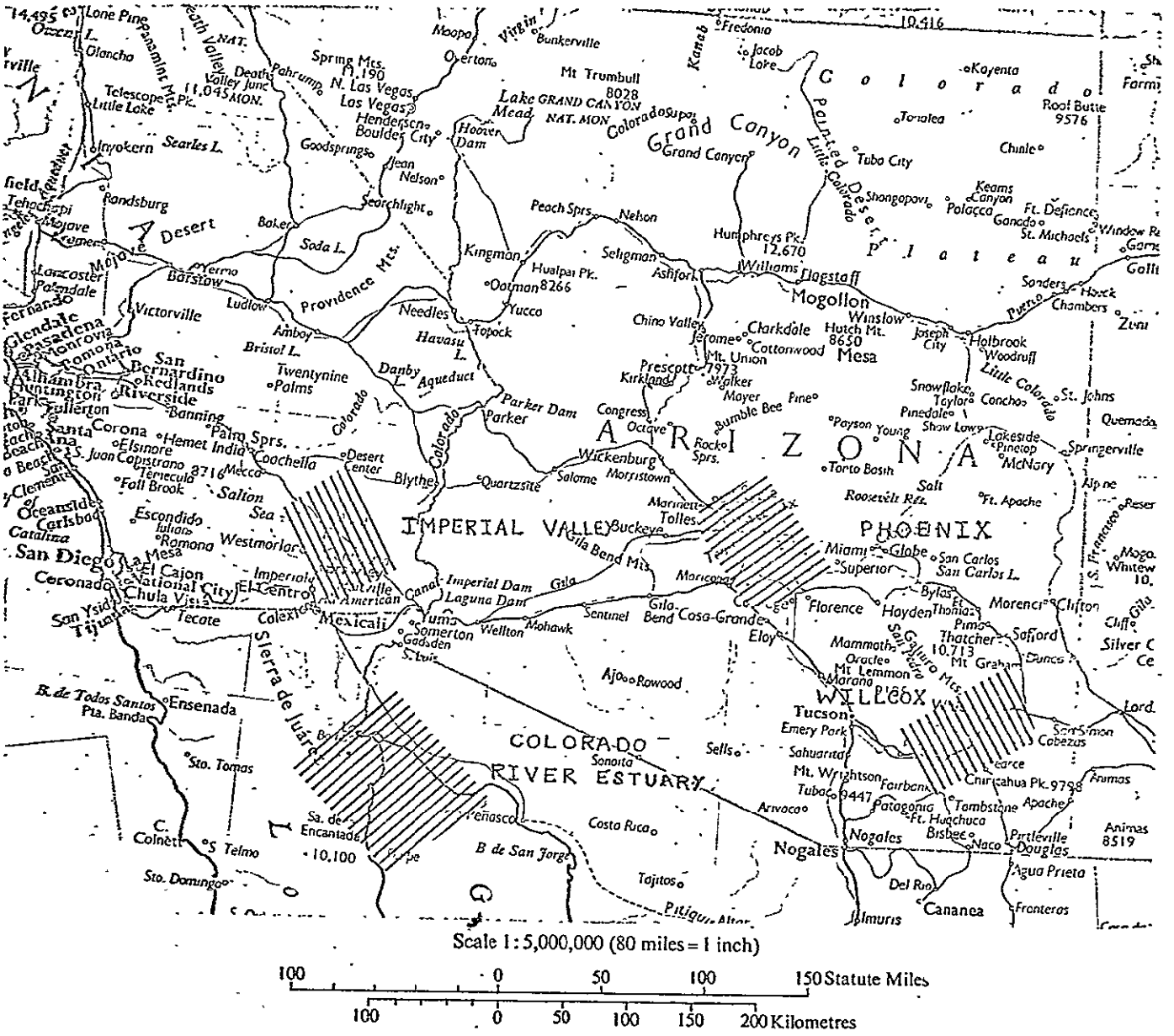

FIGURE 1 : LOCATION OF TEST SITES WHICH ARE ANALYZED IN DETAIL IN THIS REPORT.

GRAPHIC NOT REPRODUCIBLE

The results of this analysis showed that on a post facto basis, classification of vegetation, soil, and surface water could be accurately made 100 per cent of the time with the associated statistical alpha and beta errors approaching zero. An analysis of the chromaticity of the images of three crops (alfalfa, barley, and sugar beets) on a similar a posterari classification of crop type and image color indicated a 67 per cent probability of correct classification. Thus, image color was quantitatively associated with crop type two-thirds of the time.

No significant relationship was found between image brightness and either land use or crop type classifications. It was found that in general the images of soil varied much more in brightness than the images of vegetation. The greatest variability in crop image brightness was exhibited in the infrared band.

A Comparison of The Information Content of Multispectral Color and Subtractive Color Films

Again using the Imperial Valley test site, a comparison was made between the chromatic characteristics of current state-of-the-art subtractive false color films and additive color image forming techniques. Over two hundred images of soil, water and crops (alfalfa, barley, and sugar beets) were measured using three distinctly different image producing techniques. The focus of attention of this analysis was on the capability of additive and subtractive color methods to uniquely associate image color with land use categorizations of vegetation, soil, and water as well as the ability to color differentiate between images of individual

crops within the vegetation category. The three image forming techniques were: 1) enlargement of S065 multispectral additive color rendition in a color space similar to color infrared photography, 2) a four times enlargement of color infrared S065 photo, 3) color separations made from the S065 color infrared photo enlarged and reconstructed in the additive color viewer.

For each of these three renditions, unique chromatic separation of soil, water, and vegetation was achieved. That is, the convex sets of CIE chromaticity coordinates for these general categories were disjoint, implying a 100 per cent post facto correct classification. The ability to separate three crops of alfalfa, barley, and sugar beets, in the three renditions (additive color, color infrared, separation positives from color infrared) showed that in general the greatest uniqueness of correct classification was achieved in the multispectral additive color rendition. Separation positives made from the color infrared film were a close second in their ability to correctly classify these three crops on a post facto basis. Color infrared film placed third in ability to establish a unique relationship of image color to crop type.

An analysis of image brightness in the three color reproducing techniques reinforced the previous observations that it is difficult, if not impossible, to uniquely identify objects based on brightness (or density) measurements of the photographic images. A comparison of the color variations of additive color multispectral images and subtractive color films indicated that the image color of vegetation with 80 per cent or less ground cover is primarily related to per cent ground cover

and only secondarily related to crop type.

A Comparison of Space and Underflight Multispectral Photography

A comparative colorimetric analysis of the S065 space multispectral photography and the Long Island University underflight multispectral photography was also performed. The results showed that when the images of the fields in the Imperial Valley were of sufficient size and homogeneous in appearance, the per cent ground covered by the vegetation was related to image chromaticity. The underflight multispectral color photography showed however, that the relationship between per cent ground cover and image color was affected by the variations between and within fields. Therefore, it appears that ground resolution is an important factor in relating measurable characteristics of multispectral images for soil and vegetation categorization. The largest variation in brightness of vegetation image on the underflight photography existed in the infrared band and the least variation in the red band. There existed a definite non-uniqueness of image brightness and image density of crops and soils appearing on the underflight multispectral photography.

Land Use Information on Conventional Subtractive Color Films

Chromaticity measurements of the images of soils and vegetation appearing on conventional color film, taken during the Apollo 9 flight, showed that these two land use catagories could not be uniquely established on the basis of image color. The convex sets of vegetation

chromaticity coordinates was found to overlap the set of soil colors. The comparison of this conventional color photography from space with underflight color photography during the Apollo 9 orbit showed that the space and aircraft imagery produce significantly different colors for the same classes of soil and vegetation. A comparison of identical objects on the S065 infrared color film and on color film taken by the aircraft during the underflight indicated irregular variations in image saturation accompanied by increase in hue in the space color infrared images. The differences in image color between space and aircraft color photography is probably due to the inherent variability in the subtractive image forming process as well as the time difference between obtaining the space and underflight photography.

Information Extraction in Estuarine Coastal Environments

An analysis of the relative information content of the reprocessed green, red, and infrared bands of the S065 bands for imaging upper layer phenomenon and bottom effect in the Colorado River estuary was performed. The results showed considerable image detail in the red and green bands. No information relating to water mass was contained in the infrared band. Correlation of the green and red band log exposure with nominal chart depths was apparent to about 40 feet of water depth. Additive color reconstruction of the S065 multiband imagery showed that it was possible to selectively emphasize upper layer phenomenon and bottom effect by color enhancement.

The blue sensitive dye layer of conventional film showed no rela-

tionship whatever with water depth although both the green and red sensitive layers did indicate correlation of image density with mean low water soundings on hydrographic charts of the estuary. A comparative analysis of similar images on infrared color film and on multiband additive color renditions indicated that the multiband additive color presentation had at least ten times more capability in discriminating subtle detail in the water. Conventional colorimetric analyses using CIE coordinate transformations showed no significant correlation of image color and water depth as recorded on hydrographic charts of the area.

Information Extraction From Multispectral Photography Using Density Slicing

Additive color analysis of multispectral photography taken over Phoenix, Arizona was performed by reprocessing the release positives to correct for the high minimum density and low contrast in the green band. Using a sequence of precise photographic techniques, the differential density and gamma relationships in all three bands were corrected. These reprocessed positive transparencies proved to be excellent for additive color projection and analysis of the multispectral photography.

A photographic density slicing technique called the "density cut-off" process was developed. In this process it is possible to uniquely classify vegetation appearing in a set of multispectral photographs. This process allowed rapid production of vegetation maps by color identification of those images in multispectral photography which reflected energy only in the infrared band. The procedure demonstrated the feasi-

bility of the "density cut-off" technique to reproduce unique classifications of vegetation using strictly photographic process. The resultant classification, which can be produced at any scale, can readily be compiled on a conventional map sheet.

Information Extraction from Multispectral Photography Using Isoluminous Technique

A constant brightness (isoluminous) technique for preparing multispectral presentations was applied to the Apollo 9 underflight photography. This technique has the advantage in that it is capable of emphasizing subtle spectral differences between bands and also capable of eliminating the effects of brightness caused by sloping terrain and shadows. The isoluminous process is useful in detecting subtle environmental differences under dynamically changing conditions of illumination such as often encountered in vegetation and soil mapping in areas where topography is variable.

The Role of Spectroradiometric Measurements

In order to perform a quantitative analysis of the relationships between incident solar radiation, terrain reflectance, and the exposure of the S065 multiband images, ground truth measurements of the incident solar spectra at the Willcox Playa, Arizona test site were conducted during the course of the S065 experiment. Simultaneous spectroradiometric measurements were obtained of the solar radiation reflected by

the Playa as well as large plowed fields and grass areas adjacent to it. The per cent directional reflectance of homogeneous terrain objects large enough the be imaged in the space photograph was obtained through computer processing of these data. By making density measurements of the images of the Willcox Playa that appeared in the green, red, and infrared black-and-white S065 photographs obtained simultaneously with the spectroradiometric measurements, it was possible to relate the spectral brightness of ground ojects with their apparent density on the multispectral photographs. These data are helpful in quantifying the relationships between energy reflected by terrain objects and their resultant photographic characteristics as seen from space perspective.

SECTION 2

THE CHARACTERISTICS OF THE APOLLO 9 MULTIBAND CAMERA AND SUPPORTING S065 UNDERFLIGHT PHOTOGRAPHY

The arrangement of four Hasselblad cameras in a common frame resulted in an effective multiband camera array with which to obtain multispectral terrain photography. The three S065 green, red, and infrared bands which were recorded on black-and-white film were of sufficient spatial fidelity to allow additional color analysis to be performed at a level of spatial resolution comparable to the color infrared photograph in the fourth S065 camera. Not withstanding a lack of perfection within the camera system, the exposures were effectively balanced to take multispectral photography which is of significant quantitative scientific content.

At the same time the S065 experiment was being conducted from the Apollo 9 command module, the Long Island University multiband four lens camera was being used to underfly certain test sites. This aircraft mounted camera provided multiband photography in approximately the same spectral bands as recorded by the space camera. In addition, color and color infrared photographs were obtained simultaneously with the underflight multiband photography.

Nominal Characteristics of the S065 Multiband Camera System

A four camera system was used as the space borne sensor in the NASA S065 experiment. This multiband system consisted of four 70mm

format Hasselblad cameras, each with 80mm focal length Zeiss Planar lens. The optical axes of the four cameras were aligned so as to be parallel. All four cameras were actuated simultaneously by a common intervalometer. The intent of the design was to arrange the cameras in such a way that the spatial location of the images appearing on on the four photographs would be identical with respect to their principle points (the intersection of the optical axis with the camera focal plane).

Figure 2 shows the arrangement of the cameras in the mounting ring. The object at the bottom of the photograph is the common intervalometer used to actuate the cameras. In Figure 3 the multiband camera is shown mounted to the Apollo 9 hatch window. Note that the relative orientation of the four cameras is different. This 90° rotational position between each camera resulted in a different direction of film transport during the experiment. This in turn caused a different orientation of each image with respect to the film edge for each photograph in the set of multiband photos. Due to a vignetting caused by insufficient window diameter relative to the diameter of the multiband camera array, a different corner of each photo in any given set of multiband photos was vignetted (See Figures 26 , 28 , and 30).

The nominal parameters of the S065 multiband camera are shown in Table 2 . The nominal bandpass for the green, red, infrared black-and-white bands is shown along with the film-filter combinations used, the lens aperture, shutter speed and focus. The lens aperture

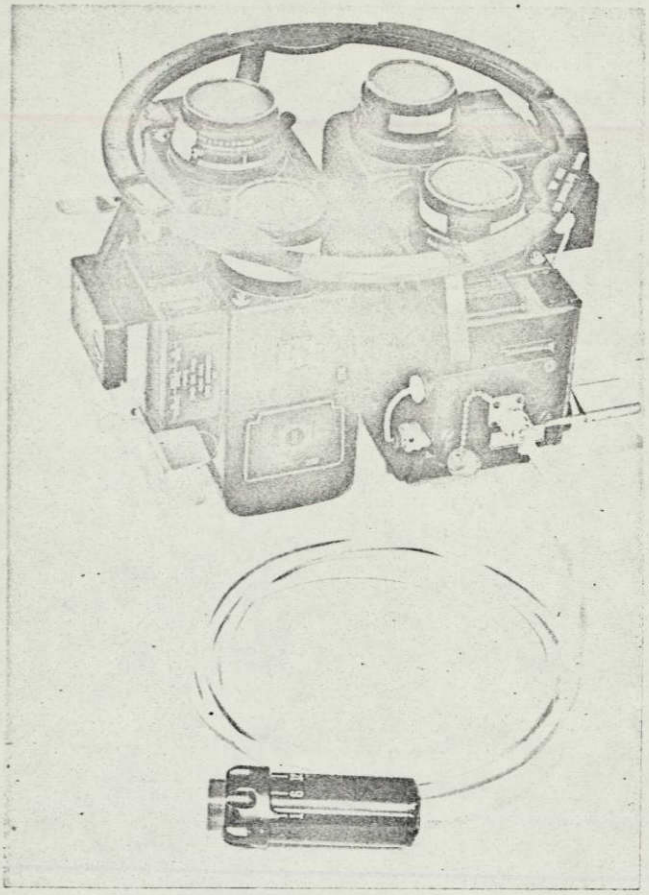

FIGURE 2 : S065 MULTIBAND SYSTEM CONSISTING OF FOUR 70MM FORMAT HASSELBLAD CAMERAS EACH WITH AN 80MM ZEISS PLANAR LENS.

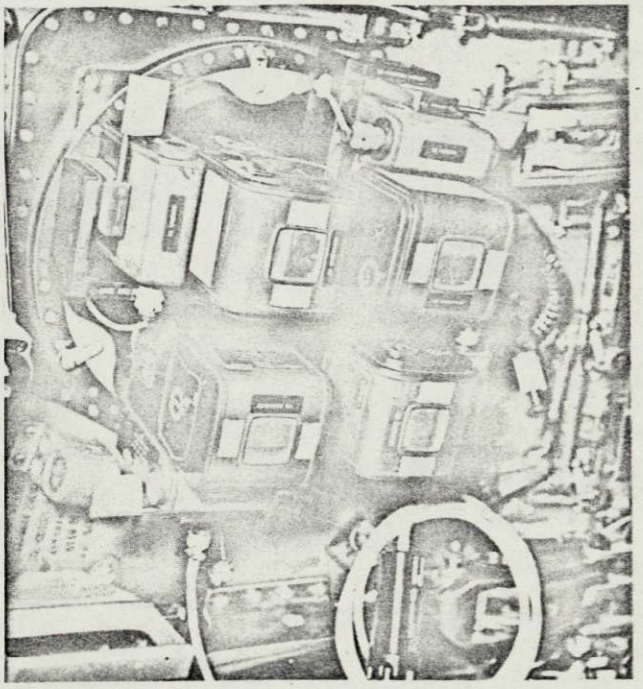

FIGURE 3 : S065 MULTIBAND CAMERA MOUNTED IN THE APOLLO 9 HATCH WINDOW.

and shutter speed were chosen such that a uniformly reflecting spectrally flat object would image the same density on each spectral negative. It is one of the purposes of this section to investigate the accuracy with which this desired result of equal film density for a uniformly reflecting object was achieved.

TABLE 2

NOMINAL SO65 MULTIBAND CAMERA PARAMETERS

BAND	NOMINAL BANDPASS (NM)	CAMERA					
		FILM	FILTER	FOCAL LENGTH (MM)	APERTURE	SHUTTER SPEED (SEC)	FOCUS
GREEN	460-610	3400	58	80	4	1/125	INFINITY
RED	580-700	3400	25A	80	4	1/250	INFINITY
INFRARED	700-900	SO246	89B	80	16	1/250	30 FT
COLOR INFRARED	3 layer sensitiv. 510-900	SO180	15	80	8	1/250	50 FT

Ideally, the SO65 multiband camera system should have produced three black-and-white spectral photographs which were spatially identical. This would require a perfect system which of course is not obtainable in practice. In theory, this implies that there would be no differential distortion in the camera lenses used, and that each photograph would have the same scale. The latter requirement infers that the focal lengths of the cameras be closely matched for the wavelengths of light transmitted. In addition, in the event that appreciable angular motion is present, each

camera must be exposed at exactly the same time to prevent image displacement. The nominal sychronization of exposure times was accomplished in the S065 multiband camera by the common actuating intervalometer. It should also be mentioned in passing that film shrinkage has been found to result in a differential relative location of the images between multispectral film formats.

The photo-optical characteristics of the S065 Hasselblad cameras were determined prior to flight (NASA/MSC, 1969). A more complete analysis was performed after the experiment which resulted in data more relavent to the actual situation that existed at the time the photography was obtained(Slater, 1969). These latter empirical tests indicated that there was considerable differential distortion present in the four S065 camera lenses. These data show that the focal lengths were as much as one millimeter different one from the other. The resolution of the four lenses was found to range between 42 lines for the black - and-white infrared camera to 59 lines per millimeter for the black-and-white green camera. A postflight analysis performed on the relative boresighting accuracies of the cameras indicated that the angular difference between the four cameras existed. The maximum value reported was that the green and red cameras possessed boresighting accuracy of boresighting errors in excess of one degree (Dornbach, 1969).

Figure 4 presents a schematic of one of the Hasselblad cameras used in the S065 experiment. The purpose of such a schematic is to show the salient photo-optical parameters which should be investigated

in order to determine the effect of each on the spectral distribution of the density of the image formed on the film. In this schematic the reader will see that radiation(reflected by the terrain) passes through the spacecraft window, through the filter and lens and is imaged on the film. The shutter time and aperture opening;of course, effect the quantity of radiation(ergs/cm^2) which impinges on the film. Thus, the characteristics of the radiation which photochemically interacts with the silver halide molecules causing a density on the black-and-white film is affected by: 1) the spacecraft window, 2) the filter, 3) the lens(including shutter speed and aperture opening), 4) film response(under prescribed processing conditions).

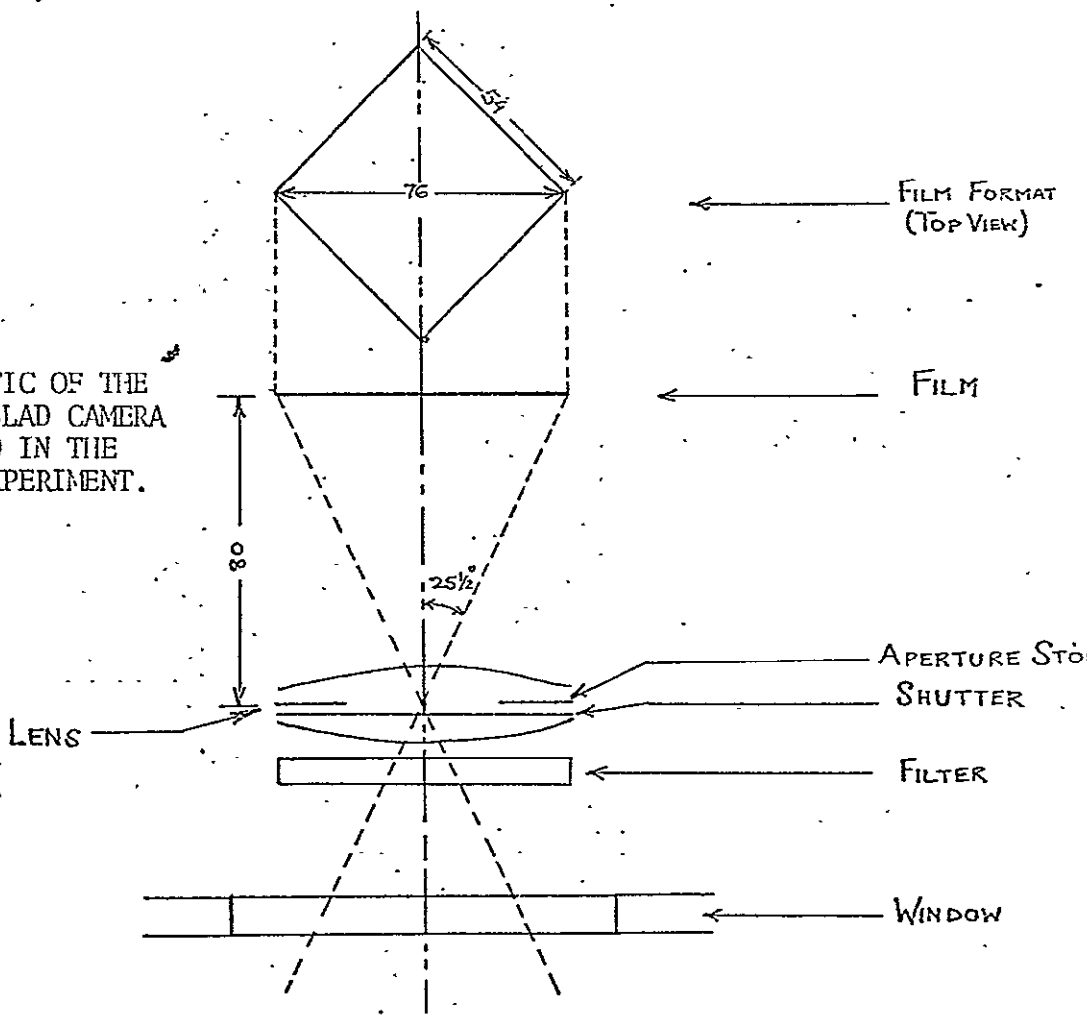

FIGURE 4 : SCHEMATIC OF THE HASSELBLAD CAMERA AS USED IN THE SO65 EXPERIMENT.

In this section we will investigate each of the preceding four components of the system. At the very top of Figure 4 , a planned view of the film format shows the approximate 54mm dimension on each side of the square film format. The approximate maximum field angle as determined by the diagonal distance of 76mm across the format is approximately 25 and 1/2 degrees for the nominal 80mm focal length.

The Spectral Characteristics of the SO65 Multiband Camera System

The pre-flight spectral transmission characteristics of the Apollo 9 spacecraft window through which the SO65 photographs were taken is shown in Figure 5 . Removal of the infrared coating from the window allowed good transmission of infrared radiation throughout the photographic infrared. It is also interesting to note that in the wavelength region of the experiment(460-900nm), although there is a slight reduction in percentage transmission with field angle, no significant differential transmission at any wavelength is apparent through the spacecraft window.

After passing through the spacecraft window and being attenuated as shown previously in Figure 5 , the radiation must next pass through the camera filter. The percentage transmission characteristics of the three filters used with the black-and-white films are shown in Figure 6 . From this Figure the reader can see that both the green Photar 58 and red Photar 25A filters transmit infrared radiation beyond that which is detectable by the human eye(i.e., 700nm). The passage of infrared

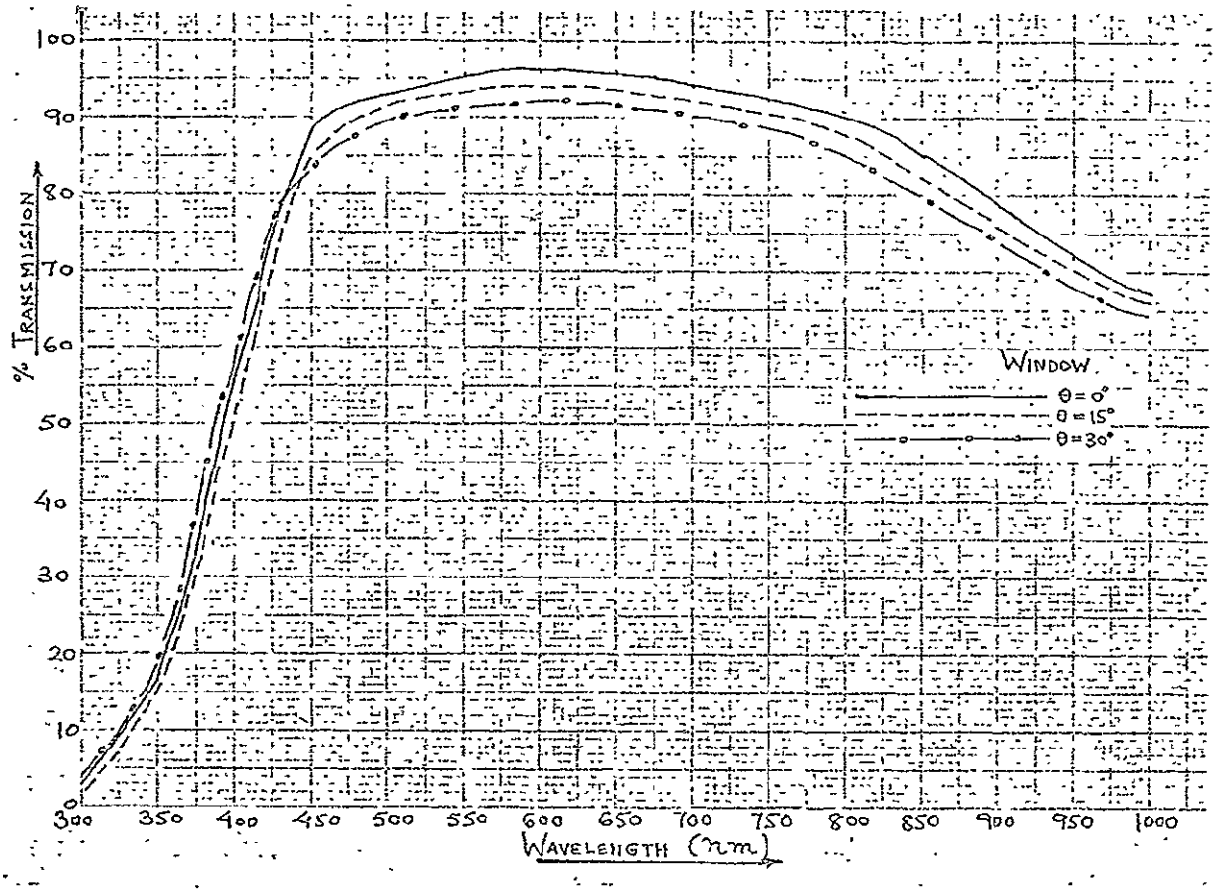

FIGURE 5 : PRE-FLIGHT SPECTRAL TRANSMISSION CHARACTERISTICS OF THE APOLLO 9 SPACECRAFT WINDOW THROUGH WHICH THE S065 MULTIBAND PHOTOGRAPHS WERE TAKEN.

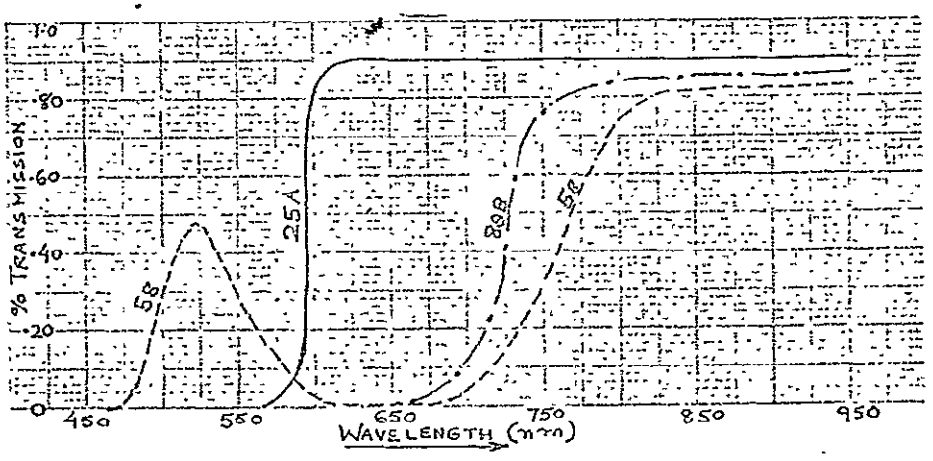

FIGURE 6 : SPECTRAL TRANSMISSION OF THE THREE FILTERS USED WITH THE S065 BLACK-AND-WHITE MULTISPECTRAL PHOTOGRAPHS.

radiation by the green filter resulted in a certain "leakage" of infrared radiation onto the green band which is discussed in subsequent paragraphs.

The spectral transmission of the Zeiss 80mm Planar lens used in the experiment is shown in Figure 8 . These data were obtained on axis at the full aperture opening. As can be seen from these curves, there is only a slight decrease percentage transmission of the radiation in the infrared region beyond 700nm compared with the visible region. It is conventional to compensate for this by adjustment of the aperture and/or shutter speed. The quantity and spectral distribution of radiation striking the film plane will of course depend on the angular distance off axis. Preliminary data indicated that the reduction in illumination as a function of field angle in the focal plane of the camera was not preferentially selective(Slater, 1970). Thus, the off-axis amplitude of the curve shown in Figure 8 would decrease but not change in shape. A reduction in the lens transmission is also affected by the aperture setting. Perhaps more significant from a photographic standpoint, the radiation per unit time falling on the film plane(ergs/cm^2) is controlled by the shutter speed of the camera. This ability to control the total quantity of radiation falling on the film by a combination of shutter speed and aperture settings is one of the great advantages of multiband photography. This degree of freedom allows one to compensate for preferential transmission of the optical system, selective spectral attenuation of the atmosphere as well as the relative distribution of

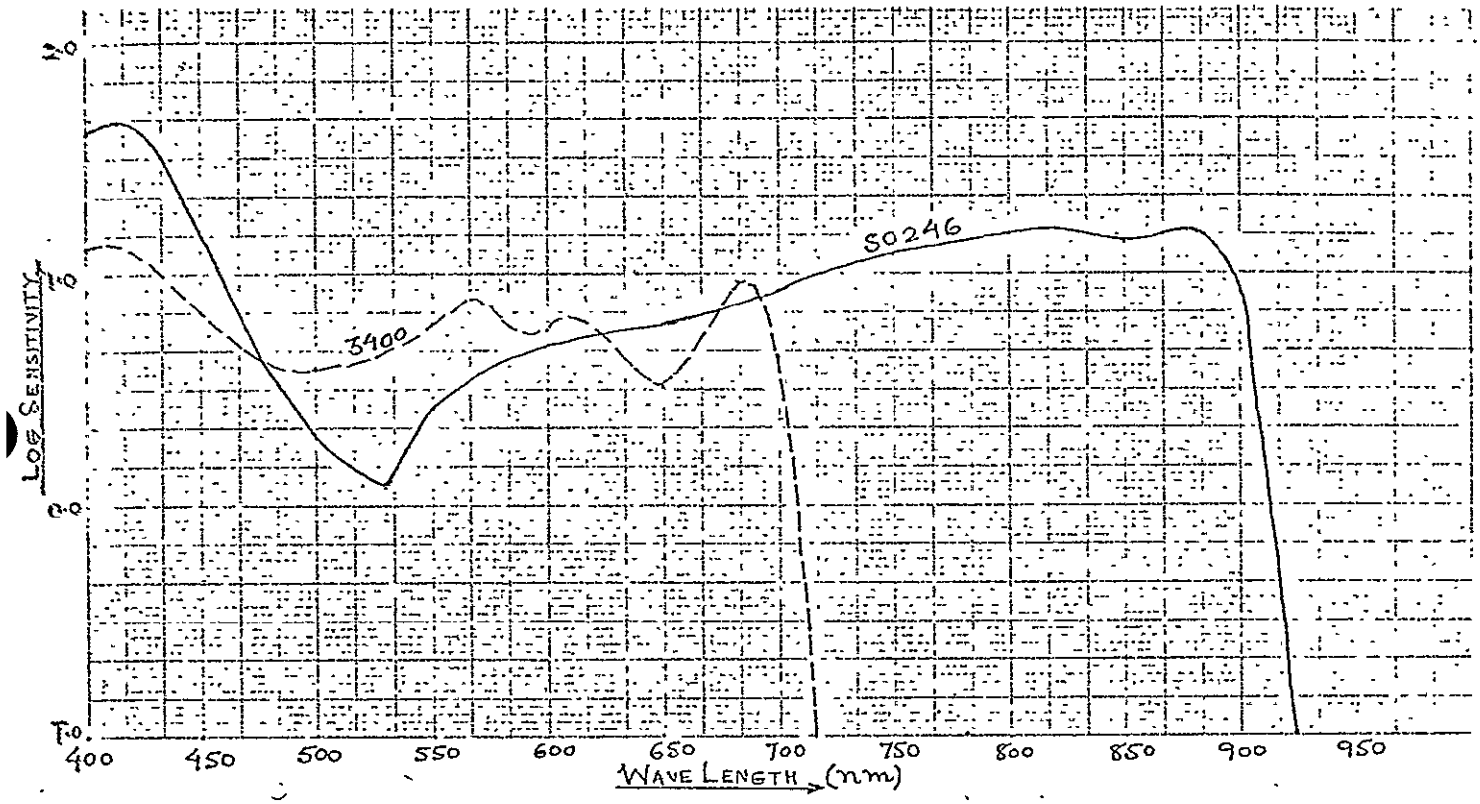

FIGURE 7 : LOG SPECTRAL SENSITIVITY OF THE FILM USED IN THE VISIBLE AND INFRARED BANDS AT A DENSITY OF .30.

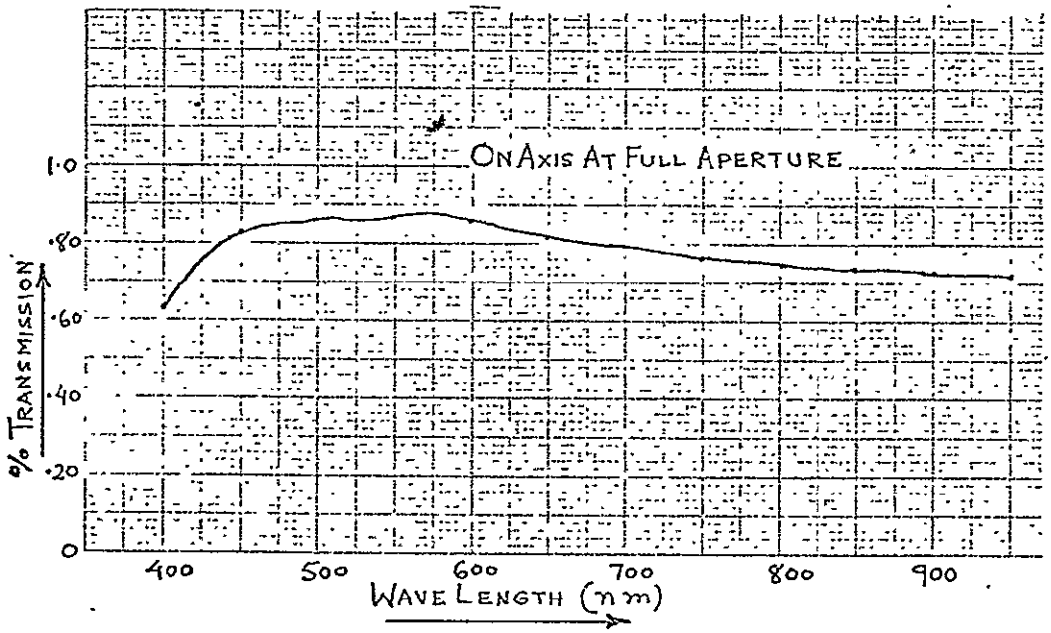

FIGURE 8 : ON AXIS SPECTRAL TRANSMISSION OF THE ZEISS 80MM PLANAR LENS (AT FULL OPEN APERTURE) USED ON THE HASSELBLAD CAMERS DURING THE SO65 EXPERIMENT.

the solar illuminant as a function of wavelength.

The log sensitivity of the two black-and-white films used in the SO65 experiment are shown in Figure 7 . These curves were prepared by the manufacturer (Eastman Kodak Co.) using equal energy sources of radiation at each wavelength, and computing the log sensitivity from the image formed at a density of .3 on the film. In addition to the non-uniformity in sensitivity of the film as a function of wavelength, one can see from these curves that the lack of sensitivity of the Panatomic X 3400 film above approximately 700nm seemed to cut-off infrared radiation. The lack of sensitivity of SO246 infrared film beyond 920nm served as the upper limit on the infrared sensitivity of the infrared band since the 89B Photar filter transmits radiation well beyond 1000nm wavelength. It is important for the reader to note that the log sensitivity curves as supplied by the manufacturer are nominal values and were not determined from the particular emulsion batch used in the experiment. Generally, there is a slight, and only sometimes significant, variation between emulsion batches. It is also noteworthy that the y axis of the curve shown in Figure 7 presents a logarithmic value of sensivity. These values are determined from the reciprocal of the exposure in ergs/cm^2 required to produce a density of .3 above base plus fog level of the film. For both the Panatomic X type 3400 and black-and-white infrared film type SO246, these data were derived by development of the film in D-19 type developer for eight minutes at 68°F. Perhaps the significant function of these curves

is the fact that it gives one an idea of the energy required to expose the film at any particular wavelength. A more sensitive film would result in a greater value of log sensitivity and, of course, the curve would be higher.

The Relative Response of the S065 Multiband Images

The relative response of the green, red, and infrared black-and-white bands has been calculated. The spectral distribution of the log response was determined by taking an equal energy source of radiation and multiplying it by: 1) the effects of the on-axis window transmission (Figure 5), 2) the appropriate filter transmission (Figure 6), 3) the lens on-axis transmission at full aperture (Figure 8), 4) the log spectral sensitivity of the film used (Figure 7). Figure 9 presents the nominal spectral log response of the S065 multiband camera system. The reader should note carefully that these are nominal values in that the data presented in the figure relate not only to the on-axis image but also the lenses at full aperture with no differential shutter speed.

The actual log spectral response of the S065 system, which takes into account the differential aperture settings of the cameras used as well as an appropriate correction factor for the different shutter speed of the green camera, is shown in Figure 10 . In the opinion of the author, these curves represent the most reasonable post facto data on the absolute spectral characteristics of the image forming energy in the three black-and-white bands used in the S065 experiment.

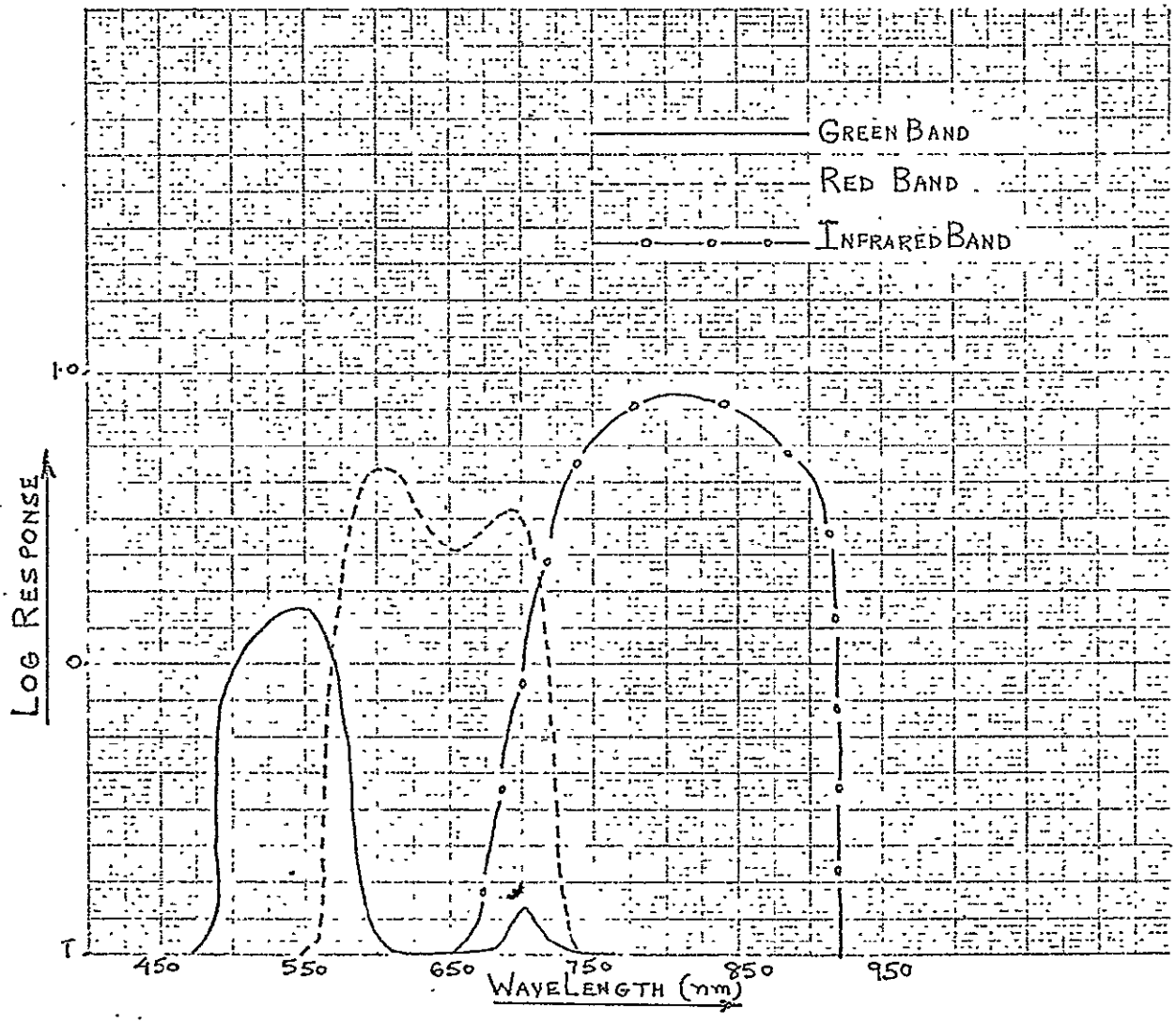

FIGURE 9 : THE NOMINAL SPECTRAL LOG RESPONSE OF THE S065 MULTIBAND CAMERA SYSTEM TO AN EQUAL ENERGY SOURCE WITH ALL LENSES AT FULL OPEN APERTURE (NO DIFFERENTIAL SHUTTER SPEED) WHICH IS REQUIRED TO PRODUCE A FILM DENSITY OF .3.

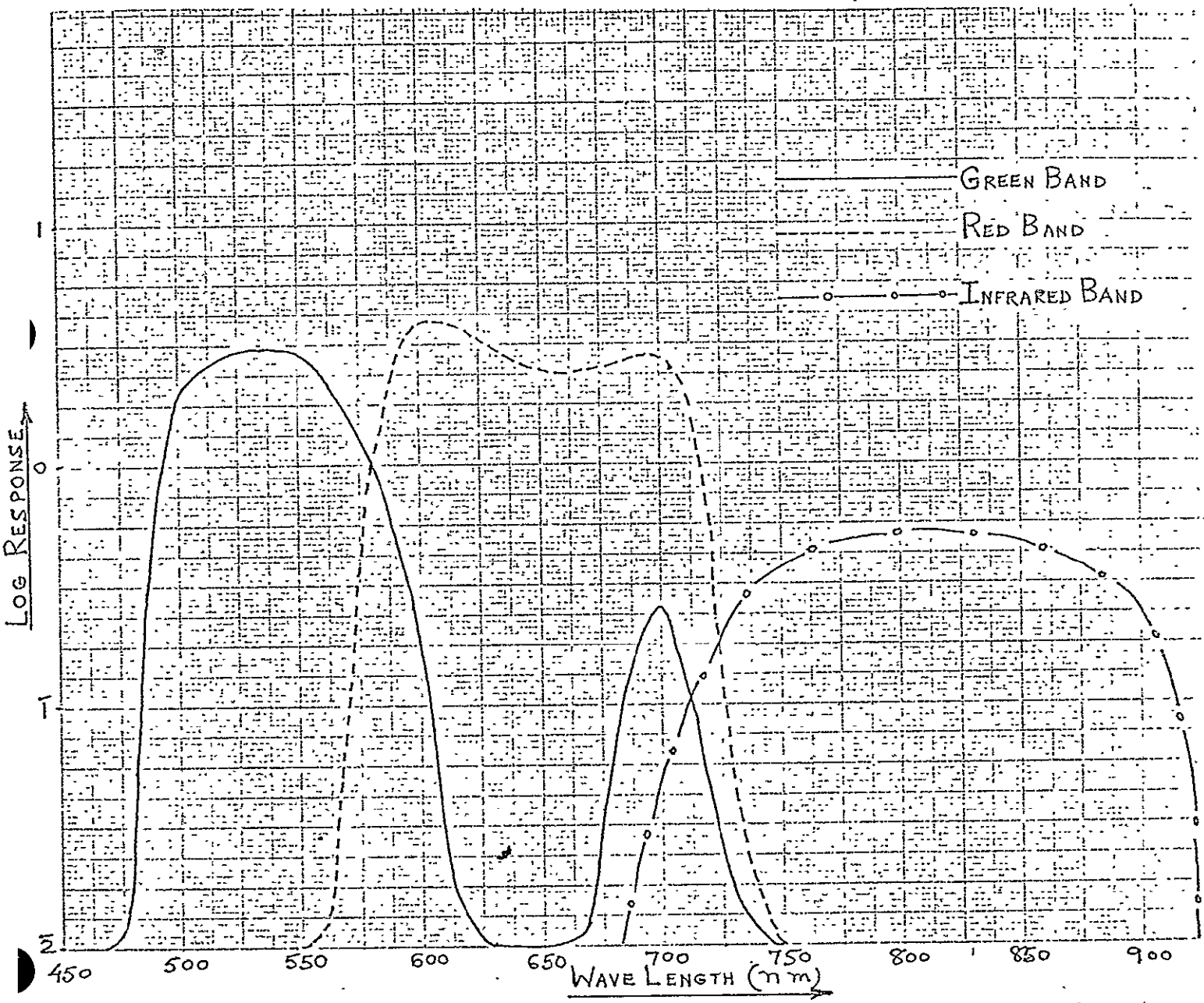

FIGURE 10 : RELATIVE LOG RESPONSE OF THE SO65 MULTIBAND CAMERA SYSTEMS TO AN EQUAL ENERGY SOURCE: SYSTEM CONSISTS OF WINDOW, FILTERS, FILM, AND LENS. THE TRANSMISSION OF THE LENS FOR EACH BAND HAS BEEN ADJUSTED TO REFLECT THE APERTURE AND SHUTTER SPEEDS USED IN THE EXPERIMENT.

It is particularly significant to note the amount of infrared radiation which is present in the green spectral image. The relative linear response of the green, red, and infrared spectral bands have been calculated. These values, normalized to unity for each of the bands and presented on a linear y axis, are shown in Figure 11 . The point of maximum transmission has arbitrarily been placed at 100% for each of the bands. Upon examination of these curves, one can see that the peak transmission of the green band occurs at approximately 550nm,and that in addition a relative response of approximately 10% occurs at 700nm due to "leakage" of infrared radiation. This is caused by a combination of extended red sensitivity of the Panatomic X 3400 film and an opening of the Photar 58 filter to infrared radiation. The relative response of the red band shows a double peak. This effect is primarily due to non-linear log sensitivity of the Panatomic X 3400 film. In the case of the infrared band, the uniform functional relationship between wavelength and relative response exists with the peak approximately at 800 nanometers.

Resolution of the S065 Multiband Photography

The NASA first generation released positives were analyzed in order to obtain a realistic idea of the operational inflight resolving capability of the S065 multiband photography. Frame number 3799 (Imperial Valley, California),a vertical photograph obtained while the spacecraft was at 129 nautical miles, was selected for analysis. The

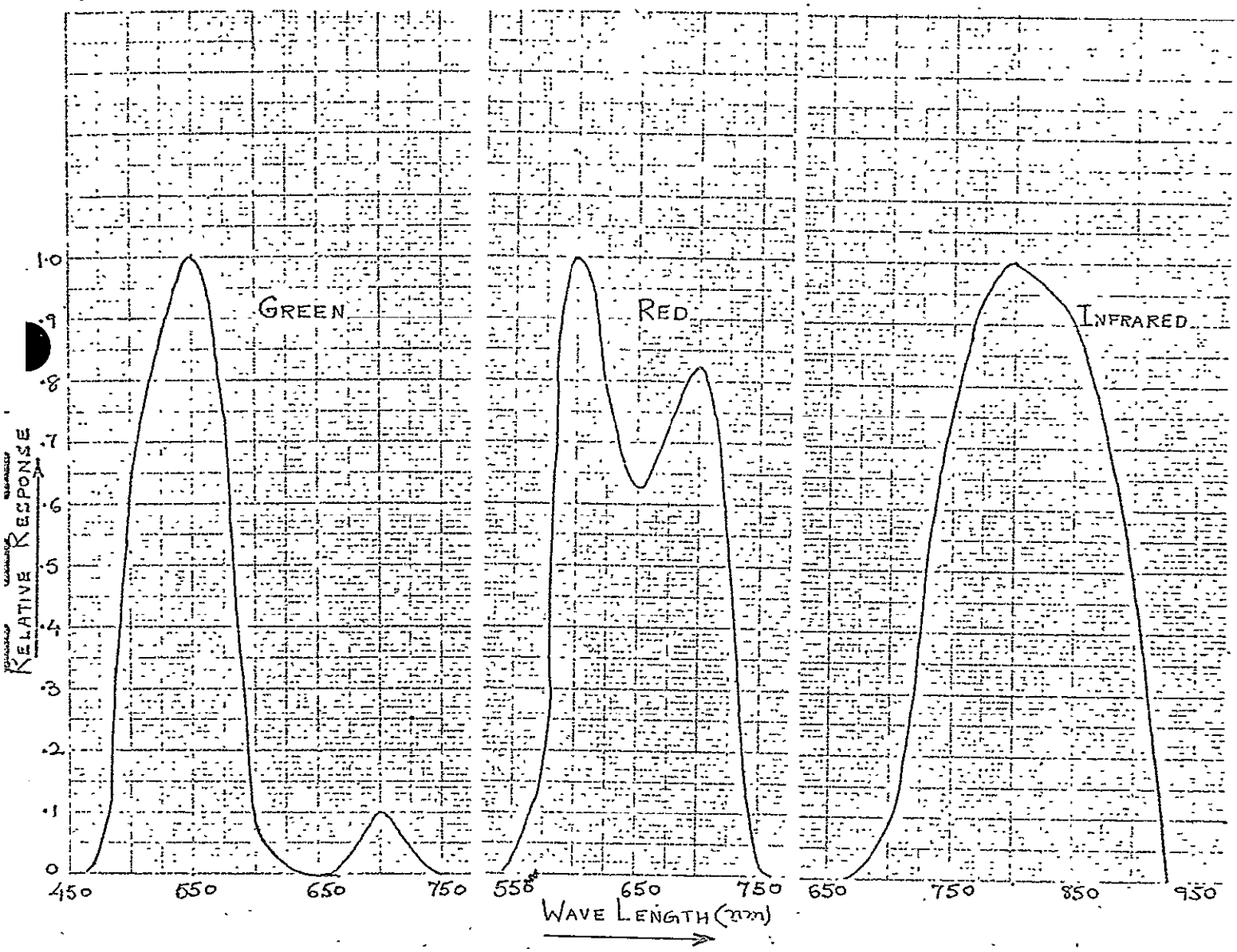

FIGURE 11 : RELATIVE PER CENT RESPONSE OF THE SO65 MULTIBAND CAMERA SYSTEM INCLUDING: FILM, LENS, FILTER, AND SPACECRAFT WINDOW. EACH CURVE HAS BEEN NORMALIZED TO UNITY TO SHOW THE RELATIVE RESPONSE OF THE SYSTEM TO AN EQUAL ENERGY SOURCE UNDER IDEAL CONDITIONS WHERE LENS APERTURE AND SHUTTER SPEED HAVE BEEN ADJUSTED TO PRODUCE IMAGES OF THE SAME DENSITY.

red band imagery showed that it was possible to detect divisions between fields which were known to be 80 feet apart on the ground. Analysis of the green and infrared bands indicated that it was possible to discern lineal objects of 120 feet in one dimension. These data thus indicate that the inflight lineal resolution (not to be confused with the Military Standard Specification 150A Bar Target Resolution) was as follows:

1) Green band---41 lines/mm

2) Red band---62 lines/mm

3) Infrared band---41 lines/mm

The multispectral composite color image was analyzed on the additive color screen (to be discussed in subsequent Sections of this report). It was found that it was possible to discern objects of 340 feet in one lineal dimension. Analysis of the color infrared photograph taken on SO180 film indicated that it was also possible to discern objects of 340 feet in a single lineal dimension. All measurements were taken on SO65 frame number 3799. The resultant computation indicated that a comparative 14 line per millimeter lineal resolution was achieved in both the composite additive color image and the associated infrared color image.

Analysis of the scale error showed that the infrared band was approximately 1% larger in relation to the green and red spectral band.

The Long Island University Multispectral Camera

During the orbit of Apollo 9, Long Island University conducted a number of underflights, primarily over the Willcox-Tuscon-Fort Huachuca Triangle and the Imperial Valley. These flights occurred between 8 March and 12 March 1969.

This airborne multispectral equipment used in support of the S065 experiment consisted of the Long Island University four lens multispectral camera and two auxilary cameras of the K-24 type which were used to obtain supplementary color and color infrared photography. The multispectral camera utilized black-and-white infrared aerographic film (emulsion #5424). The camera was equipped with filters constructed on a combination absorption and interference optical principles, covering the following four spectral bands:

Band 1	Blue	(395-610nm)
Band 2	Green	(480-590nm)
Band 3	Red	(585-715nm)
Band 4	Infrared	(700-900nm)

The log sensitivity of the film as well as the transmission of the filters and camera lenses as a function of wavelength is shown in Figure 12. The reader should particularly note that the three filters used for the visible spectral bands were specially designed to block the transmission of all infrared radiation. This blocking of infrared radiation was achieved by interference coatings placed on the surface of the filters.

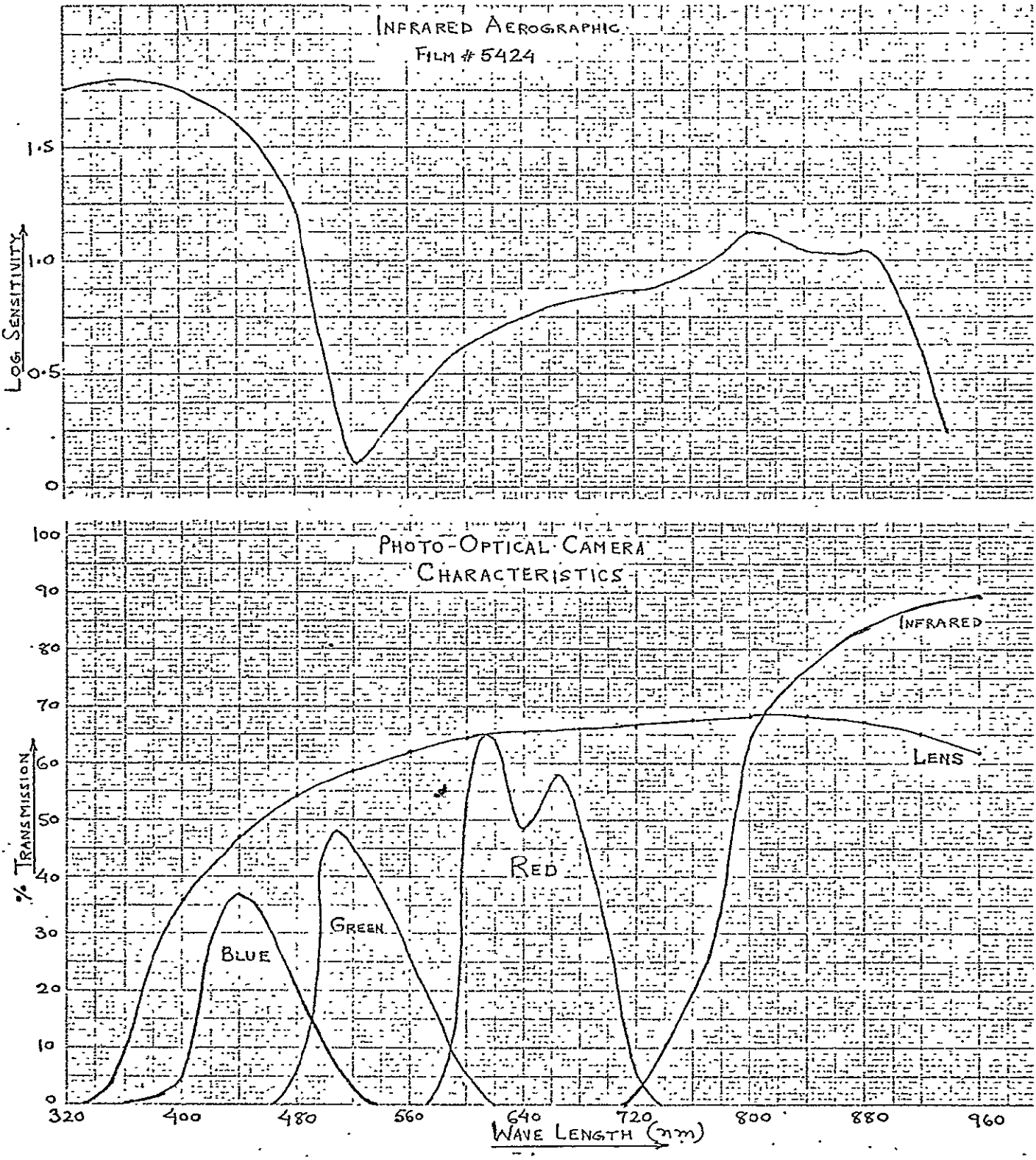

FIGURE 12: PHOTO-OPTICAL CHARACTERISTICS OF THE LONG ISLAND UNIVERSITY FOUR LENS CAMERA USED IN THE APOLLO 9 UNDERFLIGHT.

The bands used in the camera were chosen to approximate the spectral sensitivity of conventional and color infrared films. The green, red, and infrared bands closely matched those in the S065 multispectral array of cameras. The two auxilary cameras utilized aerial Ektachrome (emulsion #8442) and aerial Ektachrome infrared (emulsion #8443). These films are of the color reversal type producing positive transparencies.

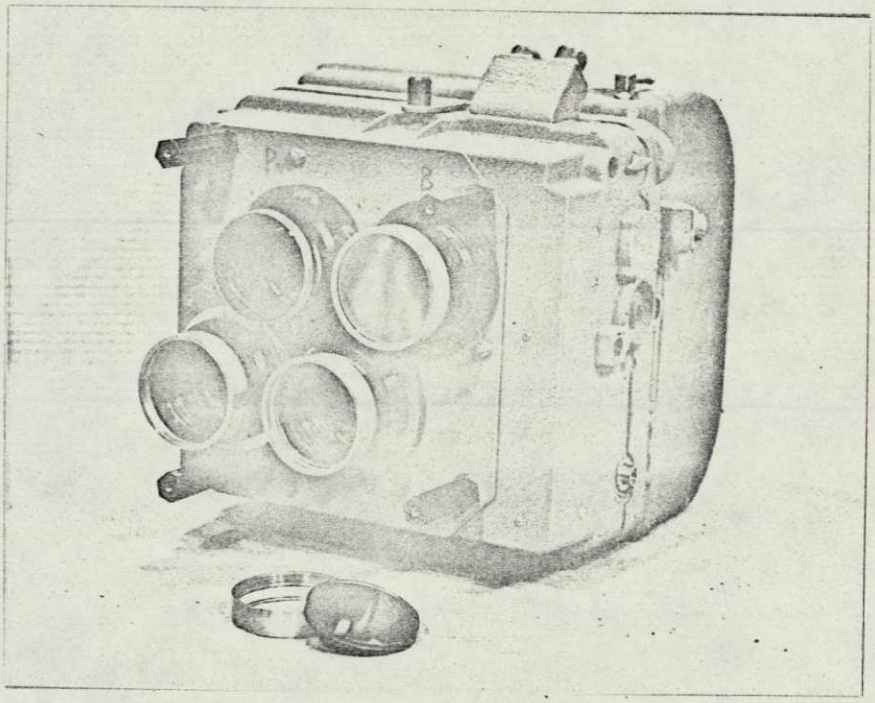

FIGURE 13: MULTISPECTRAL CAMERA: SIMULTANEOUS SPECTRAL PHOTOGRAPHY IN SPATIALLY IDENTICAL FORMATS CAN BE TAKEN IN ANY FOUR SPECTRAL BANDS BETWEEN 360 AND 900 NANOMETERS WITH THE CAMERA AND ASSOCIATED CONTROL EQUIPMENT.

The four lens multispectral camera shown in Figure 13 is of the frame type. This instrument has been designed so that the single pho-

tographic film is exposed by the four individual lenses, each one of which can be filtered to cover any desired wavlength above 360nm. In wavelengths less than this, the radiation is absorbed by the glass elements of the lens. The upper limit of radiation which is capable of being sensed is established by the film emulsion which is currently at about 920 nanometers.

The camera is designed primarily to use a single film in which four exposures are obtained on one piece of 9 1/2" wide film. However, the capability to use four different films each 2 1/4" wide has been incorporated into the design. The magazine capacity is 400 feet of standard thickness base film. The camera has been equipped with image motion compensation devices to allow the use of long exposure times at low altitudes and high aircraft velocities without causing excessive image blur. A single focal plane shutter is employed to expose all four photographs at precisely the same instant of time. This feature assists in accurate registration of multiple image in the associated additive color viewer by eliminating image displacement between the four images which might result from the aircraft angular motion during exposure.

Figure 14 is a schematic of the arrangement of the multispectral camera and two auxilary cameras in the Long Island University aircraft. This diagram shows the interconnection of the cameras and electronic control system. The system operates utilizing standard 24 volt DC aircraft power.

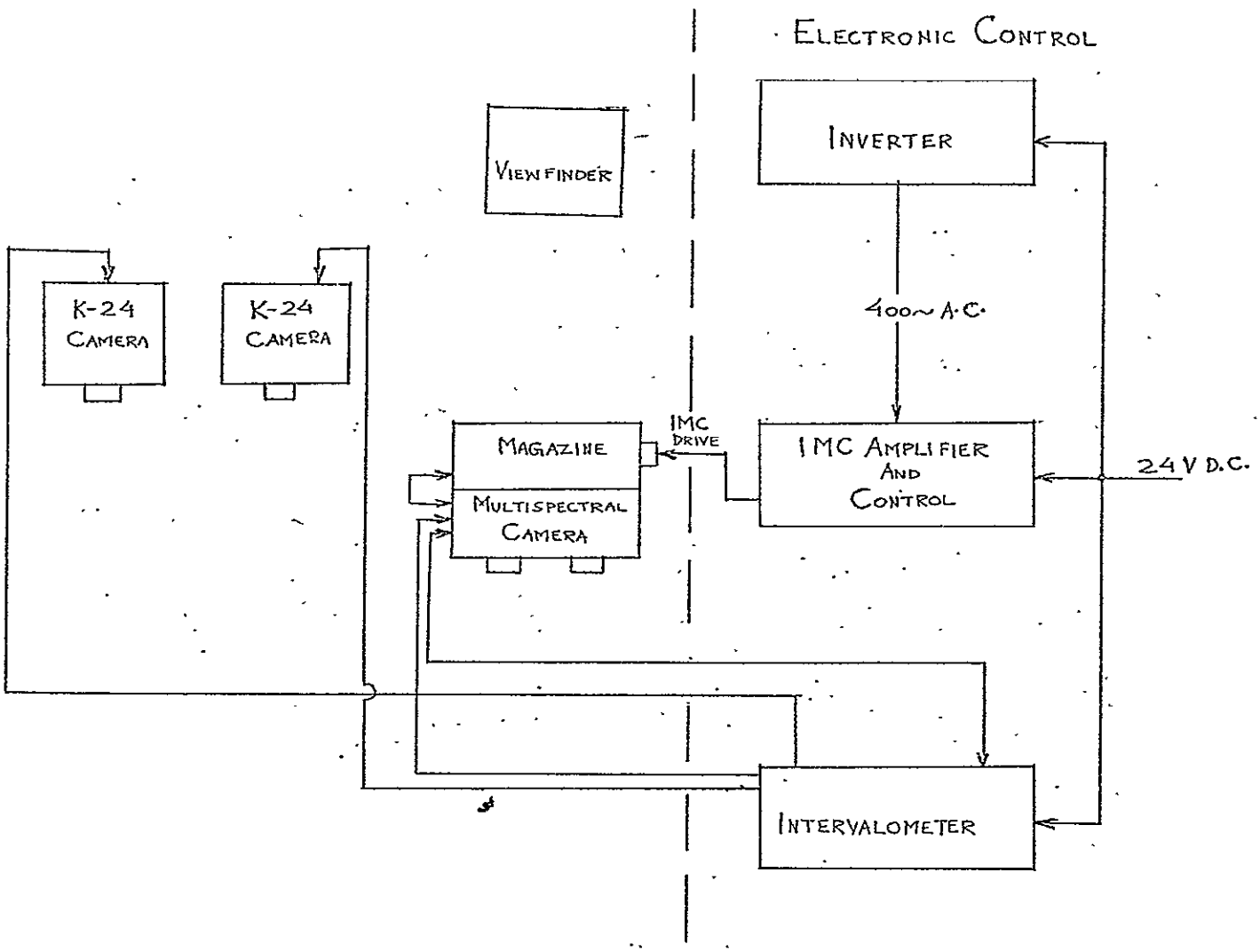

FIGURE 14: SCHEMATIC OF THE LONG ISLAND UNIVERSITY CAMERA CONTROL SYSTEM

SECTION 3

ADDITIVE COLOR ANALYSIS OF MULTISPECTRAL PHOTOGRAPHY

Multispectral additive color viewing devices provide a practical method for extracting meaningful information from sets of multiband photography. However, the photography must be of exceptional quality in that the spatial positioning of all images with respect to their principal points must be accurate. In addition, there must be a good correspondence between the image densities on all the multispectral photography and the quantity of radiation reflected by an object in that particular spectral band.

Introduction

A multispectral additive color viewer is an instrument for use in the intrepretation of multiband "black-and-white" photography. Using two or more spatially identical photos, the device produces a single color presentation by projecting the image of one photo on top of the other, using different color light sources. This technique of remote sensing permits a scientist to select a particular set of bands within the near ultraviolet, visible, and near infrared spectrum and interpret within results from a single color presentation. In addition, a multispectral viewer provides the scientist with the capability of altering the color of the presentation in order to enhance the particular relationships he may be seeking. Fundamentally, the multispectral technique allows the scientist to create a color film specifically for the purpose of

his discipline and interests. (Yost and Wenderoth. 1967, 1968, 1969)

There are three catagories of problems associated with multispectral photographic techniques which have been distinguished. These are:

The existance of instrumentation errors in multiband cameras which can seriously affect the accuracy of the image reconstituted by the multispectral viewer. The most important of these sources of error is lack of good quality image registration resulting from differential positioning of the same image on the set of multispectral positives used in projection. Such lack of good registration in the composite color image can be caused by: differences in focal length and differential distortion of the lenses in the multispectral camera array; angular variation of the optical axes of the cameras with respect to each other; differences in shutter actuation of the individual cameras when the camera platform is undergoing rapid angular motions.

There is an absence of accurate spectral reflectance data taken in situ correlated with the dynamic environmental variables such as variation in solar illumination, atmospheric scattering and absorption of radiation. As a consequence, it is difficult to predict if subtle chromatic differences will be exhibited in the multispectral

additive color image for the same earth resource phenomena photographed at different geographical locations at different times of the year.

There exist relationships in the processing and printing of photography such as the dependence of image density on wavelength of radiation, variation in gamma and reciprocity failure which are not fully understood in relation to the resultant chromaticity of the additive color image. It also should not be overlooked that, in theory, while a unique reflectance spectra exhibited by an object will produce a unique color, the inverse is not true. Identical image colors may be produced by an infinite number of different reflectance spectra. Multispectral photographic techniques have been remarkeably successful at circumventing this physical law of nature.

Additive Color Techniques

For the puroses of analysis of the operation of multispectral additive color viewers, let us assume that we have a set of three negatives taken in different bands of the spectrum; each negative being taken at the same instant by cameras having matched lenses, the optical axes of which were normal to the film plane producing four spatially identical negatives. Thus, all images will be in identical coordinate positions as measured from the principal point of each negative (the inter-

section of the optical axis with the film plane). When the film is processed and viewed on a light table, the set of spectral negatives will appear to be identical except that the densities of the same image may differ between them. This density difference is caused primarily by the selective spectral reflectance of ground objects, a fact which, in the visible spectrum, accounts for their apparent color.

Color is an effective means of discriminating density differences between similar images which appear on sets of multispectral negatives. This can be accomplished using additive color techniques first demonstrated by Clark Maxwell over 100 years ago. By projecting positives of each spectral negative on to a screen in such a fashion that one is registered upon the other (using a different colored primary light source for each), a composite color rendition of the scene is formed.

Conceptually, color may be defined as that conscious sensation which is exhibited when light of a specific spectral energy distribution enters the eye. It has been experimentally shown that differences in this energy distribution cause variations in the observed response of the eye and may be described in terms of three distinct psychophysical variables. The first is hue which is basically that quality of color which leads to the definition of an object as being red, green, yellow, etc. As white light is dispersed by a prism, it is broken up into a multitude of hues each one of which may be related to a corresponding value of wavelength producing a so-called dominant wavelength which in turn enters the eye to produce the sensation of hue. Saturation, the second quality of color, is described as the amount of white in a given hue. It may be also considered as the concentration of the color. For

instance, it is the difference between red and pink. As the amount of saturation in a color decreases, it approaches pure white. Brightness, which is the third variable of color, is described as the amount of visible energy contained in a certain hue which is saturated to a specific value. For example, the color royal blue, is identical to the color navy blue except that navy blue has a lower brightness value.

It has been estimated that the human eye can differentiate between 7,500,000 and 10,000,000 color differences over its sensitivity range. (Judd. 1952, Nickerson and Newhall 1943) For scientific purposes, it is impossible to use subjective terms for the unambiguous description of a color. The human eye is a relatively insensitive instrument when used to uniquely describe the appearence of an object with respect to its color.. It is for this reason that a mathematical conception of the three variables defined above has been employed to describe that response (by the eye or any other recording instrument) to the stimulus known as color. We may envision these three variables of hue, brightness and saturation with the aid of a three dimensional color solid shown in Figure 15. It consists essentially of a solid cone standing on its apex with the hue positioned around the periphery of the solid, the saturation existing somewhere along the line connecting the center or white point with a particular hue and the brightness varying with position along the vertical axis. More precisely, the color solid is not cone, but rather a rounded triangle. A horizontal slice through this solid, perpendicular to the brightness axes is known as a chromaticity

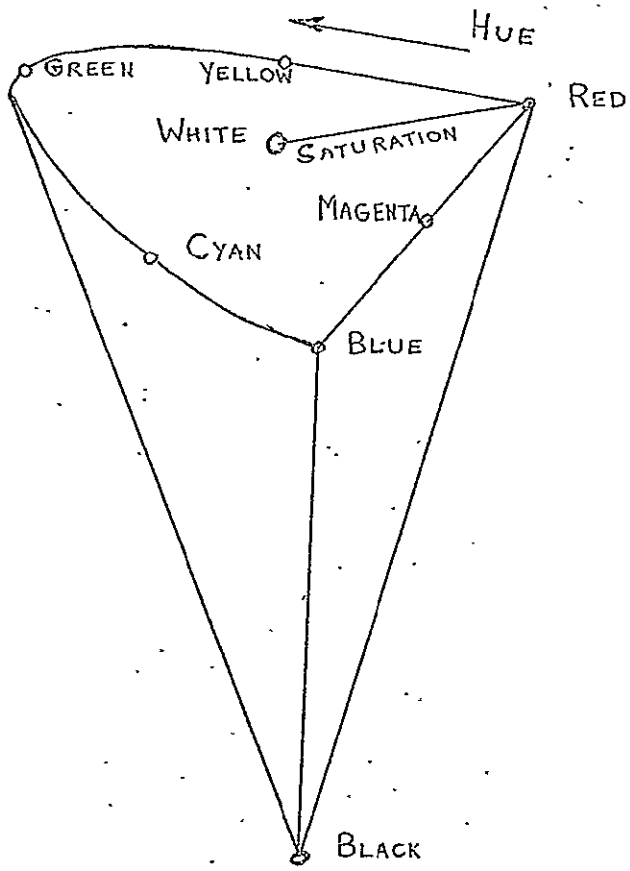

FIGURE 15 : THREE DIMENSIONAL COLOR SOLID INDICATING THE THREE VARIABLES OF HUE, BRIGHTNESS AND SATURATION.

diagram and is shown in Figure 16 , in which certain colors have been identified. In order to pictorially describe the exact hue, brightness and saturation levels of a color, it is first necessary to determine the brightness level, place an orthogonal plane through the color solid at that level and determine the hue and saturation in this plane.

It should be emphasized that the mathematical study and description of color, which is known as colorimetry, only indicates the specific values of hue, brightness and saturation which are being measured and

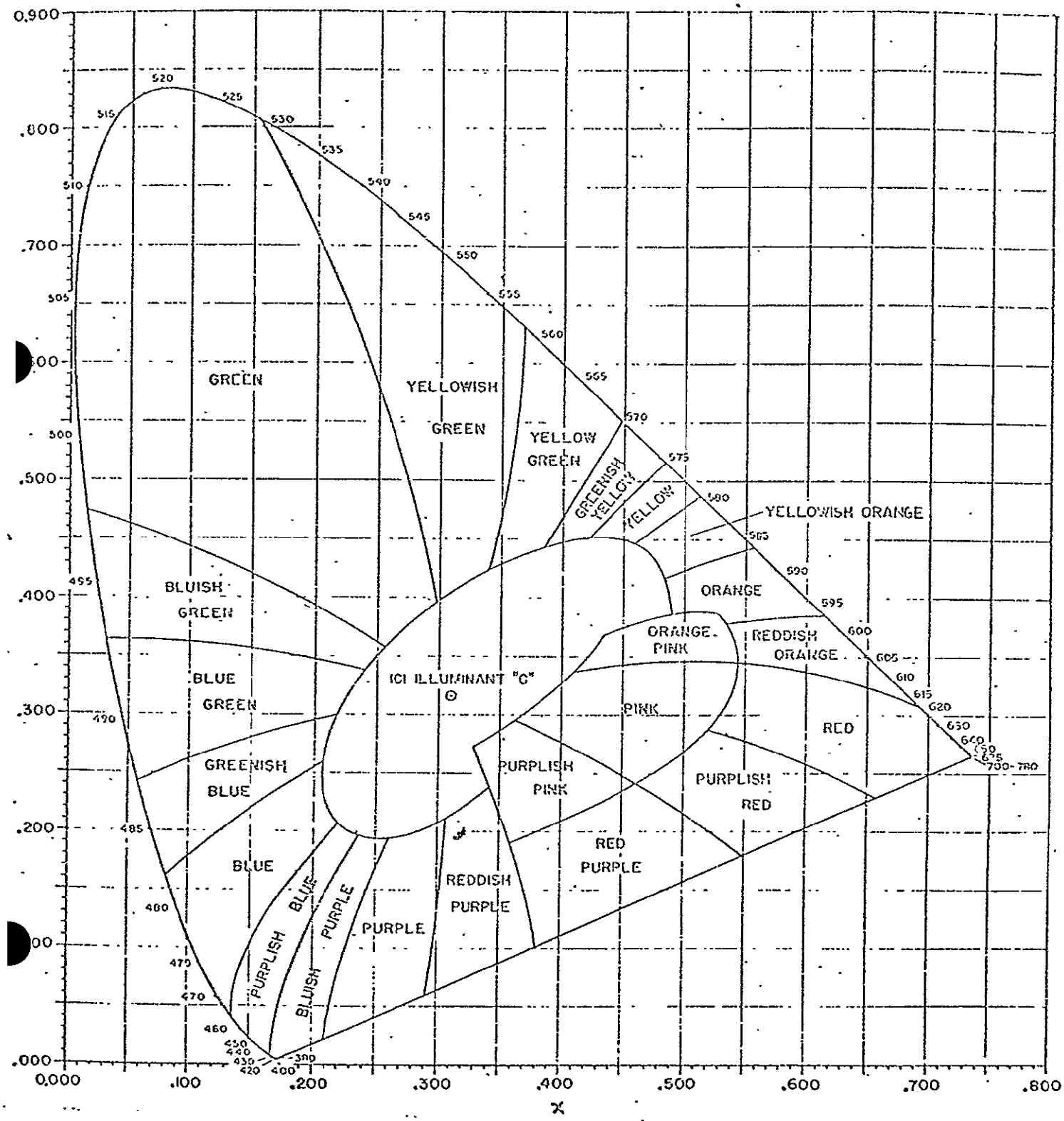

FIGURE 16: THE INTERNATION STANDARD CHROMATICITY DIAGRAM OF THE C.I.E. SYSTEM.

not the energy distribution of the color as a function of wavelength. The theory of colorimetry is based upon the concept that any color can be matched by some combination of three given colors or primaries. However, it has been demonstrated that there does not exist a single set of primary filters which can yield every color. In multispectral photography, a judicious choice of (camera) filters must be selected depending upon the spectral reflectance and the general domain of colors which are to be reproduced. For the reproduction of true color using additive methods, the primary colors shown in Figure 17, which are red, green and blue, have been selected for two distinct reasons. First,

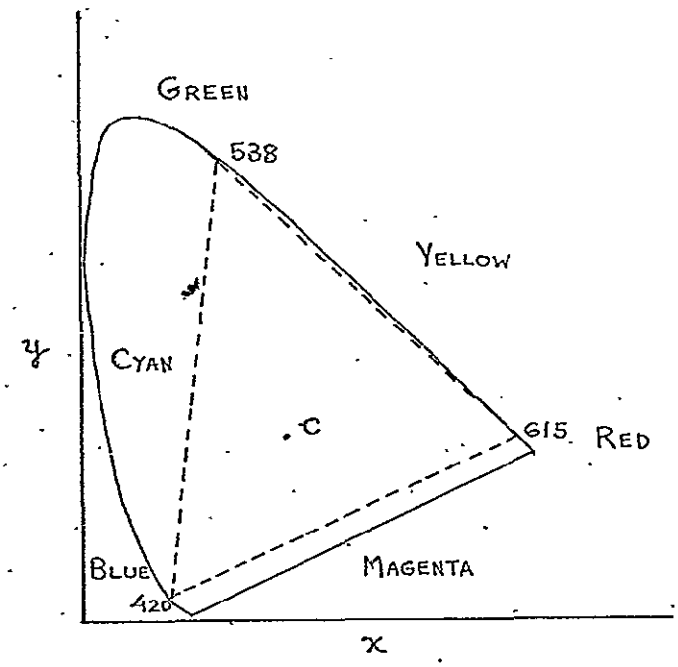

FIGURE 17 : COLOR TRIANGLE. ALL COLORS WHICH LIE ON THE BORDER OR INSIDE THE TRIANGLE CAN BE REPRODUCED BY THE PRIMARIES AT ITS APICES. SATURATED CYAN (TO THE LEFT OF THE TRIANGLE) IS RARELY, IF EVER, ENCOUNTERED IN NATURE.

it is desirable to maximize the area of the inscribed triangle since only those colors within that triangle may be reproduced by a combination of the three primaries. Secondly, the triangle is conventionally positioned so that one side lies close to the locus of the pure spectrum of the green-yellow-red colors since these colors appear in nature but the pure spectrum colors in the cyan portion of the chromaticity diagram do not.

The trichromatic system of color definition is a calculation of the fractional component of spectrally defined red and green primaries (referred to in colorimetry as the tristimulus values) for a given color. They are designated as x and y respectively and are known as trichromatic coefficients. These represent the percentage of standard red and green primaries required to produce a hue and saturation match to the color. A third value, Y represents the luminance or brightness level of the color. The standard chromaticity diagram is a plot of the color in terms of x and y. The dominant wavelength of a color is determined by the intercept of the spectrum locus with the line which connects the illuminant point (the white point) and the color itself. The relative distance between the white point, the color, and the spectrum locus is the saturation.

When analyzing the image reproduction characteristics of a multispectral viewer, colormetric measurement is a useful tool particularly in removing any anomalies associated with the visual response of the observer. The visual perceptibility of differences in the C.I.E. chroma-

ticity diagram are shown in Figure 18 . Generally, colors which appear identical on a viewer screen to an observer will not exhibit the same energy distribution and may indeed be quite different spectrally. The advantage in using a trichromatic measurement of an image is that the resultant color measure is completely dependent upon the psycho-physics of the situation without any side effects of the human eye such as simultaneous contrast enhancement.

Often, the chromaticity of an image and the background in which it is embedded lie reasonably close when plotted in the color solid. When this is the case, it is often judicious to employ a set of color projection filters which bear no resemblence to the taking filters in the multispectral camera array, but which have the effect of increasing the apparent chromatic difference between the image and its background. This so-called false color space can be made as distinct as the image densities on the transparencies permit. The use of broadband filters in the camera, which overlap along the wavelength scale, may make it impossible to chromatically separate an image from its background. Frequently in such cases, a set of narrow band filters in the multispectral camera array, which are spectrally non-overlapping, produce image densities of sufficient difference to give a marked color difference when reconstructed on a multispectral viewer.

Long Island University Viewer

The multispectral viewer shown in Figure 19 is a hardware embodi-

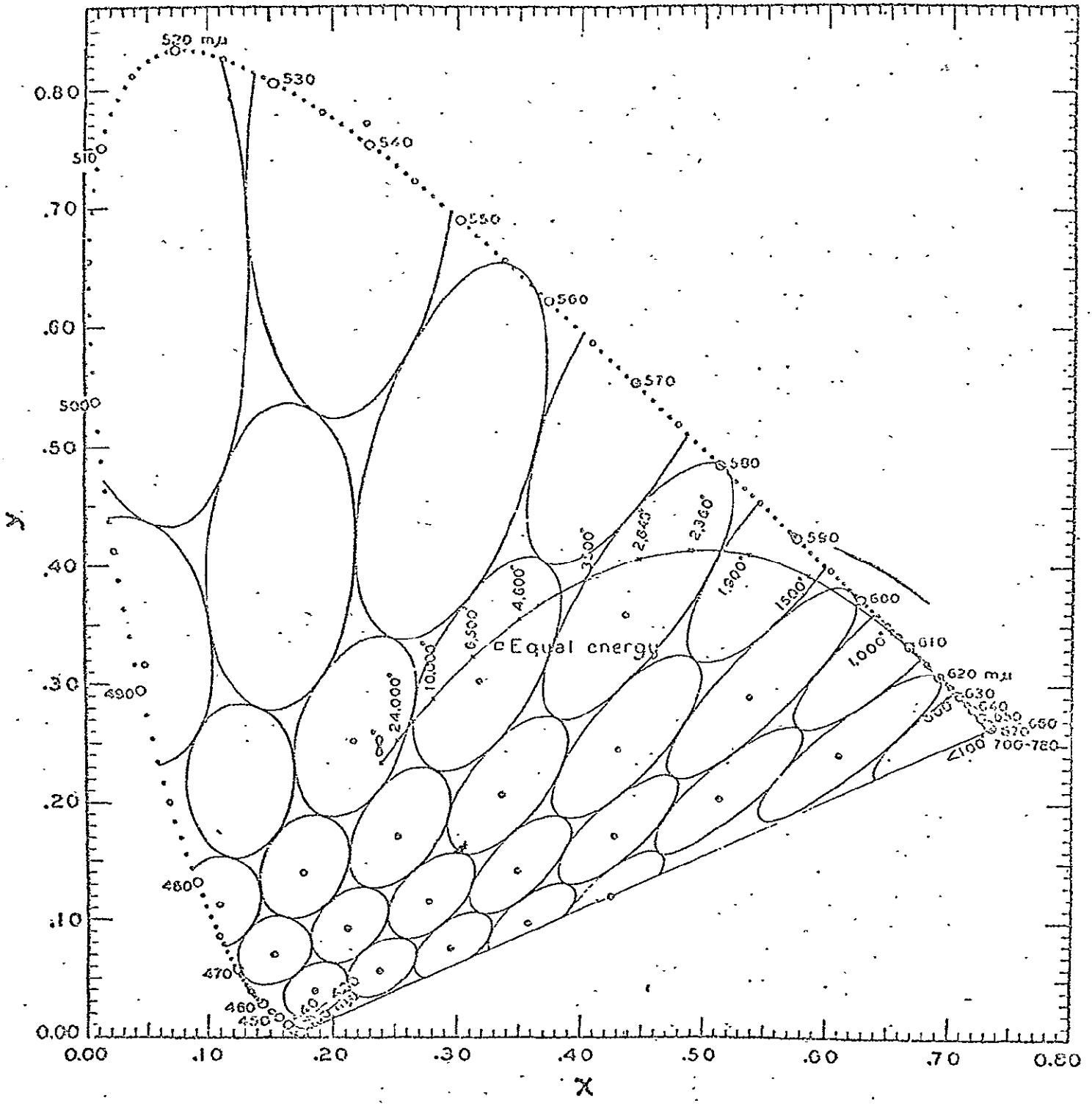

FIGURE 18 APPROXIMATE PERCEPTIBILITY OF CHROMATICITY DIFFERENCES ON THE CIE CHROMATICITY DIAGRAM. THE DISTANCE FROM POINTS ON THE BOUNDARY OF EACH ELLIPSE TO THE INDICATED POINT WITHIN IT ALL CORRESPOND APPROXIMATELY TO ONE HUNDRED TIMES THE CHROMATICITY DIFFERENCE JUST PERCEPTIBLE WITH CERTAINTY UNDER MODERATELY GOOD OBSERVING CONDITIONS.

ment of these additive color principles. It is a console which displays a rear projection screen to the operator. Optically, the viewer is an analog of the multispectral camera array. The basic principle of this device is the utilization of pre-registered sets of multispectral positives on a single roll of film. In this way registration is maintained as the operation proceeds from one multispectral presentation to the next. The four multispectral film images, each with its independent illumination system, are superimposed onto the viewer screen at a three times magnification and in precise registration, using the optical design shown in Figure 20. Misregistration of one image upon the other, when projected on the viewer screen, is not greater than .1 millimeter anywhere in the presentation, so that no blur will be discernable at a viewing distance of 18 inches. The fixed magnification projection system utilizes four, five inch focal length, f/4.5 lenses. These lenses are critically matched so that their equivalent back focus dimensions are within a few thousandths of an inch of each other. The differential distortion of the projection lens is matched in a unique way. As shown in Figure 20, a different part of the field angle of each viewer lens is used to project the image. This requires that the distortion of the lenses be <u>different</u> across their whole field but matched for all field angles associated with conjugate images.

Each of four images projected onto the viewing screen has its own dual illumination system which is also shown in Figure 20. This viewer utilizes 3200 degree Kelvin lamps which have the advantage of being quite

FIGURE 19:

ADDITIVE COLOR VIEWER REAR PROJECTION VIEWER SUPERIMPOSES FOUR SPECTRAL PHOTOS TAKEN BY THE CAMERA CREATING A COMPOSITE PRESENTATION IN COLOR

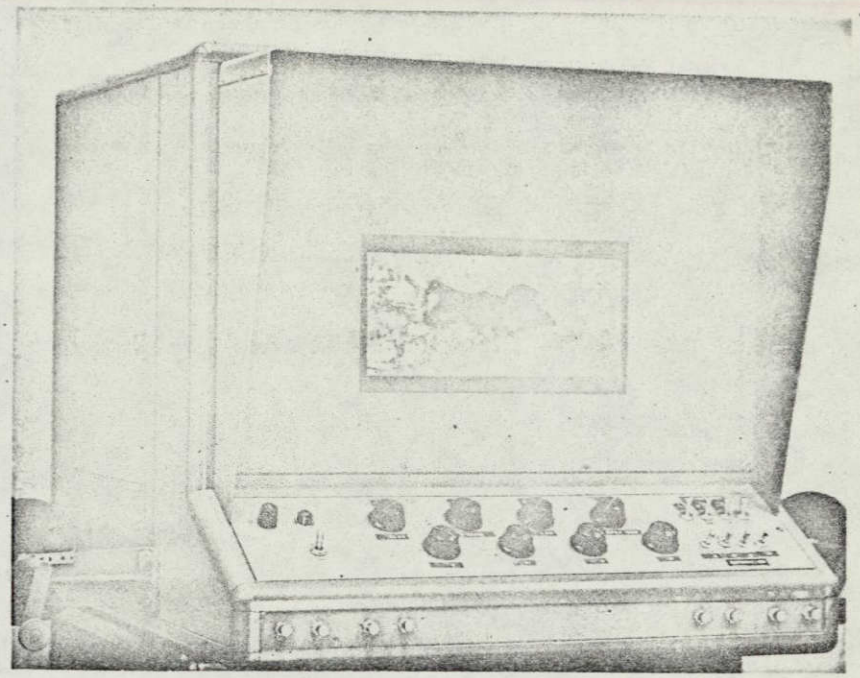

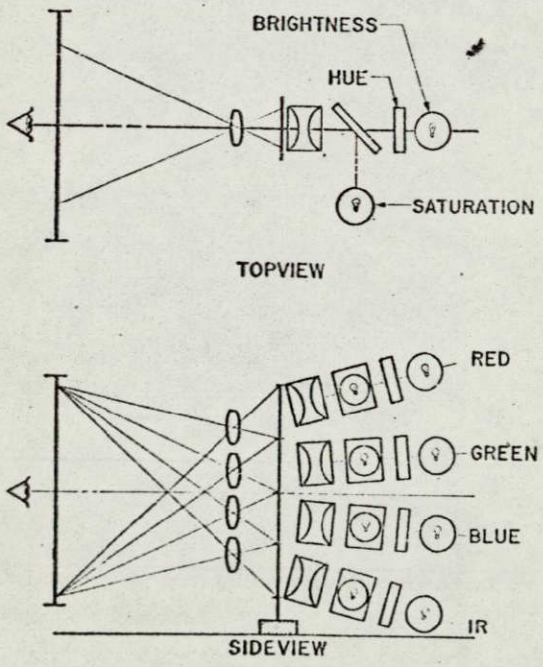

FIGURE 20:

VIEWER OPTICAL SYSTEM. THE OPTICAL PROJECTION SYSTEM OF THE VIEWER GIVES IN REGSITERED SUPERIMPOSITION ALL FOUR SPECTRAL PHOTOGRAPHS ON A REAR PROJECTION SCREEN. THE ILLUMINATION SYSTEM ALLOWS THE INTERPRETOR TO CONTROL THE BRIGHTNESS, HUE, AND SATURATION OF THE IMAGE ON THE SCREEN.

bright with the appropriate filament configuration to best fill the aperture of the projection lens. The brightness illumination passes through a neutral density filter, a spectral filter, a beam splitter and a condensing lens to illuminate the positive spectral photo. The greatest loss in energy throughout the system occurs through the spectral (or color) filter. The second half of the illumination system is set at 90 degrees to the brightness lamp and is employed for purposes of desaturation. Its illumination is reflected from the beam splitter and is added to the brightness illumination as modified by the color filter. The filters associated with the brightness illumination system controls the hue and brightness while the addition of a desaturation selection provides the photo-interpreter with complete control over the displayed color.

Film flattening is provided by two optically polished glass plates, one of which is fixed to the viewer itself and is considered the focal plane or object plane of the viewer optical system. The other is mounted off the carriage through a spring loaded cam mechanism. This moveable plate is raised off the fixed glass platen by means of a foot pedal during the transport of the film. This mechanism insures separation of the plates and avoids film scratching. A film guide is also provided to insure an even transport of the unitary film containing the four individual formats in the horizontal plane, thus maintaining the registration. The ability of the device to maintain registration of the imagery as the interpreter progresses from one multispectral image to the next, is completely dependent on pre-registration of the set of associated

multispectral photos on a single 9 1/2 inch roll of film. In order to utilize the S065 photography, mechanical disassembly of the platten and grid arrangement was necessary to accommodate the individual frames of 70mm Hasselblad photography.

Experience has indicated that the most satisfactory screen material for general rear projection viewing is a white Polacoat Lenscreen. Although other screens provide a somewhat brighter image, the fall-off with incident obliquity is more pronounced and the resolution capability is somewhat less. It was noticed however, that with the type Lenscreen used, considerable color infidelity existed when photographic reproductions of the multispectral viewing screen were attempted. A recently developed type of plexiglass Lenscreen, which is designed specifically for exposing accurate color photographs of rear projected scenes has been used for photographic reproduction of the screen image.

The multispectral viewer projects four multiband images contained on a single piece of film (each one of which has a resolution of 45 line pairs per millimeter) at a magnification of 3 times, this results in a screen resolution of about 15 lines per millimeter. Since the average eye resolves seven lines per millimeter at a normal 18 inch viewing distance, a permissible misregistration which does not exceed .0056 inches has been specified and designed into the viewer system. Each projection lens has its own brightness lamp and filter set which illuminates one of the spectral records as well as a desaturation lamp. By placing various combinations of projection filters into the optical path and by linear transportation of a filter rack, the scene on the

viewing screen appears in color. An important feature of the system is that it frequently enables, through proper choice of camera and viewing filtration, the detection, recognition and identification of objects by color differences which would not otherwise be visible.

General Effects of Photo Processing on Image Color Characteristics

The chromatic characteristics of the multispectral image formed in additive color on the viewer screen are significantly affected by the photo processing techniques used. The relationship of exposure (or its radiometric equivalent) to density on both the negative film used in the camera and the positive transparency printed for projection in the viewer is a critical consideration. Also a significant parameter, often overlooked, is the maximum and minimum density of the duplicated positive image.

The fundamental relationships of the additive color image are examined in some detail in order to present to the reader the significance of photo processing and how errors associated with processing may be reduced or eliminated.

When a multiband negative is properly exposed and processed to a gamma of 1.0, a one to one correspondence will be created on the linear portion of the characteristic curve between the radiation reflected by an object and the corresponding density of the image on the film. Frequently however, as will be demonstrated, a gamma consid-

erably greater than unity is necessary to chromatically differentiate objects whose spectral signatures are nearly similar.

An ideal set of multiband negatives will reproduce a gray scale target having uniform spectral reflectance and which is illuminated by a uniformly distributed source of radiation so that the image density of each gray scale is the same on every one of the individual multiband negatives. This exact matching of exposure and gamma in the different spectral bands which are used is very difficult and frequently not possible.

The difficulty in exactly matching the exposure density relationship (the characteristic curve) is due partially to the effect of the wavelength of radiation which strikes the photographic emulsion. When one film type is used to expose all four spectral bands of distinctly different wavelengths; in general the characteristic curve associated with each band will be different. This condition is unfortunately encountered even in panchromatic emulsions. This effect is shown in Figure 21, in which the characteristic curves for Infrared Aerographic film (5424) exposed with the filters transmitting blue (395 to 510nm), green (480 to 590nm), red (585 to 715nm) and infrared (700-900nm).

The Aerial Exposure Index (or speed) of photographic emulsions used in multiband photography also varies depending on both the spectral sensitivity and the filtration used. The Aerial Exposure Index is defined as .5 divided by the exposure (meter candle seconds) at the point where the slope of the characteristic curve is .6 times the gamma (the

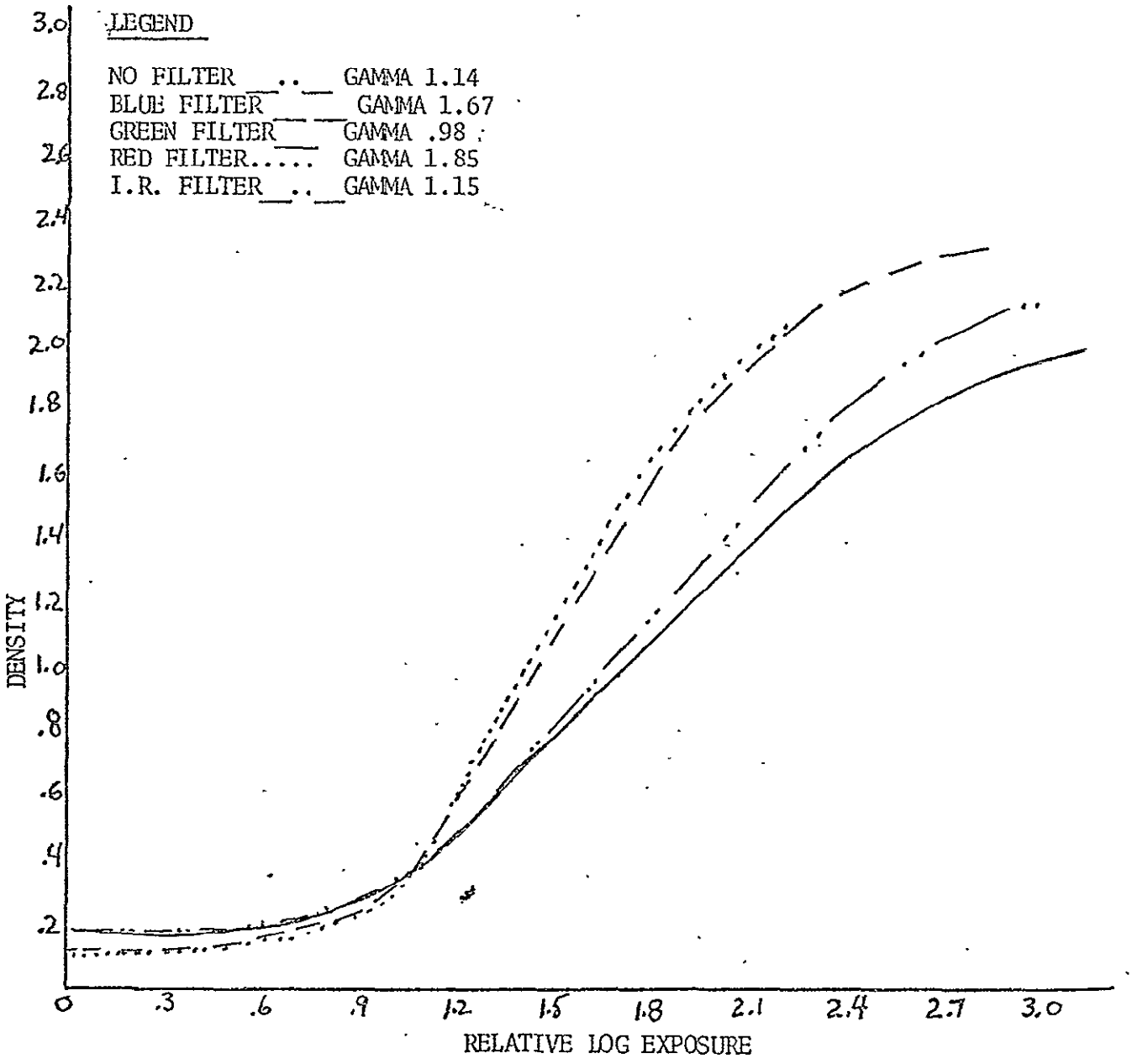

FIGURE 21: CHARACTERISTIC CURVES FOR INFRARED FILM (5424). EXPOSED WITH FILTERS USED IN THE EXPERIMENT AND MATCHED AT .6 GAMMA.

tangent of the angle made by the linear part of the curve and x axis). Figure 22 shows the absolute relationship of the characteristic curves and the differences in photographic speed for Aerographic Infrared film (5424) using filters similar to those used in the experiment.

The careful reader will note that exposure is measured in photometric units (meter candle seconds) and hence is defined only for the visible spectrum. The exposure of the infrared band contains no visible light and is really not capable of definition in terms of photometric exposure. It has been the practice in infrared and ultraviolet aerial photography to use the fiction that the exposure in this non-visible region consists of the meter candle seconds of a standard energy source (Luminant C) which has a predefined spectral distribution of both visible and infrared radiaiton. This practice has the effect of making exposure calculations for the infrared bands extremely difficult to determine because of deviations of the spectral distribution of solar radiation from this standard. Accurate and unambiguous exposure can be obtained in multiband photography by using absolute radiometric units (such as ergs per centimeter squared) in each spectral band.

It should be noted that the intensity of the energy which forms the image on the photographic emulsion of an airborne multispectral camera does not depend on the distance between the object and the lens of the sensor. That is, when an object is at sufficiently large distance with respect to the focal length of the camera, the intensity of the radiation which forms the image is:

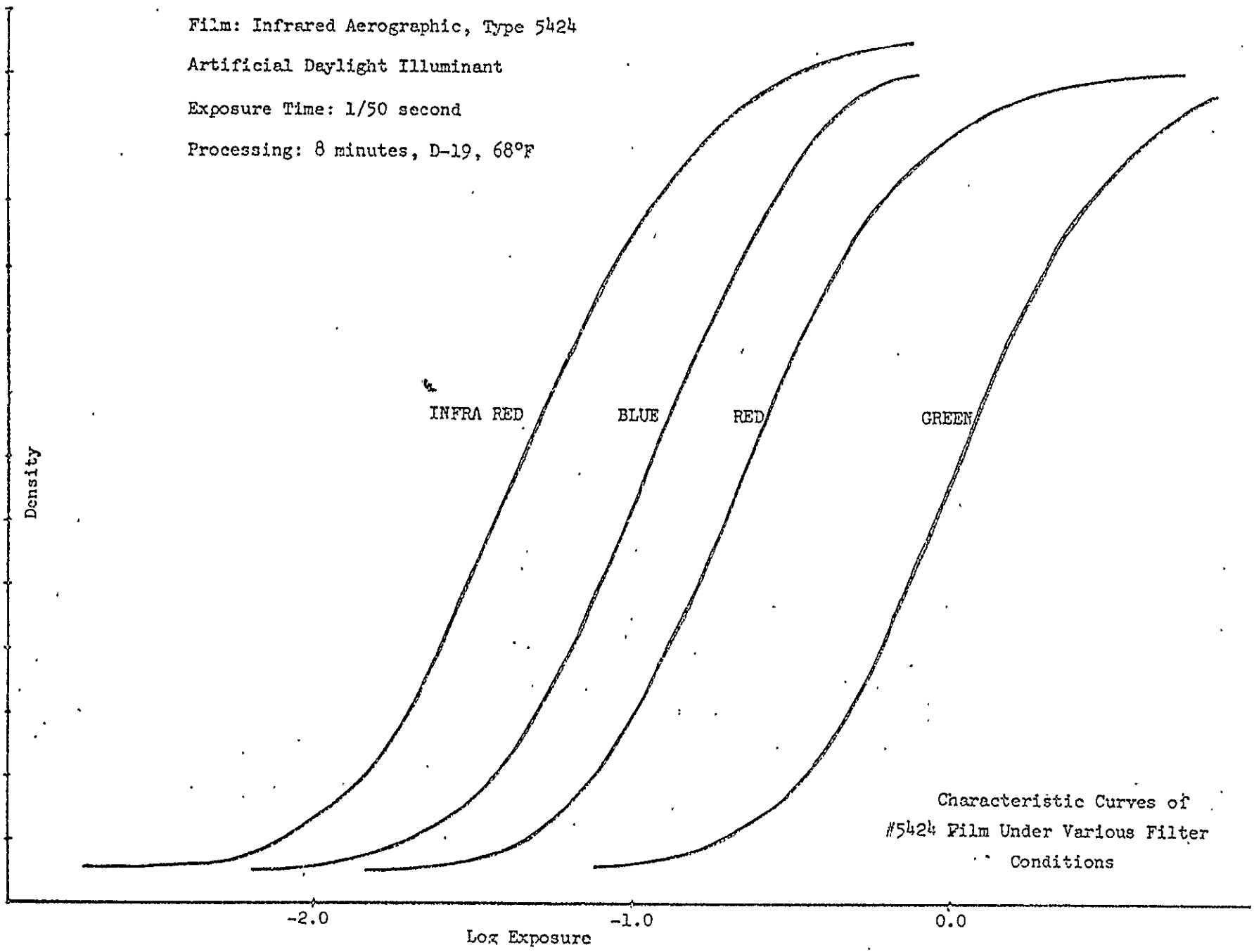

Characteristic Curves of #5424 Film Under Various Filter Conditions

$$I = \frac{B\pi}{4f^2}$$

Where: B = incident intensity of radiation times the reflectivity of the object

f = f/number of the lens

In obtaining actual multispectral photographs, the experimenter must also include the actual lens and filter transmission charactersitics in the above equation.

Photographic Tone Reproduction

In order to accurately represent to the human eye the reflected light from a particular ground scene, there must exist a one to one mapping of the object luminance into the density on the positive. Assume that the negative has been well exposed and processed to a particular gamma. A tone reproduction curve may be constructed to represent the fidelity with which combination negative and positive transparencies reproduce the brightness of the original ground scene. A typical tone reproduction curve is shown in Figure 23, which represents the fidelity with which the red spectral band reproduced the five step gray scale under noon illumination. Quadrant I of this figure shows the characteristic curve of the spectral negative. The densities on the negative of the displayed gray scales in the scene were measured and the target brightness in relative units related to the photographic exposure on the negative film. The corresponding characteristic curve of the posi-

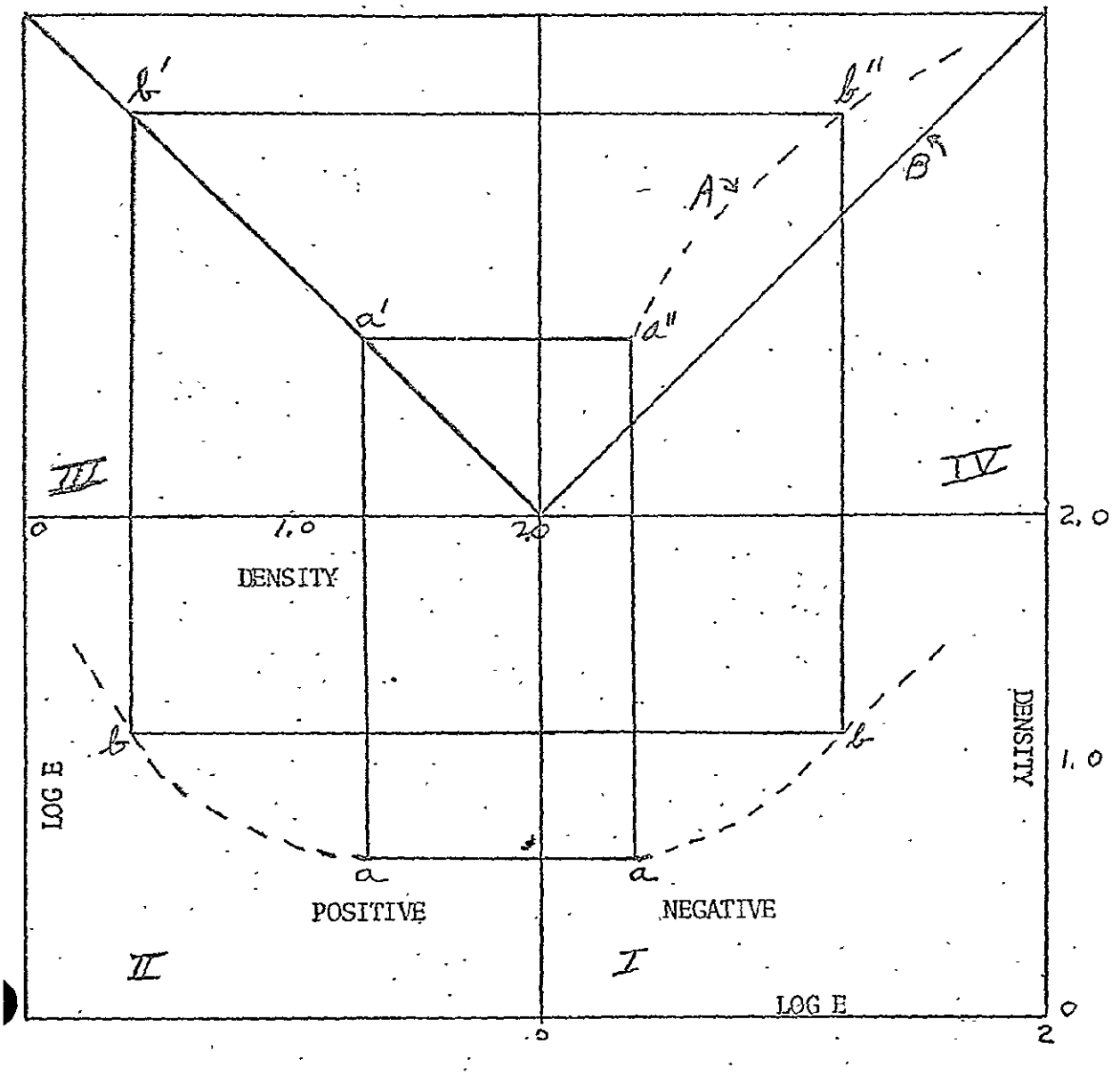

FIGURE 23: TONE REPRODUCTION DIAGRAM. THIS DIAGRAM SHOWS HOW WELL THE RED SPECTRUM NEGATIVE AND DUPLICATED POSITIVE REPRODUCED THE ORIGINAL SCENE BRIGHTNESS.

tive transparency was obtained through similar measurement of the gray scale densities of quadrant II. Vertical lines from several points connecting the negative and positive characteristic curves are made to intersect a 45 degree transfer line in quadrant III. By extending horizontal lines from quadrant III to intersect vertical lines from the original negative curve of quadrant I, and indication of reproduction process is obtained. Thus, the locus of all intersected points from the negative and positive characteristic curves yield the tone reproduction of quadrant IV. For exact reproduction, the curve in quadrant IV should appear as a straight line. An indication of the reproduced departures from this norm are made by comparing the curve A with the curve B.

How Image Density is Related to Color

In order to create an additive color presentation from a set of black and white multiband photos, each photograph must be projected by an optical system, each using a different colored light source, onto a screen in such a way that the images are accurately registered with respect to each other. A different proportion of light will be present in the screen image depending upon the densities of the image on each multiband photo which is projected.

In establishing the relationship between density of individual black and white images and the color characteristics of the corresponding recombined image that is projected on the screen, consider three

primary taking filters, blue (395 to 510nm), green (480 to 590nm), and red (585 to 715nm). When each multiband negative is exposed through one of these filters and processed to obtain a specific characteristic curve, the slope being the gamma, a positive image is then made by exposing the negative onto duplicating film and processing to obtain a specific relationship between the brightness of the ground scene and the density of the image on this positive transparency.

By projecting each of these multiband positives using similar primary blue, green and red filters to form the additive color presentation on a viewing screen, a "true color" rendition of the ground scene is created. The fidelity of the colors of the image compared to the object is not perfect. In order for the image to be a perfect reproduction of the color of the object, it would be necessary to photograph the images exactly as would be recorded by the stimulation of the visual response mechanism of the human eye, shown in Figure 24 . To date, it has not been possible to construct with complete fidelity, filters whose transmission could be duplicated by the response of a photo sensitive material and the illuminant falling on the scene such that curves are exactly reproduced. Due to the necessity to create a less than zero exposure, it is usually assumed that it is theoretically impossible to obtain absolutely perfect photographic color reproduction. These facts not withstanding, a very close true color reproduction of a ground scene is possible with the primary blue, green and red filters noted above.

As discussed previously, not all colors can be reproduced using

one particular set of filters due to the shape of the color triangle created within the chromaticity diagram (See Figure 17). No difficulty

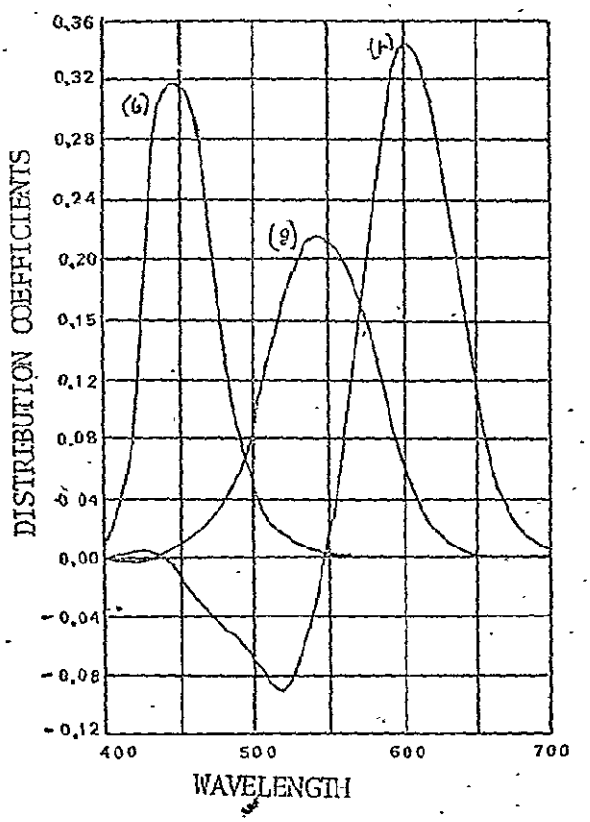

FIGURE 24: SPECTRAL DISTRIBUTION CURVES FOR THE CIE "STANDARD OBSERVER" AND MONOCHROMATIC PRIMARIES AT THE WAVELENGTHS 700, 546.1, and 435.8 NM (NEGATIVE VALUES INDICATE THAT COLOR MUST BE ADDED TO THE COLOR BEING MEASURED TO OBTAIN A COLORIMETRIC MATCH.)

will be encountered in reproducing colors whose dominant wavelengths lie close to the transmission peaks of the taking filters. However, in order to reproduce the colors of objects which reflect only dominant wavelengths associated with secondary colors yellow and cyan, it is necessary that there exist a wavelength overlap between the taking primaries as shown in Figure 25. That is, the overlap region between the

red and the green filter will yield the yellows and in similar manner, the overlap region between the blue and green filter will yield cyan color. The amount of overlap (in nanometers) indicates the spectral region in which the secondary colors can be reproduced. Fortunately, for true color reproduction, most colors in nature are composed of broadbands which cover a considerable wavelength range extending into wavelengths where the primaries transmit considerable amounts of radiation.

The reproduction of such secondary colors is also dependent on the camera exposure. Since the region of overlap does not possess the amplitude of transmission which the primary colors do, too short an exposure will render only the primaries visible. As the exposure time is increased, the secondary colors will become apparent.

In view of the foregoing, the image density on each of the multiband positives can now be related to the additive color image which they produce.

- Where the densities on all the multiband positives are equal, a condition of zero saturation exists. The image is a shade of gray (achromatic). This is due to the fact that the human eye sees equal amounts of blue, green and red, which are combined in the image as being white. The brightness or luminosity of the white color which is perceived depends on the total energy combined in the image.

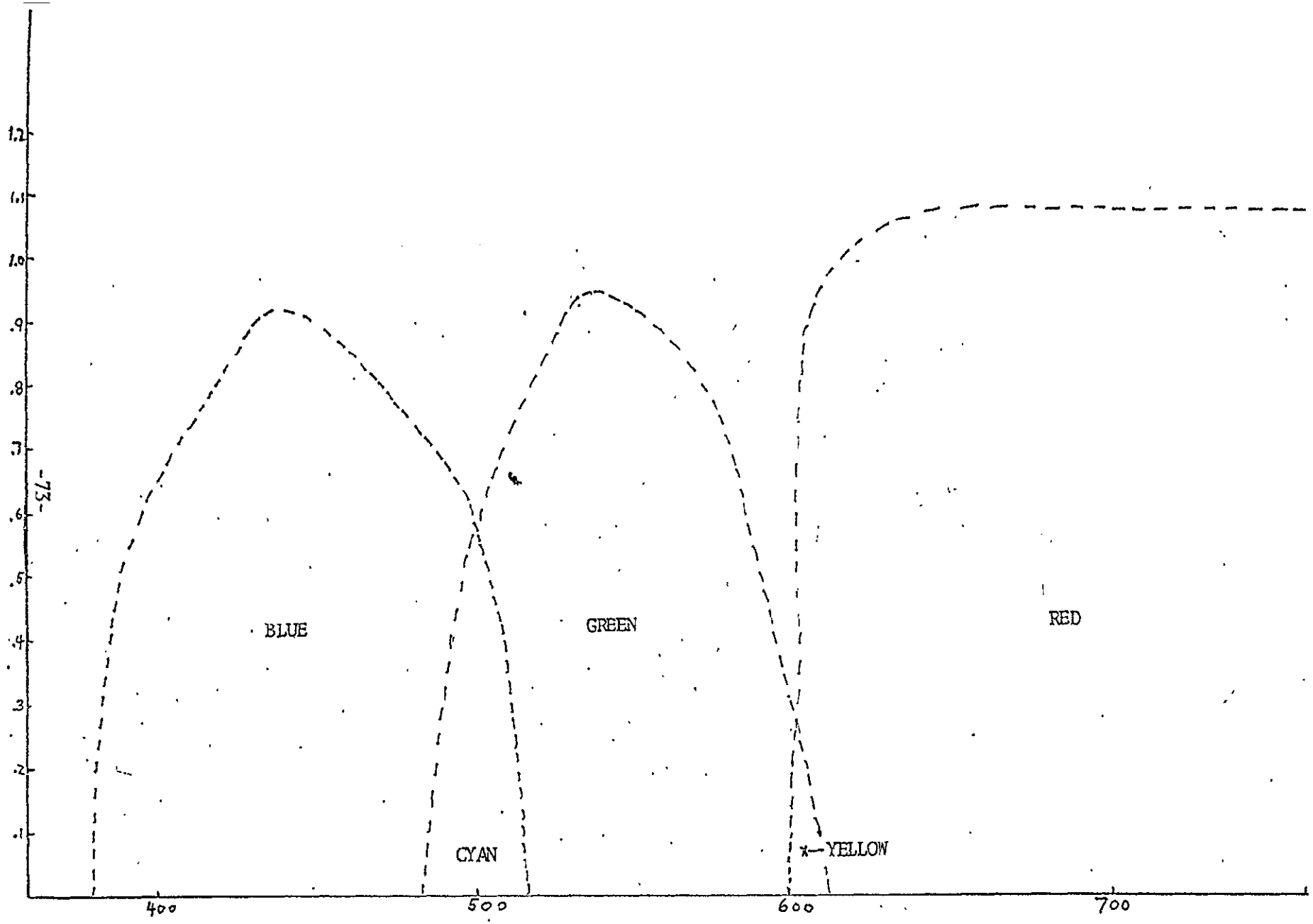

FIGURE 25: OVERLAP IN SPECTRAL TAKING FILTERS TO ACCURATELY REPRODUCE SECONDARY SPECTRUM COLORS OF CYAN AND YELLOW.

- The color of the image is a function of the ratio of the three colors which are projected to form it. Since the densities on each multiband photo are a logarithmic relation of the image forming energy, the chromaticity obtained is the weighted average of the three densities.

- The additive color image will faithfully reproduce the color of an object at a gamma of one. Increase in gamma above unity will increase the saturation of the image color above that of the object. Conversely, a gamma less than unity will decrease the saturation of the additive color image.

- The magnitude of the minimum density multispectral image establishes the brightness of the additive color image.

SECTION 4

REPROCESSING OF S065 MULTISPECTRAL PHOTOGRAPHY

In an additive color projection system, the color of an image appearing on the screen depends upon the image densities of the positives which are projected. When densities are equal in three positive images, and each is illuminated by an equal energy primary light source (blue, green, red), the screen image will be a shade of gray. This is due to the fact that the human eye sees equal amounts of blue, green and red light which are combined in the image as white. The brightness of this achromatic (colorless) image is dependent upon the magnitude of the three densities and the brightness level of the projection system.

When the densities in the three black-and-white images are unequal, the eye sees the composite screen image as a color. This color is a function of the ratio of the three densities. The hue, or dominent wavelength, is determined by the two lesser densities, and its saturation, is therefore increased by increasing the density differences existing between the black-and-white images which are projected.

The greatest possible color discrimination is achieved by expanding the density range of the areas of interest in each black-and-white image to correspond to the density range accommodated by the projection system. Investigation has shown that in the Long Island University Additive Color Viewer, densities over approximately 1.0 in one image will have no preceptible effect upon the color of the composite screen image which

is produced by the lower densities in the other images (Anderson 1968). This does not mean that all areas of interest in all three bands must have a density of less than 1.0. For example, in a photograph that includes both land and a water mass, the infrared negative will generally have very low density in the image of water, due to the absroption of infrared radiation by water. The density range in the land image of well processed green, red, and infrared positives will result in a water image density of over 1.0 in the infrared positive. In this case, any detail in the water image, as it appears on the screen, will come from the green and red positives. The color of the water image will generally be unaffected by the infrared positive.

While it is true that faithful color reproduction in an additive color projection system requires the gamma and density range of the three positives match each other, it assumes equal log exposure ranges in the three positives. As will be seen in the following analysis of a frame of multispectral photography, this assumption does not necessarily hold true in multispectral photography taken from orbit. As was evident from the previous example, the absorption of infrared radiation by water when combined with the large amount of infrared radiation reflected by most vegetation, results in a greater log exposure range in the infrared than either the green or red bands. The green band, on the other hand, typically has a shorter log exposure range than the red band. One possible explanation for this experimental fact is the increased atmospheric scattering of shorter wavelength radiation which is recorded in the

green band.

In view of the foregoing facts, the general requirements for S065 positives to be used for additive color projection are as follows:

1) a low base plus fog density, and the lowest possible minimum image density is necessary for the greatest possible screen brightness;
2) the density range of areas of interest within the image area must be relatively high, within the limitations of the projection system, for full color discrimination and saturation;
3) the overall image density, density range, and gamma, of the three positives should be matched to each other as closely as possible subject to the constraint imposed by log exposure range of each band. The best possible compromise should be achieved in view of the interpretative purpose of the additive color image.

The S065 release positives, as received, were not suitable for additive color projection because:

1) the image densities were too high, being usually above the usable range of the Long Island University additive color system;
2) the image densities were not matched to each other

in magnitude;

3) the density ranges were generally too small for full color discrimination and saturation.

Reprocessing Techniques

Selected frames of S065 multispectral photography were reprocessed. The steps taken in the reprocessing of each frame were as follows:

- the master positive of each band was contact printed, along with the pre-flight frisket exposed through the appropriate filter, to produce an internegative. Exposure and development were controlled to increase the density range of the areas of interest. A twenty-one step neutral density wedge was also included as a processing control.
- the internegative, including the negative image of the pre-flight frisket, was contact printed to produce a final positive transparency. Again, exposure and development were controlled to produce a transparency meeting the previously listed requirements, and a wedge was included as a process control. In some of the cases discussed elsewhere in this report, the internegatives and/or final positives were enlarged rather than contact printed. In these cases, scale was corrected to insure registration of the three images.

Each frame was individually reprocessed so that an additive color image optimized for an interpretative purpose would be produced. The reprocessing of frame number 3726, discussed below, is typical of the methods used for all the reprocessed SO65 multispectral photography.

Figures 26, 28, and 30 show the original "release" positive, internegative, and final positive along with the corresponding pre-flight frisket reproductions, for frame number 3726B (green band), 3726D (red band), and 3726C (infrared band). Because these images are in a different medium than the originals (paper prints rather than film transparencies), they have been printed in such a manner as to convey the visual appearance of the transparencies.

The graphs shown in Figure 27, 29 and 31 are the density versus original photometric log exposure of the pre-flight friskets (green, red and infrared) as reproduced in the master positives, internegatives, and final positives. The simulation filters (number 58, 25, and 89B) were not included in the calculation of these log exposure values. The conventional assumption of composite film and filter was used in preparing this data (Data Corp. 1969). The wedge step numbers are indicated on the log exposure scale in each case. The gamma values indicated in each figure are system gammas (that is, the gamma of the original wedge as it is reproduced in each generation) rather than process gammas (the gamma to which each generation is processed). The process gamma values of the three internegatives and final positives are listed in Table 3.

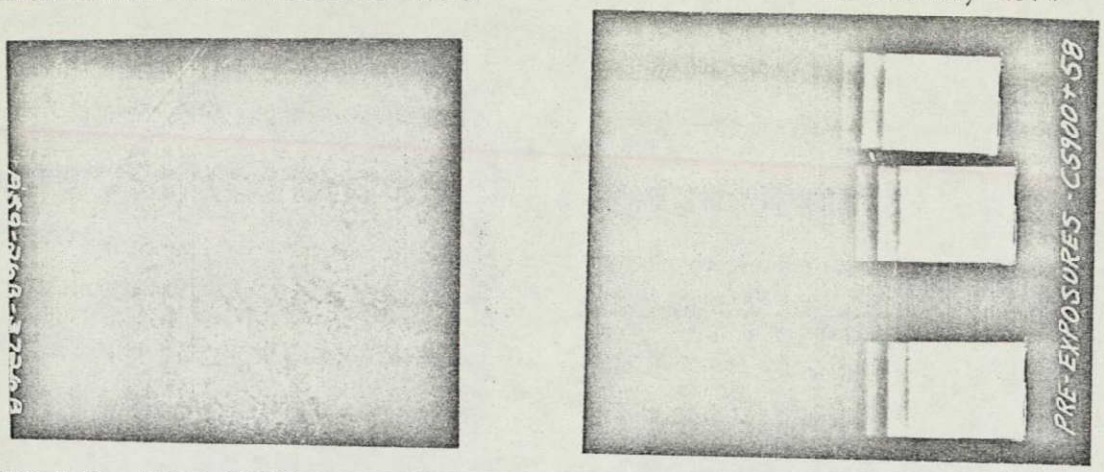

FIGURE 26A: SO65 FRAME 3726B(GREEN BAND) AND CORRESPONDING PRE-FLIGHT FRISKET AS RECEIVED.

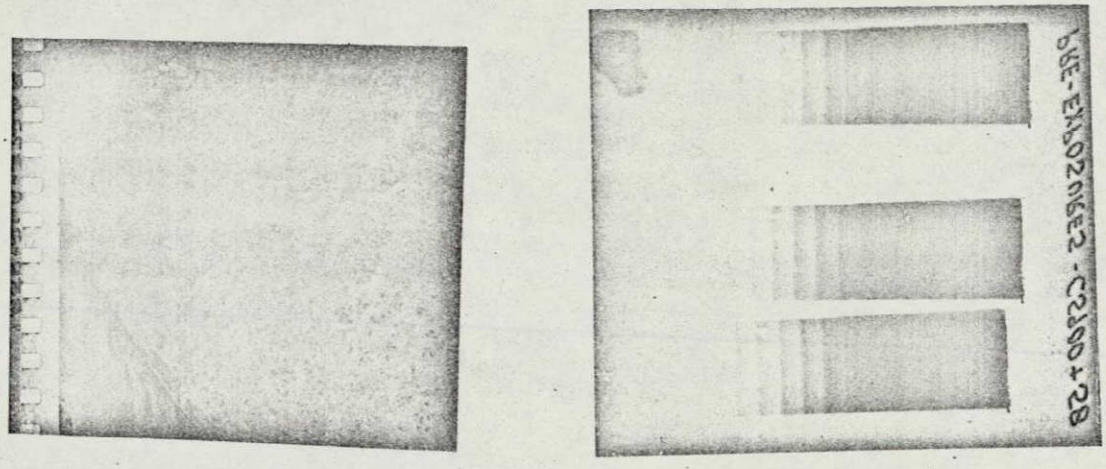

FIGURE 26B: INTERNEGATIVE STAGE OF REPROCESSED SO65 FRAME 3726B AND CORRESPONDING PRE-FLIGHT FRISKET.

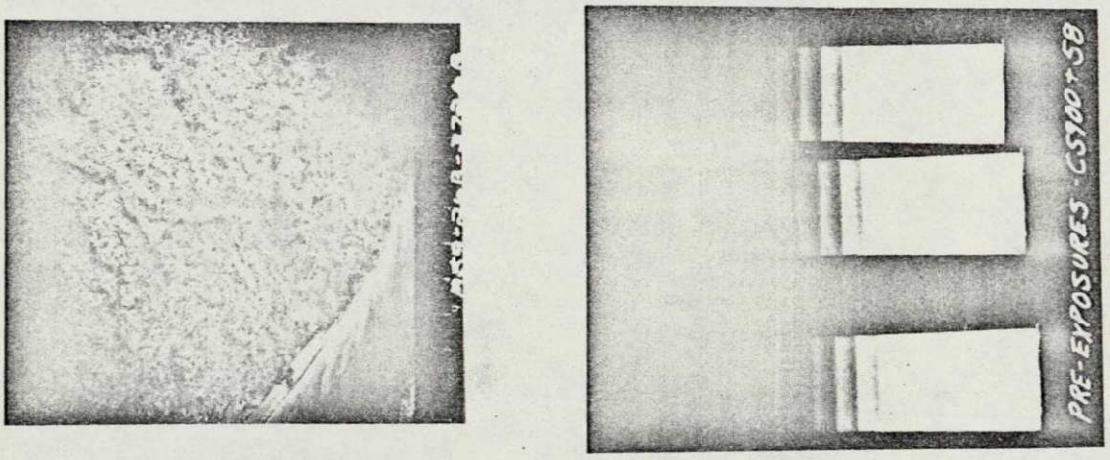

FIGURE 26C: FINAL POSITIVE STAGE OF REPROCESSED SO65 FRAME 3726B(GREEN BAND) AND CORRESPONDING PRE-FLIGHT FRISKET.

FIGURE 27 : PRE-FLIGHT FRISKET EXPOSED WITH #58 FILTER AS REPRODUCED WITH ORIGINAL POSITIVE, INTERNEG, AND REPROCESSED POSITIVE OF SO65 FRAME #3726B (GREEN BAND)

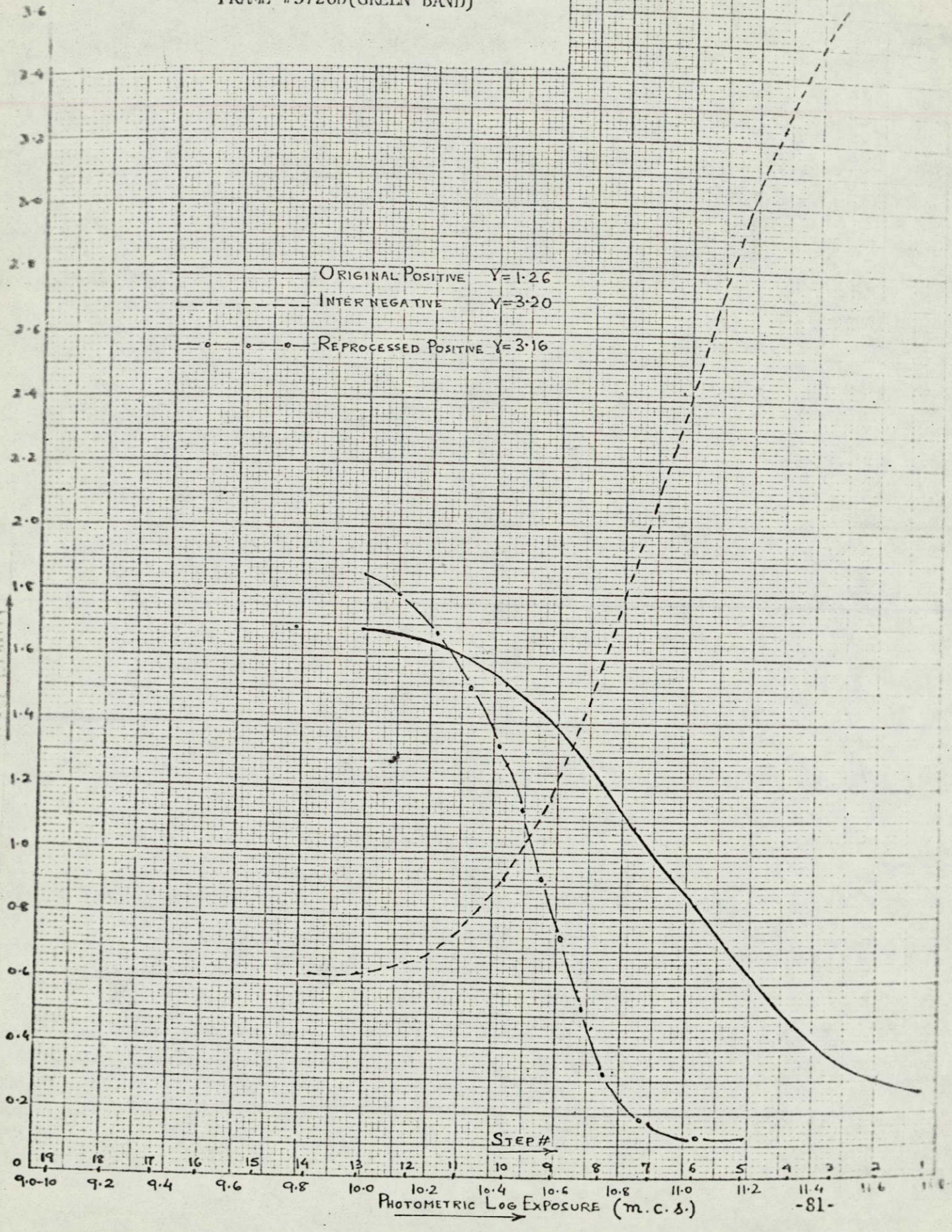

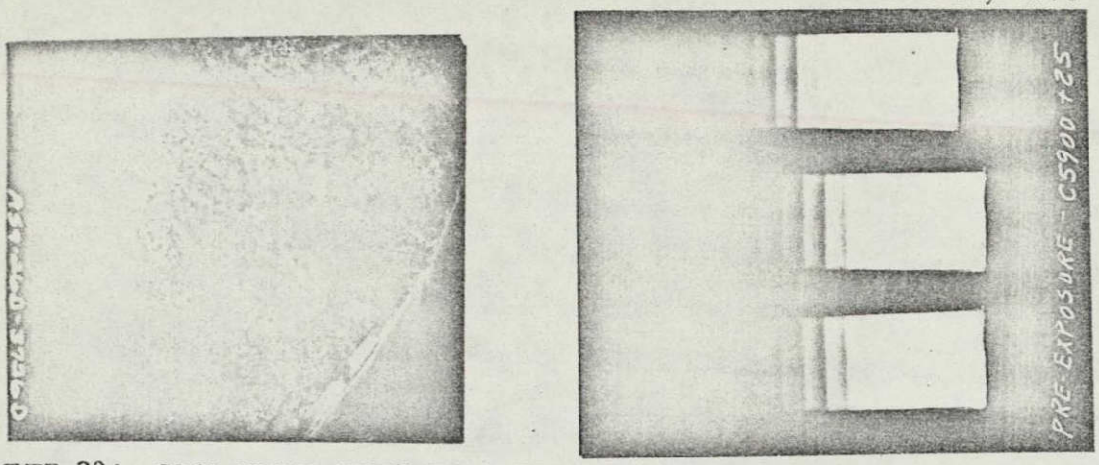

FIGURE 28A: SO65 FRAME 3726D(RED BAND) AND CORRESPONDING PRE-FLIGHT FRISKET AS RECEIVED.

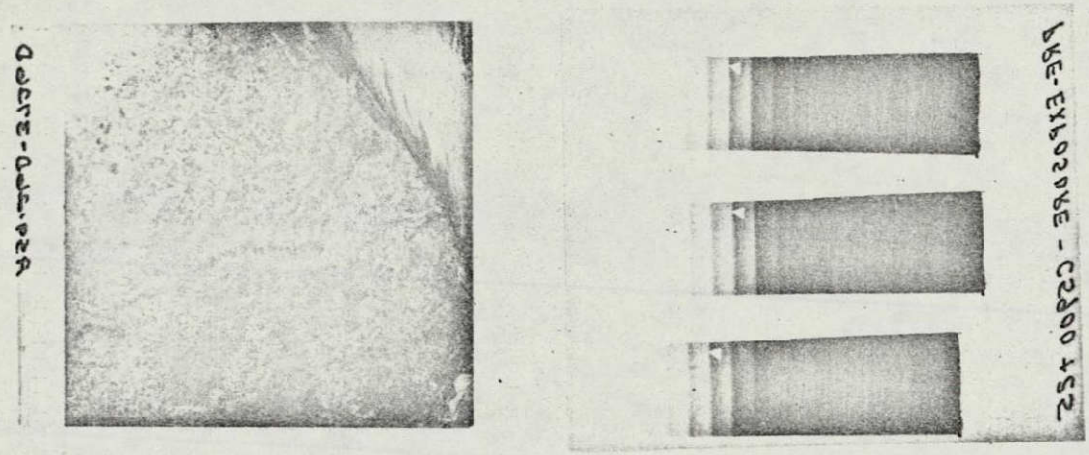

FIGURE 28B: INTERNEGATIVE STAGE OF REPROCESSED SO65 FRAME 3726D AND CORRESPONDING PRE-FLIGHT FRISKET.

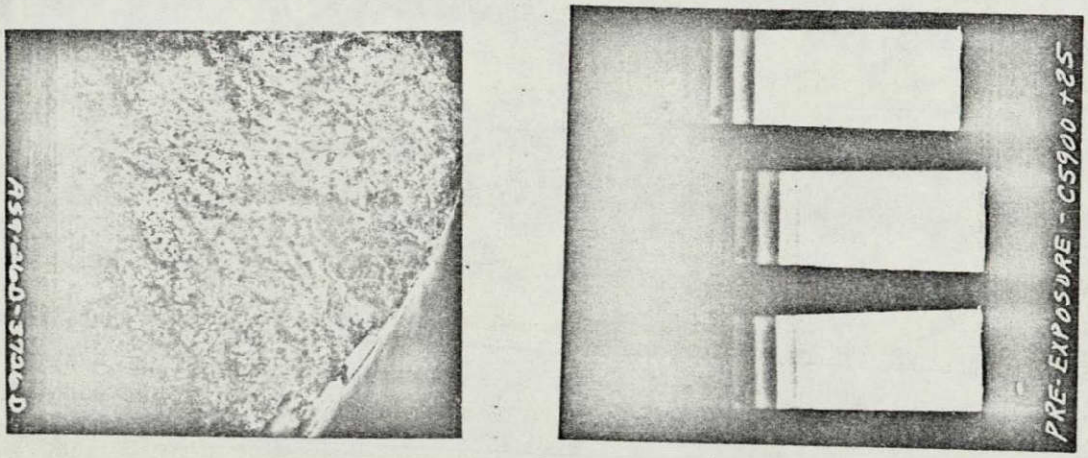

FIGURE 28C: FINAL POSITIVE STAGE OF REPROCESSED SO65 FRAME 3726D AND CORRESPONDING PRE-FLIGHT FRISKET(RED BAND).

FIGURE 29: PRE-FLIGHT FRISKET EXPOSED WITH #25 FILTER AS REPRODUCED WITH MASTER POSITIVE, INTERNEG AND REPROCESSED POSITIVES OF S065 FRAME #3726D (RED BAND)

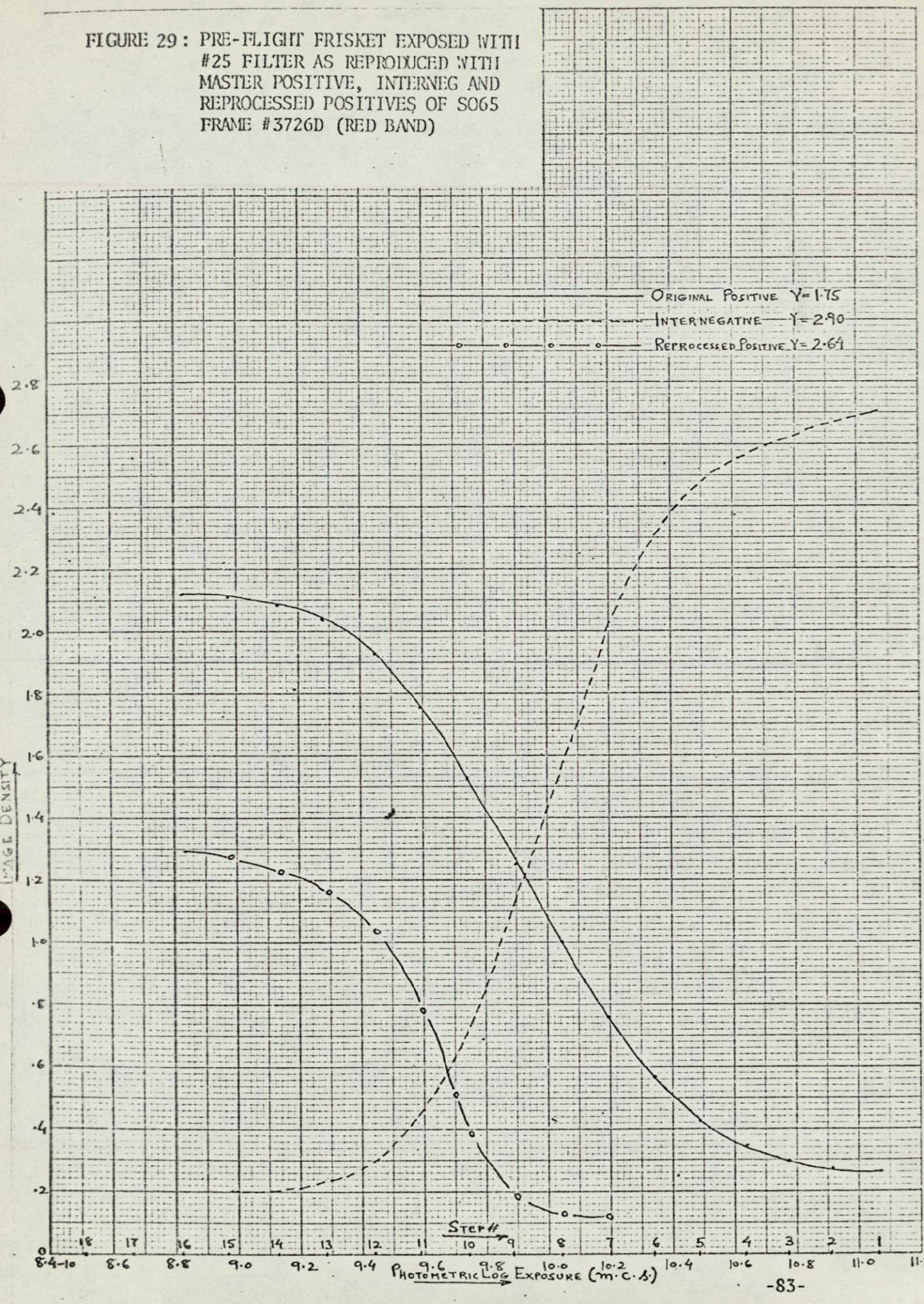

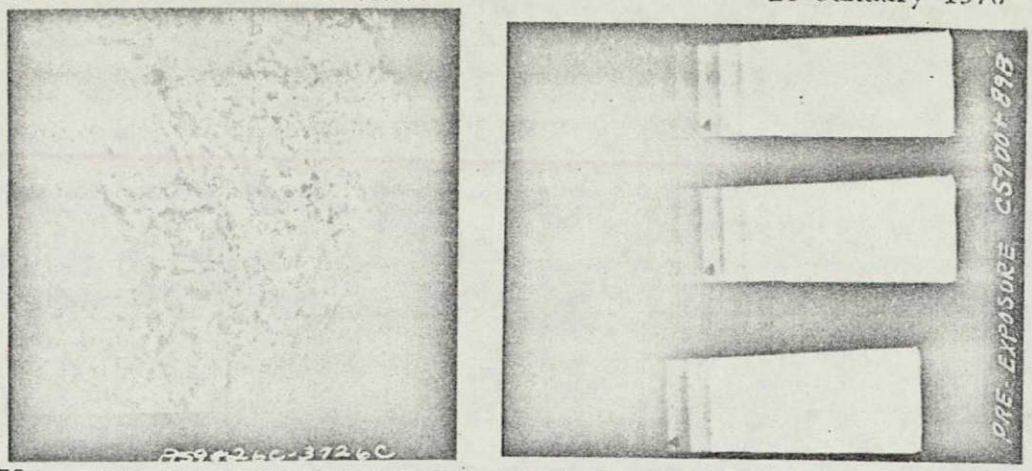

FIGURE 30A: SO65 FRAME 3726C(INFRARED BAND) AND CORRESPONDING PRE-FLIGHT FRISKET AS RECEIVED.

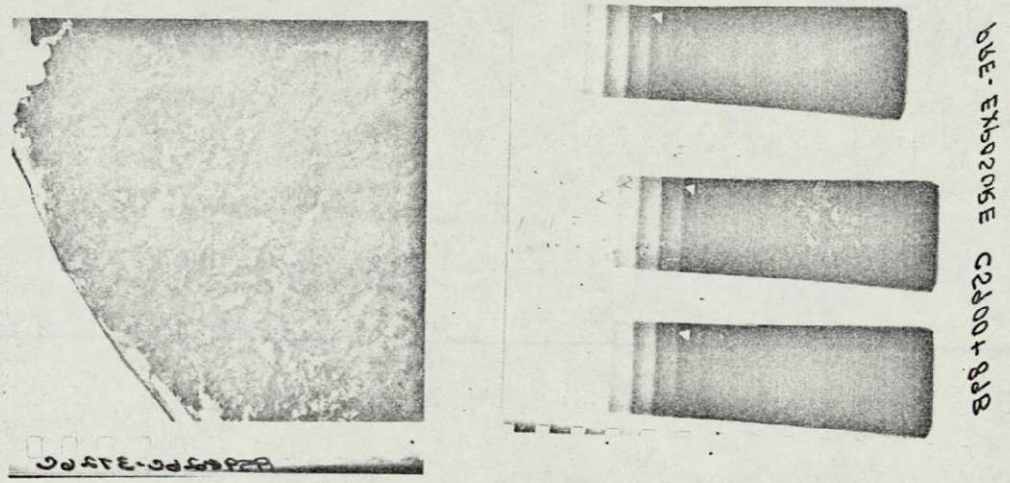

FIGURE 30B: INTERNEGATIVE STAGE OF REPROCESSED SO65 FRAME 3726C AND CORRESPONDING PRE-FLIGHT FRISKET

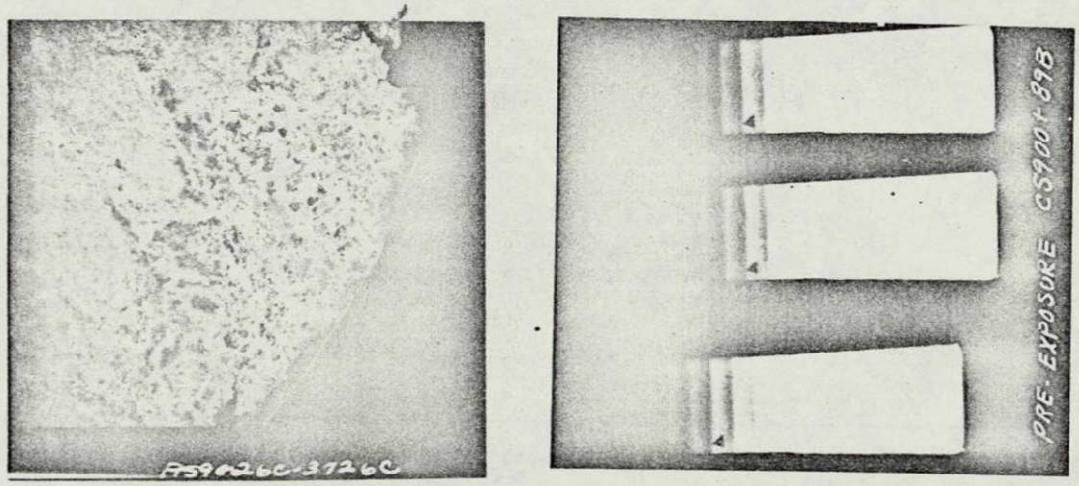

FIGURE 30 C: FINAL POSITIVE STAGE OF REPROCESSED SO65 FRAME 3726C AND CORRESPONDING PRE-FLIGHT FRISKET(INFRARED BAND).

FIGURE 31: PRE-FLIGHT FRISKET EXPOSED WITH #89B FILTER AS REPRODUCED WITH MASTER POSITIVE, INTERNEG AND REPROCESSED POSITIVE OF S065 FRAME #3726D (INFRARED BAND)

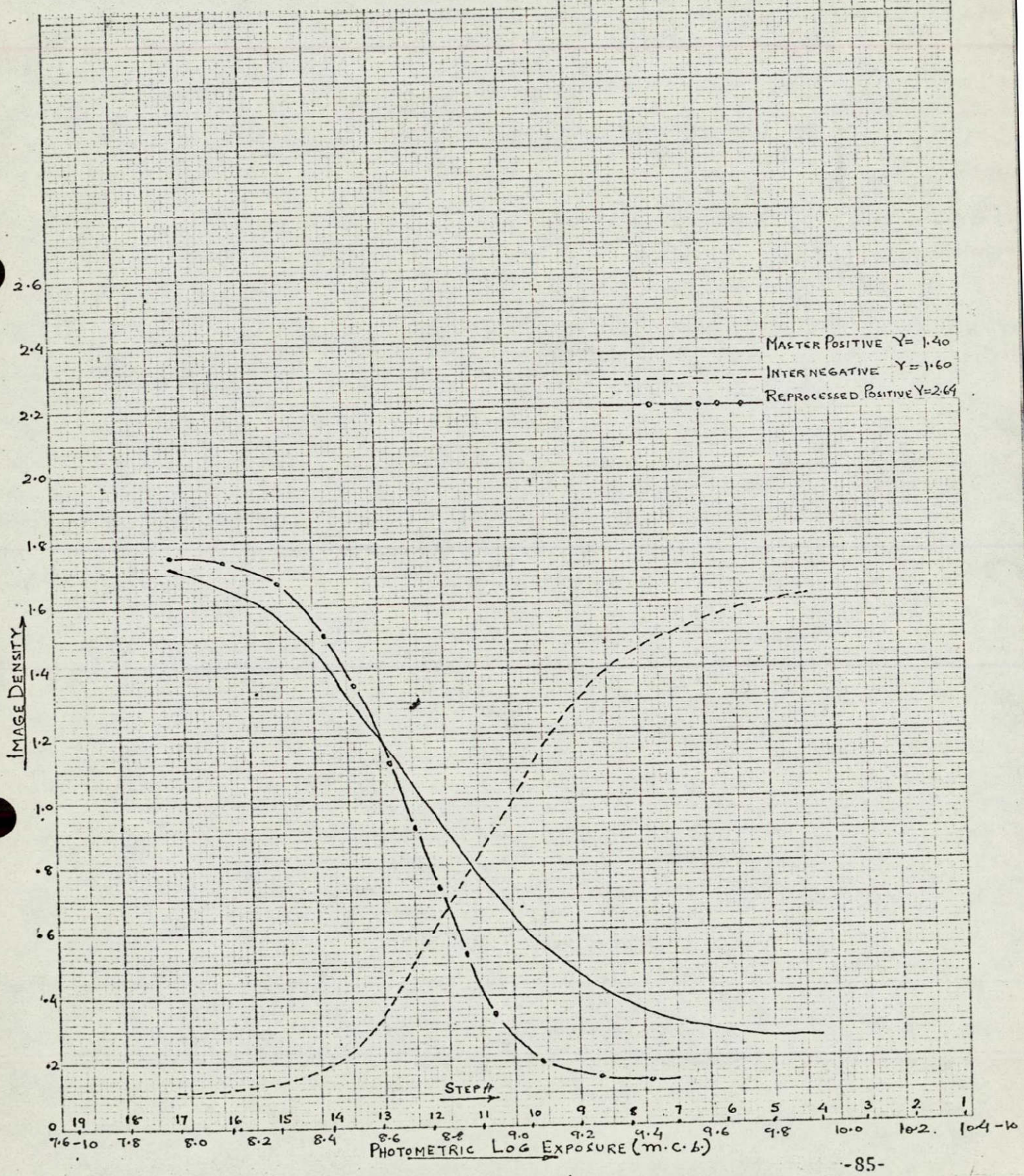

BAND	PROCESS γ OF INTERNEGATIVE	PROCESS γ OF FINAL POSITIVE
GREEN B (#58)	2.4	2.3
RED D (#25)	1.9	2.8
INFRARED C (#89B)	1.7	2.8

TABLE 3 : PROCESS GAMMAS OF INTERNEGATIVE AND FINAL POSITIVE STAGES OF REPROCESSING SO65 FRAME #3726.

Seven comparatively uniform areas of frame number 3726 were chosen for density measurements. These areas vary in brightness from comparatively deep water to relatively bright land areas. These areas are shown in Figure 32. All areas of interest are assumed to lie within the log exposure range represented by these areas. Brighter areas undoubtedly exist within the photograph, but they are too small or non-uniform to be read with the available one millimeter aperture Densitometer (MacBeth model TD 102).

The densities of these seven areas were measured in the master positive, internegative and final positive of each of the three bands. Each density was then located on the appropriate characteristic curve (Figures 27, 29 and 31) in order to determine the log exposure value that was required originally in order to produce that density in each generation. The density and corresponding log exposure values are listed in Tables 4, 5, and 6. Also included in these Tables are the

density range of areas of interest (ΔD), the corresponding log exposure range ($\Delta \log E$) of these areas, and the degree of movement along, the log exposure axis, of each area, between the master positive and the final positive (log E shift). This data is shown graphically in Figure 33. There the portion of the curves occupied by the areas of interest are shown for the master positive and final positive of each spectral band.

The significance of this data may be examined in several ways. An examination of Figure 33 graphically demonstrates the need for reprocessing the original S065 positives when additive color projection is to be used. In the green band, the magnitude of the image densities of areas of interest has been lowered to the usable range of the projection system (from minimum density of 1.35 to 0.41), and the density range has been expanded from 0.17 to 0.55. In the red band, the image minimum density has been lowered from 1.38 to 0.21 and the density range expanded from 0.58 to 0.89. In the infrared band, the image minimum density has been lowered from 0.70 to 0.26, and the density range expanded from 0.95 to 1.36. While the density ranges do not match numerically, it must be remembered that the upper density area of the infrared record represents water areas. It means merely that the additive image color of the water detail produced by the red and green bands will not be desaturated by the infrared record. It is significant that when only the land areas are considered (areas 4, 5, 6 and 7) in Figure 32, the density range becomes 0.23 for the green band, 0.34 for the red, and 0.38 for the infrared.

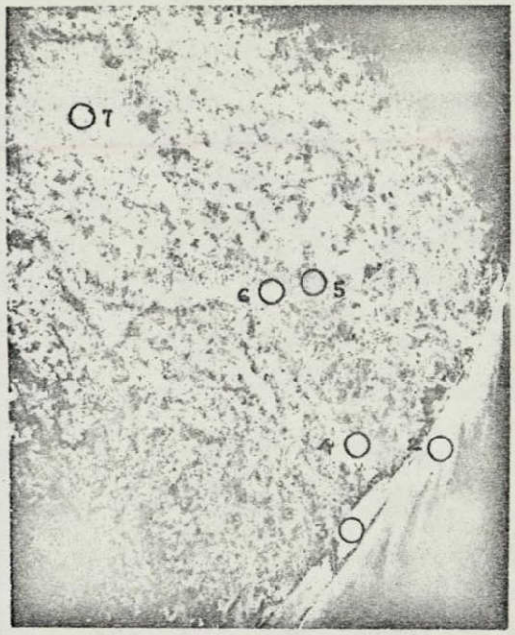

FIGURE 32: AREAS OF INTEREST CHOSEN FOR DENSITY MEASUREMENT IN S065 FRAME 3726

Some possible reasons for the difference in magnitude of the log exposure range of the areas of interest between the bands and any given generation have been discussed previously. These are:

- the compression of the log exposure range at shorter wavelengths, due to greater atmospheric scattering of the light at the shorter wavelengths;
- the expansion of the log exposure range in the infrared, due to the high absorption of infrared radiation by water, coupled with the high reflection of the infrared radiation by many types of vegetation.

The variation in log exposure range between generations of any one band, and the amount of log exposure shift of any area from original

	DENSITIES			LOG EXPOSURE (-10)			
	MASTER POSITIVE	INTER-NEGATIVE	FINAL POSITIVE	MASTER POSITIVE	INTER-NEGATIVE	FINAL POSITIVE	LOG E SHIFT
AREA 1	1.52	1.04	.96	10.44	10.51	10.54	+.10
2	1.36	1.40	.49	10.62	10.67	10.70	+.08
3	1.35	1.44	.41	10.63	10.69	10.72	+.09
4	1.38	1.38	.49	10.60	10.66	10.70	+.10
5	1.44	1.27	.64	10.54	10.62	10.64	+.10
6	1.36	1.49	.41	10.62	10.70	10.72	+.10
7	1.41	1.43	.44	10.57	10.68	10.71	+.14
ΔD	.17	.45	.55	Δlog E .19	.19	.18	

TABLE 4: IMAGE DENSITIES AND CORRESPONDING LOG EXPOSURE VALUES OF AREAS OF INTEREST IN SO65 FRAME #3726 (#58, GREEN BAND)

	DENSITIES			LOG EXPOSURE (-10)			
	MASTER POSITIVE	INTER-NEGATIVE	FINAL POSITIVE	MASTER POSITIVE	INTER-NEGATIVE	FINAL POSITIVE	LOG E SHIFT
AREA 1	1.96	.31	1.10	9.40	9.45	9.38	-.02
2	1.68	.66	.39	9.45	9.71	9.74	+.09
3	1.38	1.12	.21	9.83	9.89	9.87	+.04
4	1.52	.65	.34	9.75	9.71	9.77	+.02
5	1.74	.56	.68	9.60	9.66	9.64	+.04
6	1.54	.82	.35	9.74	9.79	9.95	+.01
7	1.50	.81	.36	9.76	9.78	9.74	-.02
ΔD	.58	.81	.89	Log E .43	.44	.49	

TABLE 5 : IMAGE DENSITIES AND CORRESPONDING LOG EXPOSURE VALUES OF AREAS OF INTEREST IN SO65 FRAME #3726 (#25, RED BAND).

	DENSITIES			LOG EXPOSURE (-10)			
	MASTER POSITIVE	INTER-NEGATIVE	FINAL POSITIVE	MASTER POSITIVE	INTER-NEGATIVE	FINAL POSITIVE	LOG E SHIFT
AREA 1	1.65	.16	1.62	8.14	8.34	8.35	+.21
2	1.60	.18	1.59	8.24	8.40	8.38	+.14
3	1.24	.38	1.12	8.56	8.62	8.63	+.07
4	.88	.77	.46	8.82	8.86	8.88	+.06
5	.97	.66	.64	8.75	8.79	8.81	+.06
6	.70	.98	.26	8.95	8.99	9.01	+.06
7	.89	.70	.56	8.81	8.82	8.84	+.03
ΔD	.95	.82	1.36	ΔlogE .81	.65	.66	

TABLE 6: IMAGE DENSITIES AND CORRESPONDING LOG EXPOSURE VALUES OF AREAS OF INTEREST IN SO65 FRAME #3726C(#89B, INFRARED BAND)

positive to final positive in a given spectral band, may be considered to be a measure of the photometric fidelity of reproduction during the reprocessing cycle. Perfect photometric fidelity would require that the log exposure range of each band be the same in the final positive as in the original positive, and that log exposure point of each area be the same in the final positive as in the original positive. Some possible causes of error which may be responsible for the deviations from this, other than the non-linearity limitations of the photographic process are as follows:

- any error in locating the same geographical area for density measurement in each image could lead to inaccurate density values;

FIGURE 33: MEASURED AREAS OF INTEREST AS REPRODUCED IN MASTER POSITIVES AND IN POSITIVE REPROCESSED FOR ADDITIVE PROJECTION (SO65 FRAME #3726)

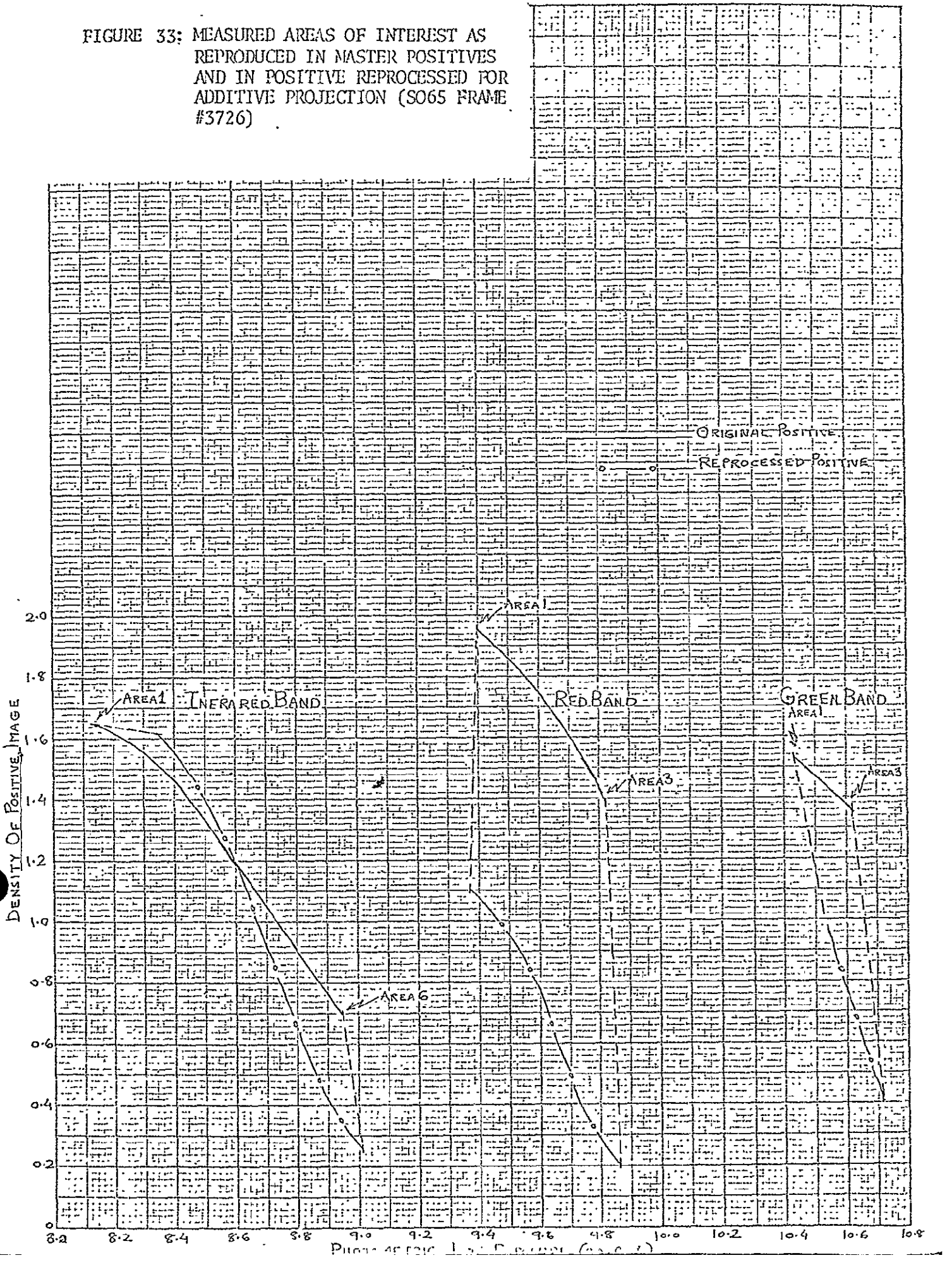

high density areas in the positive images, such as (deep water in Figure 32) in the red and particularly in the infrared bands, would have occurred near the base plus fog level of the original negative. The accuracy of corresponding log exposure values is questionable in this region, as a large log exposure difference results in a small density difference. It is significant to note that the log exposure range of the infrared band varies from 0.81 in the original positive to 0.66 in the final positive when all seven areas of interest are considered. If, however, only the land areas are considered (areas 4,5,6 and 7 in Figure 32), the log exposure range is a constant 0.20 in the original positive, the internegative and the final positive. Similarly, the log exposure range of the red band varies from 0.43 in the original positive to 0.49 in the final positive when all seven areas are considered. When the deep water area (area 1 in Figure 32) is exluded from consideration, the log exposure range is a constant 0.23 in all three generations.

This anlaysis of photometric fidelity is concerned only with the reprocessing cycle, from the original positive received from NASA, through the final positive used for additive color projection. An analysis of the photometric fidelity to the original negative would require density readings of these areas in the original negative.

SECTION 5

ANALYSIS OF MULTISPECTRAL ADDITIVE COLOR PHOTOGRAPHY FOR DETERMINING AGRICULTURAL LAND USE IN THE IMPERIAL VALLEY, CALIFORNIA

The Imperial Valley of California was used as a controlled test site in order to evaluate the utility of multispectral additive color photography for land use classification. Not only was excellent ground truth of the area available during the time of the Apollo 9 flight but also this agricultural unit is of considerable economic significance. The gross value of crop and livestock production exceeds $232 million of which $92 million are represented by field crops.

Two areas of the Valley were chosen for detailed analysis. Ground truth was available for both. Colorimetric analysis of 45 times enlargements of the SO65 multispectral additive color images showed that the classifications of vegetation, soil and surface water could be reliably made.

An analysis of the chromaticity of images of three crops (alfalfa, barley and sugar beets) on a post facto cross classification of crop type and image color indicated a 67% a posterari probability of correct classification. That is, image color was quantitatively associated with crop type two thirds of the time.

No significant relationship was found between image brightness and these land-use classifications. In general, the images of soils varied much more in brightness than vegetation. The greatest variability

in crop brightness was exhibited in the infrared image.

Some Geographical, Agricultural and Economic Characteristics of Imperial Valley, California

The Imperial Valley is an impressive monument to man's ingenuity. In just sixty years, a once dry and desolate desert has been turned into a half million acre agricutural area. This has been accomplished by diversion of water from the Colorado River in a network of canals. Several dams on the Colorado River provide a well controlled flow of water in the 80 mile long All-American Canal and through some 300 miles of smaller canals. Imperial Valley is now the largest single irrigated acreage in the Western Hemisphere. The gross value of crop and live stock production in 1968 exceeded $232 million.

The Imperial Valley, located some 220 miles southeast of Los Angeles and 60 miles west of Yuma, Arizona, was once partially submerged under the Gulf of California. In time the flow of the Colorado River built a vast dam of silt between the Gulf and the Valley creating the desert. A large portion of the Imperial Valley is below sea level, the Salton Sea being 235 feet below the Pacific Ocean. The mean temperature of the valley is 72.8°F with a mean January temperature of 53.4°F. The average humidity is 26%.

Today no single area in the world of comparable size produces as many beef-pounds as the Imperial Valley. The latest figures indicate that some 750,000 head of cattle pass through the feedlots and fields

of the Valley annually producing a cash flow of more than $73 million. Alfalfa, the richest of all livestock feed plants grows well on the irrigated farm land of the Valley all year long. Barley and milo (sorghum) are used as alternates to alfalfa. The value of all field crops (which includes sugar beets and cotton and a sprinkling of other crops) was valued at $92 million in 1968.

During certain parts of the winter, from 75 to 90% of all the vegetables Americans eat come from the Imperial Valley. Most of the Valley's produce is grown for immediate consumption--only a small portion is frozen or canned. Lettuce is the largest vegetable investment with more than 40,000 acres planted in 1968 which had a value of $34 million. This was more than one half the $66 million total value of all the Valley's vegetable crops in 1968.

Irrigation of vegetables was almost totally by the furrow method until the fall of 1965 when an estimated 1,500 acres were treated with sprinklers. The next season 7,000 acres were sprinkled and in 1968 an estimated 15,000 were under sprinkler irrigation. However, most all irrigation is still accomplished by either constant or intermittant flooding.

The problem of excess salt accumulation in the soil, which restricts the growth and germination of many crops, arises from the saline water table and from concentration of salt in the irrigation water. Control of the salinity in the soils of the valley is maintained by a network of sub-surface drainage tiles which facilitates leaching. More

salt is removed from the soils per unit time by constant flooding, a practice which is used in the higher land valued areas. However, since irrigation water is expensive, the usual practice is to achieve the maximum salt removal per gallon of water applied by using intermittant flooding techniques.

During the period from March 8 through March 14, 1969, extensive "ground truth" was collected in certain sections of the Imperial Valley by a joint University of Michigan and Department of Agriculture field team. The stated objectives of the ground data collection effort were to obtain identification of fields as to crop (or other condition) as well as per cent cover, height, row direction and other conditions which might affect the multispectral experiment. Because of the limited time available for ground data collection, every field was not visited. The ground truth data contains the disclaimer that vegetation heights and cover estimates were obtained from one observation point within each field and "may not be representative of height and ground cover conditions throughout each field". Interpretation of selected ground truth areas from low level aircraft photography showed that the ground truth appeared reasonably accurate, gross errors appearing in only a few instances (such as per cent cover in field 73). The reader is referred to University of Michigan Report 2264-7-X(1969) for the details of the ground truth (Spansail, et.al., 1969).

Characteristics of Apollo 9 Space and Underflight Multispectral and Color Photography--The Technique of Analysis

The cloud free conditions that existed at the time the set of four S065 photographs (frame #3799) was obtained on 12 March 1969 at 0828 Pacific Standard Time (1628GMT) afforded an excellent opportunity for the quantitative analysis of multispectral space photography. Since the Imperial Valley--Salton Sea area of California was covered in the photographs, the focus of attention was on agricultural land uses. These space borne multispectral and infrared color photographs were taken at an altitude of 129 miles while the sun angle was 30 degrees above the horizon.

In addition to the space photography, the following additional sources of data were available: 1) S065 color photography, 2) Long Island University underflight color, color infrared and multispectral photography, 3) University of Michigan ground truth.

The S05 photographic experiment coverage of this area was obtained on March 9, 1969 at1002PST(1802GMT) using Kodak color emulsion, special order 368(frame #3287). Multispectral photography was taken on 8 March 1969 at 1536 Pacific Standard Time(2336GMT) at an altitude of 14,000 feet above mean terrain level using the Long Island University multispectral camera. The ground truth was taken continuously during the orbit of Apollo 9 (Spansail, 1969). Figure 34 is an enlargement of the red frame of the set of multispectral photographs showing the Imperial Valley, All-American Canal, Mexican Border, Salton Sea, Chocolate Mountains, and

other geographic features of the area.

The first step performed in evaluating the suitability of the S065 photography for the determination of agricultural land use was to make enlargements of the two areas shown in Figure 35. These are denoted as Area I and Area II. Area I appearing in the three multispectral photographs was enlarged using a precision apparatus to obtain 15 times enlargements in positive form. Precise control was maintained over the reproduction of the density-exposure relationships in the images. These enlargements were made from reprocessed and photographically balanced multispectral photos (see Section 4). These fifteen times enlargements were placed in the additive color viewer. Since this instrument has a fixed three times enlarging capability, the resultant image on the viewer screen was 45 times the original photo scale.

A variety of false color renditions were created by manipulating the hue, brightness and saturation controls of the viewer. The resulting screen images were photographed in color transparency form. Selected images of fields were densitometrically measured on the color transparency and the chromaticity coordinates computed using two computer programs developed for the purpose. A similar technique was used for Area II except in order to obtain images of sufficient size, twenty-five enlargements were used. This produced a seventy-five times enlargement on the viewer screen, which was photographed and subsequently colorimetrically analyzed.

The S065 color infrared photograph and S05 color photographs were enlarged four times the original photo scale. They were, of course, pro-

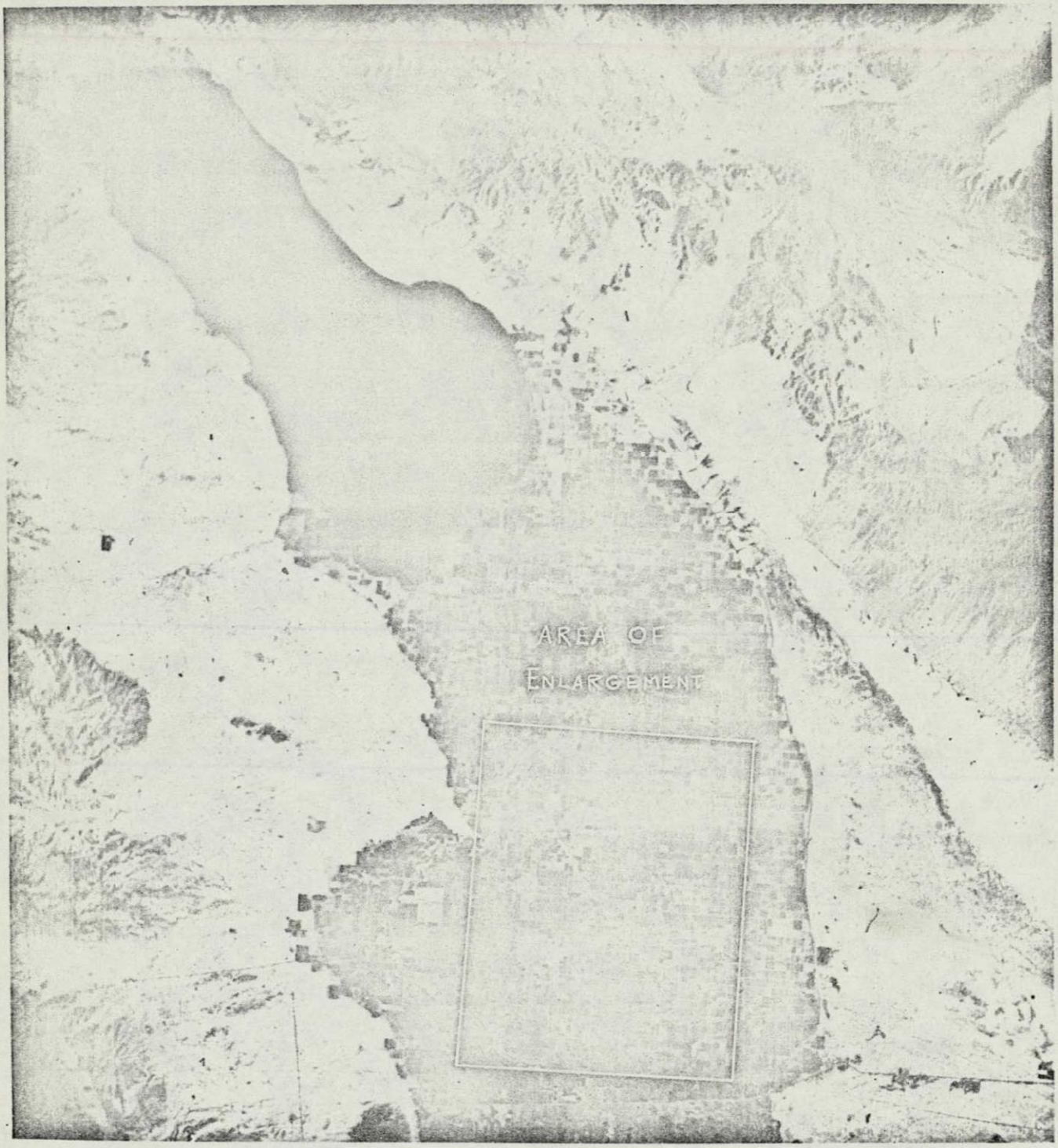

FIGURE 34: S065 RED BAND MULTISPECTRAL PHOTOGRAPH (FRAME #3799) SHOWING THE IMPERIAL VALLEY--SALTON SEA AREA OF CALIFORNIA. ANALYSIS WAS CONDUCTED IN THE ANNOTATED AREA, ENLARGED AREA SHOWN IN FIGURE 35.

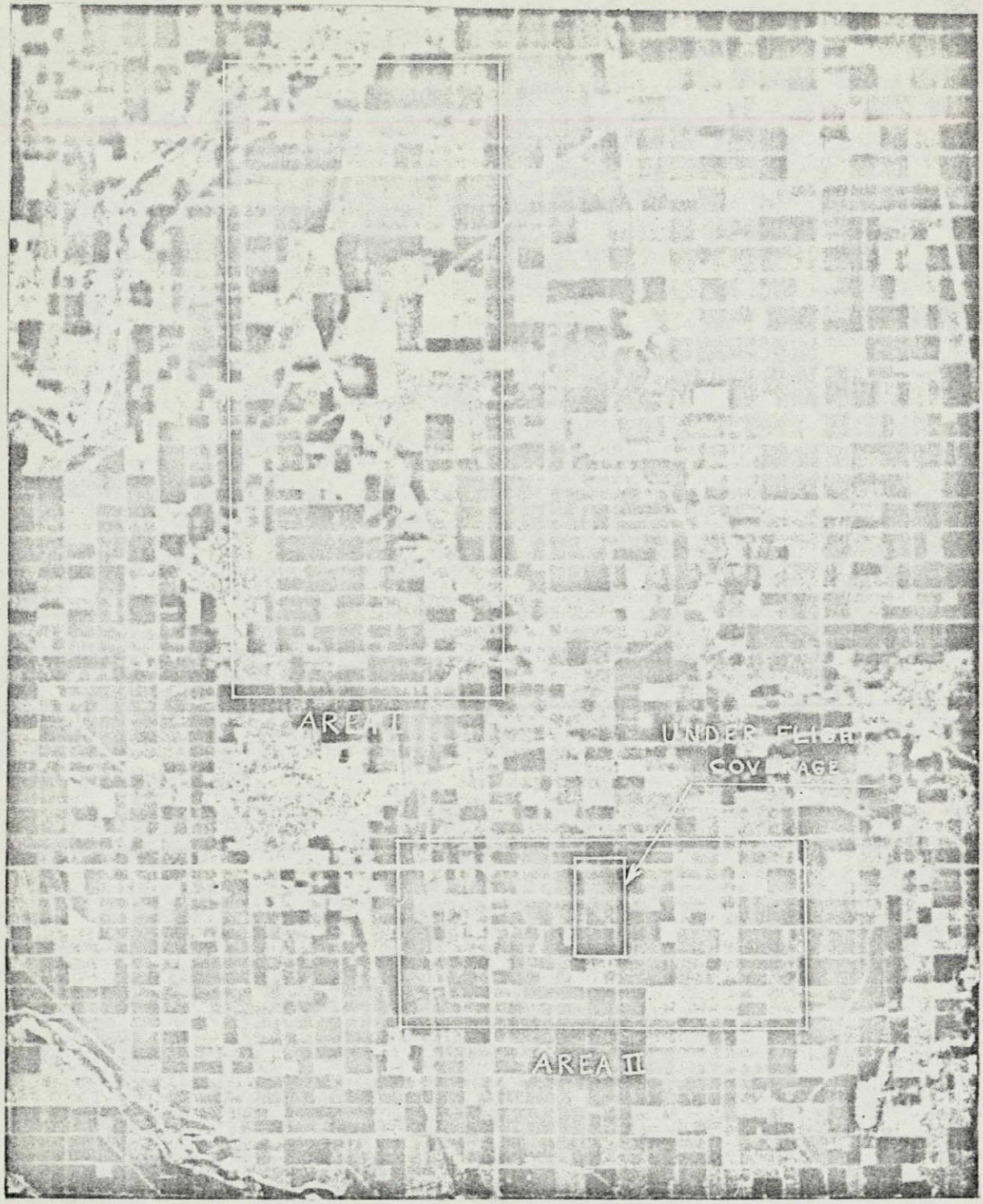

FIGURE 35: ENLARGED SECTION OF S065 MULTISPECTRAL FRAME #3709 SHOWING THE TWO AREAS OF THE IMPERIAL VALLEY WHICH WERE ANALYZED.

GRAPHIC NOT REPRODUCIBLE

duced in color transparency form. The highest precision was used in the reproduction process with the state-of-the-art. This procedure insured image units of sufficient size on the reproduced image to be measurable with the requisite spatial precision.

The Long Island University multispectral imagery was colorimetrically analyzed in the same manner as used for the S065 multiband photography. Color transparencies were reproduced from the viewer screen, densitometrically measured and chromaticity values determined using computer programs. Measurements of the underflight color and color infrared imagery were obtained by densitometric measurement in the duplicate photography supplied by NASA.

In all, over one thousand image measurements were made. In general, the sample size on each photographic rendition for each of the land use categories was between six and nine. The convex set containing all the measurements in each land use category was computed in the international standard CIE chromaticity diagram. The image catagories were classified on the basis of the 100% ground truth. Such a convex set (more properly called the convex hull) is a set of points such that when a line is drawn between any pair of points in the set, the entire line will also be in the set (Hadley, 1964).

The reader should note that the color space used is of a mathematical form based upon colorimetric theory. The distance between any two points in this space is <u>not</u> a measure of the perceivable color difference. The existance of a color space in which equal distances repre-

sent equal units of perceivable color is the subject of much debate in the literature (Mac Adam 1967).

The purpose of these measurements and associated computations is to define the relative capability of currently available color producing photographic techniques for classifying land use, crop type, soils and the presence of surface water. The intention is to determine the uniqueness of chromatic image characteristics in relation to the environment.

Figure 36 shows a multispectral color rendition of the Apollo 9 S065 multispectral photograph #3799. This area covers the Imperial Valley--Salton Sea region of California. This photographic rendition was made from the additive color viewer screen; the green band was projected as red, the red band projected as green and the infrared band as blue. Color measurements of images of fields for which one hundred per cent ground truth was available were made using similar color space as shown in Figure 36. These measurements are plotted in the chromaticity diagram in Figure 37. Note that the location of image colors relating to crop, soil and water categories plot in entirely different parts of the diagram. This indicates a unique association of image colors with these land use classifications. The data shown represent the convex hull of all points in each of the three catagories, vegetation, soil and water.

The second reproduction of a multispectral additive color image is shown in Figure 38. The green band has been projected as red, the

FIGURE 36: ADDITIVE COLOR RENDITION OF APOLLO 9 SO65 MULTISPECTRAL PHOTOGRAPH #3799 SHOWING THE IMPERIAL VALLEY--SALTON SEA AREA OF CALIFORNIA:

GREEN BAND PROJECTED AS RED
RED BAND PROJECTED AS GREEN
INFRARED BAND PROJECTED AS BLUE

SIGNIFICANT COLOR DIFFERENCES HAVE BEEN ACHIEVED BETWEEN CROPS AND PLOWED FIELDS AS SHOWN BY IMAGE CHROMATICITY VALUES.

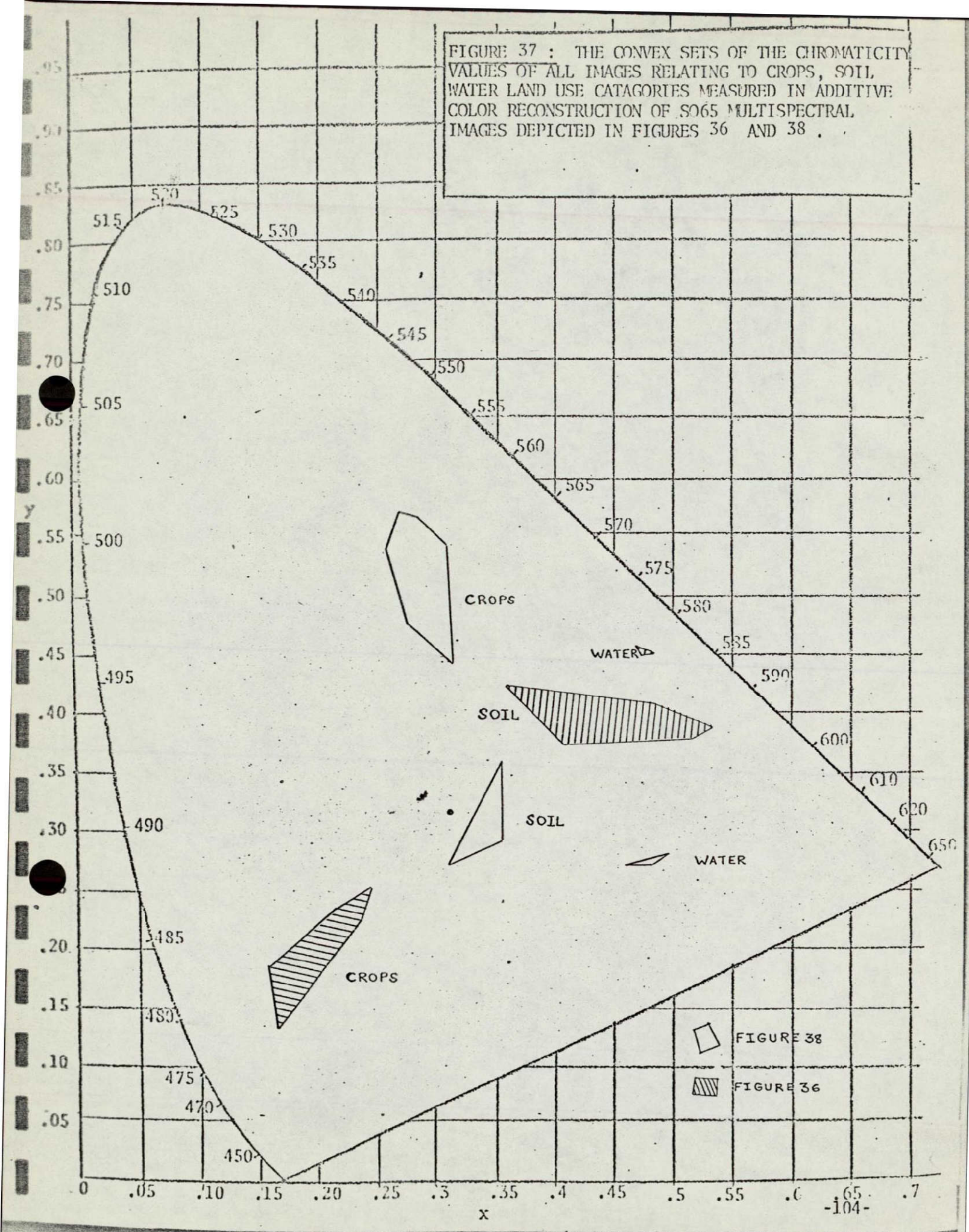
FIGURE 37 : THE CONVEX SETS OF THE CHROMATICITY VALUES OF ALL IMAGES RELATING TO CROPS, SOIL WATER LAND USE CATAGORIES MEASURED IN ADDITIVE COLOR RECONSTRUCTION OF SO65 MULTISPECTRAL IMAGES DEPICTED IN FIGURES 36 AND 38 .
520
515
525
530
535
540
545
550
555
560
565
570
575
580
585
590
600
610
620
650
510
505
500
495
490
485
480
475
470
450
CROPS
WATER
SOIL
SOIL
WATER
CROPS
FIGURE 38
FIGURE 36
.95
.90
.85
.80
.75
.70
.65
.60
.55
.50
.45
.40
.35
.30
.20
.15
.10
.05
0
.05
.10
.15
.20
.25
.3
.35
.4
.45
.5
.55
.6
.65
.7
x
y

FIGURE 38 : AN ADDITIVE COLOR RENDITION OF S065 MULTISPECTRAL PHOTOGRAPH #3799. THE PROJECTION COLORS HAVE BEEN ADJUSTED SO THAT: GREEN BAND PROJECTED AS RED, RED BAND PROJECTED AS BLUE, INFRARED BAND PROJECTED AS GREEN. THE COLOR DIFFERENCE BETWEEN VEGETATION, SOIL AND WATER IS SIGNIFICANTLY ENHANCED SO THAT NO COLOR OVERLAP EXISTS BETWEEN THESE LAND USE CATAGORIES.

red band has been projected as blue, and the infrared band as green. Again, as we would expect, the transformation of the color space yields categorizations of crop, soil and water which are unique for these three land use categories. As for the previous multispectral rendition, the convex hull of all measurements is shown in Figure 37. Note that there is large color separation between these three land use catagories.

Additive Color Analysis of Reprocessed S065 Photography--Area I

It was seen in the preceding paragraphs that land use classifications of soil, vegetation and water could be readily differentiated on a post facto basis. The wide chromatic separation evidenced by the chromaticity coordinates shown in Figure 37 showed that the α errors (identifying two images as belonging to different classification when actually they represent the same class of object) and β errors (saying two images relate to objects of the same classification when the objects are of different classes) would approach zero. This excellent ability to make these three land use categories is based on multispectral color as the only identifying image characteristic.

In all six additive color renditions constructed from the photography, these three land use categories were widely separated in image color. This, of course, implies that there exists separation of the density vectors in three dimensional space. Thus, on the reprocessed black-and-white S065 multispectral photography there exists density data in the images which allows soil, water and separation classification

using either photographic techniques or photometric techniques such as film scanning and computer processing of the resultant data.

A detailed colorimetric analysis was conducted of all the multispectral additive color renditions. One of these is shown in Figure 40 . In this rendition, the green band was projected as red, the red band as blue and the infrared band as green. This analysis showed the following:

1) There exists significant chromatic separation between crops, soil and water in the reprocessed S065 multiband photography when reconstructed in additive color.
2) There exists overlap between crop types alfalfa, barley and sugar beets in all additive color multispectral renditions.
3) The a posterari probability that these three crops growing on fields with 80% or greater ground cover will be correctly classified is 67%. This probability of correct classification is based upon a post facto definition of the convex sets containing image colors which are related to a unique crop type

The convex sets of each crop type and the overlap of these sets, as well as individual image chromaticity coordinates, are shown in

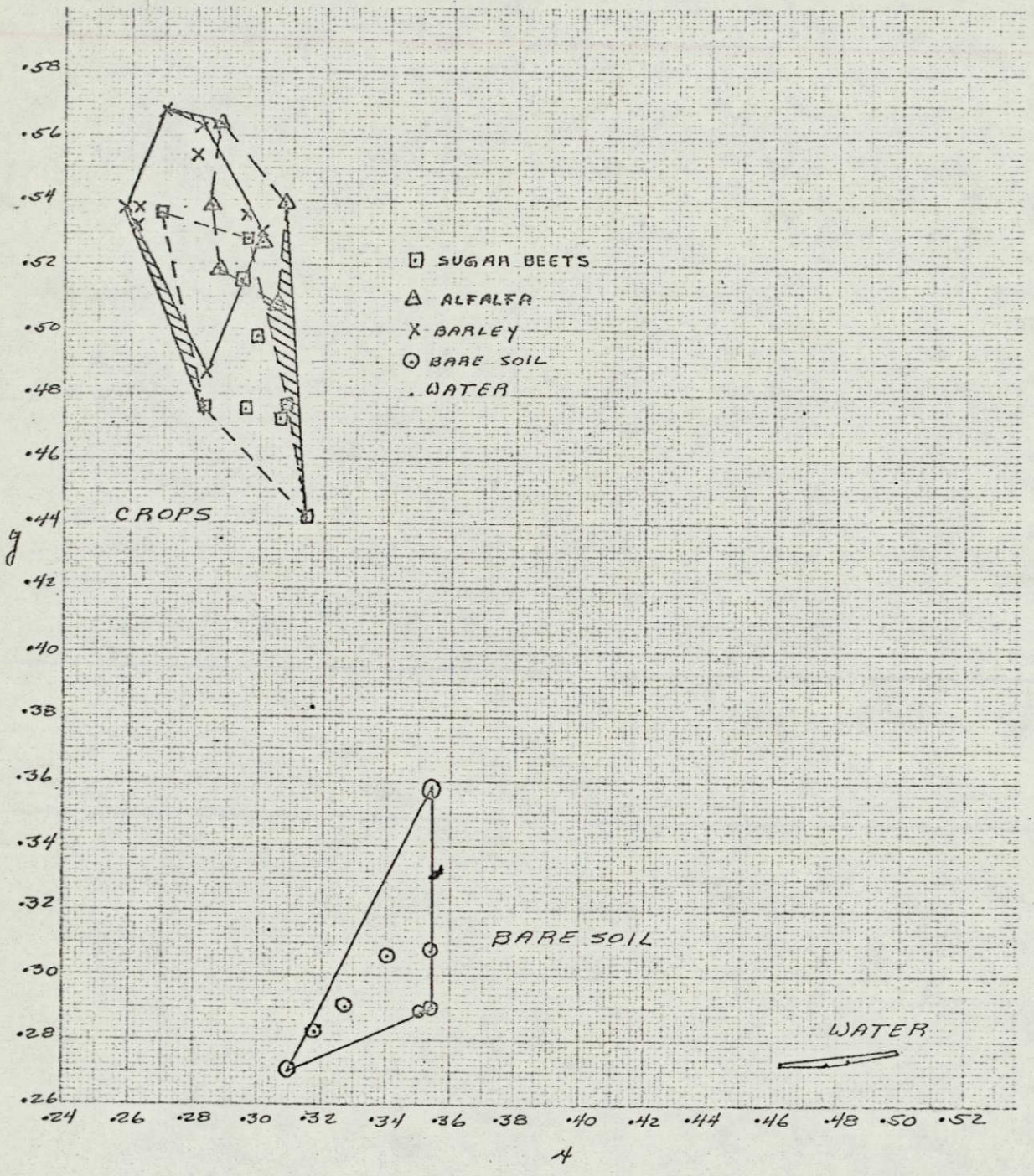

FIGURE 39: THE CHROMATICITY COORDINATES OF WATER, SOIL AND THREE CROPS (ALFALFA, BARLEY AND SUGAR BEETS) APPEARING IN S065 MULTISPECTRAL PHOTOGRAPH ON THE FOLLOWING PAGE.

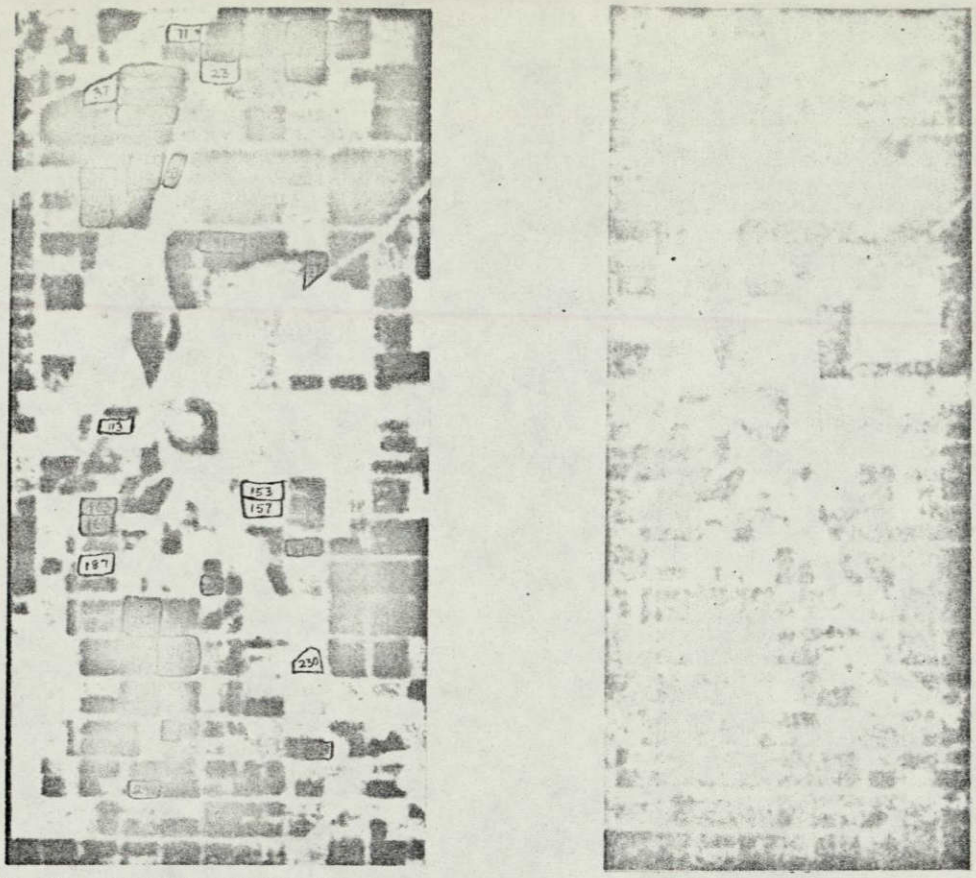

FIGURE 40: TWENTY TIMES ENLARGEMENT OF S065 MULTISPECTRAL FRAME #3799 SHOWN IN ADDITIVE COLOR WITH GREEN BAND PROJECTED AS RED, REND BAND AS BLUE AND INFRARED BAND AS GREEN.

LEGEND:

BARE SOIL			ALFALFA				BARLEY				SUGAR BEETS			
FIELD NOS	ROW DIR.	REMARK	FIELD NOS	ROW DIR.	CROP HEIGHT INCHES	% COVER	FIELD NOS	ROW DIR.	CROP HEIGHT INCHES	% COVER	FIELD NOS	ROW DIR.	CROP HEIGHT INCHES	% COVER
11	EW	BED. FOR COTT.	14		10-12	100	12	NS	18-24	95	52	EW	12-18	90
23	NS	PLOW.	15	EW	10-12	100	17	NS	18-24	100	53	EW	12-14	90
37	NS	BED FOR COTT.	22		10-12	90	19		18-24	100	66	EW	12-18	80
115	EW	BED FOR COTT.	39	NS	10-12	85	25	NS	18-24	95	77	NS	12-15	90
153		RECEN. PLOW.	50	EW	10-12	80	71		18-24	100	163	NS	12-18	90
157			299	NS	10-12	95	213	NS	18-24	95	164	NS	15-20	90
187	NS	BED. FOR COTT.					270	NS	18-30	95	174	NS	15-18	80
230	NS	BED.					279	NS	18-22	100	205	NS	13-18	80
											242	NS	8-20	80

Source: (Spansail, N., 1969)

Figure 39. The ability to correctly identify crop type as a function of multispectral image color is shown in Table 7 . This classification is based upon a tabulation of the location of each image point in each set. The correct identification of barley, alfalfa and sugar beets is based only on the chromaticity of the multispectral image. The definition of colors which pertain exclusively to a particular crop were made on a post facto basis.

The image colors which fell in each sub-set of the convex set of all crops is tabulated in Table 7 . For instance, sixty-seven per cent of fields containing barley fell in the convex set of all barley fields. Twenty-two per cent of barley was misclassified as alfalfa and eleven per cent was misclassified as sugar beets. The same analysis is shown for alfalfa and sugar beets.

Image Brightness Analyses

The brightness of the additive color images are shown in Figures 41 and 42. These analyses show that for any rendition:

1) No single correlation exists between image brightness and any crop or soil.
2) In general, the image brightness of soils is much more varied than the image brightness of crops (80% or better ground cover).
3) The greatest variation in image brightness of crops exists in the infrared band. This can be seen when the infrared band is projected as green, which is shown in Figure 41 and 42. This condition is generally

	TOTAL NUMBER OF IMAGE	NUMBER IN EACH SET	RATIO TOTAL # TO # IN EACH SET	A POSTE-RARI PROBABIL-ITY	
ALFALFA IMAGES IN THE FOLLOWING SETS:	6	--	--	--	--
ALFALFA(ONLY)	--	4	4/6	.67	CORRECT
BARLEY	--	1	1/6	.17	INCORRECT
SUGAR BEETS	--	0	0	0	INCORRECT
BARLEY & SUGAR BEETS	--	1	1/6	.17	INCORRECT
BARLEY IMAGES IN THE FOLLOWING SETS:	9	--	--	--	--
BARLEY(ONLY)	--	6	6/9	.67	CORRECT
ALFALFA	--	2	2/9	.22	INCORRECT
SUGAR BEETS	--	1	1/9	.11	INCORRECT
ALFALFA & SUGAR BEETS	--	0	0	0	INCORRECT
SUGAR BEET IMAGES IN THE FOLLOWING SETS:	9	--	--	--	--
SUGAR BEETS(ONLY)	--	6	6/9	.67	CORRECT
ALFALFA	--	0	0	0	INCORRECT
BARLEY	--	1	1/9	.11	INCORRECT
ALFALFA & BARLEY	--	2	2/9	.22	INCORRECT

THE A POSTERIORI PROBABILITIES OF CORRECT CROP CLASSIFICATION BASED ONLY ON IMAGE CHROMATICITY CHARACTERISTICS--S065 MULTISPECTRAL ADDITIVE COLOR RENDITION OF IMPERIAL VALLEY.

TABLE 7

attributed to the variation in the mesophyl reflection of leaves. The data in Figures 41 and 42 show that green and red sensitive bands display much less variability in the image brightness of vegetation.

4) The infrared band exhibits the greatest average image brightness. The green band exhibits the next greatest brightess with the red band the least. The reduced brightness of crops in the red band is undoubtedly due to the chlorophyll absorption at 680nm.

Recapitulation of The Techniques Used

Precision photographic techniques were used to reproduce the enlargements of Area I of the Imperial Valley using S065 black-and-white Frame #3799. A specially adapted Omega enlarger was used to make the necessary positive transparencies. Special photographic sensitometric controls were used to insure that high fidelity tone reproduction was maintained in the enlarging process. Color transparencies were made of the additive color image as it appeared on the viewer screen. Since a three times enlargement exists in the additive color viewer, the photo scale on the viewer screen was 45 times that of the original S065 photography.

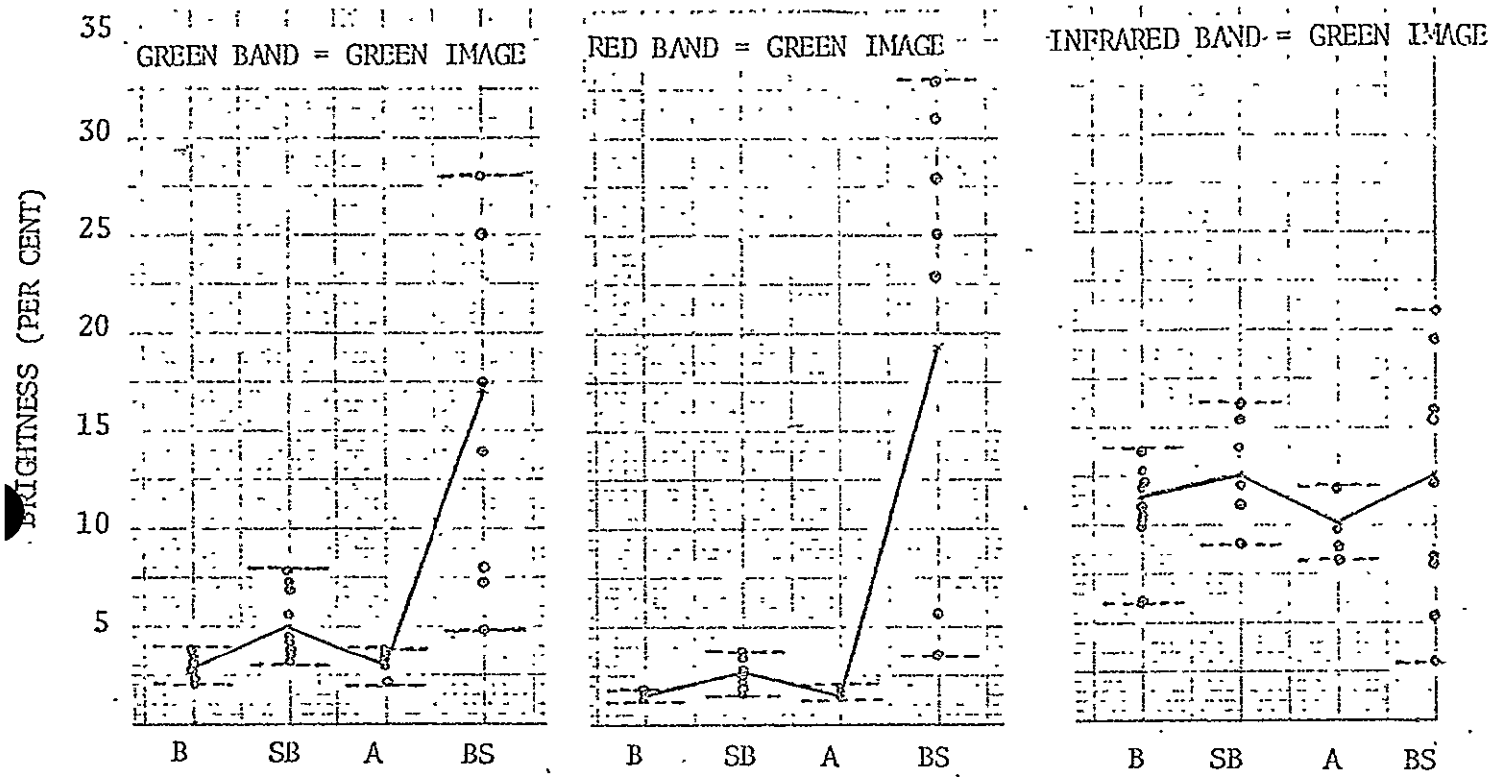

FIGURE 41: IMAGE BRIGHTNESS OF ALFALFA (A), BARLEY (B), SUGAR BEETS (SB), AND BARE SOIL (BS), IN THE GREEN, RED AND INFRARED BANDS WHEN DISPLAYED IN ADDITIVE COLOR

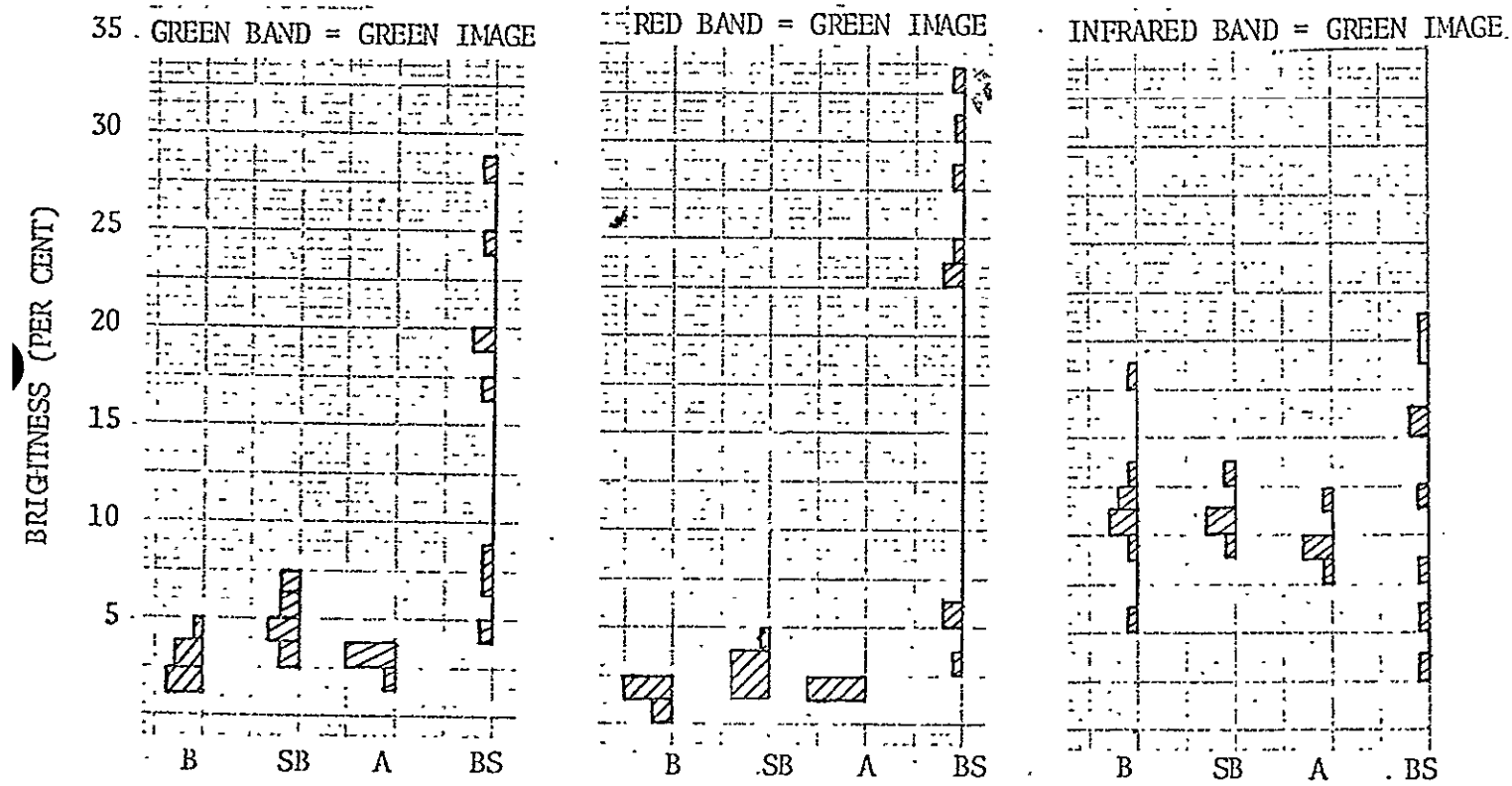

FIGURE 42: HISTOGRAM DEPICTING THE DISTRIBUTION OF IMAGE BRIGHTNESS OF ALFALFA (A), BARLEY (B), SUGAR BEETS (SB), AND BARE SOIL (BS) IN THE GREEN, RED AND INFRARED BANDS WHEN DISPLAYED IN ADDITIVE COLOR.

The color reproductions made with high speed Ektachrome Type B were sensitometrically controlled in processing to produce the best color transparencies within the state-of-the-art. In the photographic reproduction, the scale was reduced to twenty times the scale of the original S065 photography.

The six possible primary color spaces were analyzed in terms of their CIE coordinates, three of which are reproduced in this report.* These color values were computed from per cent transmission measurements made on the transparencies by using two computer programs developed specially for this purpose. Thirty-three fields were measured: nine barley fields, nine sugar beet fields, six alfalfa and eight bare soil, one water (four measurements). The fields were chosen based on the homogenous quality of their image on the color transparencies. The numbers of the fields exhibiting a homogenous image for which ground truth was available are shown in Figure 40.

A detailed examination of the color and brightness of the thirty-two fields was performed. Brightness is the third vaiable of color. The brightness of each of the three renditions (not ground object brightness) was analyzed using the green band approximation to the brightness function. The green filter used in making these measurements approximates quite well the brightness function of the human eye as can be seen from the graph on the following page. The distribution of approximate image brightness of each crop and bare soil is given in Figure 41 along

*There are 3! permutations of the blue, green and red primaries.

with a histogram of the distribution of brightness values (Figure 42).

SECTION 6

COMPARATIVE COLORIMETRIC ANALYSIS OF S065 MULTISPECTRAL ADDITIVE COLOR AND INFRARED SUBTRACTIVE COLOR IMAGES

A colorimetric analysis was undertaken to compare the chromatic characteristics of current state-of-the-art additive and subtractive false color image forming techniques. Images of soil, water and crops (alfalfa, barley and sugar beets) appearing on S065 frame #3799, Imperial Valley, California, were measured using three distinctly different methods of producing color images. The focus of attention was not only the capability to uniquely associate image color with vegetation, soil and water land use catagorizations but also the ability to differentiate between individual crops.

The first image analyzed was an additive color enlargement of S065 frame number 3799 with the green band projected as blue, the red band projected as green and the infrared band projected as red. Area I of the Imperial Valley was selected (see Figure 35). The choice of viewing filters used in projection simulated the response of color infrared film. The image on the viewer screen was forty-five times the scale of the original S065 photography. The crop, soil and water images were then compared with a four times enlargement of the associated S065 color infrared photograph. The third comparison made was conducted using a set of black-and-white separation positives made from the S065 color infrared photo and placed in the additive color viewer; the chro-

maticity measurements were made from a photographic reproduction of the additive color image as it appeared on the viewer screen.

Thirty-seven different images were measured on each of these three renditions. Identical replications were made (i.e., the same images were measured on each rendition). Twenty-four different fields of crops were measured consisting of six (6) alfalfa, nine (9) barley and nine (9) sugar beet fields. Nine (9) different plots of bare soil were measured. The one large ground area which contained water was measured in four (4) locations.

The reader should note that identical areas were compared on:

1) an enlargement of the S065 multispectral additive color rendition with the green band projected as blue, the red band projected as green and the infrared band projected as red;
2) a four times color enlargement of the color infrared of S065 frame #3799;
3) color separations made from the S065 color infrared photo enlarged four times and reconstructed on the additive color viewer screen.

The largest convex sets containing each of the four different land use categories was determined for each of the three crops as well as for soil and water. The number of image points in each set and intersection of sets was determined graphically. These convex sets represent an after-the-fact (a posteriori) classification of alfalfa,

barley, sugar beets, bare soil and water. It will be seen by examining the associated chromaticity diagrams, that for each of the three renditions analyzed, unique separation of soil, water and crops was achieved. That is, the convex sets of chromaticity coordinates for these general catagories were disjoint. This implies 100 per cent (a posteriori) correct classification of crops, soil and water.

A measure of the separation of the soil, crop and water convex sets is given in the large chromaticity diagram associated with each of the three image producing techniques which have been analyzed. The significant chromatic separation which exists implies that it is possible, and indeed highly probable, that correct classification based upon before-the-fact (a priori) definitions of image color can be achieved. That is, an area of the chromaticity diagram can be assigned to the image color of all objects of a particular class, say bare soil. When an image falls in this area of the CIE diagram, it is classified as bare soil. The effectiveness of this methodology of classifying objects by image color of course depends on the precision reproducibility of the color by the image forming systems used.

Color Analysis of the SO65 Additive Color Rendition

Figure 43 graphically depicts the wide color separation between crops, soil and water in the multispectral additive color rendition shown in Figure 44. Figure 45 shows the convex sets of the images of individual crops, alfalfa, barley, and sugar beets. These data were

obtained by computation from density measurements of a color transparency made of the multispectral additive color image which appeared on the viewer screen. This reproduction is shown in Figure 44. Note there is an overlap between the crop types. In general, it can be seen that a saturation difference exists between sugar beets and barley. Barley is the more saturated, with a dominant wavelength of 612nm. Alfalfa has a slightly higher dominant wavelength approximately 616nm and an intermediate saturation between the other two crops.

The possibility of correct classification based on an after-the-fact definition of image color has been computed and is shown in Table 8. This tabulation indicates that there exists a 50% a posteriori probability of correct classification of alfalfa and a 78% probability of correct classification of both sugar beets and barley. This classification is based upon the number of image measurements falling in the various convex sets shown in Figure 45 which has been established post facto based on knowledge of the object represented by the image. Achievement of such high probabilities of correct classification before-the-fact (a priori) by image color requires a high degree of color reproducibility in the image forming process.

Characteristics of The S065 Subtractive Color Infrared Image

Figure 47 shows the reproduction of the S065 color infrared frame #3799. Measurements of the same images discussed above again indicate that the color catagories of soil, crops and water are uniquely separated

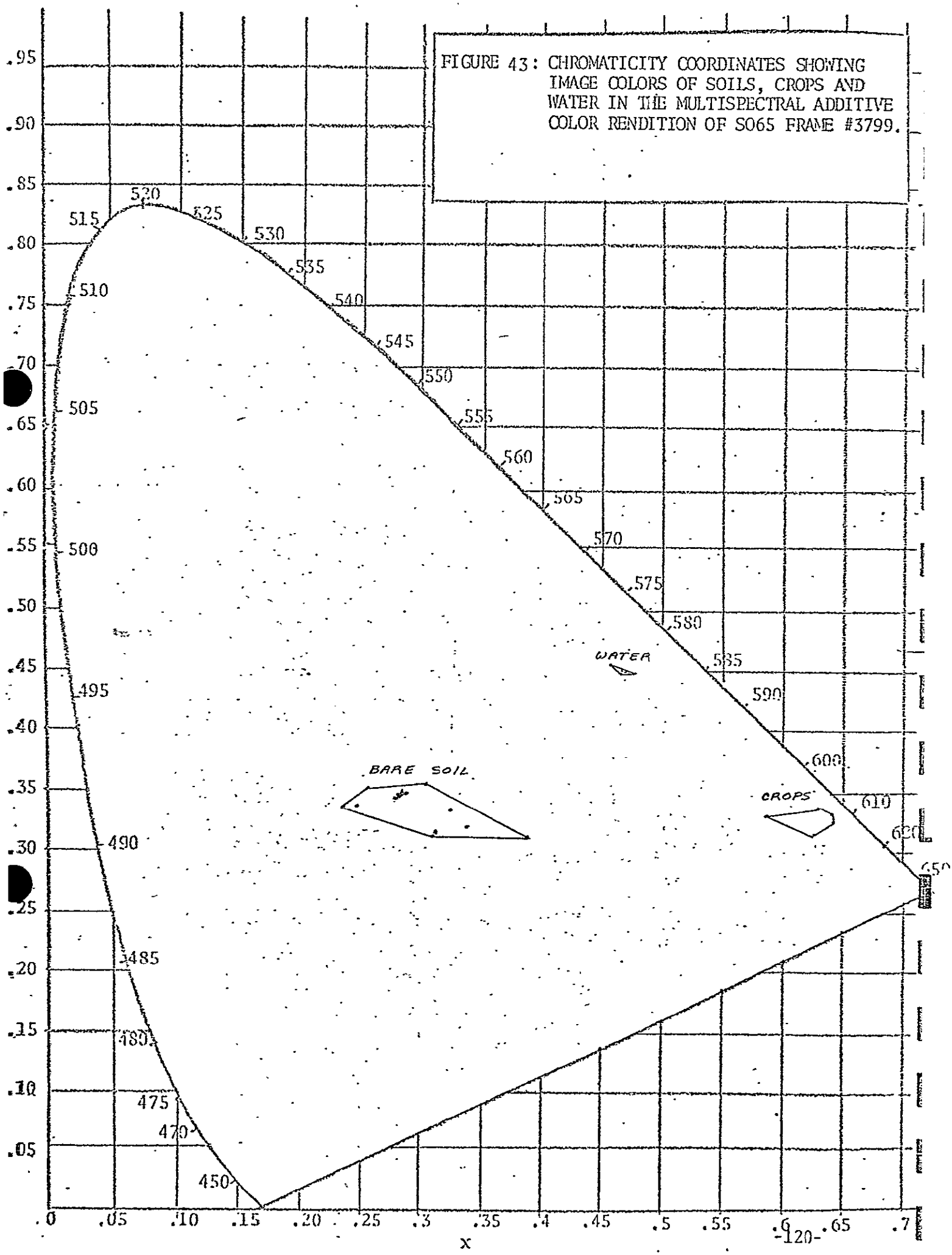

FIGURE 43: CHROMATICITY COORDINATES SHOWING IMAGE COLORS OF SOILS, CROPS AND WATER IN THE MULTISPECTRAL ADDITIVE COLOR RENDITION OF S065 FRAME #3799.

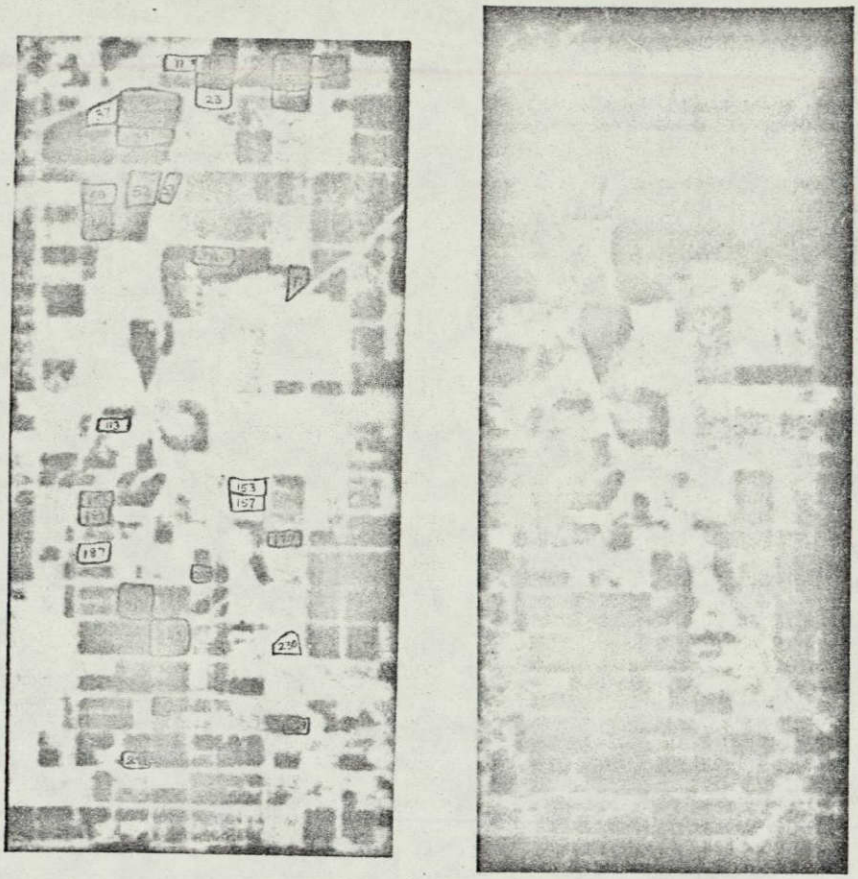

FIGURE 44: ENLARGEMENT OF S065 ADDITIVE COLOR MULTISPECTRAL RENDITION OF S065 FRAME #3799. GREEN BAND PROJECTED AS BLUE, RED BAND AS GREEN AND INFRARED AS RED. (FOR LEGEND OF FIELDS MEASURED SEE PAGE 109)

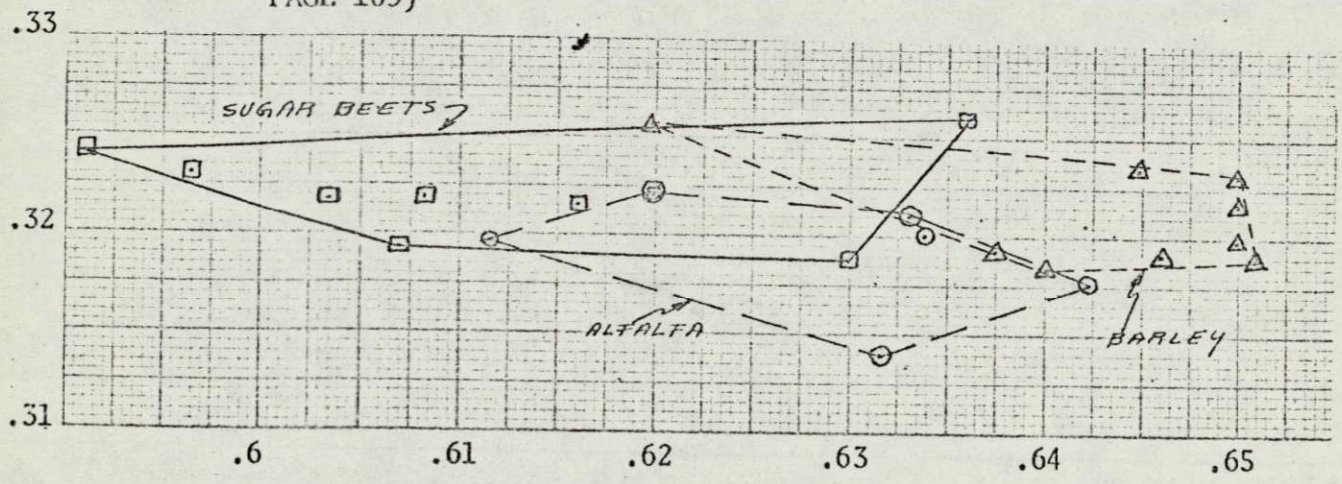

FIGURE 45: COLOR MEASUREMENTS OF IMAGE OF ALFALFA, BARLEY AND SUGAR BEETS FROM THE ABOVE MULTISPECTRAL COLOR PHOTO.

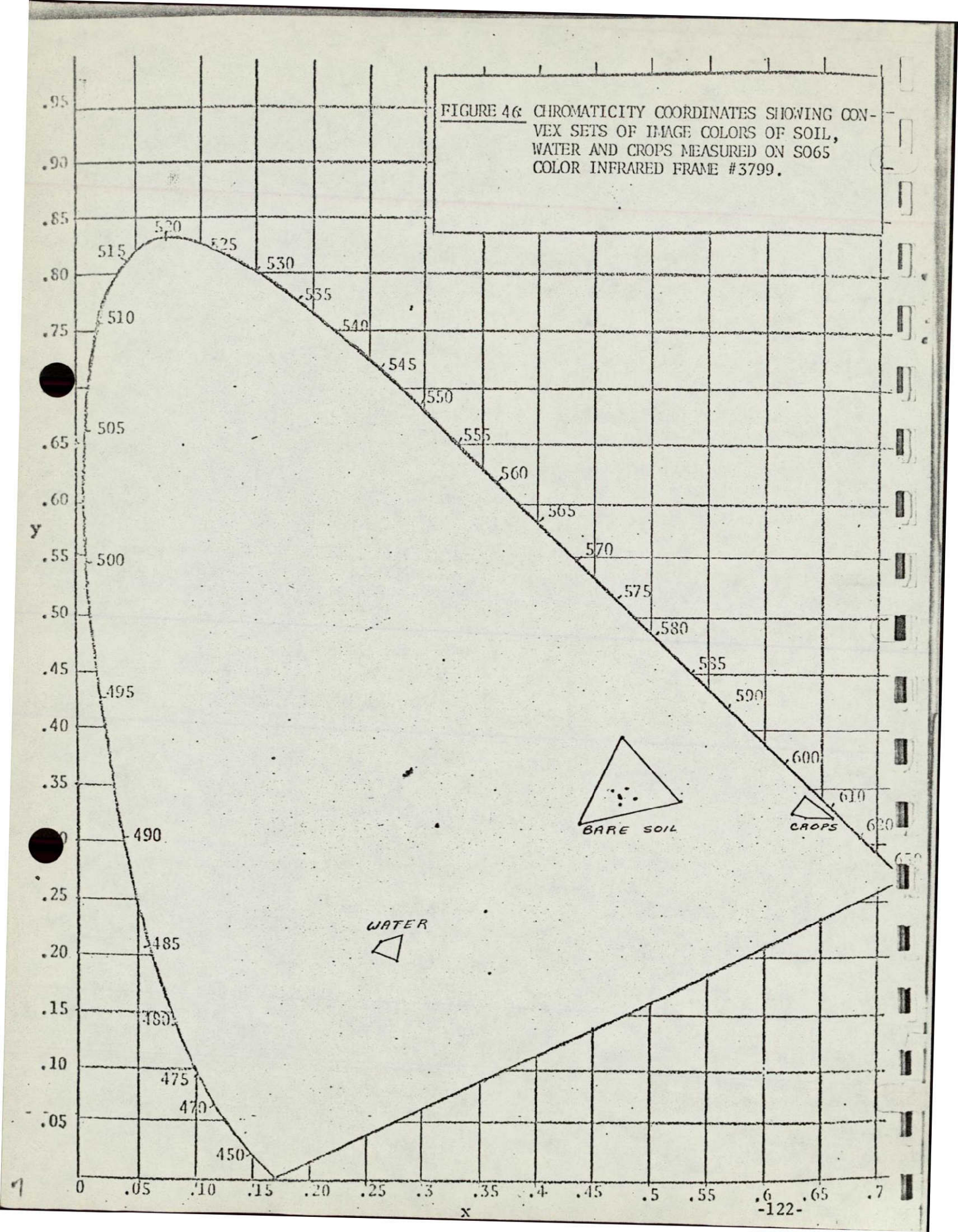
FIGURE 46: CHROMATICITY COORDINATES SHOWING CONVEX SETS OF IMAGE COLORS OF SOIL, WATER AND CROPS MEASURED ON S065 COLOR INFRARED FRAME #3799.
520
515
525
530
535
510
540
545
550
505
555
560
565
570
500
575
580
585
495
590
600
610
490
485
480
475
470
450
BARE SOIL
CROPS
WATER
.95
.90
.85
.80
.75
.65
.60
.55
.50
.45
.40
.35
.25
.20
.15
.10
.05
y
0
.05
.10
.15
.20
.25
.3
.35
.4
.45
.5
.55
.6
.65
.7
x

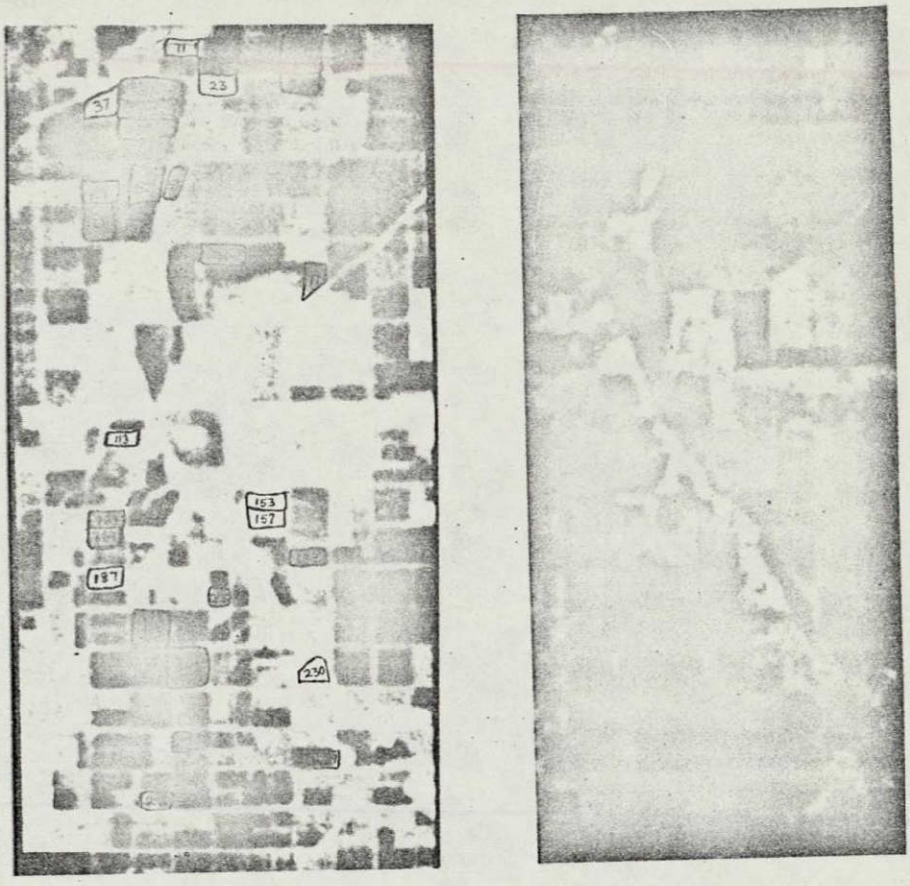

FIGURE 47 ENLARGEMENT OF S065 COLOR INFRARED FRAME #3799, IMPERIAL VALLEY, CALIFORNIA. (FOR LEGEND OF FIELDS MEASURED SEE PAGE 109)

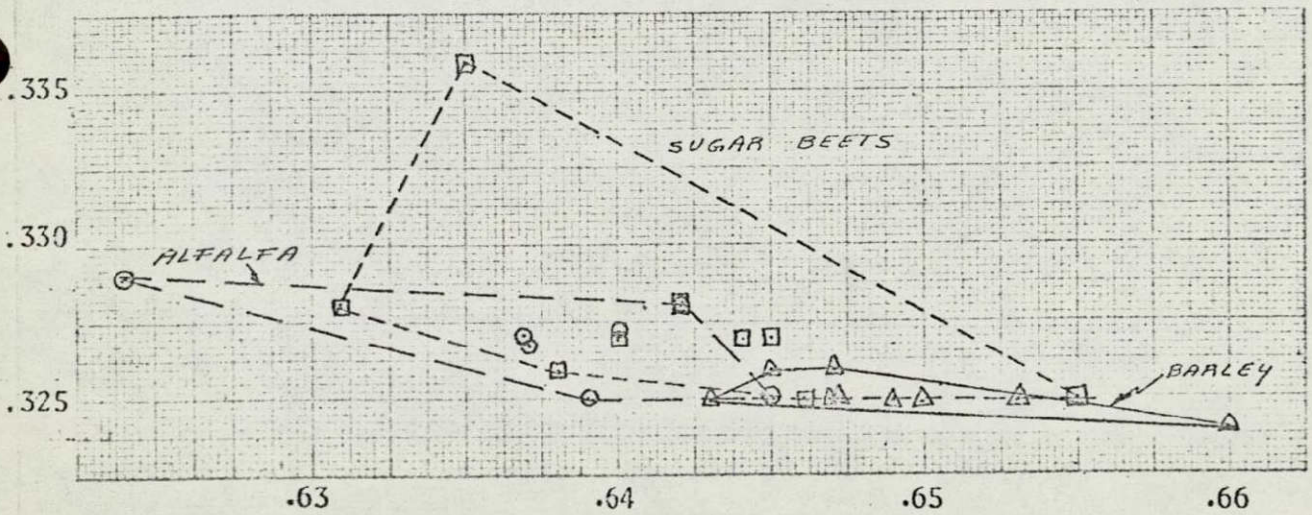

FIGURE 48 CHROMATICITY MEASUREMENTS OF CROPS: ALFALFA, BARLEY AND SUGAR BEETS ENLARGED FROM THE ABOVE COLOR PHOTOGRAPH.

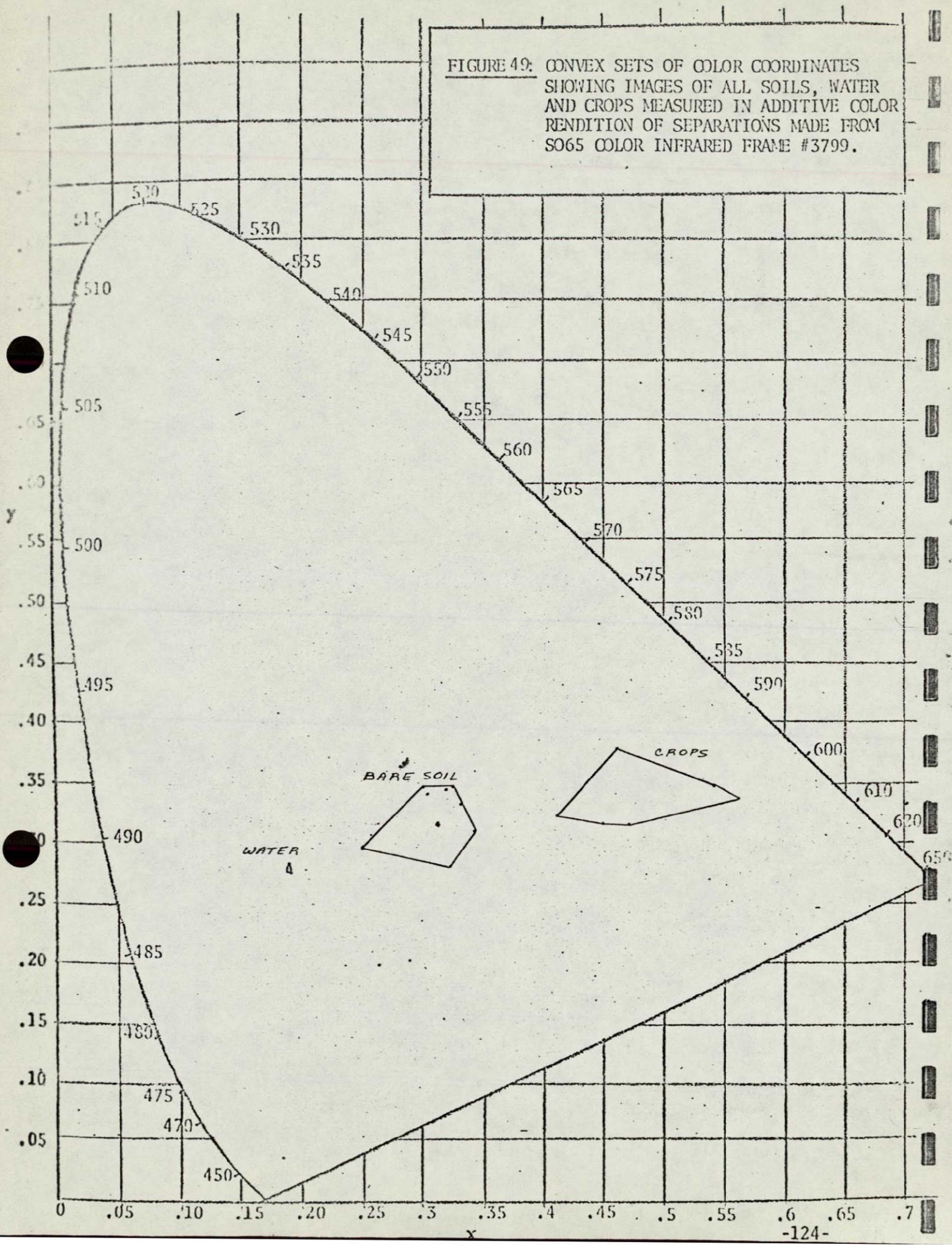

FIGURE 49: CONVEX SETS OF COLOR COORDINATES SHOWING IMAGES OF ALL SOILS, WATER AND CROPS MEASURED IN ADDITIVE COLOR RENDITION OF SEPARATIONS MADE FROM SO65 COLOR INFRARED FRAME #3799.

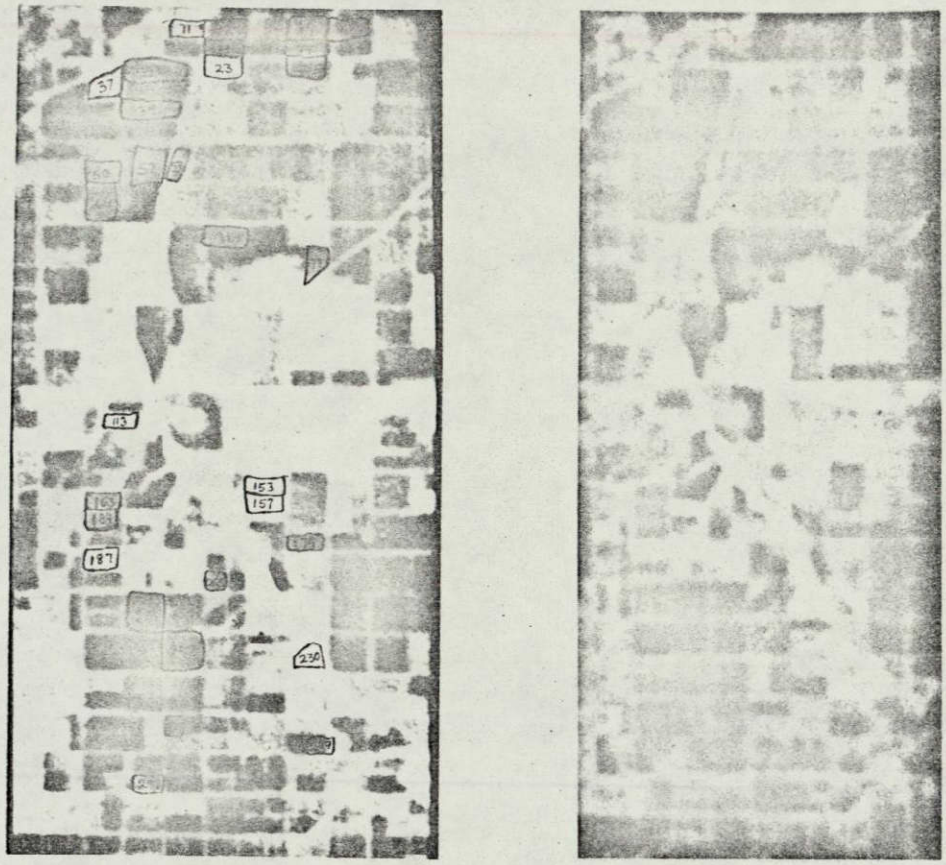

FIGURE 50: ADDITIVE COLOR RENDITION OF SEPARATION POSITIVES MADE FROM BLUE, GREEN AND RED IMAGE FORMING LAYERS IN COLOR INFRARED FRAME #3799. (FOR LEGEND OF FIELDS MEASURED SEE PAGE 109)

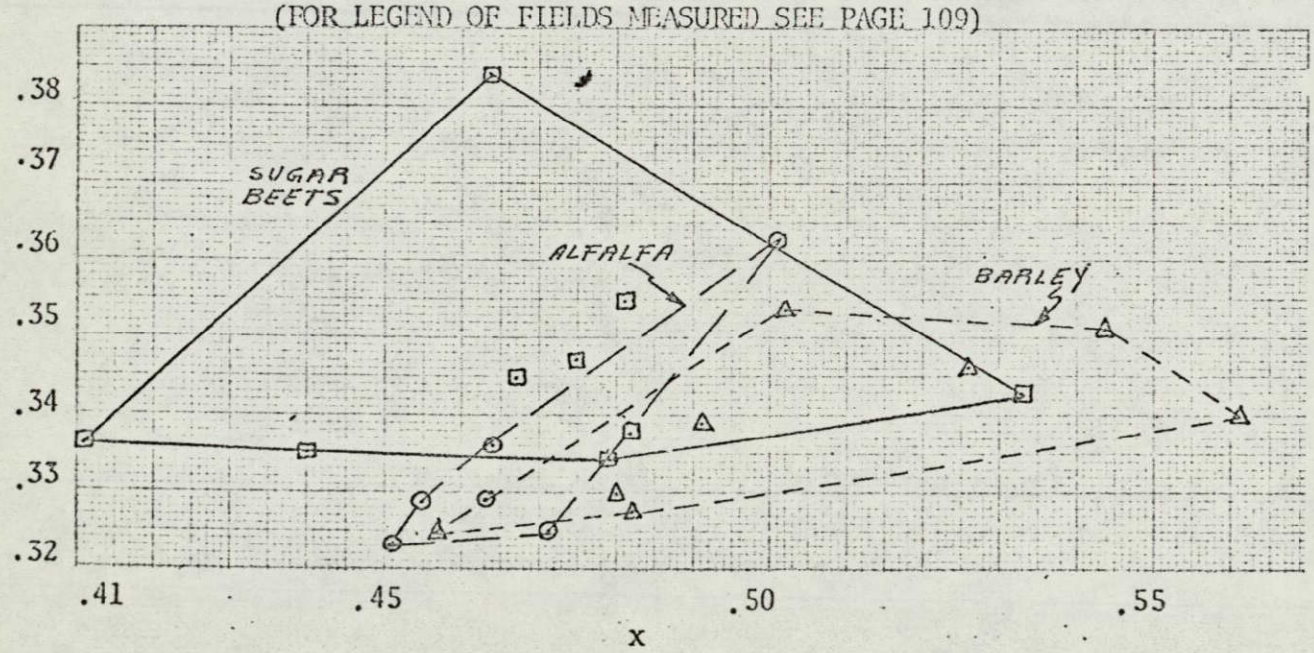

FIGURE 51: CHROMATICITY MEASUREMENTS OF IMAGES OF ALFALFA, BARLEY AND SUGAR BEETS FROM THE ABOVE COLOR RENDITION

TABLE 8

COMPARISON OF THE A POSTERIORI PROBABILITIES OF CORRECT CROP CLASSIFICATION BY IMAGE COLOR USING ADDITIVE AND SUBTRACTIVE IMAGE FORMING TECHNIQUES

	MULTISPECTRAL ADDITIVE COLOR		COLOR INFRARED FILM		SEPARATION POSITIVES FROM COLOR IR FILM PROJECTED ADDITIVELY	
ALFALFA IMAGES IN THE FOLLOWING SETS:	(Total number of alfalfa images--6)					
Alfalfa(only)	3	3/6=.50	2	2/6=.33	3	3/6=.50
Barley	1	1/6=.16	1	1/6=.16	1	1/6=.16
Sugar Beets	2	2/6=.33	3	3/6=.50	2	2/6=.33
Barley & Sugar Beet	0	0/6=0	0	0/6=0	0	0/6=0
BARLEY IMAGES IN THE FOLLOWING SETS:	(Total number of barley images--9)					
Barley(only)	7	7/9=.78	1	1/9=.11	4	4/9=.44
Alfalfa	1	1/9=.11	1	1/9=.11	2	2/9=.22
Sugar Beets	1	1/9=.11	7	7/9=.78	3	3/9=.33
Alfalfa & Sugar Beet	0	0/9=0	0	0/9=0	0	0/9=0
SUGAR BEET IMAGES IN THE FOLLOWING SETS:	(Total number of sugar beet images--9)					
Sugar beets(only)	7	7/9=.78	4	4/9=.44	6	6/9=.67
Alfalfa	2	2/9=.22	3	3/9=.33	0	0/9=0
Barley	0	0/9=0	2	2/9=.22	3	3/9=.33
Alfalfa & Barley	0	0/9=0	0	0/9=0	0	0/9=0

chromatically. A closer examination of the crop colors however, shows less separation of chromaticity coordinates than was evident on the additive color reproduction of the separate multispectral photographs. The data presented in Table 8 shows that the a posteriori probability of correct classification of alfalfa in the color infrared film image is reduced to 33%. Similarly, where the correct classification of sugar beets is 78% in multispectral additive-color rendition, it is only 11% using color infrared film. Likewise, where the a posteriori probability of correct classification of sugar beets is 78% in mulitspectral photography, it is reduced to 44% using the color infrared film. This decrease in color separation of individual crops is depicted by the small size of the convex sets of individual crop types shown in Figure 48 as well as the intersection between the various crop convex sets.

Separation Additive Color Images from S065 Color Infrared Photography

Similar measurements were made using separation positives obtained from the blue, green and red image forming layers of the S065 color infrared film. These black-and-white enlargements were precision processed to achieve faithful tone reproduction and placed in the additive color viewer. The same color space as used for the multispectral rendition was used. Again, the bare soil, crop and water categories were uniquely distinguished. However, the individual crops (alfalfa, barley and sugar beets) were not unique. The probability of a posteriori correct classification based on the non-overlapping nature of these convex sets of

the three crop types shows intermediate improvement compared to the subtractive color infrared image. This can be seen from Table 8 . Figure 51 also shows the general spreading out of the colors which is evidenced by the increase in the dominant wavelengths associated with each crop class. The color image of barley is still most saturated of the three crop types. The dominant wavelength of all crops is between 585 and 605nm. Saturation differences however, predominate.

Average and Range of The Color Space Associated with Crops

Figures 52, 53and 54 show graphically the average value and range of the chromaticity coordinates for all measurements of the three crops in each of the three renditions. Note that all three methods used for producing color results in overlapping of the image colors of these three crops. This joint intersection of the three crops, is smallest in the multispectral rendition. The choice of filters in the SO65 Hasselblad cameras made it impossible to give a unique a priori definition of image color which would result in 100% correct crop classification.

Probabilities of Correct Crop Classification

Table 8 presents the relative capability of each image forming technique for correct classification of crop type based on the probabilistic notion of convex sets. The number of correct responses is determined by the number of image measurements falling in each convex set.

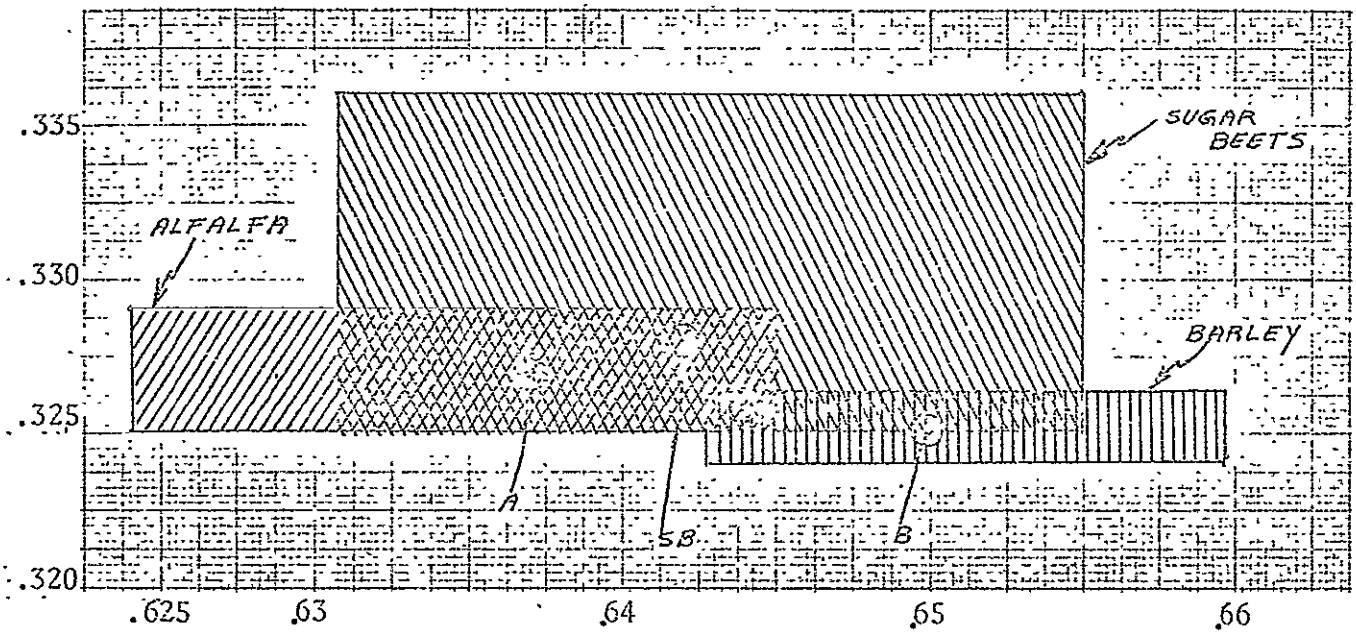

FIGURE 52: SO65 COLOR INFRARED IMAGE CHROMATICITY DEFINED BY THE RANGE OF BARLEY, ALFALFA AND SUGAR BEET CROP IMAGE COLORS.

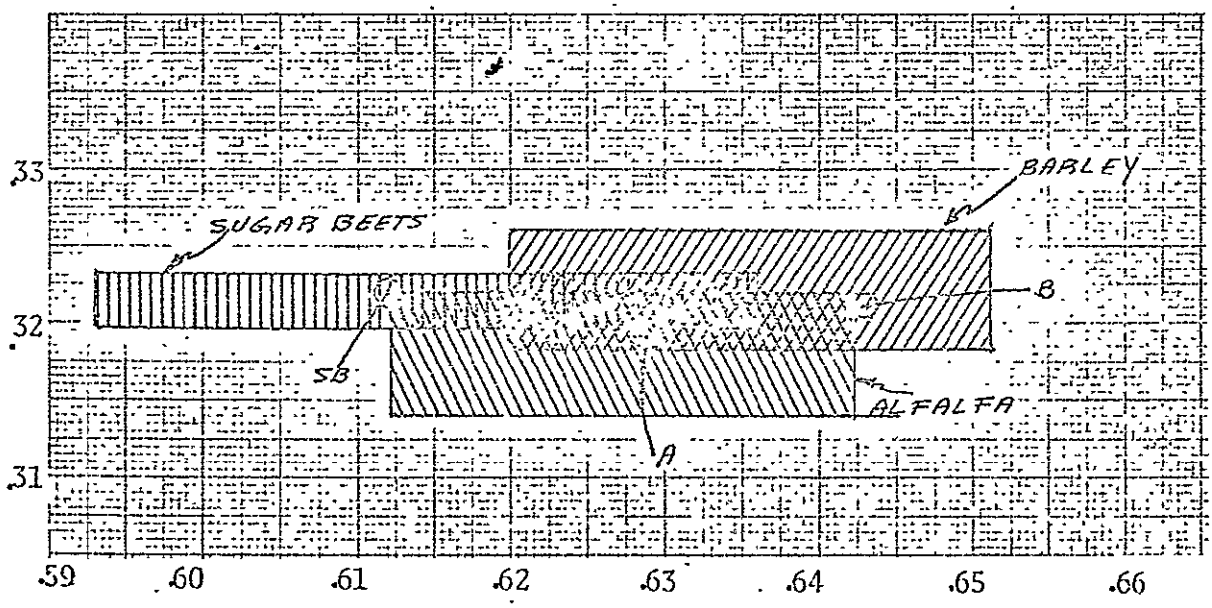

FIGURE 53: MULTISPECTRAL RENDITION COMPARABLE TO THE ABOVE SHOWING AVERAGE VALUE AND RANGE OF COLORS OF CROP IMAGES DEFINED IN CIE DIAGRAM.

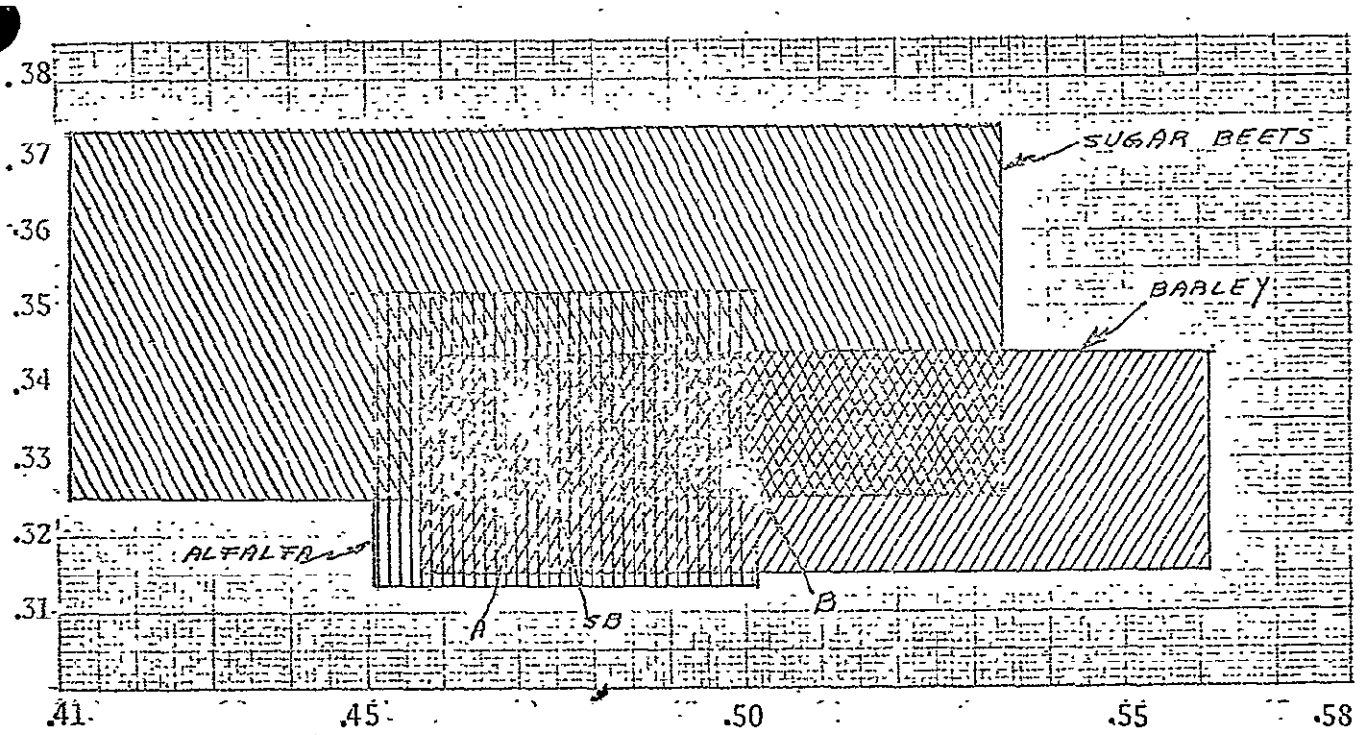

FIGURE 54: AVERAGE AND RANGE OF IMAGE COLORS APPEARING ON SEPARATION POSITIVES MADE FROM THE CYAN, YELLOW AND MAGENTA DYE LAYERS OF SO 65 COLOR INFRARED PHOTOGRAPHY

For instance, only three of the six measurements of the image of alfalfa fell uniquely in the convex set identifying alfalfa; therefore, the ratio of three divided by six or 50 per cent correct classification is assigned. Note that one alfalfa image fell in the barley and therefore a one sixth or 16 per cent incorrect classification is assigned to barley. Similarly, where two alfalfa plots fell in the convex set of all sugar beets, there exists a two sixths or 33 per cent misclassification of alfalfa as sugar beets.

These tabulations are shown in Table 8 and give a graphical measure of the uniqueness of image color based upon not only the overlap of the convex sets of all measurements in each crop category but also the number of image colors falling in each convex set.

While the small sample size may leave open the question of the relative accuracy of these measurements, it is clear that the magnitude of the difference between correct classification using multispectral photography vis a vis color infrared photography is probably indicated. Apparently multispectral additive color imagery leads to a greater probability of correct classification than does subtractive color infrared film.

Image Brightness

Figure 55 presents measurements of image brightness in the three color producing renditions. Here the per cent transmission of the green image is placed on the Y axis. Since the green filter in the color

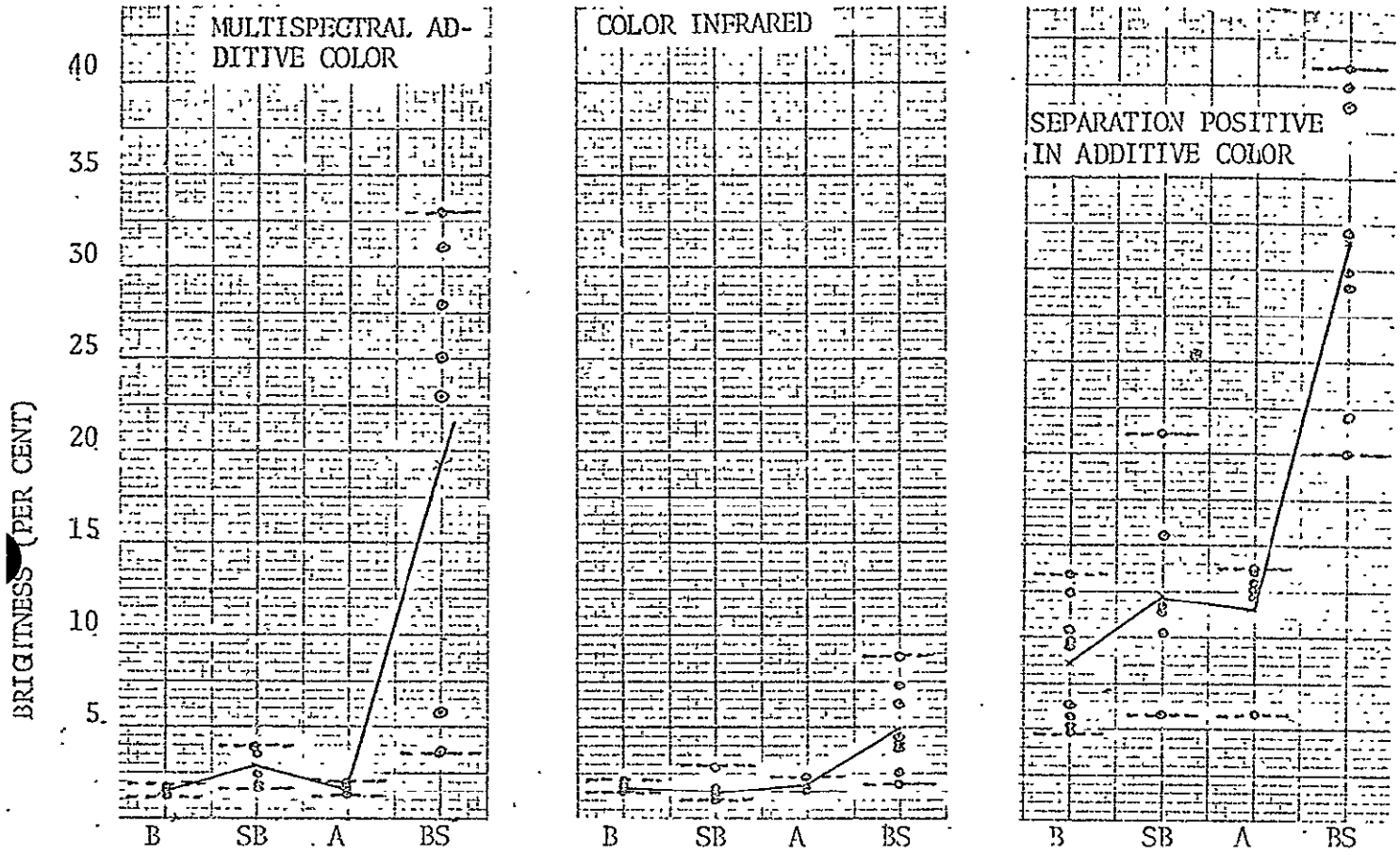

FIGURE 55: THE SO65 IMAGE BRIGHTNESS OF BARLEY(B), SUGAR BEETS(SB), ALFALFA(A) AND BARE SOIL(BS) USING ADDITIVE AND SUBTRACTIVE METHODS OF COLOR FORMATION

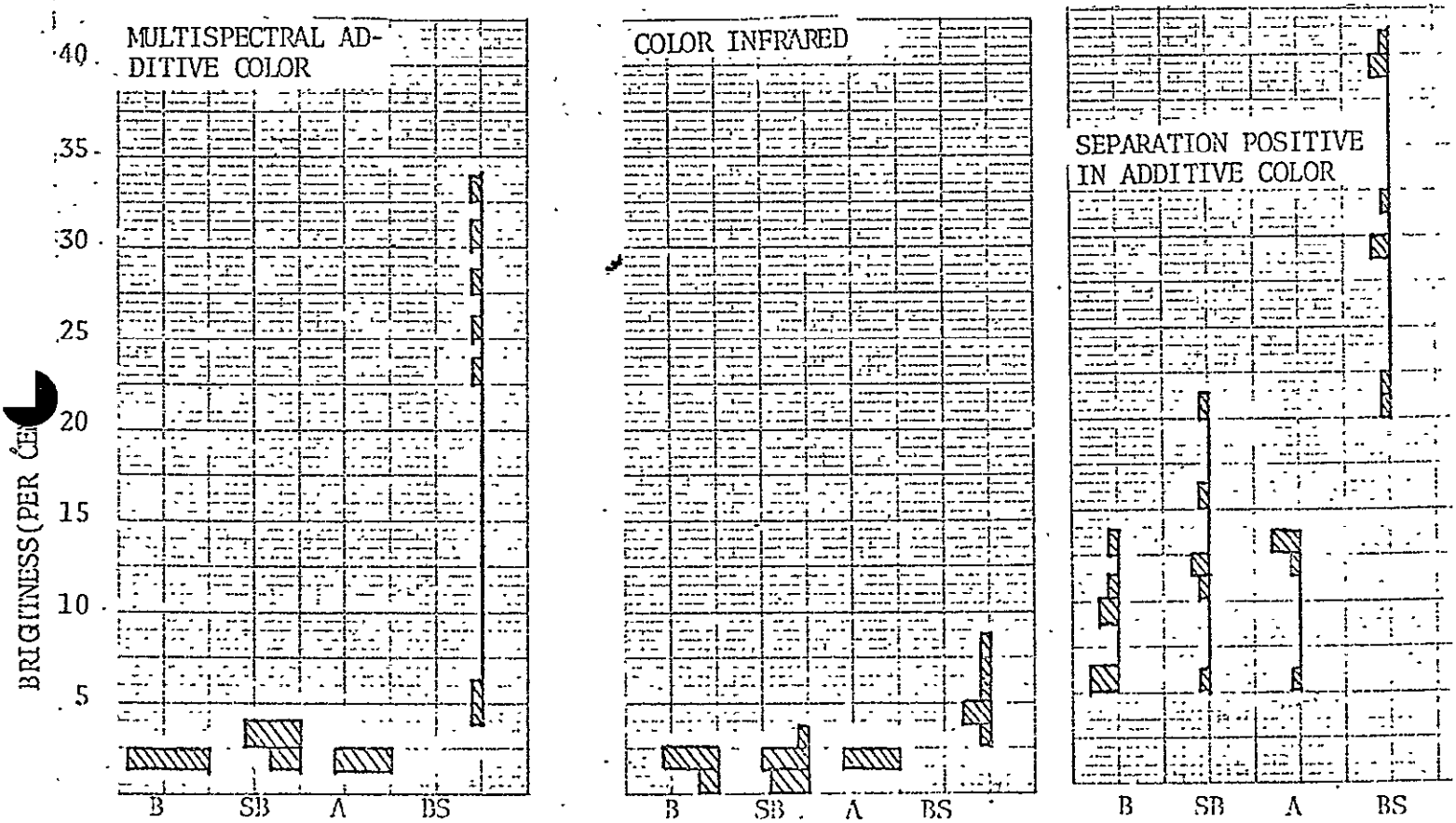

FIGURE 56 : HISTOGRAM OF DISTRIBUTION OF IMAGE BRIGHTNESS IN ADDITIVE AND SUBTRACTIVE COLOR IMAGES.

densitometer rather well approximates the brightness function of the human eye, it has been used as a measure of image brightness.

Note that the magnitude and range of image brightness for each category shown is much greater in both the multispectral additive color renditions than in the subtractive color infrared image. From the histogram on the bottom of the page, it would seem that the multispectral additive color transformation of the individual color infrared dye layers has the effect of strtching out the image brightness values. It is interesting to note that the range of brightness values associated with bare soil are greatest in all three renditions but particularly in the additive color renditions. These data reinforce the observation that it is difficult, if not impossible, to uniquely identify objects based on brightness (or density) measurements of photographic images.

Comparative Variations in Chromaticity of Additive Color Multispectral Images and Subtractive Color Film Images

The variability of image chromaticity within three alfalfa fields is shown graphically in Figure 57. Therein are plotted the convex sets associated with the range of chromaticity coordinates for the following underflight photography:

A) multispectral additive false color rendition, (green band projected as blue, red band as green, and infrared as red.)

B) aerial ektachrome (emulsion 8442) subtractive true color,

FIGURE 57: MAXIMUM COLOR VARIATION WITHIN FIELDS CAUSED PRIMARILY BY DIFFERENCES IN PER CENT GROUND COVER.

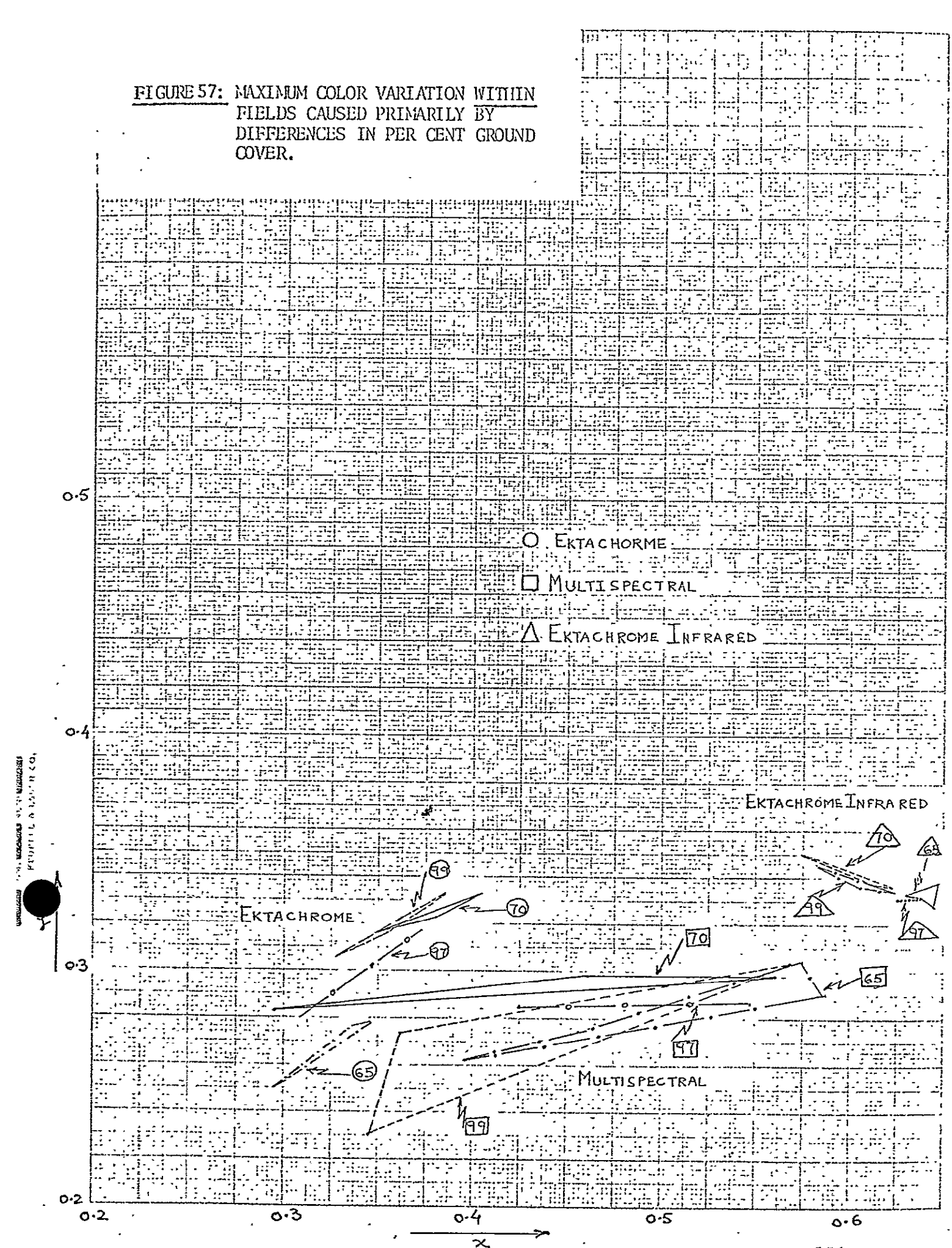

C) aerial ektachrome infrared (emulsion 8443)

subtractive false color.

These data emphasize the sensitivity of multispectral additive color methods of analysis to the variation in the ground cover of vegetation. The variation in color is far greater than that exhibited by color infrared film.

The data and associated illustration (Figure 58) indicate that for these true and false color emulsions as well as for this set of multispectral camera-viewing filters, image color of vegetation is primarily related to per cent ground cover and only secondarily related to crop type.

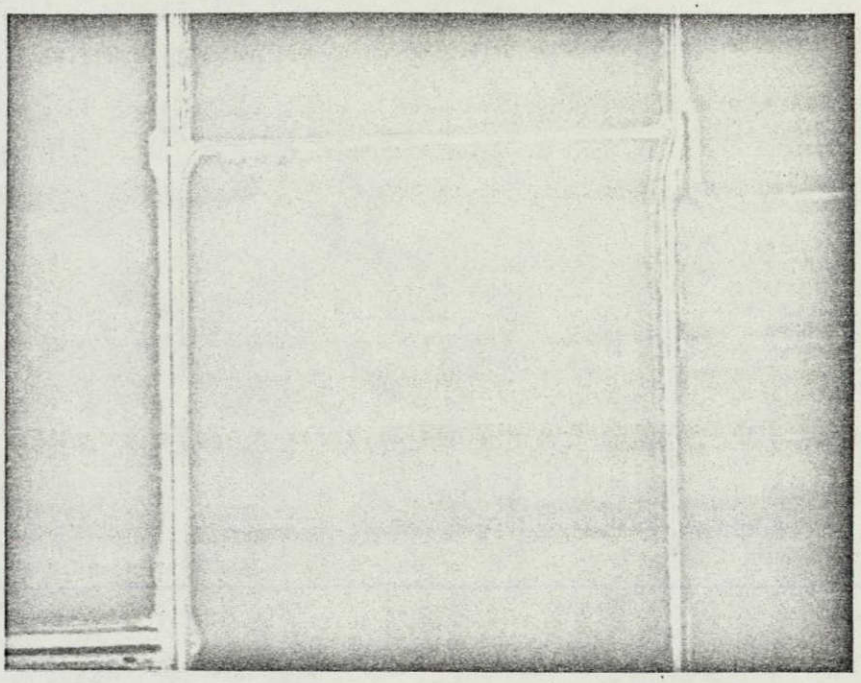

FIGURE 58 : AN ENLARGMENT OF UNDERFILGHT PHOTOGRAPH SHOWING THE GREAT VARIABILITY IN IMAGE COLOR CAUSED BY VARIATION IN PER CENT GROUND COVER OF VEGETATION.

Variations In Image Color Among The S065 Space Photos

As part of Long Island University's on-going activity in space photography, the color characteristics of selected photographs, from the Gemini through the Apollo flights, are being colorimetrically evaluated. This evaluation has as its purpose establishing the uniqueness and reproducibility of the color images of various ground objects. This includes analysis of color films (emulsion numbers S0217 and S0121), color infrared films (emulsion number S0180) as well as multispectral additive color rendition constructed from the S065 black-and-white multiband photography.

In order to make a meaningful comparison of the chromatic accuracy between the subtractive and additive techniques of obtaining color images, as well as among the individual color films, a standard test object must be used. Such a physical object must, of course, exist naturally in the environment. The scale of typical space photography in the past (in excess of 1:1,000,000) necessitates a very large and relatively natural homogenous features be used as the "standard object".

The area to the east and west of the Imperial Valley is currently being used as the standard target area. This portion of the Imperial Valley contains numerous large and relatively homogenous semi-arid areas and mountains which appear to have relatively uniform spectral characteristics over most of the solar day. These areas are also free from glaring variations in spectral reflectance with seasonal changes.

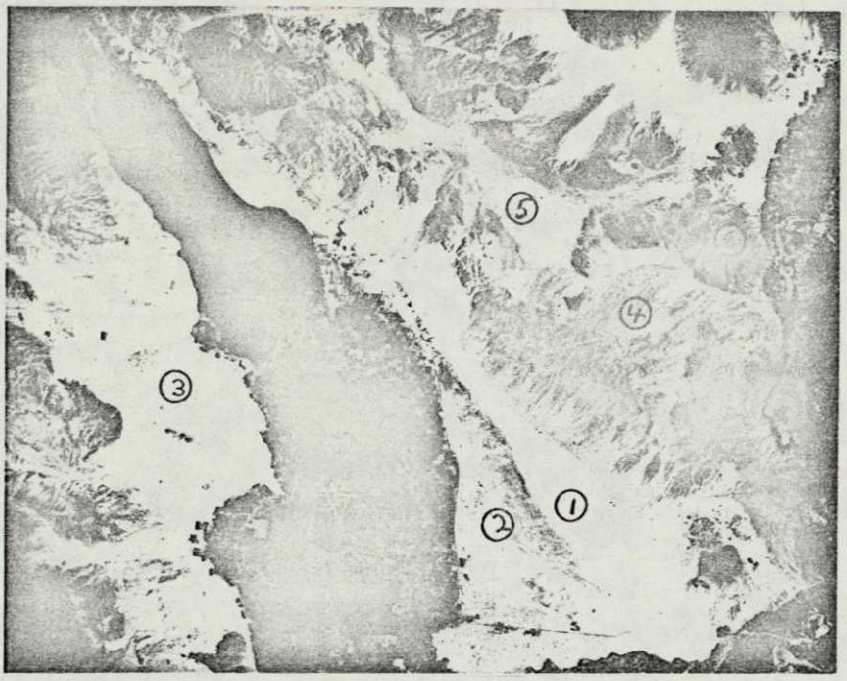

FIGURE 59 : STANDARD TARGET AREAS IN THE VICINITY OF THE IMPERIAL VALLEY, CALIFORNIA USED TO EVALUATE THE IMAGE COLOR REPRODUCIBILITY ON SPACE COLOR PHOTOGRAPHS.

TABLE 9

GEOGRAPHICAL DESCRIPTION OF TARGET AREAS USED AS STANDARDS TO MEASURE REPRODUCIBILITY OF COLOR IMAGES

ANNOTATION NUMBER	DESCRIPTION
1	Desert east of Amos, Calif. in foothills of Chocolate Mountains.
2	Desert west of Amos, Calif.
3	Desert west of Westmoreland, Calif.
4	Chocolate Mountains north of Quartz Peak.
5	Chuckawalla Mountains
6	Palo Verde area, Trigo Mountains.

The specific locations of the six target areas in the Imperial Valley are shown in Figure 59 . The reader will note, there is great diversity in topography between these areas. The geographical location and associated conventional names of these standard target areas are tabularized in Table 9 . All the areas shown are essentially achromatic, that is colorless, with what appears to be uniform spectral reflectance out to 900nm. One would expect then that the color of these objects would be essentially neutral, varying from one to the other only in brightness.

The following two chromaticity diagrams indicate the reproducibility of color on two geographical locations. Area 1, which is the desert area east of Amos, California in the foothills of the Chocolate Mountains, exhibited the most uniform color characteristics on all the media used. These media are tabulated in Table 10 . The reader will note that the imagery used varies from Gemini color photography through the Apollo additive color multispectral photos. The Trigo Mountains, near the Palo Verdes on the Colorado River, exhibited the greatest image variability in color as shown in Figure 61 . Here it is apparent that image color is greatly affected by the topography and slope. The lack of reproducibility in the two areas may be ascribed not only to the media on which the color image is recorded but also changes in the apparent color of objects due to different illumination conditions.

TABLE 10

SIX RENDITIONS OF COLOR IMAGES ANALYZED FOR CHROMATIC VARIATIONS OF STANDARD TARGET AREAS

RENDITION	TYPE	REMARKS
A	S065 Multispectral additive color frame #3799	Green band projected as green Red band projected as blue IR band projected as red
B	S065 Multispectral additive color frame #3799	Green band projected as red Red band projected as green IR band projected as blue
C	S065 Multispectral additive color frame #3799	Green band projected as red Red band projected as blue IR band projected as green
D	S065 Color Infrared frame #3799	Color Infrared emulsion number S0180
E	Gemini V frame #S-65-45747	Multispectral Ektachrome color emulsion #S0217
F)	Apollo VII frame #AS7-11-2023	Color emulsion #S0121

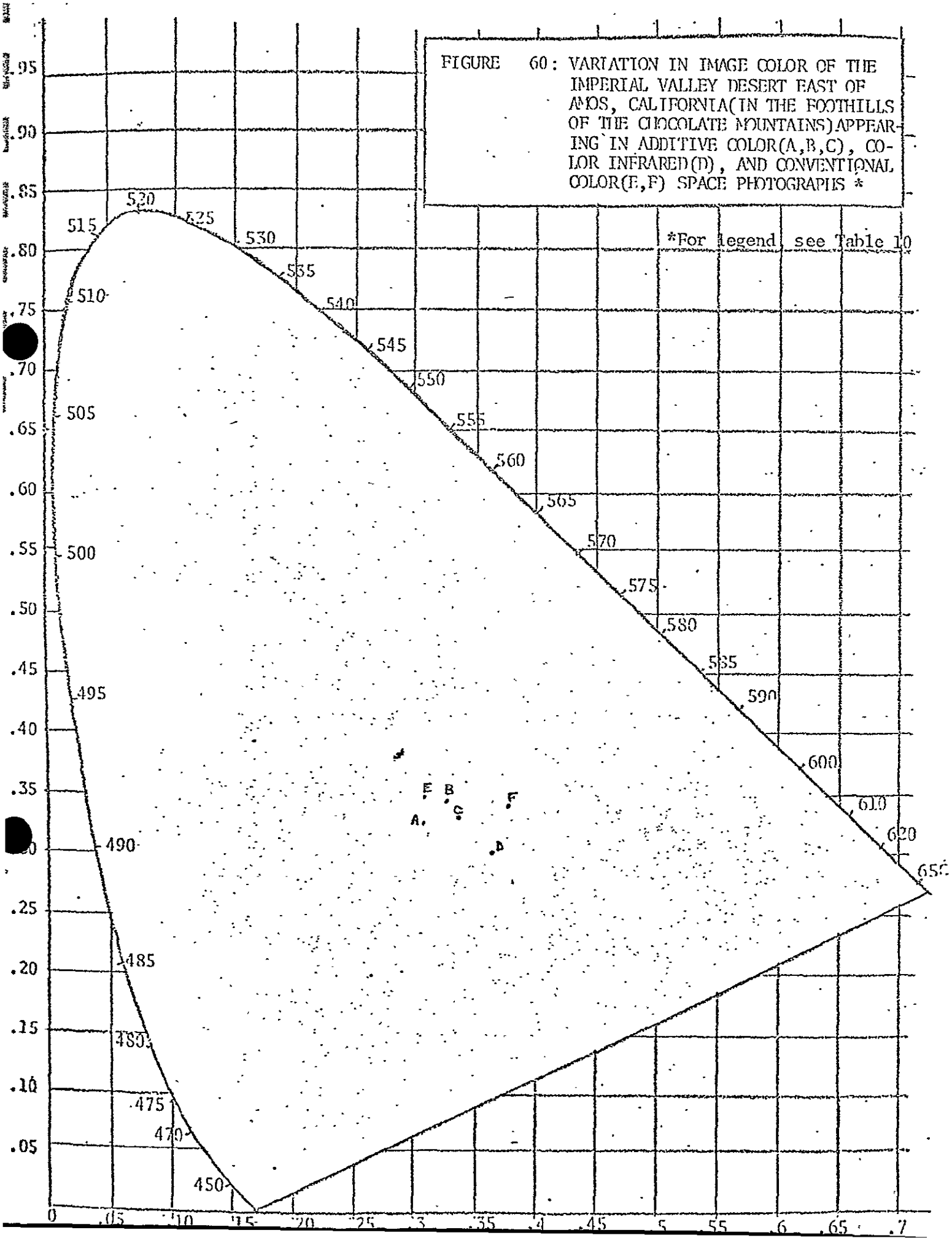

FIGURE 60: VARIATION IN IMAGE COLOR OF THE IMPERIAL VALLEY DESERT EAST OF AMOS, CALIFORNIA (IN THE FOOTHILLS OF THE CHOCOLATE MOUNTAINS) APPEARING IN ADDITIVE COLOR (A,B,C), COLOR INFRARED (D), AND CONVENTIONAL COLOR (E,F) SPACE PHOTOGRAPHS *

*For legend see Table 10

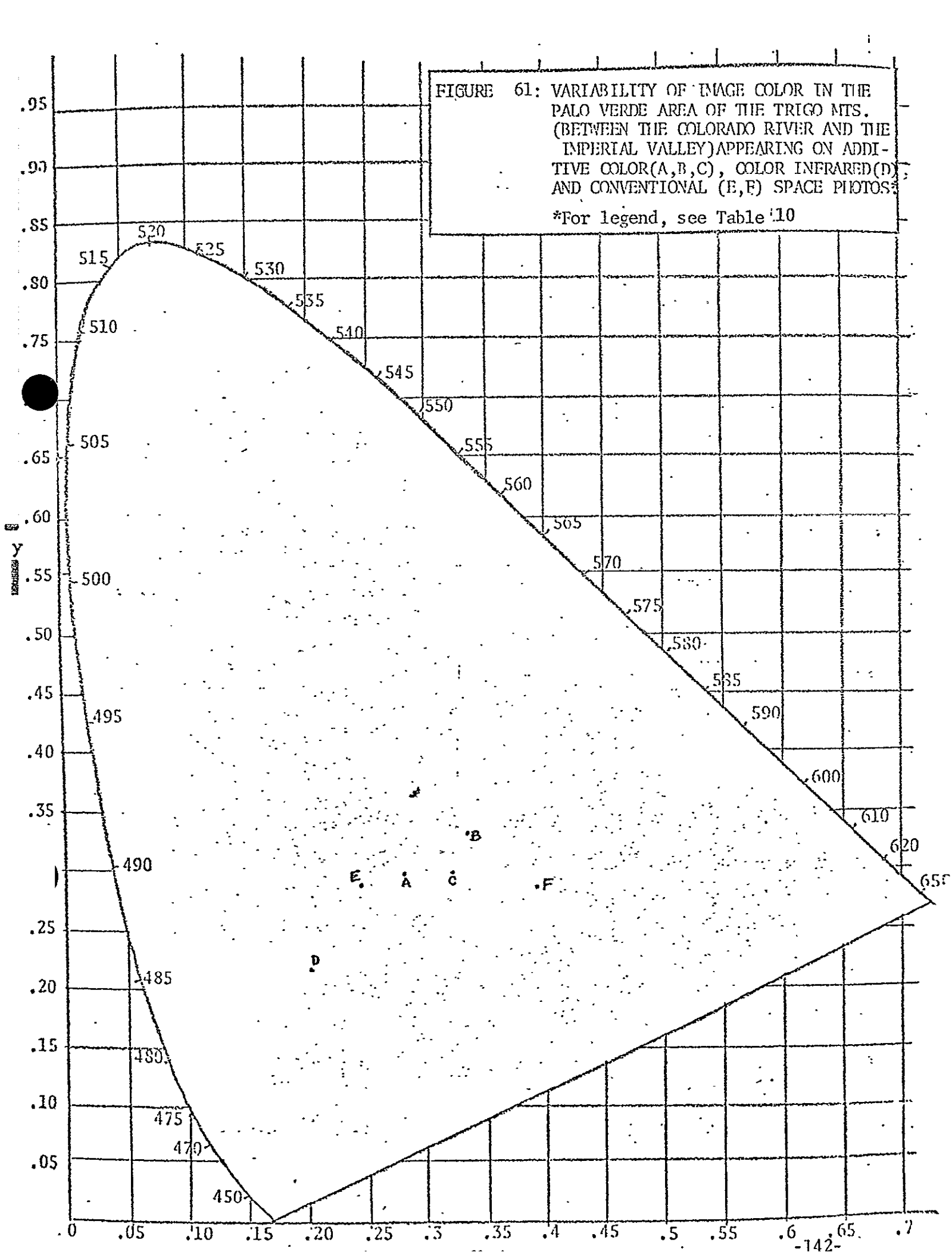
FIGURE 61: VARIABILITY OF IMAGE COLOR IN THE PALO VERDE AREA OF THE TRIGO MTS. (BETWEEN THE COLORADO RIVER AND THE IMPERIAL VALLEY) APPEARING ON ADDITIVE COLOR (A,B,C), COLOR INFRARED (D), AND CONVENTIONAL (E,F) SPACE PHOTOS.
*For legend, see Table 10
y
.95
.90
.85
.80
.75
.65
.60
.55
.50
.45
.40
.35
.25
.20
.15
.10
.05
0
.05
.10
.15
.20
.25
.3
.35
.4
.45
.5
.55
.6
.65
.7
520
515
525
530
535
540
545
550
555
560
565
570
575
580
585
590
600
610
620
650
510
505
500
495
490
485
480
475
470
450
A
B
C
D
E
F

SECTION 7

A COMPARISON OF SO65 SPACE MULTISPECTRAL PHOTOGRAPHY AND LONG ISLAND UNIVERSITY UNDERFLIGHT MULTISPECTRAL PHOTOGRAPHY

Colorimetric analysis of the additive color renditions of reprocessed and enlarged multispectral space photography of the Imperial Valley (SO65 frame #3799) and underflight imagery obtained using the Long Island University multispectral camera were performed. The results indicated that when the images of fields were of sufficient size and homogeneous in appearance, the per cent of the ground covered by vegetation was related to image chromaticity.

Analysis of underflight multispectral photography indicated that the relationship between the per cent ground cover and image color was affected by variations between and within fields. For this reason, it appears that ground resolution is an important factor in relating measureable characteristics of a multispectral image for soil and vegetation mapping when accuracy relative to the ground truth and precision among the measurements are required.

The largest variation in brightness of vegetation imaged on the underflight photography was found to exist in the infrared band and the least variation in the red band. Great overlap exists between the brightness (and of course, density) of crop and soil catagories in the underflight multispectral photography.

SO65 Multispectral Image Chromatic Characteristics

Figure 62 presents a photo reproduction of the additive color viewer screen on which was projected, in color, the SO65 multispectral photography (frame #3799). In order to simulate the sensitization of color infrared film, the green band was projected as blue, the red band projected as green and the infrared band as red. The area of the Imperial Valley covered by this photograph is shown in Figure 35 on page 100 . The 25 times enlargements of the original SO65 images used to form the additive color image were processed to obtain precision tone reproduction in the image when projected. The screen image was 75 times the scale of the original photography.

Colorimetric analyses of various fields were performed, the purpose being to determine if any significant repeatable chromatic characteristic could be discerned from space. Fields were selected on the basis of size and image homogenity. Colorimetric transformations were made by computer program from the dye layer densities of color transparency reproductions made from the screen image.

It should be emphasized that only fields which exhibited homogeneous image quality were measured. For instance, fields 65, 70, 97 and 99 were not measured because of apparent image mottling. Fields which were too small (such as 63, 64 and 67) were not possible to differentiate even on the seventy-five times enlargement of the SO65 photography.

FIELD NO.	FIELD CODE	ROW DIR.	EST. AVE. CROP HEIGHT (in.)	EST. AVE. % GROUND COVER	FIELD TREATMENTS PRIOR TO AND DURING FLIGHTS, AND OTHER GROUND OBSERVATIONS
40	Sugar beet	NS	18-24	80	20% weed cover
45	Bare soil				Bedded for cotton
48	Barley	NS	18-24	90	
60	Barley	NS	24-36	100	
61	Bare Soil				
63	Sugar beet	NS	15-18	90	
64	Barley		12-18	80	
66	Sugar beet	EW	18-24	100	
67	Onions	EW	20-30	60	
68	Carrots	EW	10-12	80	
69	Rye	EW	2-4	70	
71	Alfalfa	NS	4-12	80	
72	Alfalfa	EW	3-8	90	
73	Alfalfa	EW	4-6	80	
74	Sugar beet	NS	14-18	90	
75	Barley	NS	18-24	95	
76	Bare soil				
77	Bare soil				
78	Bare soil	NS			Bedded for cotton
93	Idle				80% weed cover
95	Idle				80% weed cover
98	Alfalfa & rye	NS		60	large patches of bare soil in SE portion of field
99	Alfalfa	EW	10-12	100	
100	Barley	NS	24-30	100	
102	Alfalfa	NS	3-4	80	Recently cut
103	Bare soil	NS			Bedded for cotton
122	Bare soil	EW			Bedded for cotton
123	Bare soil				Recently plowed

GROUND TRUTH FOR PART OF THE IMPERIAL VALLEY (MC CABE ROAD AREA) OBTAINED DURING APOLLO 9 MISSION MARCH 1969

TABLE 11

*Source:

N. Spansail, et.al., "Imperial Valley, Ground Truth for Apollo 9 Overflight of March 1969, University of Michigan.

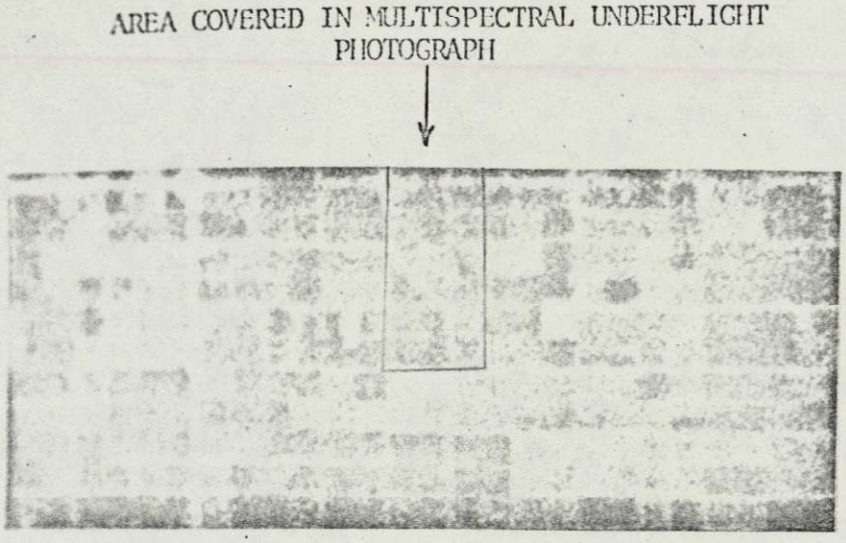

FIGURE 62: IMPERIAL VALLEY AREA II FALSE COLOR REPRODUCTION OF S065 MULTISPECTRAL FRAME #3799 OBTAINED AT 0828PST(1628GMT) ON 12 MARCH 1969. ENLARGEMENT IN ADDITIVE COLOR VIEWER WITH GREEN BAND PROJECTED AS BLUE, RED BAND AS GREEN AND INFRA-RED BAND AS RED.

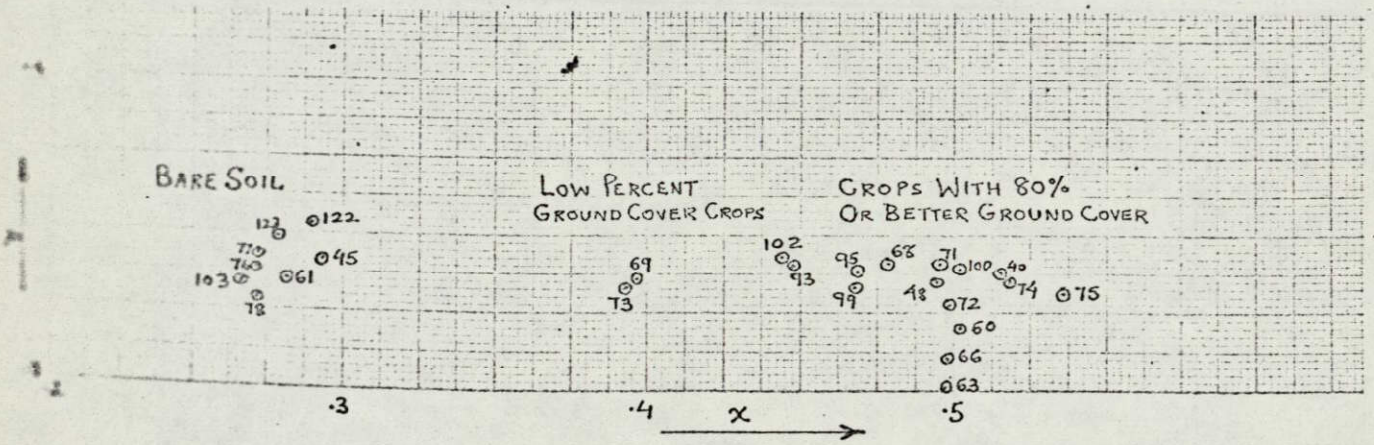

FIGURE 63: ENLARGEMENT OF COLOR COORDINATES OF CROPS APPEARING IN ABOVE S065 MULTISPECTRAL COLOR PHOTOGRAPH.

The results of these measurements are shown in compact form in Figure 63. While there is not sufficient data to compute probability measures for the various crops based upon the mathematical notion of convex sets, the data clearly do depict a significant colorimetric effect.

The chromaticity coordinates plotted in Figure 63 on the bottom of page 146 show the distinct soil and vegetation classes of chromaticity depicted in the preceeding section. However, note the position of crops with low percentage ground cover. These crops lie among a line segment connecting bare soil with "high density" ground cover crops. This suggests that reasonably accurate method of computing per cent ground cover of fields in a particular area may be devised. Measurement of image chromaciticity of a few known bare soil areas and a few known 100% covered vegetated areas could be used as a reference for determining the percentage cover of the remaining unknown fields. It is obvious that the precision of such a technique depends greatly on the accuracy of the photographic tone reproduction in the image as well as on the choice of spectral filters in the camera and colorimetric presentation in the viewer.

Chromatic Analysis of Underflight Multispectral Photography

Three additive color renditions of Long Island University multispectral photographs obtianed during the Apollo 9 mission are shown in Figures 64, 66 and 68. These photographs were taken four days prior to the Apollo 9 space photo shown in Figure 62. The photography was

obtained in the afternoon (1536PST) while the comparison S065 photography was taken in the morning (0828PST).

This elapsed time of four days and different sun angle not withstanding, significant insight can be gained by the comparison of these photos with the S065 overflight photography. The chromatic separation of bare soil, intermediate cover crops (idle fields and fields with 60% or less ground cover) and crops with 80% or greater coverage is apparent from the data in Figures 65 , 67 and 69 . One must remember that determination of ground cover was made on the ground and while generally appears to be quite good is, in some cases, in error(for instance, field 73).

The underflight photography clearly shows the great variability in per cent ground cover between fields and within fields. The effects of variable ground cover tend to integrate the perceived chromaticity of the space image. However, not withstanding this integrating effect and the comparative desaturation of the space image,(perhaps due to atmospheric effects) a functional relationship is seen to exist between per cent ground cover and image chromaticity.

The greater separation of the CIE coordinates achieved in some additive color renditions strictly results from the international standard transformations used in colorimetric analysis. It is not due to any alteration of the black-and-white positives which are projected.

Image Brightness of the Underflight Multispectral Photographs

The image brightness of the three previous underflight multispectral

FIELD#	CROP	HEIGHT	%COVER
[1,2,3,4]	Bare soil		
63	Sugar beets	15-18"	90%
64	Barley	12-18"	80%
66	Sugar beets	18-24"	100%
67	Onions	20-30"	60%
68	Carrots	10-12"	80%
69	Rye	2-4"	70%
71	Alfalfa	4-12"	80%
72	Alfalfa	3-8"	90%
73	Alfalfa	4-6"	?
74	Sugar beets	14-18"	90%
75	Barley	18-24"	95%
93	Idle		
95	Idle		
98	Alfalfa & Rye		60%
99	Alfalfa	10-12"	100%
100	Barley	24-30"	100%

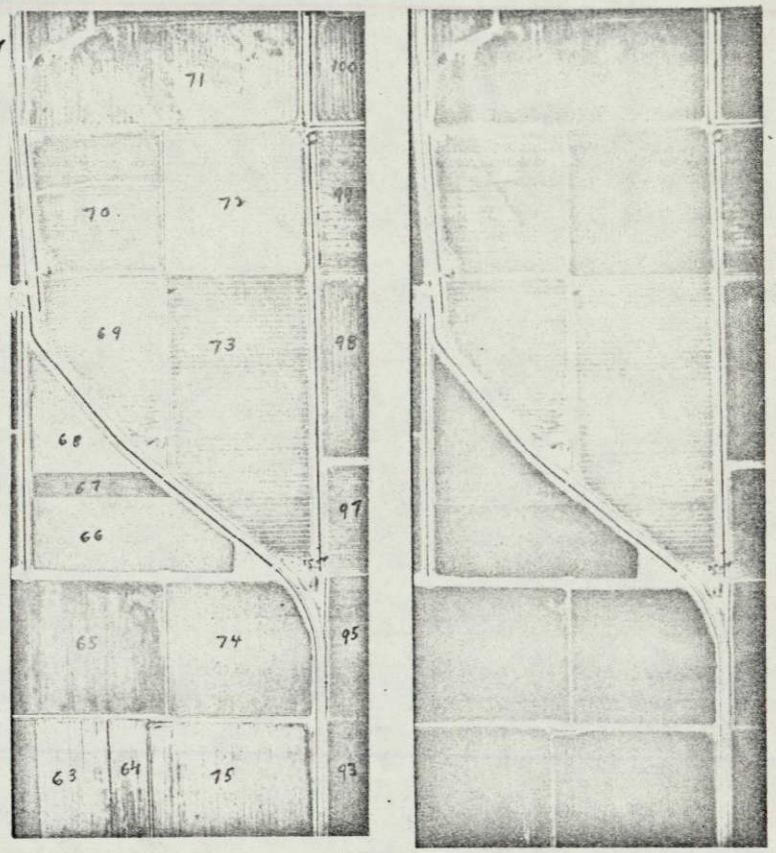

FIGURE 64: MULTISPECTRAL FALSE COLOR REPRODUCTION OF UNDERFLIGHT MULTISPECTRAL PHOTOGRAPH. GREEN BAND IMAGED AS BLUE, RED BAND AS GREEN AND INFRARED BAND AS RED. TAKEN WITH LIU MULTISPECTRAL CAMERA AT 14,000 FT. MSL AT 1536PST (2336GMT) ON 8 MARCH 1969.

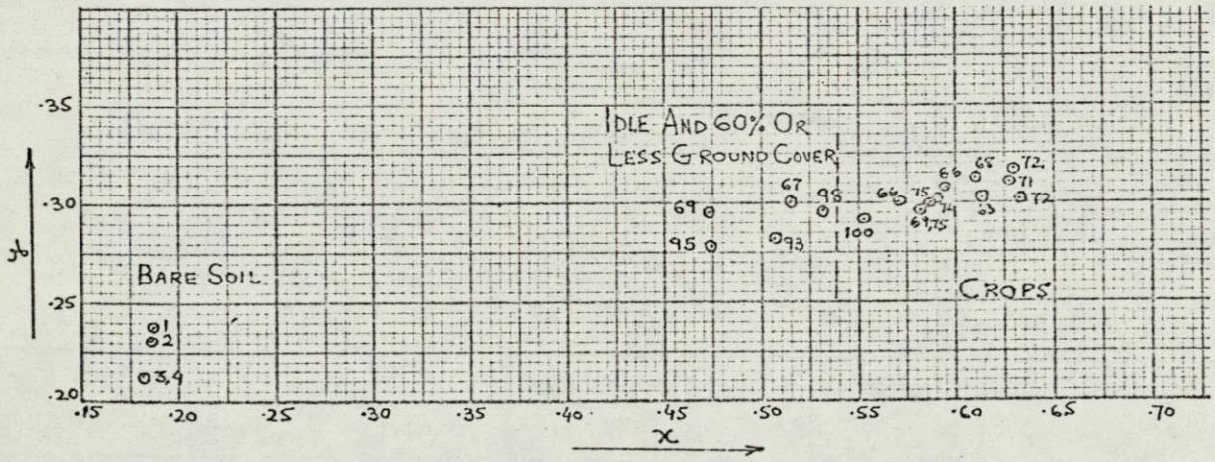

FIGURE 65: ENLARGEMENT OF CHROMATICITY PLOT OF CROP COLORS APPEARING IN ABOVE MULTISPECTRAL COLOR PHOTOGRAPH.

FIELD#	CROP	HEIGHT	%COVER
[1,2,3,4]	Bare soil		
63	Sugar beets	15-18"	90%
64	Barley	12-18"	80%
66	Sugar beets	18-24"	100%
67	Onions	20-30"	60%
68	Carrots	10-12"	80%
69	Rye	2-4"	70%
71	Alfalfa	4-12"	80%
72	Alfalfa	3-8"	90%
73	Alfalfa	4-6"	?
74	Sugar beets	14-18"	90%
75	Barley	18-24"	95%
93	Idle		
95	Idle		
98	Alfalfa & Rye		60%
99	Alfalfa	10-12"	100%
100	Barley	24-30"	100%

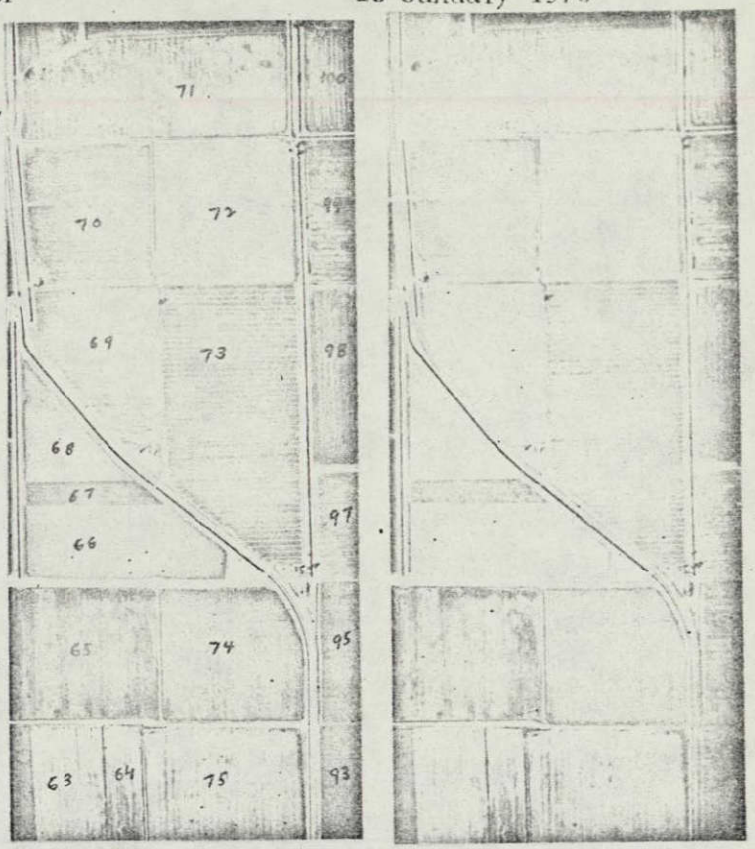

FIGURE 66: MULTISPECTRAL FALSE COLOR REPRODUCTION OF UNDERFLIGHT MULTISPECTRAL PHOTOGRAPH. GREEN BAND PROJECTED AS RED, RED BAND AS GREEN AND INFRARED AS BLUE. TAKEN WITH THE LIU MULTISPECTRAL CAMERA AT 14,000 FT, MSL AT 1536PST(2386GMT) ON 8 MARCH 1969.

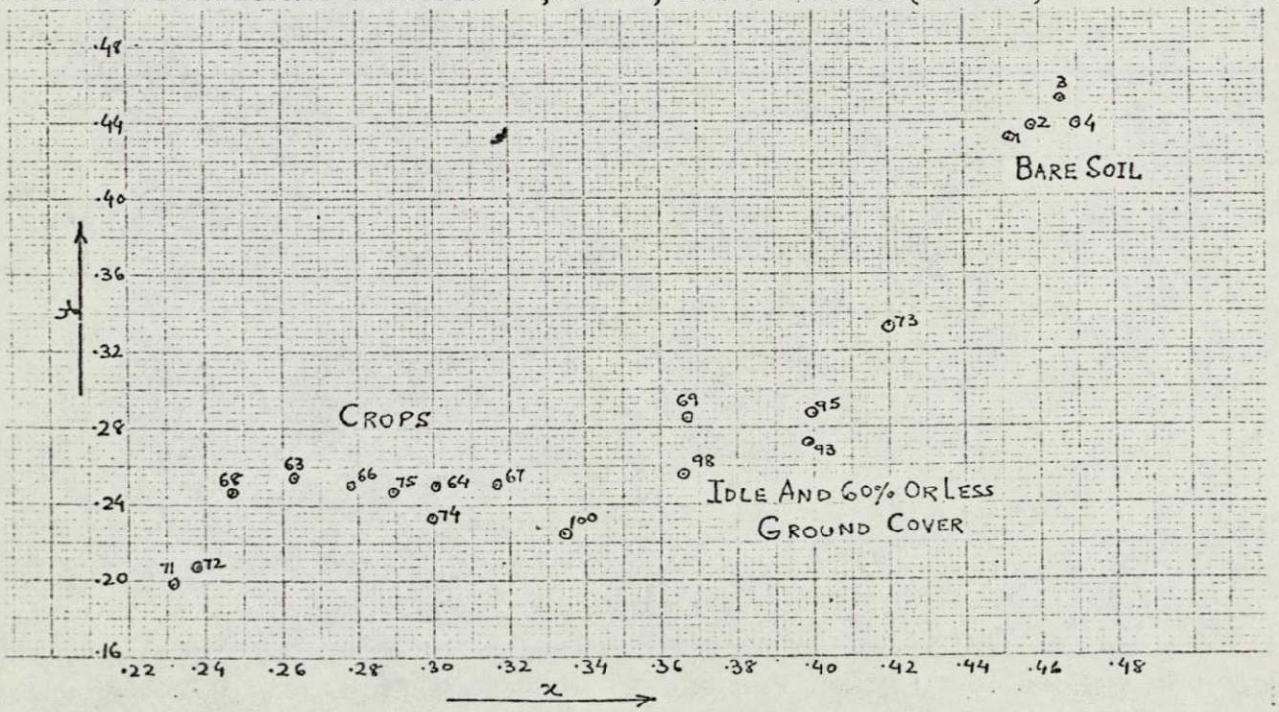

FIGURE 67: ENLARGEMENT OF COLOR COORDINATES OF CROPS APPEARING IN THE ABOVE COLOR PHOTOGRAPH.

FIELD [1,2, 3,4]	CROP Bare soil	HEIGHT 15-18"	% COVER
63	Sugar beets	12-18"	90
64	Barley	12-18"	80
66	Sugar beets	18-24"	100
67	Onions	20-30"	60
68	Carrots	10-12"	80
69	Rye	2-4"	70
71	Alfalfa	4-12"	80
72	Alfalfa	3-8"	90
73	Alfalfa	4-6"	?
74	Sugar beets	14-18"	90
75	Barley	18-24"	90
93	Idle		
95	Idle		
98	Alfalfa & Rye		60
99	Alfalfa	10-12"	100
100	Barley	24-30"	100

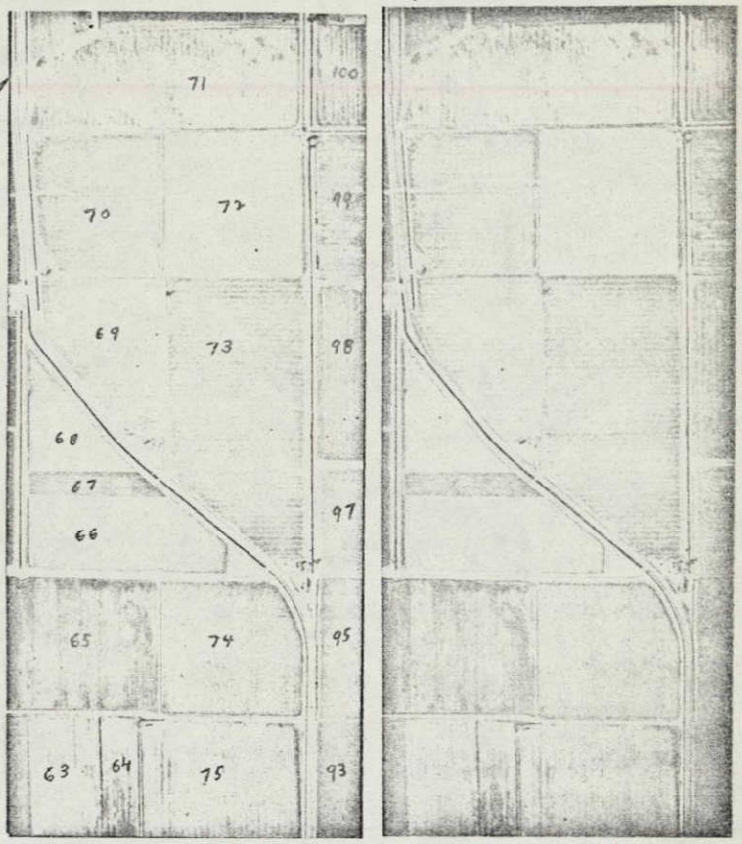

FIGURE 68: MULTISPECTRAL FALSE COLOR REPRODUCTION OF UNDERFLIGHT MULTISPECTRAL PHOTOGRAPH. GREEN BAND PROJECTED AS RED, RED BAND AS BLUE AND INFRARED BAND AS GREEN. TAKEN WITH THE LIU MULTISPECTRAL CAMERA AT 14,000 FT, MSL AT 1536PST (2386GMT) ON 8 MARCH 1969.

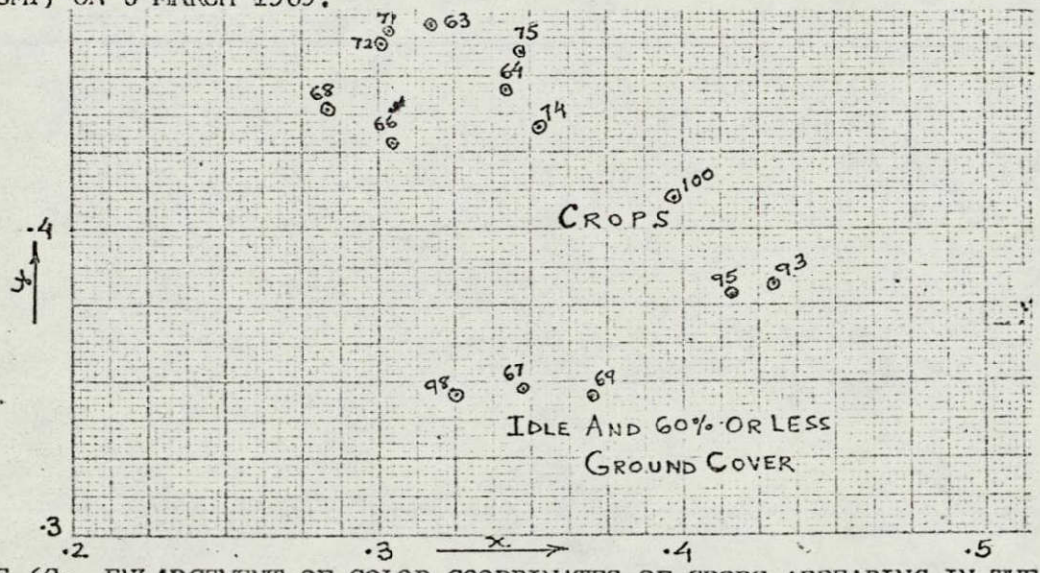

FIGURE 69: ENLARGEMENT OF COLOR COORDINATES OF CROPS APPEARING IN THE ABOVE COLOR PHOTOGRAPH.

color renditions is shown in Figure 70 . The data on the y axis were obtained by measuring the transmission of the transparency reproduction of the screen image to green light using a densitometer with a 1mm aperture.

Even with the small sample available, the data indicate that:

1) the greatest variability in crop image brightness occurs in the infrared followed by the green band,
2) very little brightness variation of crops is present in the red band (undoubtedly due to absorption of radiation in photosynthesis,
3) due to the overlap in image brightness, it is not possible to differentiate soils and vegetation on this basis.

The lack of variability in the brightness of soils shown in Figure 70 compared to S065 multispectral color data previously presented is probably due to the small sample size of the data available for analysis.

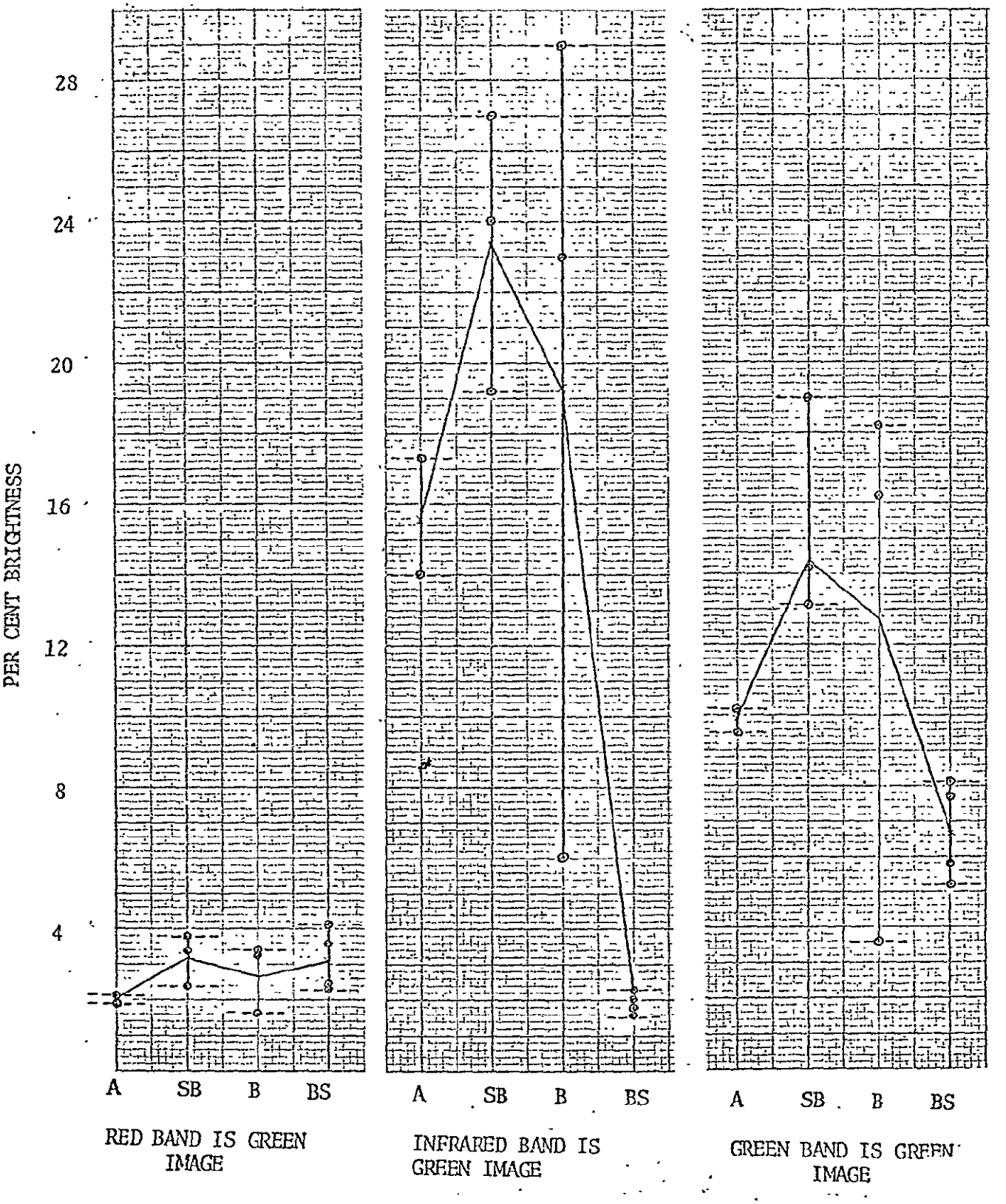

FIGURE 70: IMAGE BRIGHTNESS OF CROPS (ALFALFA, SUGAR BEETS, BARLEY) AND BARE SOIL APPEARING ON APOLLO 9 UNDERFLIGHT MULTISPECTRAL PHOTOGRAPHY.

SECTION 8

THE CHROMATIC CHARACTERISTICS OF S065 AND UNDERFLIGHT SUBTRACTIVE COLOR FILM IMAGES

The chromatic characteristics of vegetation and soil images appearing on an Apollo 9 conventional color photograph, taken with a hand-held Hasselblad camera using Kodak Special Order emulsion #368, were measured. It was found that on these color photographs, soils and vegetation could not be uniquely identified on the basis of image color. The convex set of vegetation chromaticity coordinates overlapped the set of soil chromaticity coordinates.

The chromaticity of images representing similar classes of vegetation (although not identical objects) was also measured on Apollo 9 underflight photography. These photographs, taken with Aerial Ektachrome (emulsion #8442) produced images of critically different chromaticity values compared to the space photograph using special order #368 color film.

A comparison of the images of identical objects of S065 infrared color film (emulsion #180) and on Long Island University underflight color film (emulsion #8443) indicated irregular variations in image saturation accompanied by an increase in hue in the space color infrared images. These differences in image color were probably due to the inherent variability in the subtractive image forming process as well as the time difference between obtaining the space and underflight photography.

Space and Underflight Images on Subtractive Color Infrared Film

The image chromatic characteristics of three crops appearing on S065 color infrared film (emulsion S0180) were measured using a precision color enlargement of the first generation duplicate of S065 frame #3799. This space image was obtained on March 12, 1969 at 0828 Pacific Standard Time. Image identification was based on 100 per cent ground truth (Spansail 1969). The images of exactly the same fields were also measured on the Apollo 9 color infrared underflight photograph (emulsion #8443). This subtractive color imagery was obtained by Long Island University using a K-24 camera equipped with a seven inch focal length lens at an altitude of 14,000 feet above terrain on 8 March 1969 at 1536PST.

The comparative plot of the same fields on both the space and underflight color infrared photography is shown in Figure 71. These data show a decrease in the y trichromatic coefficient of all space acquired images relative to underflight imagery. In this portion of the chromaticity diagram, this results in increasing dominant wavelength. There is, however, no regular pattern between change in x trichromatic coefficient and the two photographic altitudes. As can be seen from Figure 71, some vegetation images increase in saturation (x becomes larger), and some decrease. There appears to be no regularity present in the data.

In addition to changes in image color, which may be caused by the film dyes and variations in processing, the four day time period coupled with a change in the distribution, intensity and angle of the solar illuminant is known to affect the chromaticity of subtractive infrared

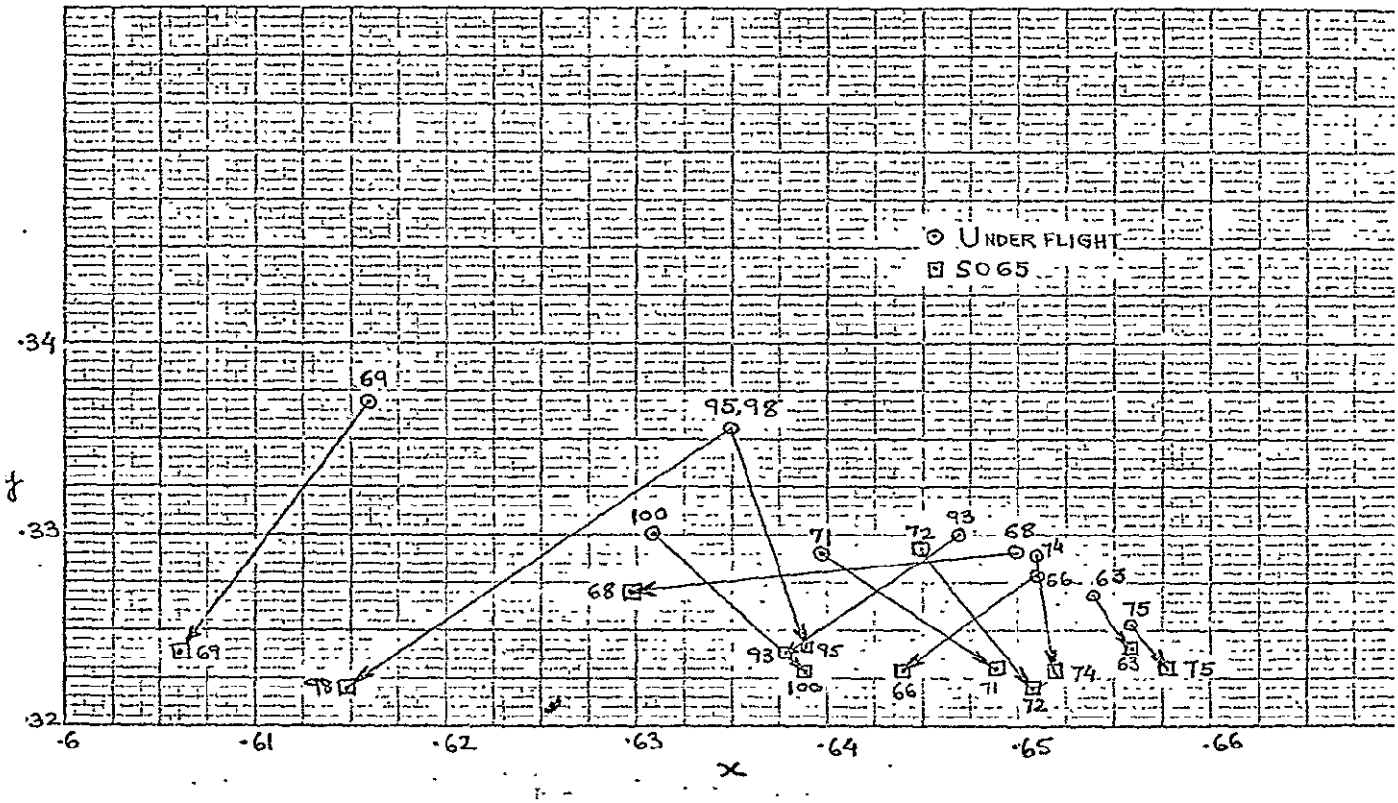

FIGURE 71 : COMPARATIVE IMAGE CHROMATICITY PLOT OF VEGETATION ON S065 COLOR INFRARED FILM (FRAME #3799) AND ON COLOR INFRARED FILM OBTAINED DURING APOLLO 9 UNDERFLIGHT. THE UNDERFLIGHT PHOTOGRAPHY WAS TAKEN IN THE AFTERNOON ON MARCH 8, 1969 WHILE THE SPACE IMAGERY WAS OBTAINED ON MARCH 12, 1969 IN THE MORNING AT 0828 LOCAL TIME. NUMBERS REFER TO FIELDS (SEE PAGE 151).

color film images. It is clear from the data that great variability exists in the chromaticity of images of vegetation obtained on color infrared film.

Color Photography--Space and Underflight

During the Apollo 9 mission, a number of "targets of opportunity" were photographed using a Hasselblad camera with an 80mm focal length lens similar to those used for the S065 experiment. On March 9, 1969 at 1002 Pacific Standard Time (1802 Greenwich Mean Time) an oblique photo was obtained of the Imperial Valley, California, while the spacecraft was in a 107 nautical mile orbit and the sun 47 degrees above the horizon. The image characteristics of the space photography were determined using the procedure described below.

A four times enlargement was made from a first generation NASA release transparency. State-of-the-art control was maintained over the color reproduction and processing. Densitometric measurements were made of the images of fields identified as being a particular crop or bare soil. The following numbers of image measurements were made: six (6) alfalfa, nine (9) sugar beets, nine (9) barley, eight (8) bare soil. Chromaticity coordinates were computed from the dye layer density measurements using special computer programs developed for the purpose.

Chromaticity coordinates derived from these image measurements are shown in Figure 72. It is interesting to note that there is very little difference in hue of the images. A dominent wavelength of 595nm

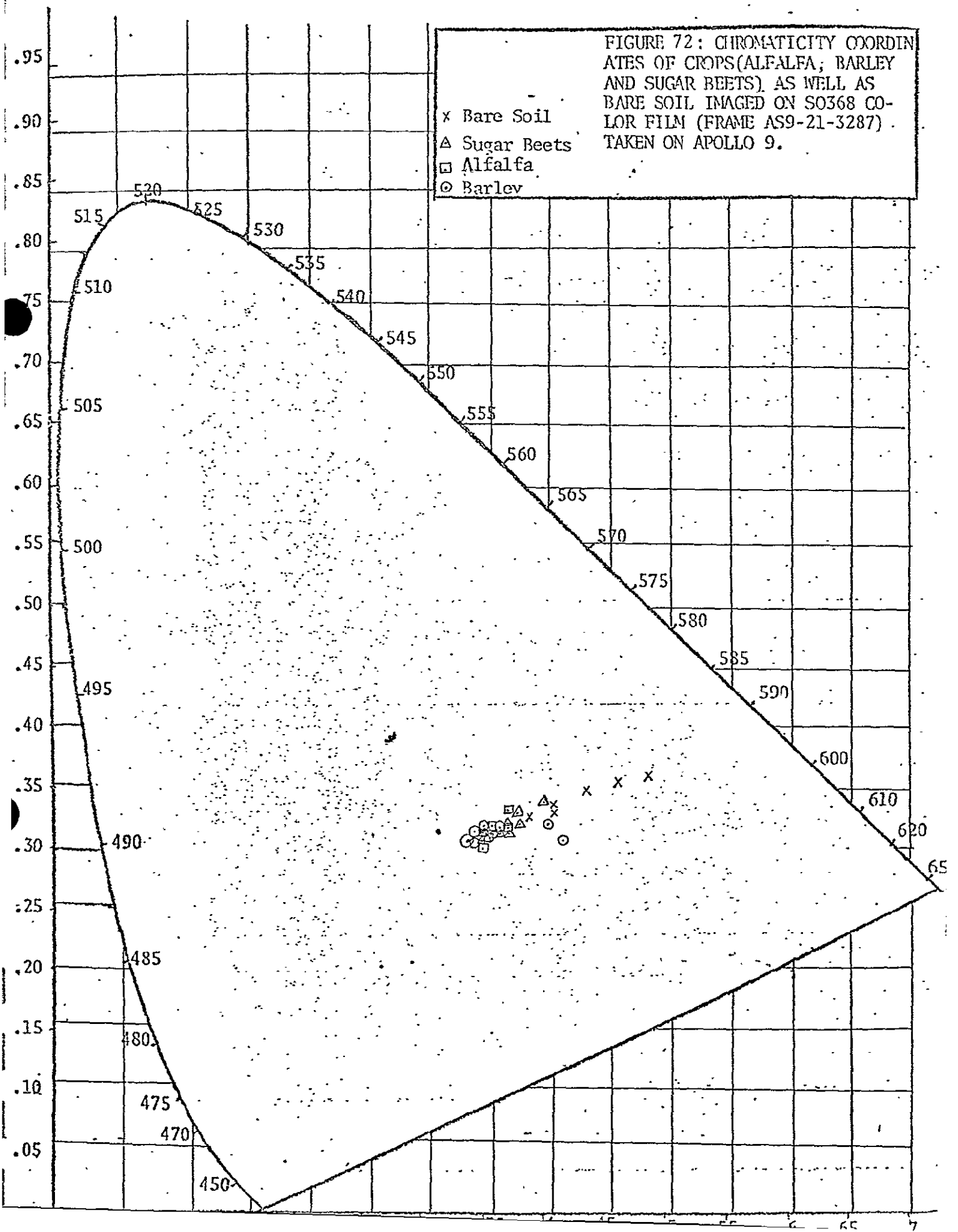

FIGURE 72: CHROMATICITY COORDINATES OF CROPS(ALFALFA; BARLEY AND SUGAR BEETS) AS WELL AS BARE SOIL IMAGED ON SO368 COLOR FILM (FRAME AS9-21-3287) TAKEN ON APOLLO 9.

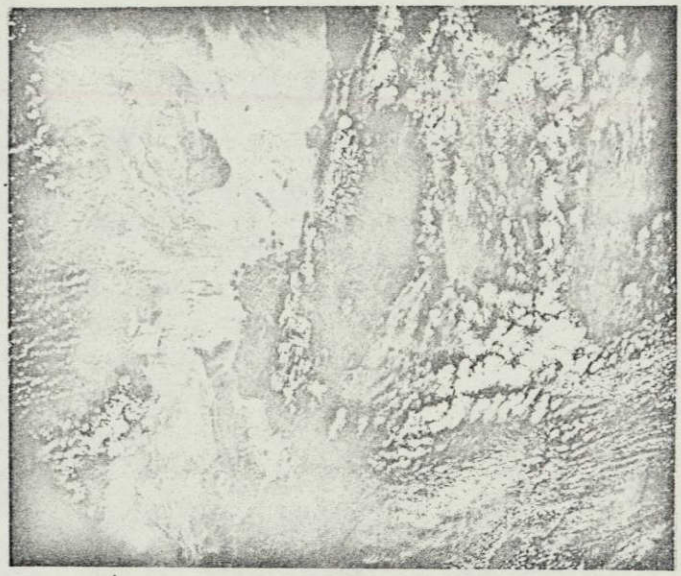

FIGURE 73 : COLOR PHOTOGRAPH OF THE IMPERIAL VALLEY OBTAINED DURING THE APOLLO 9 MISSION AT 1002 PDT (1802GMT) ON 9 MARCH 1969. THE FLIGHT ALTITUDE WAS 107 NAUTICAL MILES AND THE APPROXIMATE SUN ANGLE 47 DEGREES. ORIGINAL FILM WAS KODAK SO368 COLOR EMULSION.

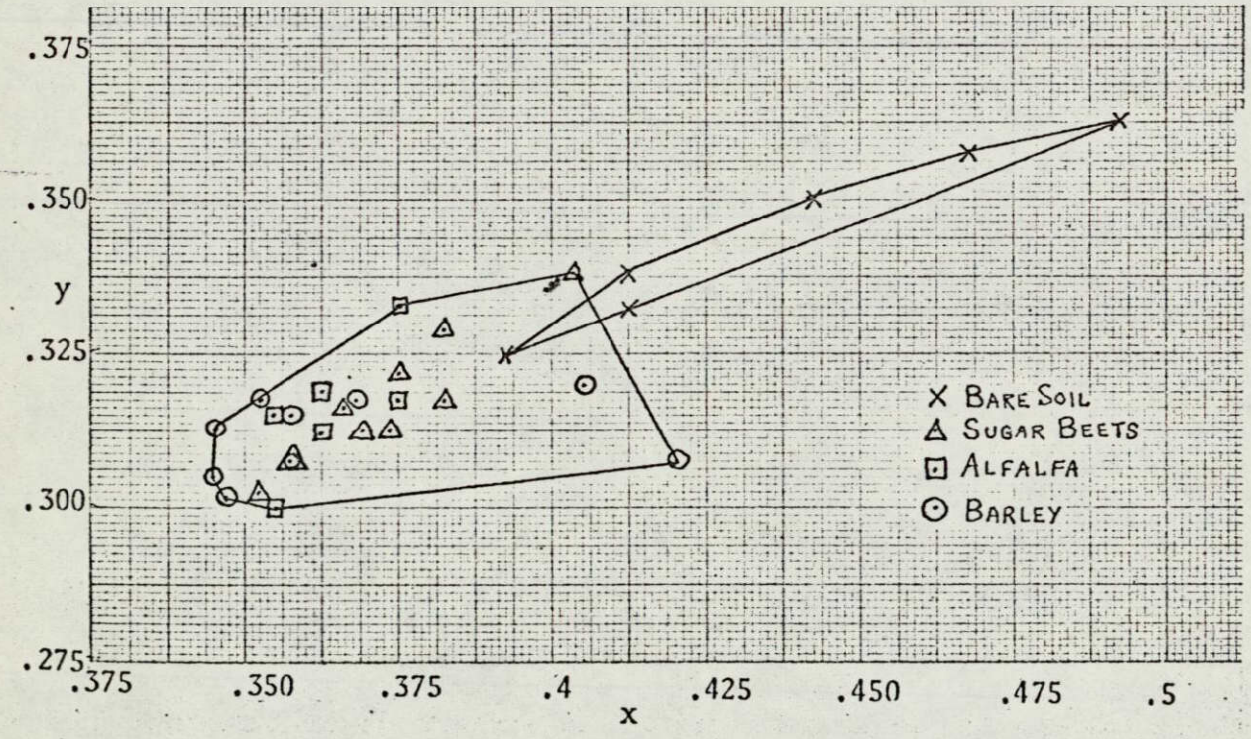

FIGURE 74 : CHROMATICITY OF VEGETATION AND BARE SOIL IMAGES APPEARING IN THE ABOVE COLOR PHOTOGRAPH.

is generally characteristic. Chromaticity differences between images appear to be due to saturation differences.

Figure 74 below the reproduction of the space photograph is an enlargement of a number of image color measurements. The convex set of all chromaticity measurements of the three crops has been plotted along with the convex set of all soil chromaticity measurements. It is significant that the set of measurements of soil and vegetation image colors overlap on subtractive color film, as can be seen in this figure.

The color characteristics of a small number of different crop types and idle fields obtained by Long Island University on Aerial Ektachrome (#8442 emulsion) during the Apollo 9 underflight were measured on the NASA release color duplicate. The original photography was obtained at 1536 Pacific Standard Time on 8 March 1969.

These data which are plotted in Figure 75 show entirely different color characteristics than the associated space color photography analyzed previously. It is uncertain whether this difference can be attributed to: (a) different fields being measured, (b) different taking emulsions, (c) different processing techniques, (d) different duplicating stock, (e) atmospheric effects or sun angle at time of exposure. It is clear however, that it is not possible to relate an image uniquely with a ground object forming it by a measurement of image color on conventional subtractive color film.

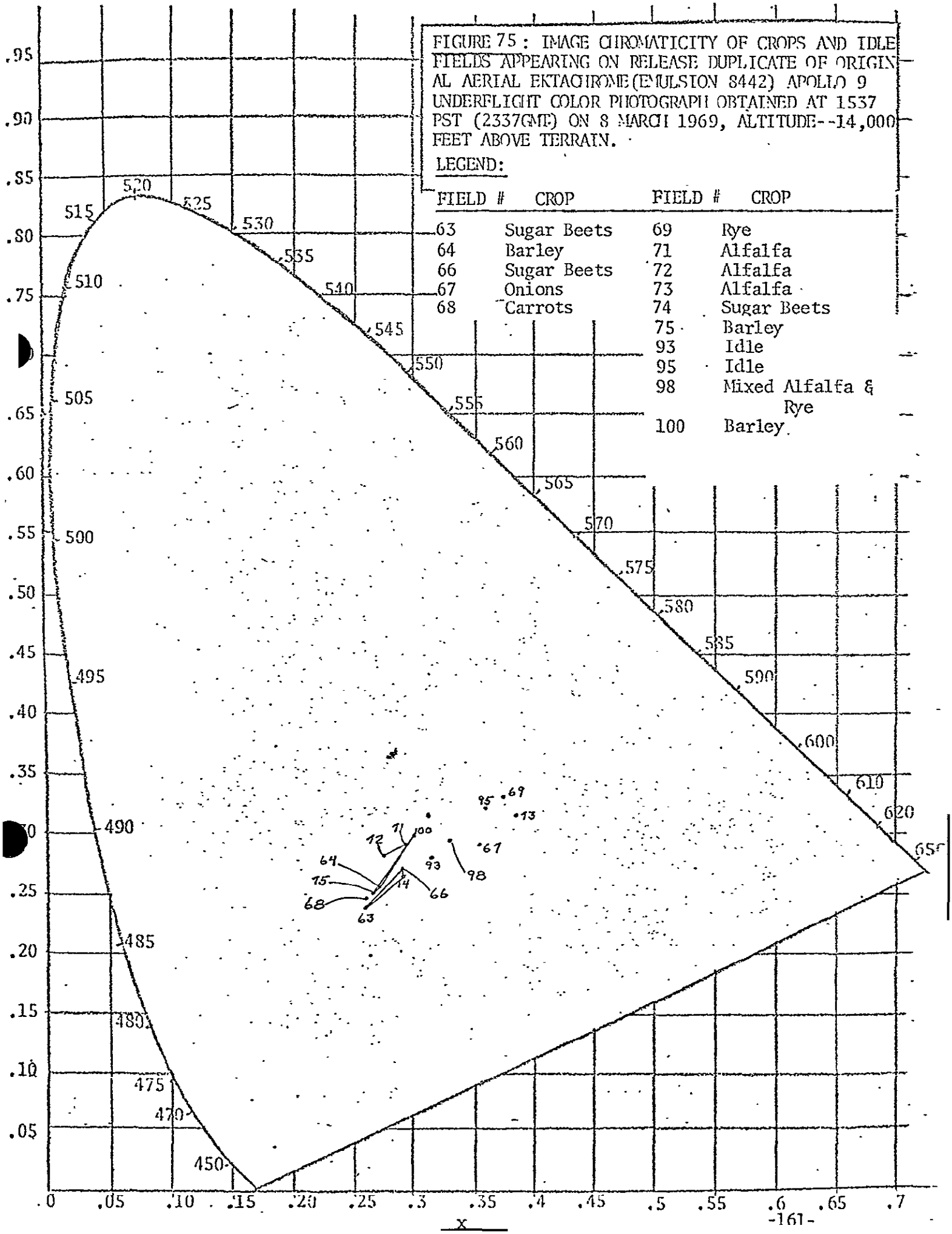

FIGURE 75 : IMAGE CHROMATICITY OF CROPS AND IDLE FIELDS APPEARING ON RELEASE DUPLICATE OF ORIGINAL AERIAL EKTACHROME (EMULSION 8442) APOLLO 9 UNDERFLIGHT COLOR PHOTOGRAPH OBTAINED AT 1537 PST (2337GMT) ON 8 MARCH 1969, ALTITUDE--14,000 FEET ABOVE TERRAIN.

LEGEND:

FIELD #	CROP	FIELD #	CROP
63	Sugar Beets	69	Rye
64	Barley	71	Alfalfa
66	Sugar Beets	72	Alfalfa
67	Onions	73	Alfalfa
68	Carrots	74	Sugar Beets
		75	Barley
		93	Idle
		95	Idle
		98	Mixed Alfalfa & Rye
		100	Barley

SECTION 9

MULTISPECTRAL SENSING OF COASTAL ENVIRONMENTS IN THE COLORADO RIVER ESTUARY

Excellent multispectral space photography was obtained of the Colorado River mouth and of the extreme northern part of the Gulf of California in SO65 frame #3781. This set of multiband imagery was obtained on 11 March 1969 at an altitude of 126 nautical miles at 1614 GMT (0814 Pacific Standard Time). The sun was at an elevation of approximately 31 degrees above the horizon.

An analysis of the relative ability of the reprocessed green (460-610nm), red (580-700nm) and infrared (700-900nm) bands for imaging upper layer phenomena and bottom effect in the estuary was performed. The results showed considerable image detail in the red and green bands. No information relating to the water mass was contained in the infrared band. Correlation of green and red band log exposure with nominal chart depths was apparent to about 40 feet of water depth.

Additive color reconstruction of the SO65 multiband imagery showed it was possible to selectively emphasize upper layer phenomena and bottom effect by color enhancement.

The blue sensitive dye layer of conventional color film showed no relationship whatever with water depth although both the green and red sensitive layers did indicate correlation of image density with mean low water soundings on hydorgraphic charts of the estuary.

A comparative analysis of similar images on infrared color film

and on multiband additive color renditions indicated that the multiband additive color presentation had at least 10 times more capability in discriminating subtle detail in the water. The extreme care that was used in reprocessing the SO65 multiband photography insured that water detail was not an artifact of the photographic process.

Conventional colorimetric analyses using CIE coordinate transformations showed no significant correlation of image color and water depth as recorded on hydrographic charts of the area.

Ground Truth Data

A hydrographic chart, corrected to the March 1969 Notice to Mariners, is shown in Figure 76 . Thereon are marked the locations of the image measurements made on the SO65 and Gemini photography discussed in subsequent paragraphs of this section. A determined effort was made to make the densitometric measurements on the photographs as accurate as possible with respect to this chart. Of course, the usual attention was directed to the relative precision in repeatably measuring the same image within each photograph.

Water depths on this chart are shown in fathoms (one fathom equals six feet) at mean low water. Both tidal variations and shifting bottom will change the relative depths between the points measured as well as the absolute depths given on the chart. Available data indicate that it is not possible to determine tidal depths by normal use of tide tables in this part of the Gulf of California. Abnormally large tidal ranges are reported to exist (Sherman, 1970).

FIGURE 76: HYDROGRAPHIC CHART OF THE COLORADO RIVER ESTUARY AND EXTREME NORTHERN PART OF THE GULF OF CALIFORNIA. ANNOTATIONS SHOW LOCATIONS OF IMAGE DENSITOMETRIC MEASUREMENTS MADE ON SO65 AND GEMINI PHOTOGRAPHS.

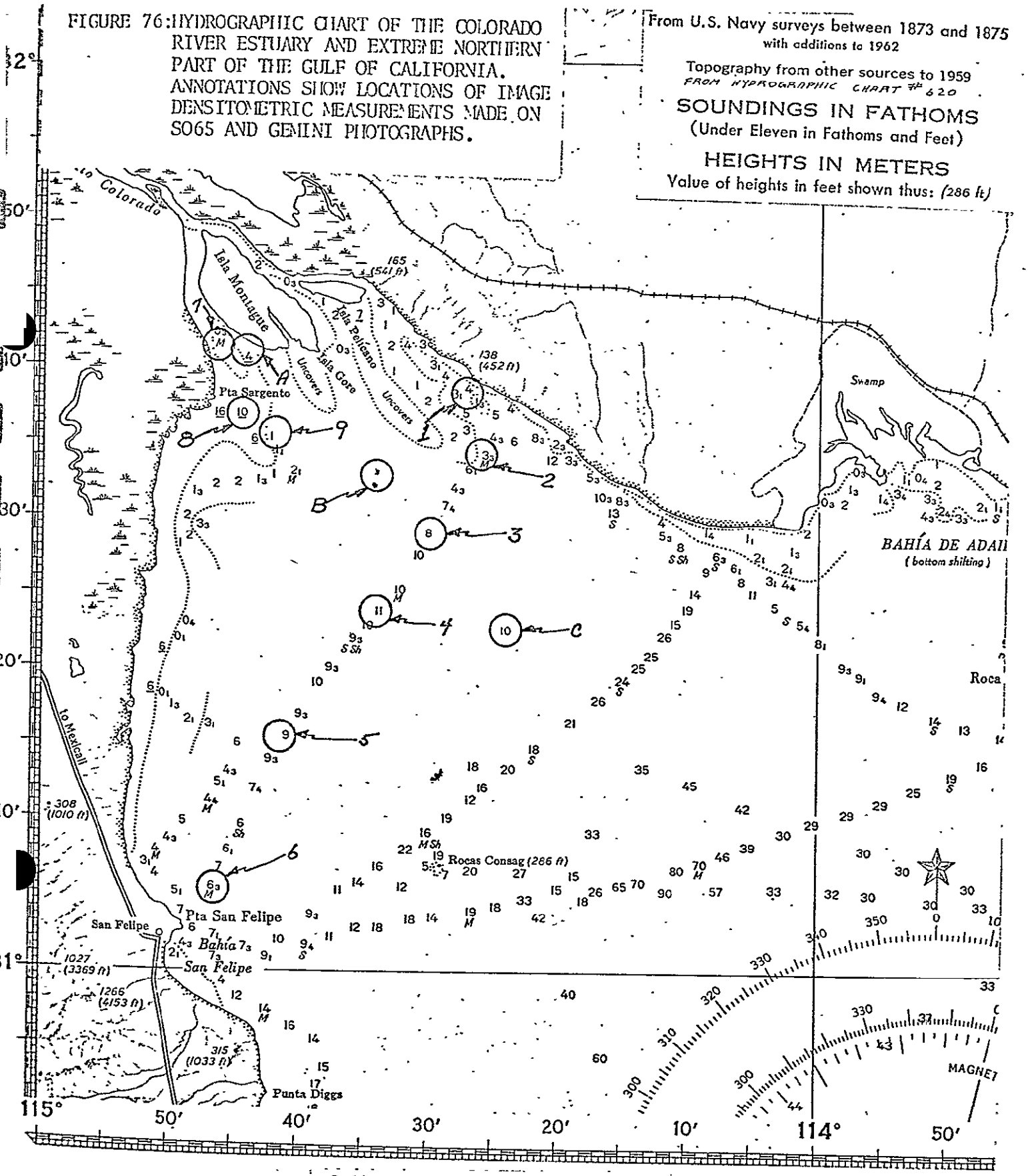

Golfo de California—Northern Part

SOUNDINGS IN FATHOMS—SCALE 1:639,400

Figure 77 shows a geologic map of the area surrounding the mouth of the Colorado River. The major land forms and character of the shore area in this northern part of the Gulf of California should be particularly helpful to the photo geologists in an examination of the multispectral color photographs in Figures 84 and 86 .

Analysis of Black-and-White S065 Imagery

The four black-and-white S065 photographs appearing in Figures 78, 80 and 81 have been included to demonstrate the comparative detectability of water phenomena in the Colorado River estuary in the green, red and infrared bands as well as on color infrared film. The multiband photography was reprocessed from first generation duplicate positives, supplied by NASA, by going through an internegative.

It is evident that even though the infrared multispectral photo has been printed to bring out low contrast images (at the expense of shore detail), little, if any, information relating to either suspended particulant or bottom effect can be detected in this band of the spectrum (700-900nm).

The situation is quite different in the green and red bands where conditions which are anomalous with respect to deeper water further to the south are being detected in the estuary. The phenomena imaged in the 460-610nm green band are clearly different from that depicted in the 580-700nm red band.

In coastal aquatic environments, it is difficult to say with certainty just what effect causes this difference which is perceived in

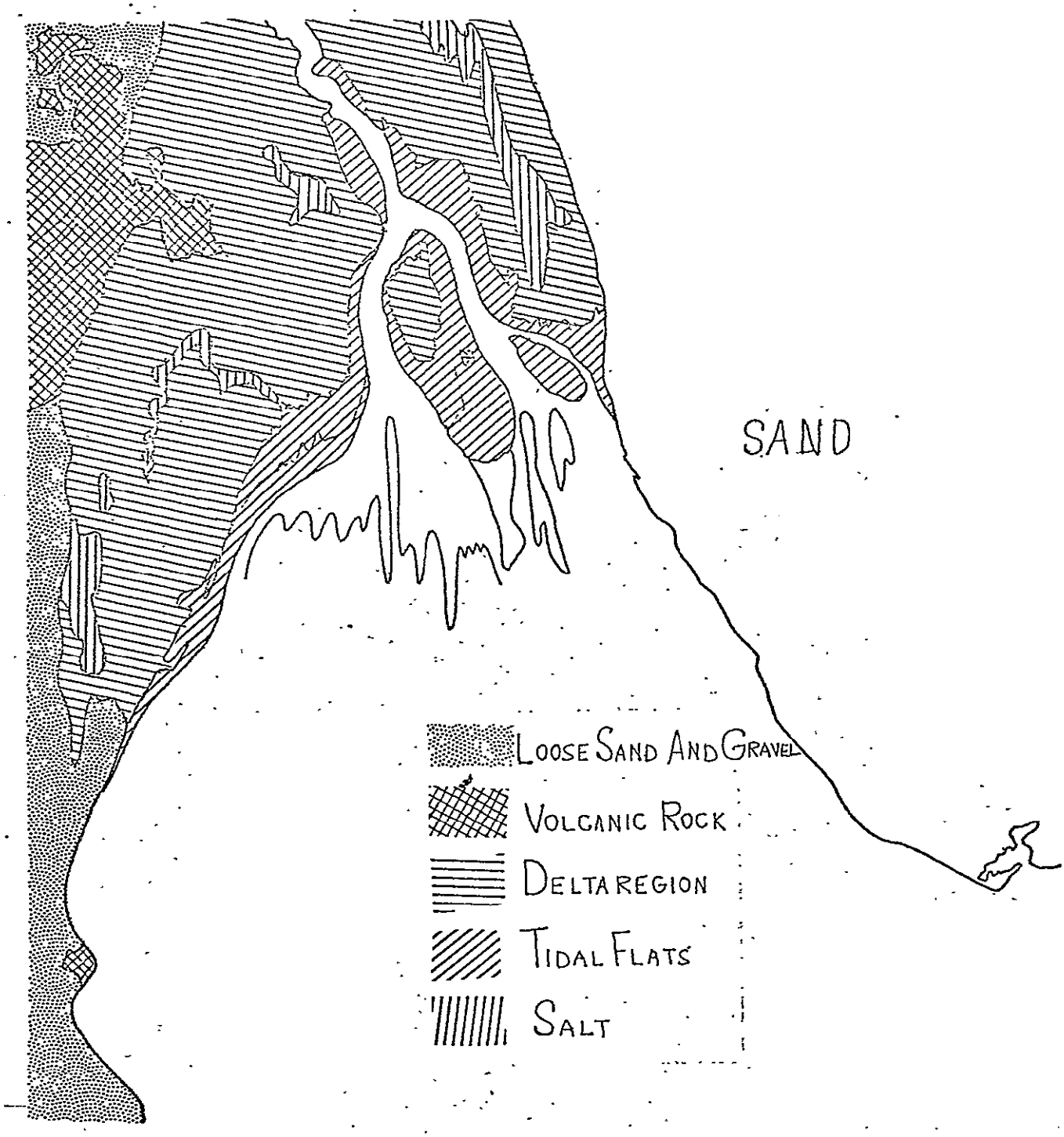

FIGURE 77: GEOLOGIC MAP OF LAND AREAS BORDERING THE COLORADO RIVER ESTUARY.

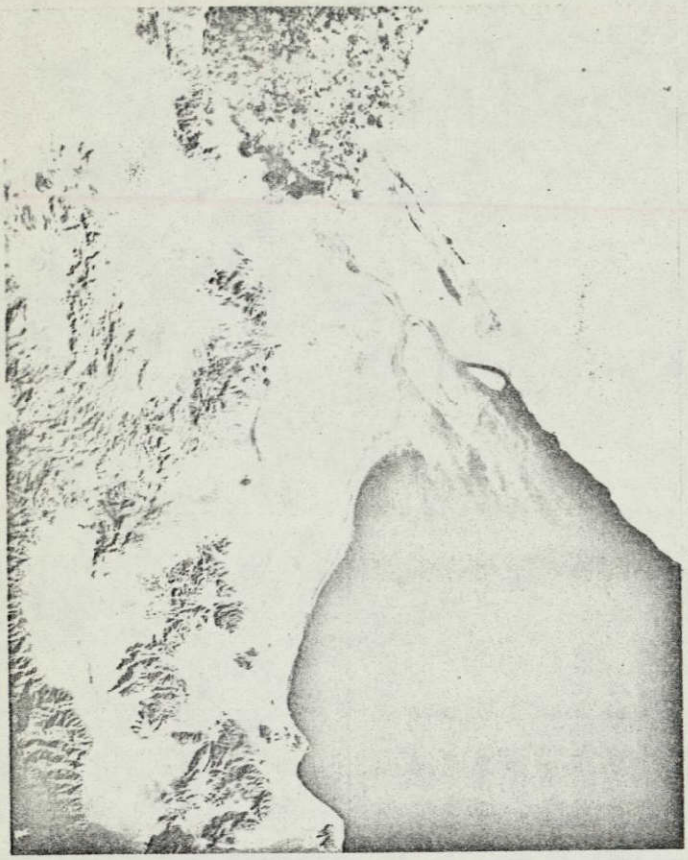

FIGURE 78 : ENLARGMENT OF PORTION OF THE S065 FRAME #3781 SHOWING ESTUARIAN EFFECTS IMAGED IN THE 580 TO 700 NM BAND.

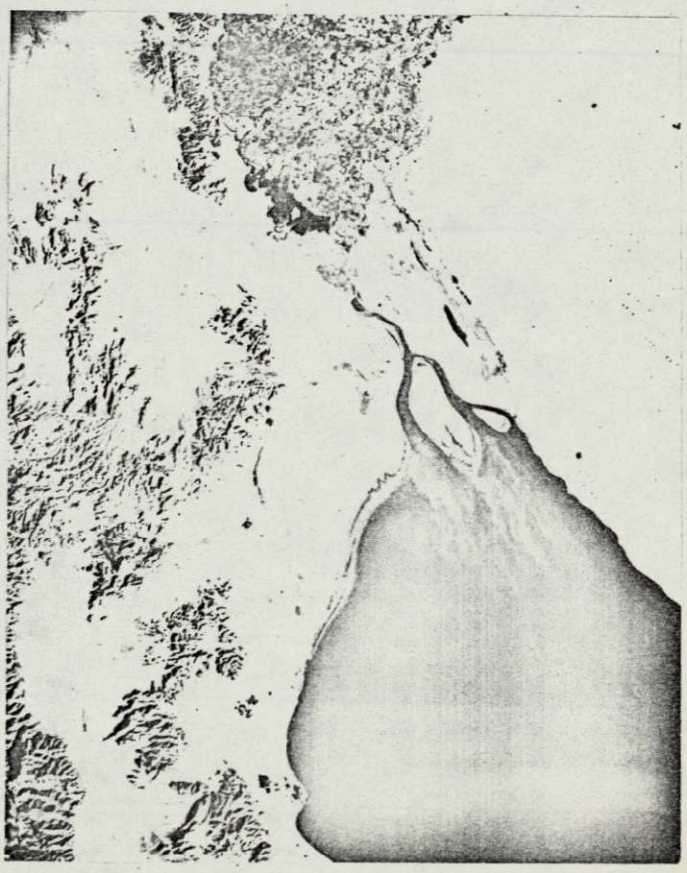

FIGURE 79 : INFRARED COLOR, BLACK AND WHITE ENLARGEMENT OF S065 COLOR INFRARED PHOTO. DUPLICATION WAS PERFORMED TO ACHIEVE THE MAXIMUM WATER DETAIL. TOTAL SENSITIVITY OF THE THREE DYE LAYERS 510 TO 900 NANOMETERS.

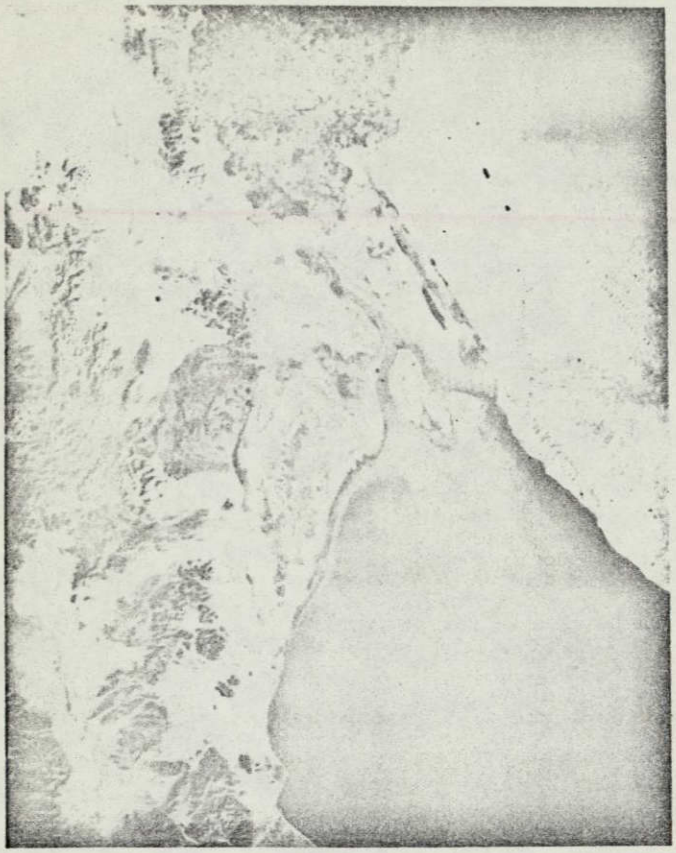

FIGURE 80 : GREEN BAND
WATER EFFECTS IN THE COLORADO RIVER ESTUARY WERE EMPHASIZED IN PRINTING THIS REPRODUCTION SENSITIVE TO THE 460 TO 610 NANOMETER BAND.

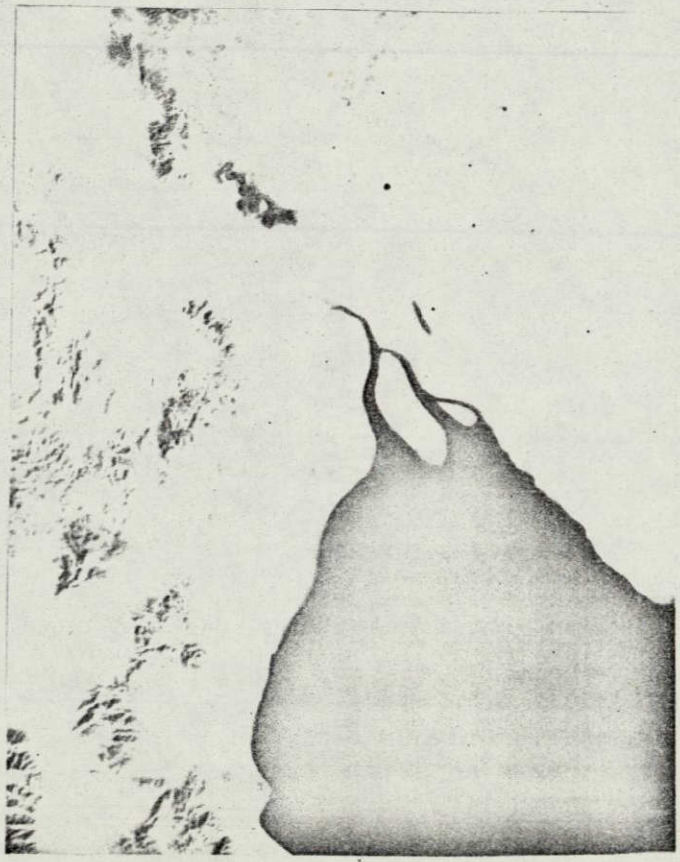

FIGURE 81 : INFRARED BAND

THIS ENLARGEMENT OF S065 FRAME # 3781 WAS EXPOSED FOR MAXIMUM WATER DEFINITION IN THE 700 TO 900 NANOMETER BAND.

the images. The transmission properties of sea water suggest that due to the greater optical penetration of green light, the bottom effect is detected in the green band and suspended particulant in the red (Jerlov 1968, Sharkov and Kurditsk 1956, Yost and Wenderoth 1968). However, recent research has suggested that this condition can be significantly altered by the amount and size of suspended particulant in the water mass (Yost and Wenderoth 1970). When the particle sizes are large and dense, even the green wavelengths are absorbed and consequently it is the longer wavelengths which penetrate to greater depths.

A comparative analysis of the density on each of the three multispectral black and white first generation duplicate positives of S065 frame #3781 suggests that this might be the situation being depicted in this multiband space photography. Figure 82 shows a graph of the water depth as recorded on the associated hydrographic chart (Figure 76) as a function of image density. It can be seen that both the red and green bands show correlation for water depths between 3 and 40 feet. However, in the red band the effect is more pronounced but somewhat more irratic as indicated by the deviations of the points from the regression line. There is no correlation between depth and image density in these visible bands for indicated depths greater than 40 feet. This figure also shows that density and water depths are essentially uncorrelated in the infrared band (700-900nm).

To remove the effects of differential processing which is a common problem with multiband photography (Yost and Wenderoth 1967), the

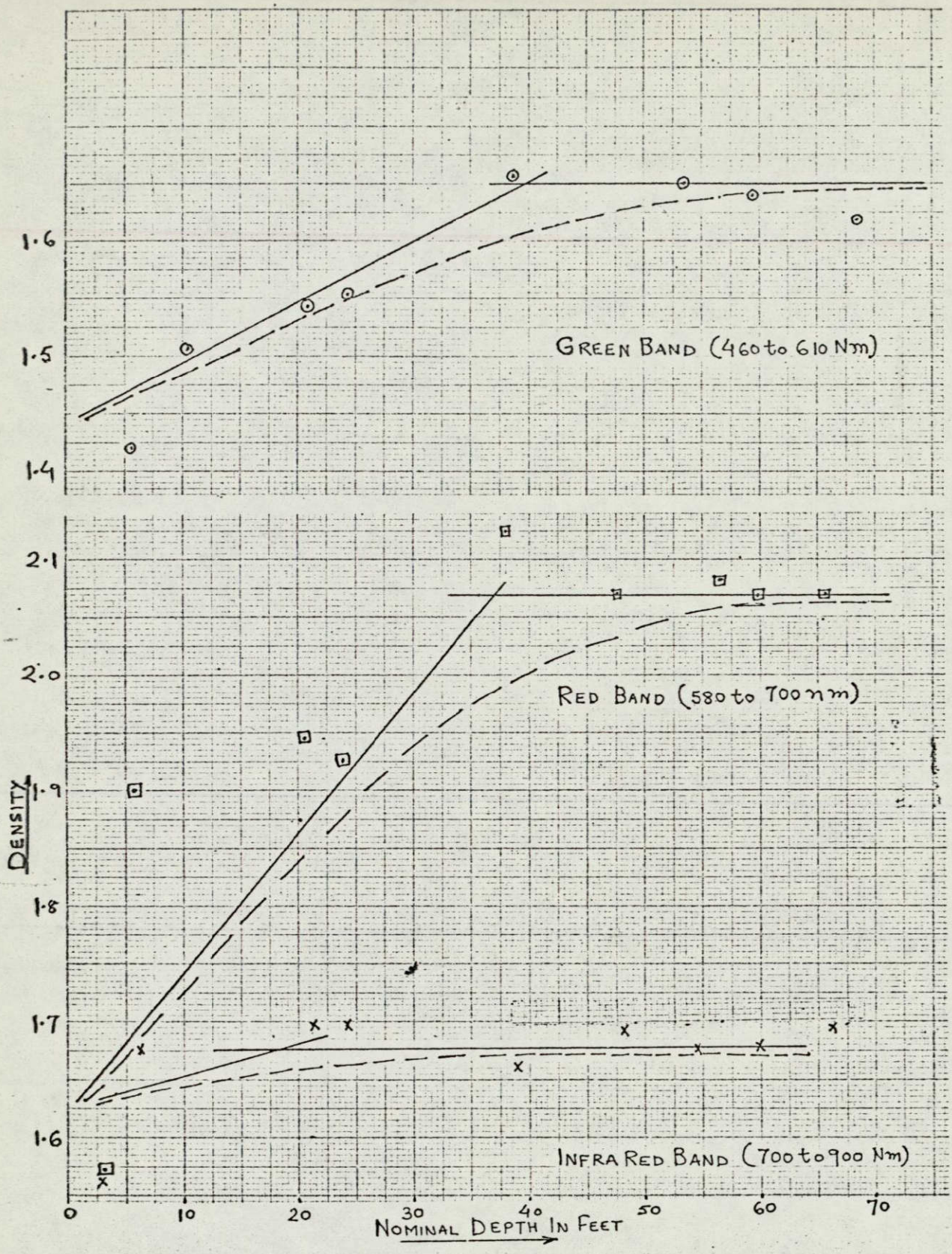

FIGURE 82: IMAGE DENSITY VERSUS DEPTH ON FIRST GENERATION POSITIVE OF APOLLO 9 SO65 MULTIBAND PHOTOGRAPHY FRAME #3781.

density data have been replotted in terms of nominal exposure (meter candle seconds). The infrared as well as the visible exposure can be expressed in terms of equivalent photometric exposure in the sensitometric data since the spectral distribution of the image forming energy is known (Data Corp. 1969).

These data shown in Figure 83 again show that:(1) the image forming energy in the infrared band is unrelated to depth and has a range of 0.20 log exposure units, (2)the log exposure in the green band is expanded compared to the density on the green spectral photo and is surprisely well correlated with depth between 3 and 40 feet; the log exposure range is 0.42 m.c.s., (3) the red band shows the greatest correlation with depth with a 0.92 m.c.s. log exposure range.

The reader should note that in the black-and-white reproduction of the associated color infrared S065 photo (Figure 79), the image detail in the water appears to more closely correspond to the red band multispectral image (Figure 78). Some detail shown in the green band (Figure 80) can also be detected. There appears to be absolutely no addition to the water image detail contributed by the infrared band (Figure 81).

Additive Color Analyses of Multispectral Photographs

A multispectral additive color rendition of S065 frame #3781 is shown in Figure 84 . In this rendition the green band has been projected as green, the red band projected as red and the infrared band

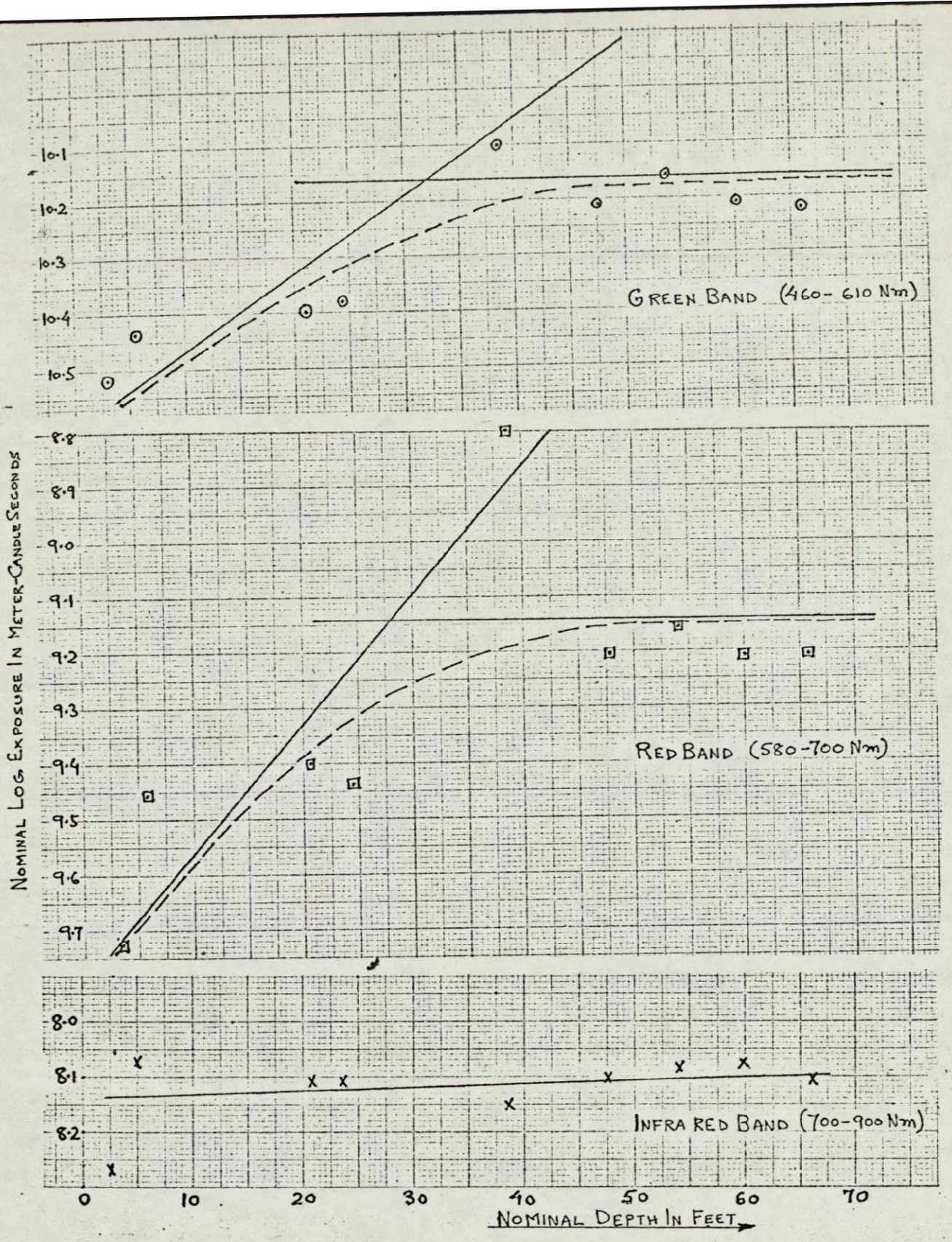

FIGURE 83: EQUIVALENT LOG EXPOSURE VERSUS DEPTHS OF THE COLORADO RIVER ESTUARY AS COMPUTED FROM AN S065 MULTIBAND FIRST GENERATION POSITIVE #3781 ALONG WITH PRE AND POST FLIGHT SENSITOMETRY.

as blue. Qualitatively from an interpretative standpoint, it is obvious that chromatically enhanced water detail is present in the multispectral color image.

An analysis of the relationship between the optical density of the blue, green and red image forming layers has been made to test for the presence of any bottom effect in the image. The results presented in Figure 85 show reasonably good correlation of water depth with the image density of the color image (up to 40 feet) in both the green and red image colors. The slight relationship of water depth and image density in the infrared band probably results from "cross talk" between the green and blue images due to the manipulation of the color space in the additive color viewer. The reader should note that the density measurements shown in Figure 85 were made from color transparencies which in turn were made of the image on the viewer screen.

Figure 86 shows another multispectral additive color rendition. The color space in this presentation was adjusted to emphasize sub-surface water detail which appeared to be primarily bottom effect. The data appearing in Figure 87 support the contention that phenomena in the lower water layers are being detected. Not only is there good correlation in the blue and green images at depths up to 40 feet but also to the depth of 66 feet in the red image. The variation of the individual points about the red image regression line is considerable, however.

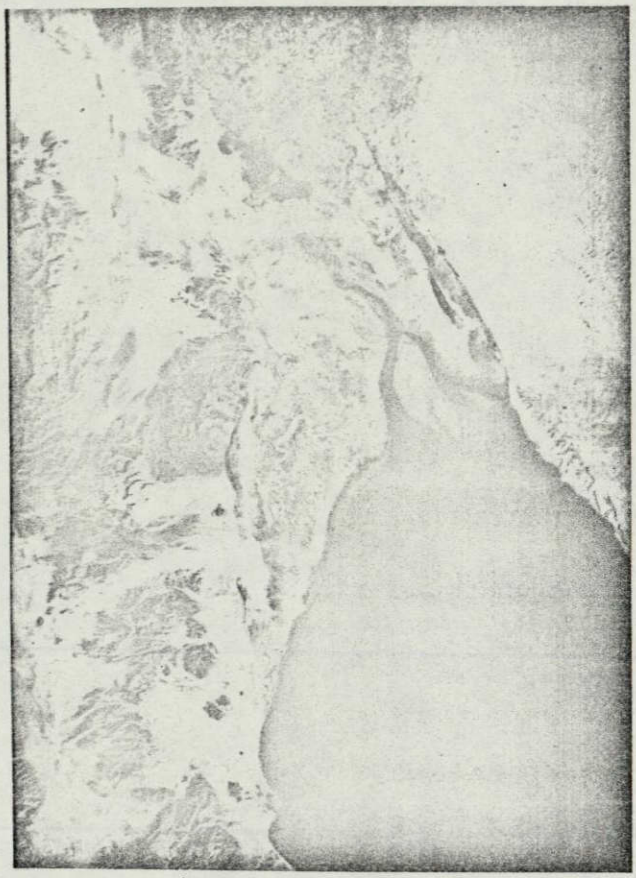

FIGURE 84 : MULTISPECTRAL ADDITIVE COLOR RENDITION OF SO65 FRAME #3781 GREEN BAND IS PROJECTED AS GREEN, RED BAND PROJECTED AS RED AND INFRARED BAND AS BLUE. IMAGE COLOR EMPHASIZES UPPER WATER DETAIL.

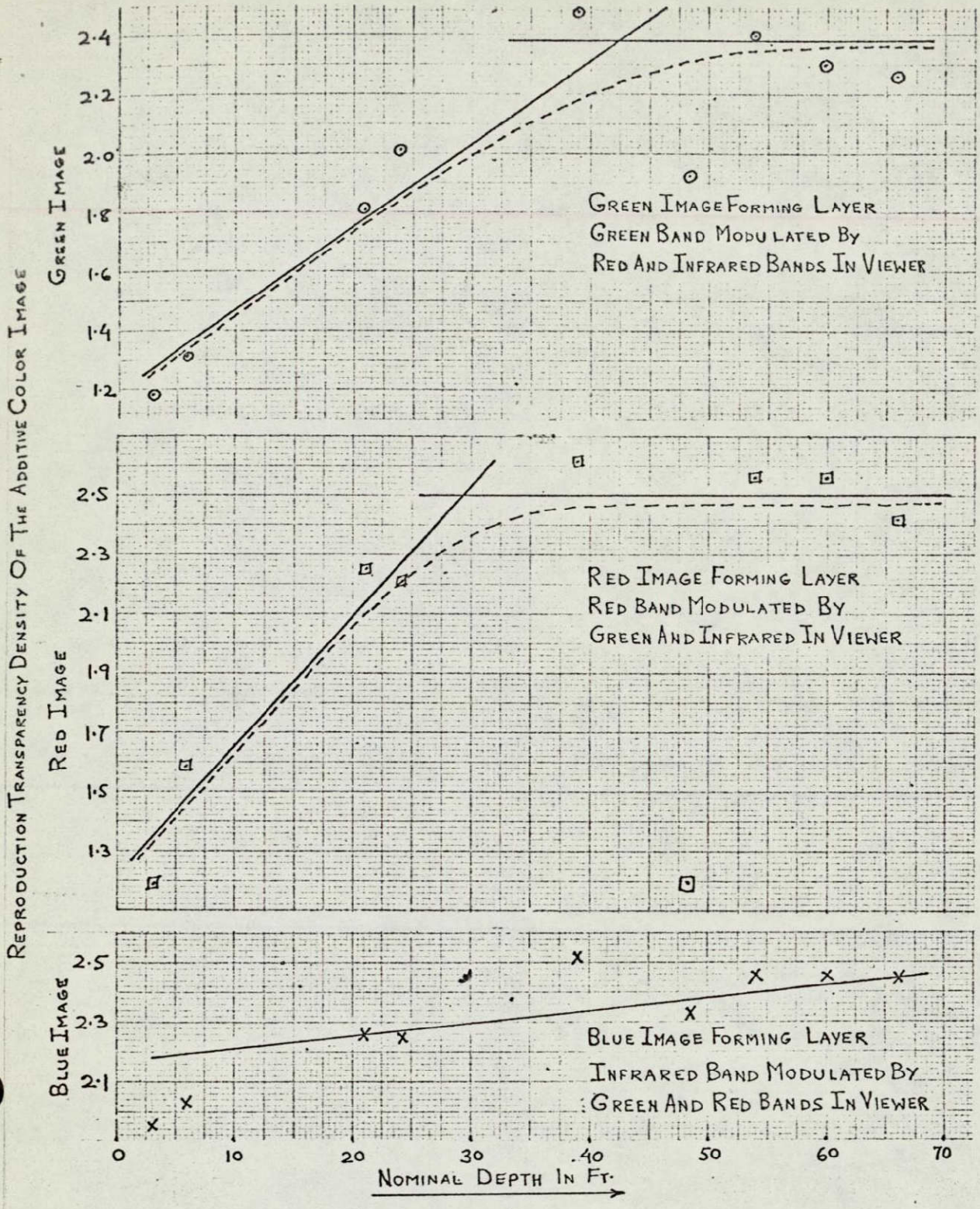

FIGURE 85 : TRANSPARENCY REPRODUCTION COLOR DENSITIES IN THE BLUE, GREEN AND RED IMAGE FORMING LAYERS OF THE ADDITIVE COLOR COMPOSITE OF SO65 MULTIBAND PHOTOGRAPHY SHOWN ON PRECEDING PAGE.

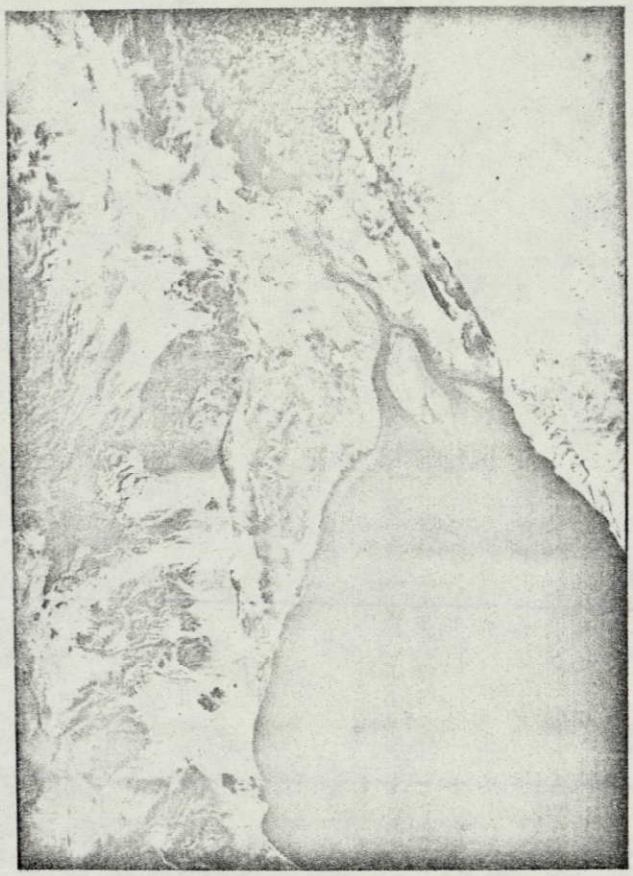

FIGURE 86 : S065 FRAME #3781 MULTI-SPECTRAL ADDITIVE COLOR RENDITION. GREEN BAND PROJECTED AS RED, RED BAND PROJECTED AS BLUE AND INFRARED BAND AS GREEN. THIS COLOR RENDITION CHROMATICALLY EMPHASIZES DETAIL IN THE LOWER WATER LAYERS INCLUDING BOTTOM (SEE FIGURE 87).

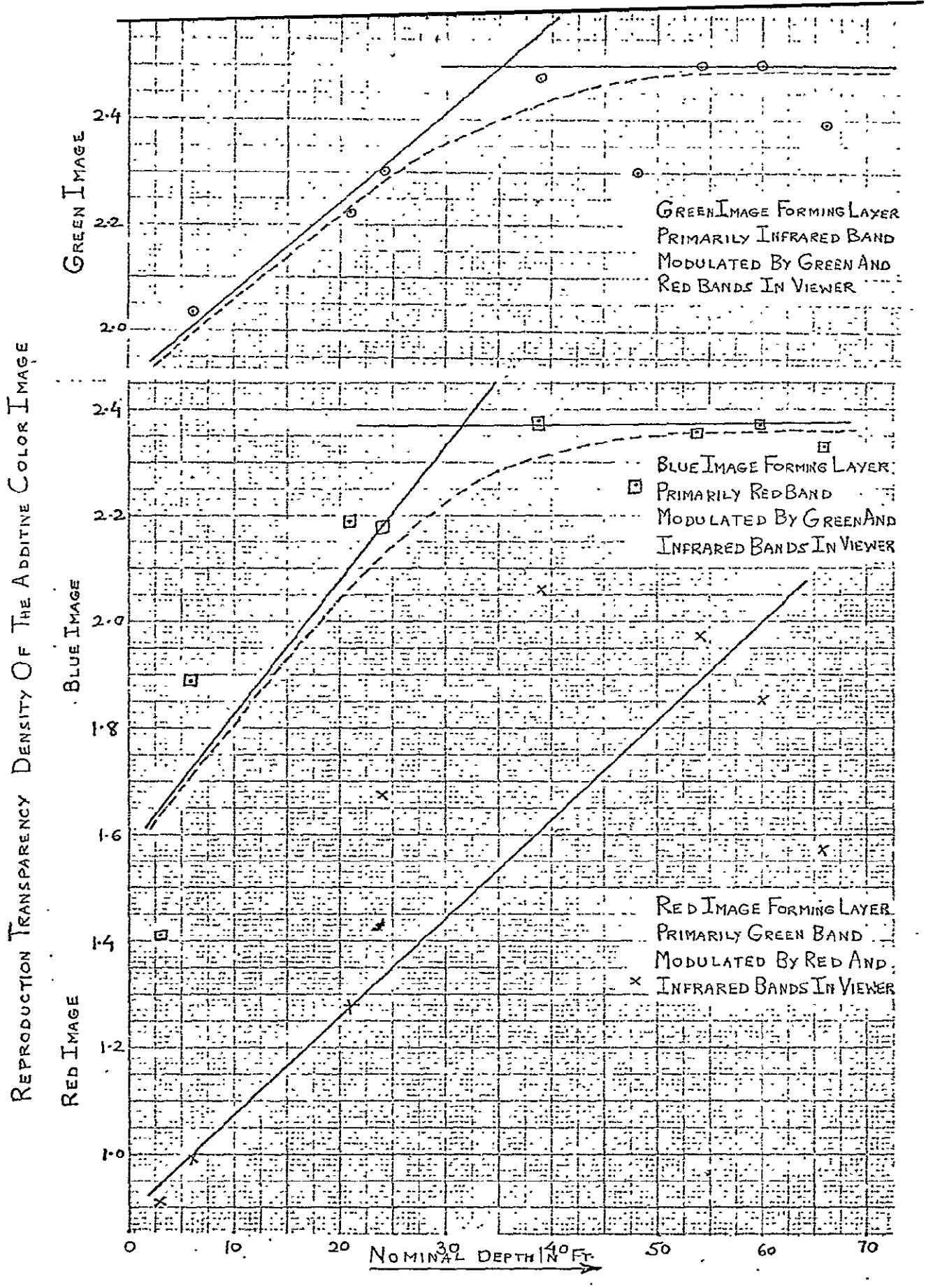

FIGURE 87 : DENSITIES OF THE TRANSPARENCY REPRODUCTION OF THE ADDITIVE COLOR VIEWER RENDITION OF S065 MULTIBAND PHOTOGRAPH SHOWN ON THE PRECEDING PAGE.

Colorimetric Analysis of Color Infrared Photograph

The SO65 color infrared photograph associated with frame number 3781 was colorimetrically analyzed. The same image areas in the Colorado River Estuary that were measured on the additive color images were densitometrically measured on each dye layer of the first generation release color infrared transparency. Using the same computer program, the dye layer densities were transformed into chromaticity coordinates. The intent of this analysis was to establish the extent to which color and dye layer density were related to nominal water depths in the estuary.

As can be seen from Figure 88 , the greatest image density range appears in the blue and green image forming layers. When imaged through the Photar 15 filter, at unity sensitivity, the blue image forming layer is sensitized by green radiation in the 500-600nm part of the spectrum; the green band is sensitized by the red radiation in the 500-700nm portion of the spectrum; and the red image forming layer is sensitized by the infrared radiation in the 580-890nm part of the spectrum.

As can be seen from the curves in Figure 88 , the greatest correlation in all three bands appears for water depths between zero and thirty feet. The infrared band shows the least density range. The fact that the infrared band shows any density variation in the water area at all is probably due to the "cross talk" between the red and infrared sensitive dye layers on the SO180 color infrared emulsion.

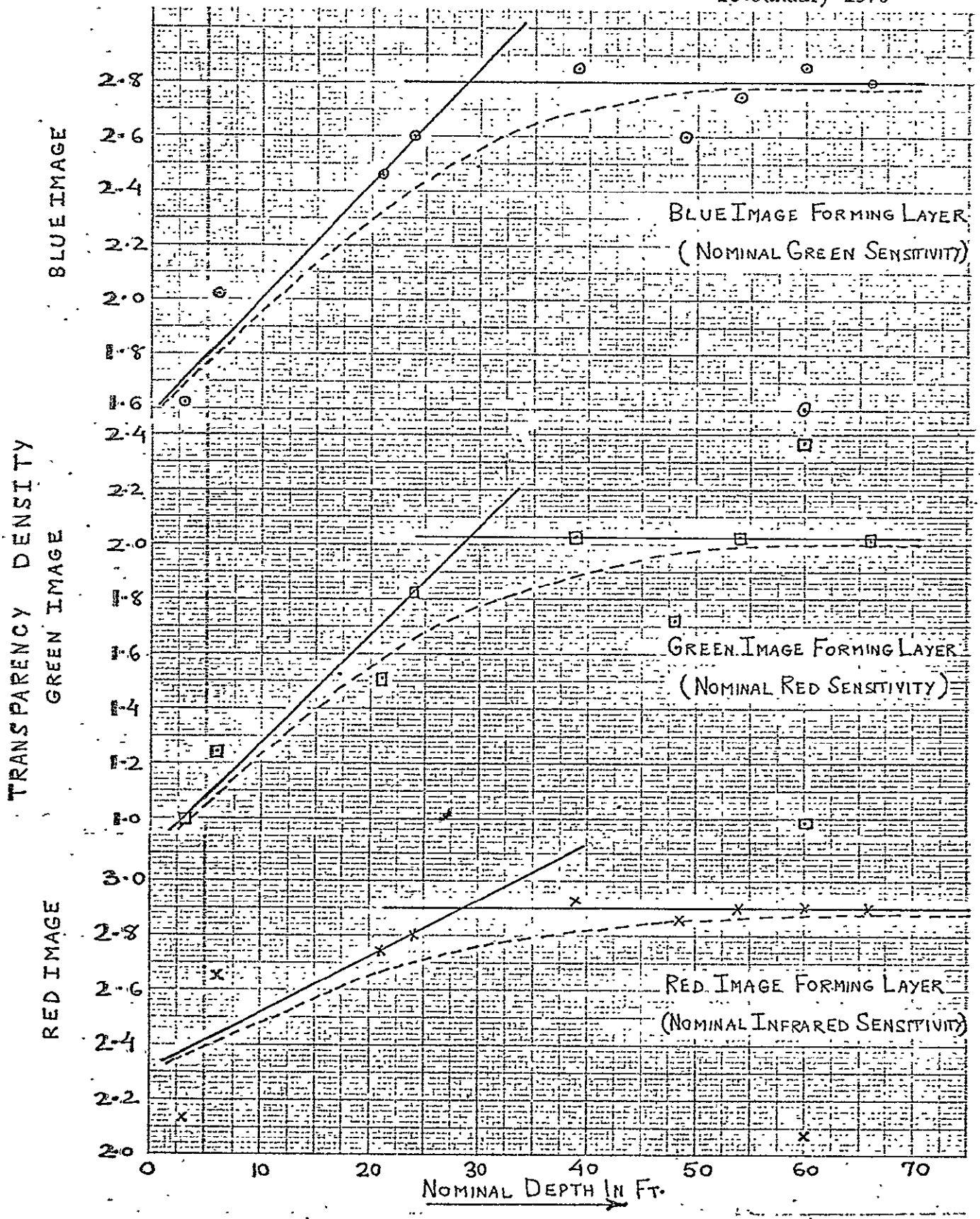

FIGURE 88 : SO65 COLOR INFRARED DYE LAYER DENSITIES IN THE BLUE, GREEN, AND RED IMAGE FORMING LAYERS AS A FUNCTION OF NOMINAL WATER DEPTH.

Densitometric Analysis of Gemini Photography

A color reproduction of Gemini IV photography frame #S-65-34673 taken on 5 June 1965 was densitometrically analyzed. This color film image was processed by the Precision Photo Laboratory at the NASA Manned Spacecraft Center. The original film was Kodak SO217(MS Ektachrome).

The data presented in Figure 89 show that there is no relation between nominal water depth and image density in the blue image forming layer. Correlation does exist, however, in both the green and red sensitive layers. Note that the variation of the data points from the regression line is less when the nominal water depths are under 25 feet.

Comparison of Multispectral Additive Color and Color Infrared Film

The comparative usefulness of the photographic infrared (either black-and-white multispectral photography or the infrared sensitive dye layer of infrared color film) for water studies has been questioned on theoretical grounds due to the almost total absorption of infrared radiation by water. In order to quantitatively evaluate the usefulness of the photographic infrared for recording either suspended particulant or bottom effects, a number of density measurements were made on: 1) transparency reproductions of the color image on the additive color viewer screen and 2) on the associated infrared color transparency.

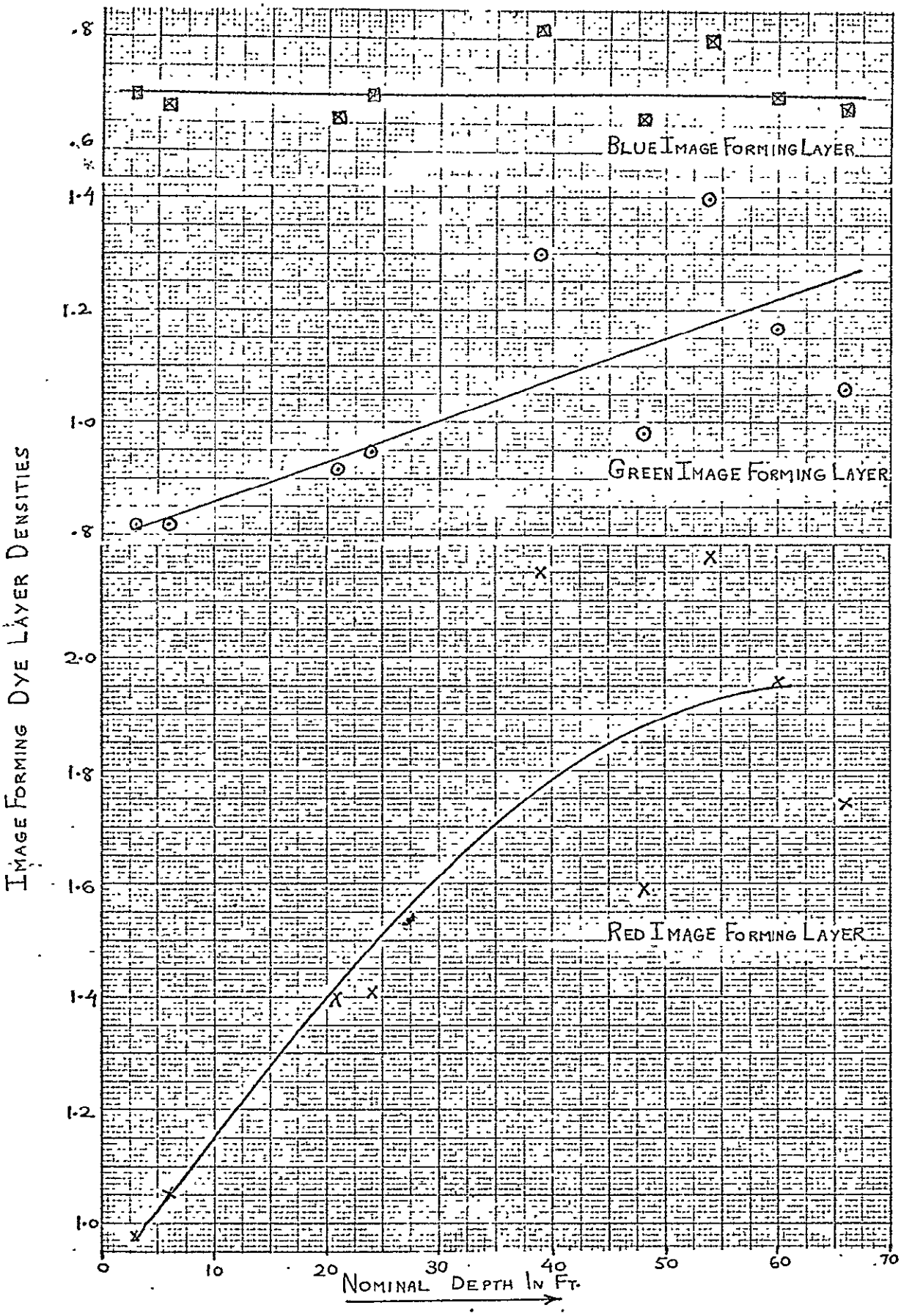

FIGURE 89: IMAGE FORMING DYE LAYER DENSITIES VERSUS NOMINAL WATER DEPTH IN GEMINI IV PHOTOGRAPH FRAME #S-65-34673.

TABLE 12

IMAGE DENSITIES OF TRANSPARENCY COPIES OF THE ADDITIVE COLOR VIEWER SCREEN AND OF INFRARED COLOR FILM APOLLO 9 SO65 FRAME NUMBER 3781.

	FIGURE (CX15-4) MULTISPECTRAL TRANSPARENCY			FIGURE (CX15-6) MULTISPECTRAL TRANSPARENCY			INFRARED COLOR FILM		
FILM SENSITIVE TO	GREEN	RED	IR	GREEN	RED	IR	GREEN	RED	IR
PROJECTED AS	GREEN	RED	BLUE	RED	BLUE	GREEN	BLUE	GREEN	RED
A. Colorado River	1.28	1.34	2.03	.96	1.48	1.81	1.11	1.78	2.63
B. Punta Sargento	1.92	2.46	2.37	1.44	2.35	2.36	1.72	2.70	2.68
C. Gulf of Calif.	2.35	2.66	2.51	2.08	2.47	2.60	2.00	2.82	2.66
Density(C minus A)	1.07	1.32	.48	1.12	.99	.79	.89	1.04	.03

From the above table, it is evident that a very small density difference between the relatively shallow turbid Colorado River and the comparatively clear and deep Gulf of California exists on infrared color film (.03 density difference in the above table). However, note that it was possible to increase the density difference between these two water masses on the infrared forming image to between .48 and .79 in the multispectral rendition. This suggests that multispectral photography incorporating the infrared as one of the bands might be useful in modulating the chromatic effects of the visible bands in an additive

color display and thus be quite beneficial in the environmental studies of coastal waters.

Colorimetric Image Analysis

Plotted in the following chromaticity diagrams are the CIE coordinates of the two multispectral photographs depicted in Figures 84 and 86 as well as a Gemini IV photograph (Frame #S-65-34673). The numbers shown on the graph refer to the nominal depth of the water (at mean low water) taken from the hydrographic chart shown in Figure 76 .

Upon examination the reader will observe that there is little, if any, correlation between the chromaticity coordinates and nominal water depth in any of the three images depicted in Figure 90 . Assuming at least the relative water depths are approximately correct, it is clear these data show that both multispectral additive color chromaticity coordinates as well as subtractive color chromaticity coordinates are unrelated to bottom effect in the Colorado River estuary.

As can be seen from the chromaticity plot in Figure 91 , the chromaticity coordinates of images on color infrared SO65 frame number 3781 and water depths are unrelated.

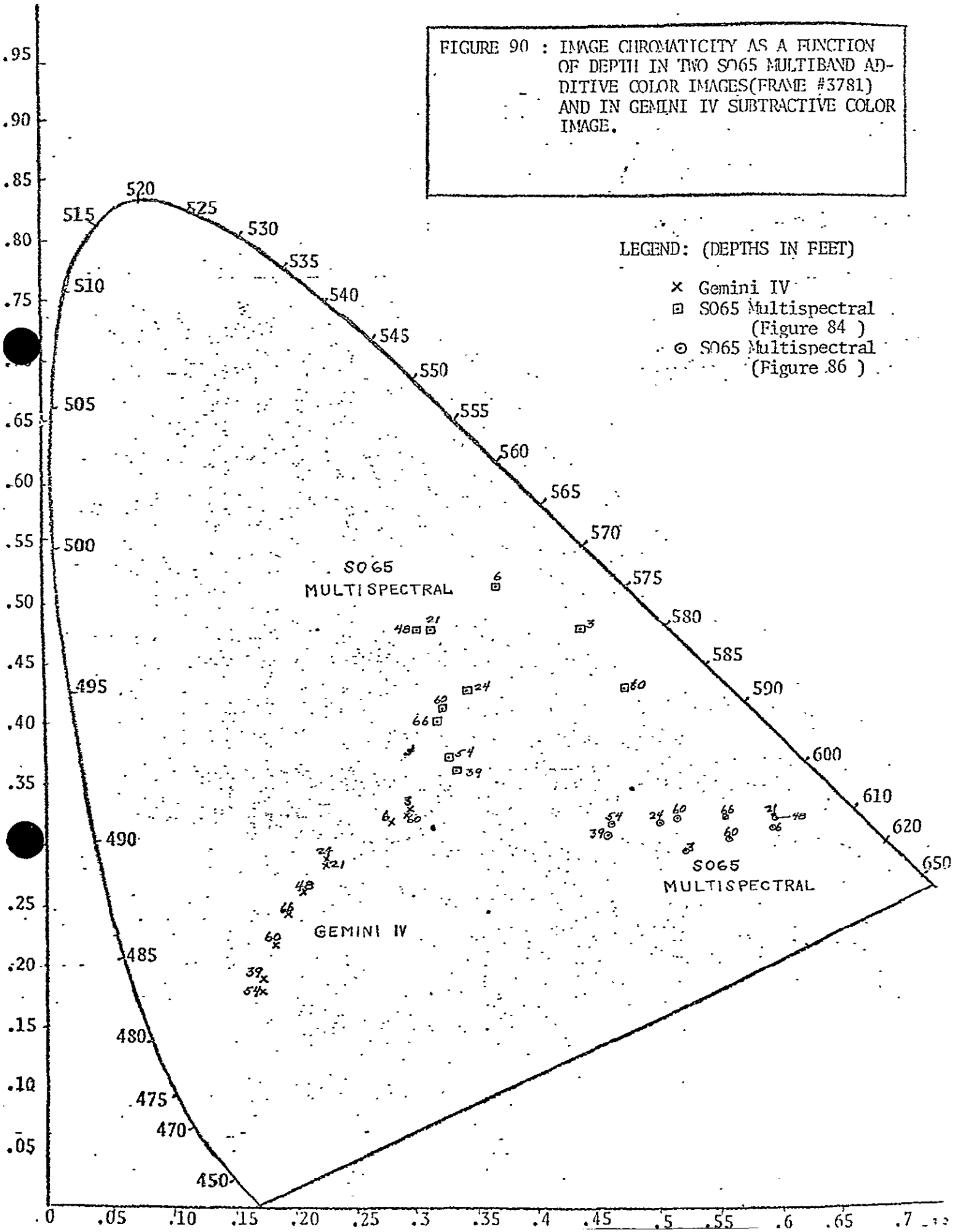
FIGURE 90 : IMAGE CHROMATICITY AS A FUNCTION OF DEPTH IN TWO S065 MULTIBAND ADDITIVE COLOR IMAGES(FRAME #3781) AND IN GEMINI IV SUBTRACTIVE COLOR IMAGE.
LEGEND: (DEPTHS IN FEET)
× Gemini IV
⊡ S065 Multispectral (Figure 84)
⊙ S065 Multispectral (Figure 86)
S065 MULTISPECTRAL
GEMINI IV
S065 MULTISPECTRAL
520
515
525
530
535
540
545
550
555
560
565
570
575
580
585
590
600
610
620
650
510
505
500
495
490
485
480
475
470
450
.95
.90
.85
.80
.75
.65
.60
.55
.50
.45
.40
.35
.25
.20
.15
.10
.05
0
.05
.10
.15
.20
.25
.3
.35
.4
.45
.5
.55
.6
.65
.7

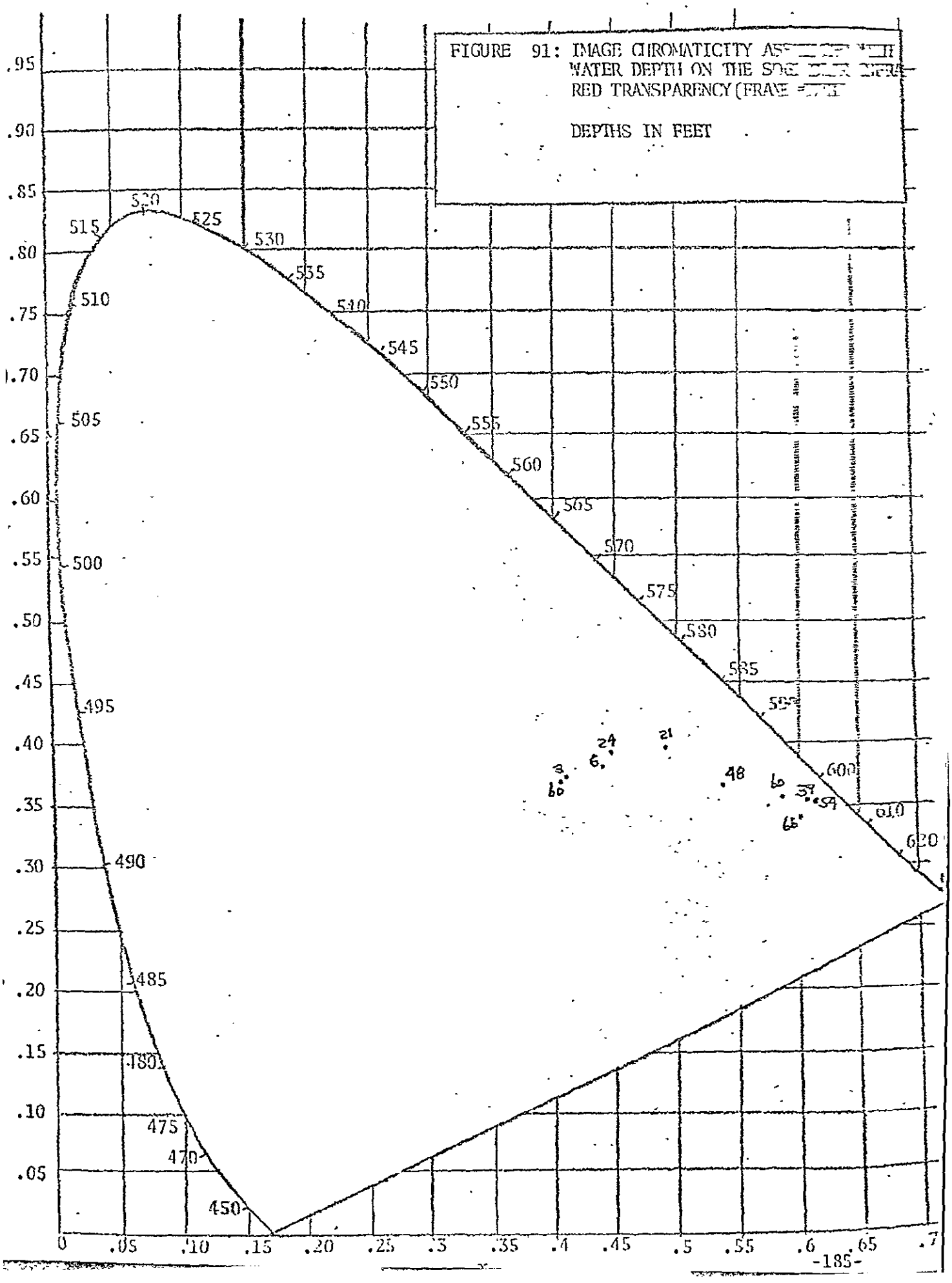

FIGURE 91: IMAGE CHROMATICITY AS[illegible] WITH WATER DEPTH ON THE SO[illegible] RED TRANSPARENCY (FRAME [illegible]

DEPTHS IN FEET

SECTION 10

ADDITIVE COLOR ANALYSIS OF MULTISPECTRAL PHOTOGRAPHY AND VEGETATION CLASSIFICATION BY DENSITY SLICING

SO65 frame number 3801 taken over Phoenix, Arizona at 0928 Mountain Standard Time on 12 March 1969 was reprocessed to correct for the high minimum density and low contrast in the green band. Using a sequence of precise photographic techniques, it was also possible to correct the differential density and gamma relationships in all three bands. These reprocessed positive transparencies proved to be quite good for additive color projection of the multispectral photography.

A number of multispectral additive color renditions were created on the Long Island University additive color viewer, using this reprocessed photography. The resultant color images showed clear differentiation of subtle vegetation detail in the desert area surrounding Phoenix. In addition, considerable agricultural land use information was apparent in the Mesa area.

By using a photographic density slicing technique called "density cut-off" process, it was possible to uniquely classify vegetation appearing in this set of SO65 multispectral photographs. By use of this photographic process, it was possible to achieve both a vegetation map and a vegetation photograph by color identification of those images in the multispectral photography which reflected only in the infrared band. The procedure demonstrates the feasibility of the "density cut-off" technique to reproduce unique classifications of vegetation using strictly a photographic

process. The resultant classification which is produced at the photo scale can readily be compiled on either a black-and-white photograph or a conventional map sheet. It is significant that these results were produced from the multispectral photography and not from the S065 color infrared photograph. To further refine this photographic process it will be necessary to determine the optimum density cut-off points for classification of any arbitrary group of objects and to investigate other methods for displaying the data.

Reprocessing The S065 Photography

The relatively high minimum density of the S065 positives when coupled with the low contrast in the green band, hampered information extraction from the imagery. This condition probably arose from a combination of differential exposure in the three multiband cameras along with incorrect gamma compensation when the original photography was processed.

The green, red and infrared bands of S065 frame #3801 were reprocessed. This frame was taken during the orbit of Apollo 9 over Phoenix, Arizona at 0928MST on 12 March 1969, while the spacecraft was at an altitude of 127 nautical miles and the sun was 32° above the horizon. The reprocessing procedure involved making sensitometrically controlled internegatives and duplicate positives.

A set of enlargements of frame #3801 before and after processing

are shown in the six following photographs. These reproductions are indicative of the improvement in contrast and detectability of terrain detail in the reprocessed photography. Not only have the high minimum density and differential gamma relationships been corrected in three bands, but also the three exposures have been balanced. The reader should particularly note that the low contrast in the green band, commented upon by many investigators, have been significantly improved.

Multispectral Additive Color Renditions

Two multispectral additive color renditions of this S065 frame are shown in the following figures. The ground area covered by this space photo included the city Phoenix itself, Mesa, Gila Bend, as well as nearby cultivated fields and surrounding desert. Figure 98, in which the green band is projected as blue, red band as green, and the infrared band as red, quite clearly detects range vegetation in mountain areas (shown as pink) and differentiates the boundaries between agricultural lands (shown as red), urban areas, uplands and desert.

The multispectral additive color rendition shown in Figure 99 was achieved by projecting the green band as red, the red band as blue, and the infrared band as red. This particular color rendition shows great detail in the agricultural lands east of Phoenix and near Mesa. In addition, many variations in color can be discerned in the desert areas. These chromatic differences are probably due to the combination of different

FIGURE 92: SO65 FRAME #3801B (GREEN BAND) AFTER REPROCESSING

FIGURE 93: GREEN BAND SO65 FRAME #3801B BEFORE REPROCESSING

FIGURE 94: SO65 FRAME #3801D (RED BAND) AFTER REPROCESSING

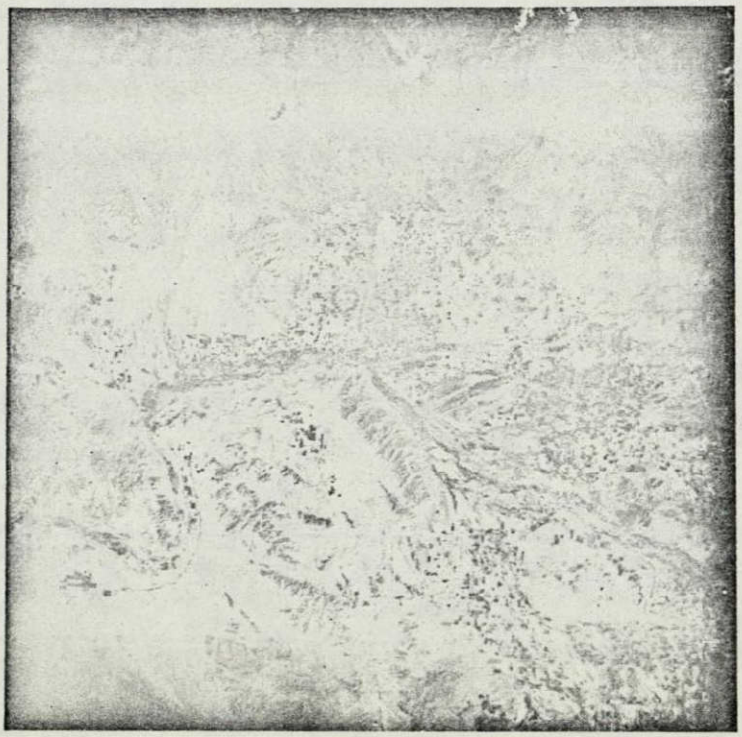

FIGURE 95: RED BAND SO65 FRAME #3801D BEFORE REPROCESSING

FIGURE 96: S065 FRAME #3801C (INFRARED BAND) AFTER REPROCESSING

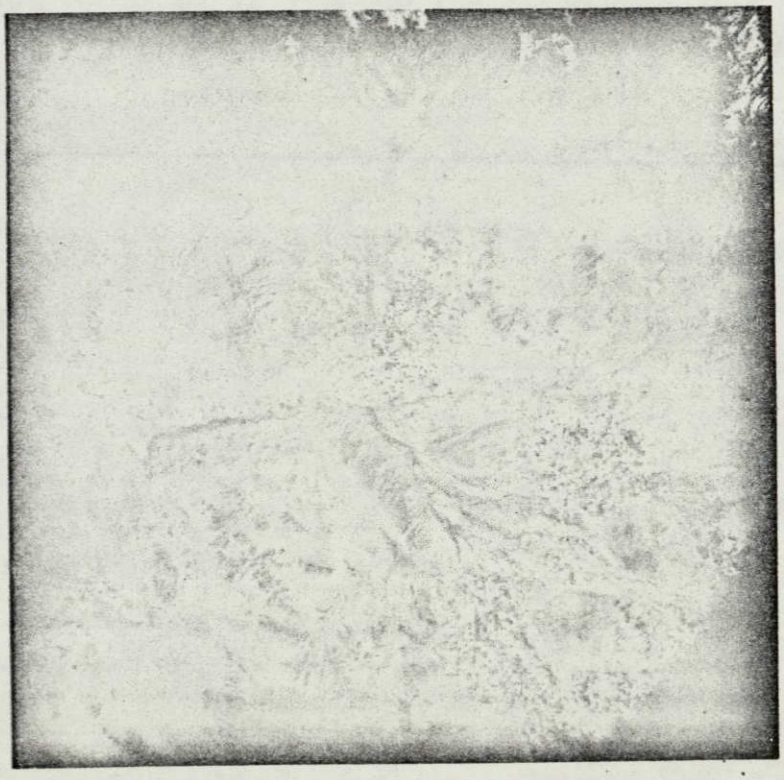

FIGURE 97: INFRARED BAND S065 FRAME #3801C BEFORE REPROCESSING

FIGURE 98 : MULTISPECTRAL ADDITIVE COLOR RENDITION OF S065 FRAME #3801 SHOWING PHOENIX, ARIZONA. GREEN BAND IS IMAGED AS BLUE, THE RED BAND AS GREEN AND THE INFRARED BAND AS RED. THE APOLLO 9 MULTISPECTRAL PHOTOGRAPHS WERE TAKEN AT 0928 MOUNTAIN STANDARD TIME ON 12 MARCH 1969.

THIS COLOR RENDITION IS USEFUL FOR DISCERNING RANGE VEGETATION IN MOUNTAIN AREAS (PINK SHADING AT THE TOP) AS WELL AS THE BOUNDARY BETWEEN AGRICULTURAL LANDS (RED), URBAN AREAS AND DESERT.

FIGURE 99 : MULTISPECTRAL ADDITIVE COLOR RENDITION OF S065 FRAME #3801 (PHOENIX, ARIZONA) THE GREEN BAND IS IMAGED AS RED, THE RED BAND AS BLUE AND THE INFRARED AS RED. THIS COLOR RENDITION IS USEFUL FOR ANALYZING THE DETAILS OF HOW AGRICULTURAL LANDS ARE BEING USED.

soil types and varying density of vegetation on the terrain.

Vegetation Photographs and Maps by Density Slicing

Figure 100 shows vegetated areas appearing in the western portion of S065 frame #3801. The reader will note that all vegetation is shown as red and that all other detail has been suppressed. This vegetation photograph has been achieved by differentiating areas that reflect highly and exclusively in the infrared band. These images have been distinguished from all other areas including those that reflect highly in all spectral bands. This vegetation photograph has been constructed from an additive color rendition of multispectral photography in which the green band was imaged as blue, the red as green and the infrared as red.

Figure 101 is a vegetation map constructed by overlaying the vegetation photograph on a black-and-white photograph of the Phoenix area. All vegetation is clearly differentiated in the red image. Location is achieved by exact superimposition on the base photograph to make the simulated map. It would be just as easy to construct a map by projection of the red vegetation photograph on an image of a map sheet. This technique should find considerable application to problems of rapid vegetation mapping in short periods of time. Similar presentations could be constructed from imagery which reflects uniquely in any multispectral photographic band.

The Density Cut-off Process

The "density cut-off" process is a method of clearly and uniquely

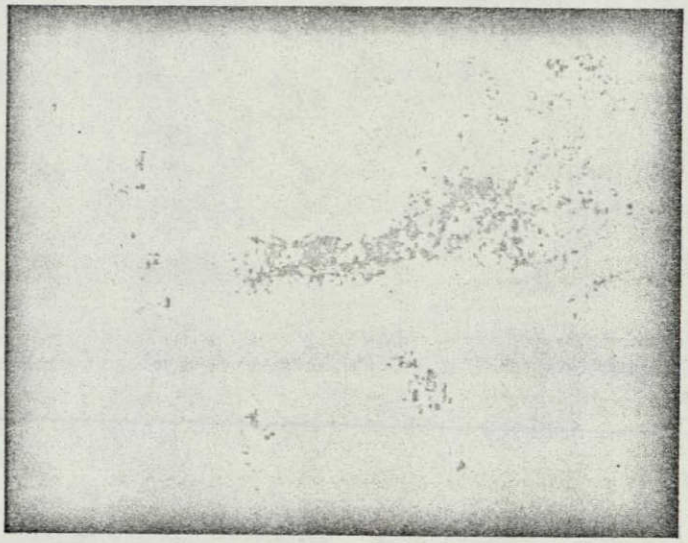

FIGURE 100 VEGETATION PHOTOGRAPH CREATED BY THE DENSITY CUT-OFF PROCESS. ONLY VEGETATION APPEARING IN THE WESTERN PORTION OF SO65 FRAME #3801 IS SHOWN, ALL OTHER DETAIL HAS BEEN ELIMINATED.

FIGURE 101 THE VEGETATION "SLICE" SHOWN IN THE PRECEEDING PHOTOGRAPH HAS BEEN SUPERIMPOSED ON A BLACK-AND-WHITE SPACE PHOTOGRAPH TO PROVIDE LOCATION DATA.

classifying areas that exclusively reflect in one spectral band (for instance, the near infrared) from all other areas including those that reflect highly in all spectral bands. For instance, this technique can be used to clearly classify vegetation from orbital multispectral photography. The result can be presented as a "vegetation photograph" or the uniquely classified image can be superimposed on a black-and-white photograph or map sheet to produce a "vegetation map". This photographic process produces a classification of images that are below a certain density level (or density cut-off point) in only one of the three bands. In the example discussed below, it is the infrared band.

The original image used here to demonstrate the feasibility of the density cut-off technique was a color transparency reproduction of a multispectral additive color image, in which the green band was projected as blue, the red band as green, and the infrared band as red. The steps required to produce the uniquely classified image of vegetation are listed below, and are diagrammed in Figure 102. The reader should note that all photographic printing was done by contact and pin registration was utilized to insure registration of all masked images.

Step One

A high contrast negative image of the blue and green dye layers was produced by printing from the color transparency. This is a photo of areas that reflect highly in the green and/or red bands.

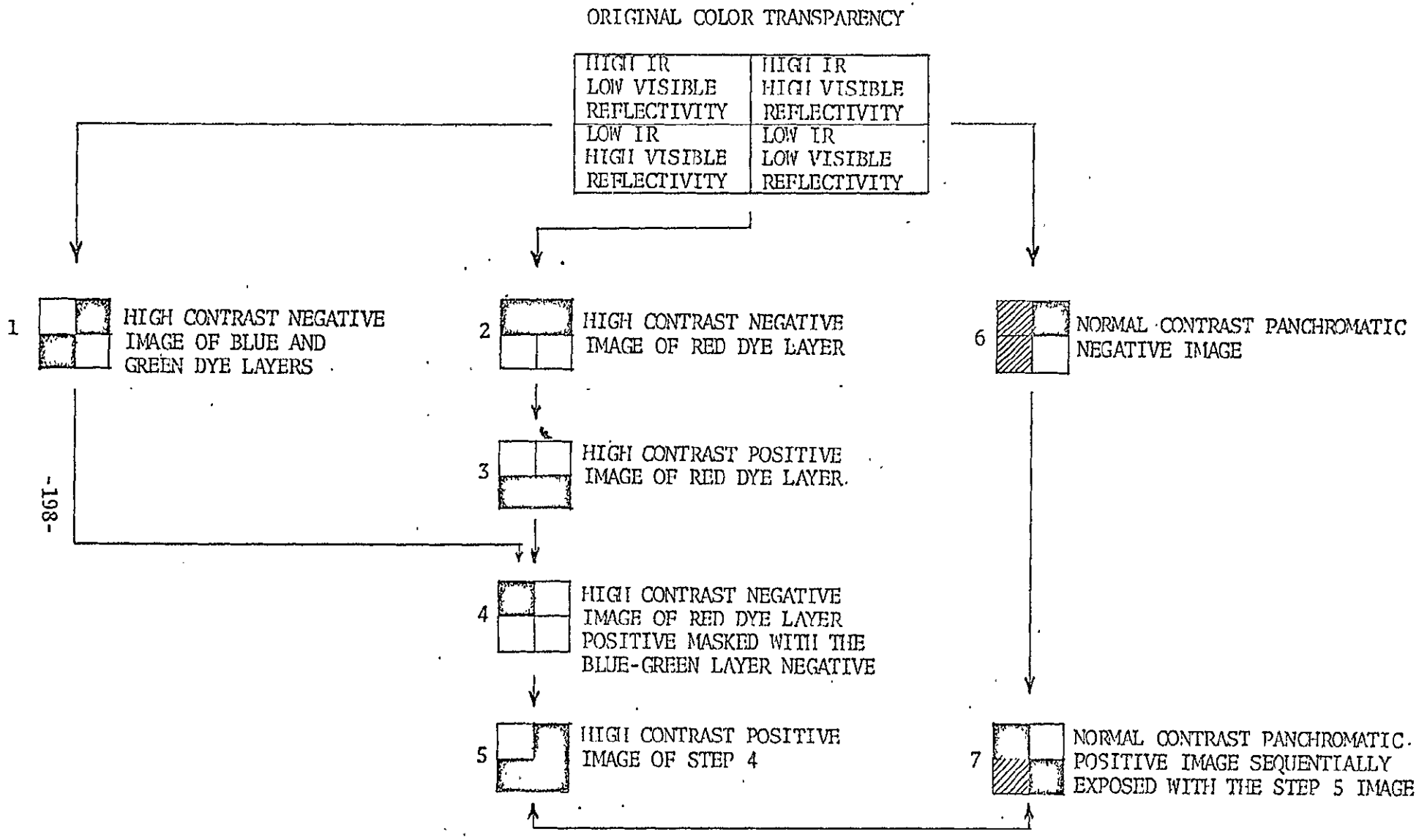

FIGURE 102: DIAGRAM OF THE DENSITY CUT-OFF PROCESS. THE ORIGINAL COLOR TRANSPARENCY IS HERE REPRESENTED BY A FOUR BLOCK SYMBOL, CONTAINING THE FOUR POSSIBLE RATIOS OF INFRARED TO VISIBLE REFLECTANCE IN THE ORIGINAL TERRAIN. THE APPEARANCE OF THE IMAGE IS SHOWN FOR EACH STEP OF THE PROCESS AS HIGH DENSITY ▩, MEDIUM DENSITY ▨, OR LOW DENSITY □. STEP FOUR IS PRODUCED BY PRINTING A SANDWICH OF STEP ONE AND STEP THREE IMAGES. STEP SEVEN IS PRODUCED BY SEQUENTIALLY EXPOSING STEP SIX AND STEP FIVE.

Step Two

A high contrast negative image of the red dye layer was made by printing the color transparency, exposing by red light on medium contrast film. This is a photo of areas that reflect highly in the infrared region.

Step Three

A high contrast positive image of the red dye layer was produced by printing the step two negative.

Step Four

A high contrast composite image was produced by printing a sandwich of the step one negative of the blue and green dye layer and the step three positive of the red dye layer. The resulting high density image is a record of the areas that had high infrared and comparatively low visible reflectance. All other areas are clear (base plus fog density). The color image shown in Figure 100 was made by additively projecting this image with green light, along with non-image red light. In this way, the image is displayed as red against a yellow non-image surrounding.

The remaining three steps are required to display the vegetation image superimposed on a monochromatic image of the terrain.

Step Five

The step four image was printed on high contrast film to produce a record which displays vegetated areas as low density, and all other areas as high density.

Step Six

A normal contrast black-and-white negative image of the terrain was produced by printing the original color transparency.

Step Seven

A normal contrast positive image of the terrain, with vegetated areas displayed as high density, was made by sequentially exposing duplicating film to the step six negative and to the step five image. The vegetation photo shown in color in Figure 101 was produced by additively projecting the positive terrain image with white light, in register with the step five high contrast image projected with red light. In this way, the vegetated area is displayed as uniform red within a black-and-white positive image of the terrain.

This photographic process has been developed as a feasibility study, and further experimentation will be necessary to:

1) determine optimum density cut-off for the primary image band (in this case, the red band),
2) determine applicability to classifications other than vegetation,

3). investigate different methods of displaying the data obtained.

This photographic process may of course be adapted to make direct use of multispectral black-and-white positives, provided the scale of the photographs has been corrected to match each other.

SECTION 11

ISOLUMINOUS MULTISPECTRAL COLOR PHOTOGRAPHY

Herein is described a constant brightness (isoluminous)technique for preparing multispectral color presentations. This new technique has the advantage of both, a) emphasizing subtle spectral differences between bands by greatly enhancing the color of the superimposed composite of all bands and, b) eliminating the effects of brightness caused by sloping terrain and shadows. The technique is useful in detecting subtle environmental spectral differences under dynamically changing illumination, such as often encountered in vegetation and soil mapping in areas where the topography is variable.

Conventional photographic techniques, black-and-white or subtractive color films, associate image density with the brightness of the object. Similarly, in the conventional additive color display of multispectral photography, a positive color space is presented in which the brightness of the color image (not necessarily the chromaticity of the image) increases as a function of increasing brightness in the original scene. The exact relationship depends on the characteristic curves of the individual spectral bands used.

It is evident in the multispectral black and white photographs as well as in the associated additive color renditions presented in preceding sections of this report that large brightness differences in the terrain frequently prevent detection of subtle spectral differences be-

tween objects when they differ considerably in brightness.

An example of this effect is shown in the following S065 photograph taken in the red band (frame number 3752). Note that variations in terrain elevation, such as exists in the Dragoon Mountains or on the east side of the Gunnison Hills, affects ground brightness. The resultant effect on the density of this S065 frame is more pronounced between the west slopes, which are in direct sunlight, and east slopes, which are less fully illuminated. Most density differences between two images which appear in a set of multispectral photographs in sparsely vegetated desert areas are caused by the relative orientation of the sun and the terrain. Spectral reflectance differences between bands are much less in magnitude but of critical importance in uniquely identifying objects under constantly changing illumination conditions. Spectrophotometric data have shown that the spectra of vegetation types are frequently so small compared to brightness differences, that a means is required for precise determination of the image chromaticity of such terrain features (Yost & Wenderoth 1970).

Isoluminous Principles

All brightness effects can be eliminated from the multispectral display projected on the additive color viewer screen. This is accomplished by employing photographic masking techniques to cancel overall brightness differences from the multispectral black-and-white positives. This creates a set of black-and-white spectral photographs in which all

FIGURE 103: ENLARGEMENT OF APOLLO 9 S065 RED BAND MULTISPECTRAL PHOTOGRAPH, FRAME #3752, SHOWING WILLCOX PLAYA, ARIZONA AND SURROUNDING AREA. CLOUD COVER REDUCED THE VISIBILITY OF MUCH OF THE GROUND. NOTE HOW DENSITY OF TERRAIN IMAGE VARIES WITH SLOPE AND SUN ANGLE.

density differences represent hue and saturation differences only. When such a set of multispectral masked photographs are projected in an additive color viewer, using any combination of filters to generate a particular color space, a display which is "isoluminous" will be formed. In this type of display, all achromatic (colorless) objects are projected at a fixed brightness level. Any colored object will also be projected at this same brightness level. Strictly speaking, an isoluminous display of this type is neither negative or positive, since such terms are applied to the ordering of image brightness.

An Example

The salient features of isoluminous multispectral color photography can be presented by an example. Figure 104 shows reproductions of the four spectral photographs taken by the Long Island University four lens multispectral camera during the Apoll 9 underflight mission. The photographs were taken at 10,000 feet above the terrain at 1145 Mountain Standard Time on March 9, 1969.

The area covered in these photographs comprises the western slope of the Gunnison Hills between Willcox and Tuscon, Arizona. The coverage of these photographs is plotted on two joined quadrangle topographic maps shown in Figure 105. As can be seen from the latter map, the elevation difference between Big Draw, on the right, and the Gunnison Hills, on the left, is approximately 400 feet.

The surface geology of the area is depicted in Figure 108. In

BLUE BAND
(395-510nm)

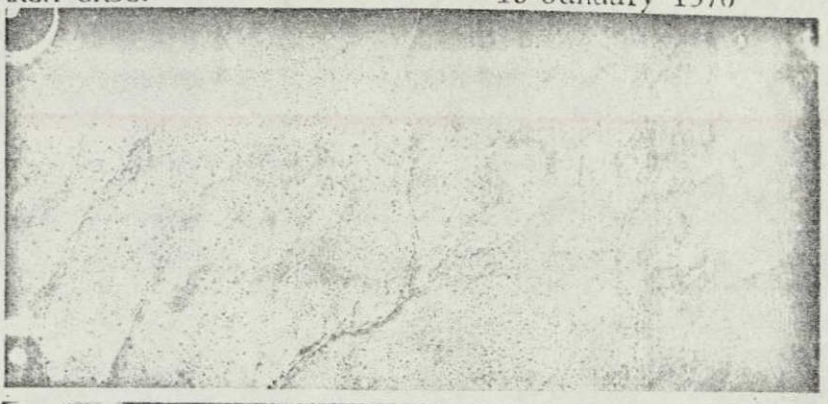

GREEN BAND
(480-590nm)

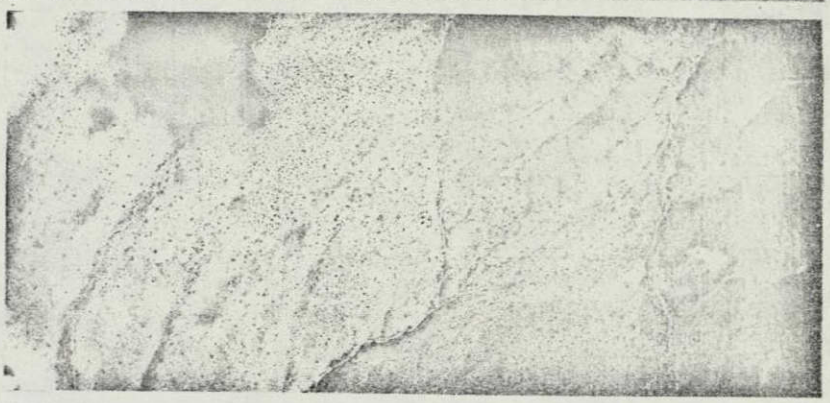

RED BAND
(585-715nm)

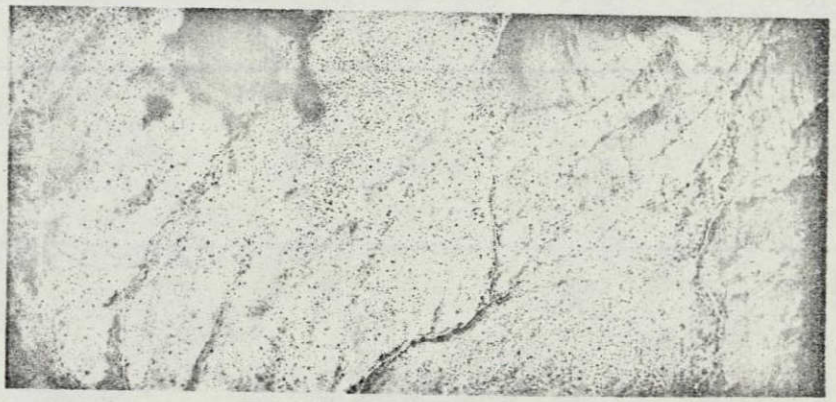

INFRARED BAND
(700-900nm)

FIGURE 104: APOLLO 9 UNDERFLIGHT PHOTOGRAPHY OBTAINED USING FOUR LENS MULTISPECTRAL CAMERA, MARCH 9, 1969, 1145MST, 10,000 FT. ALTITUDE ABOVE GUNNISON HILLS, ARIZONA. TERRAIN IS 400FT. HIGHER AT RIGHT THAN LEFT OF PHOTO.

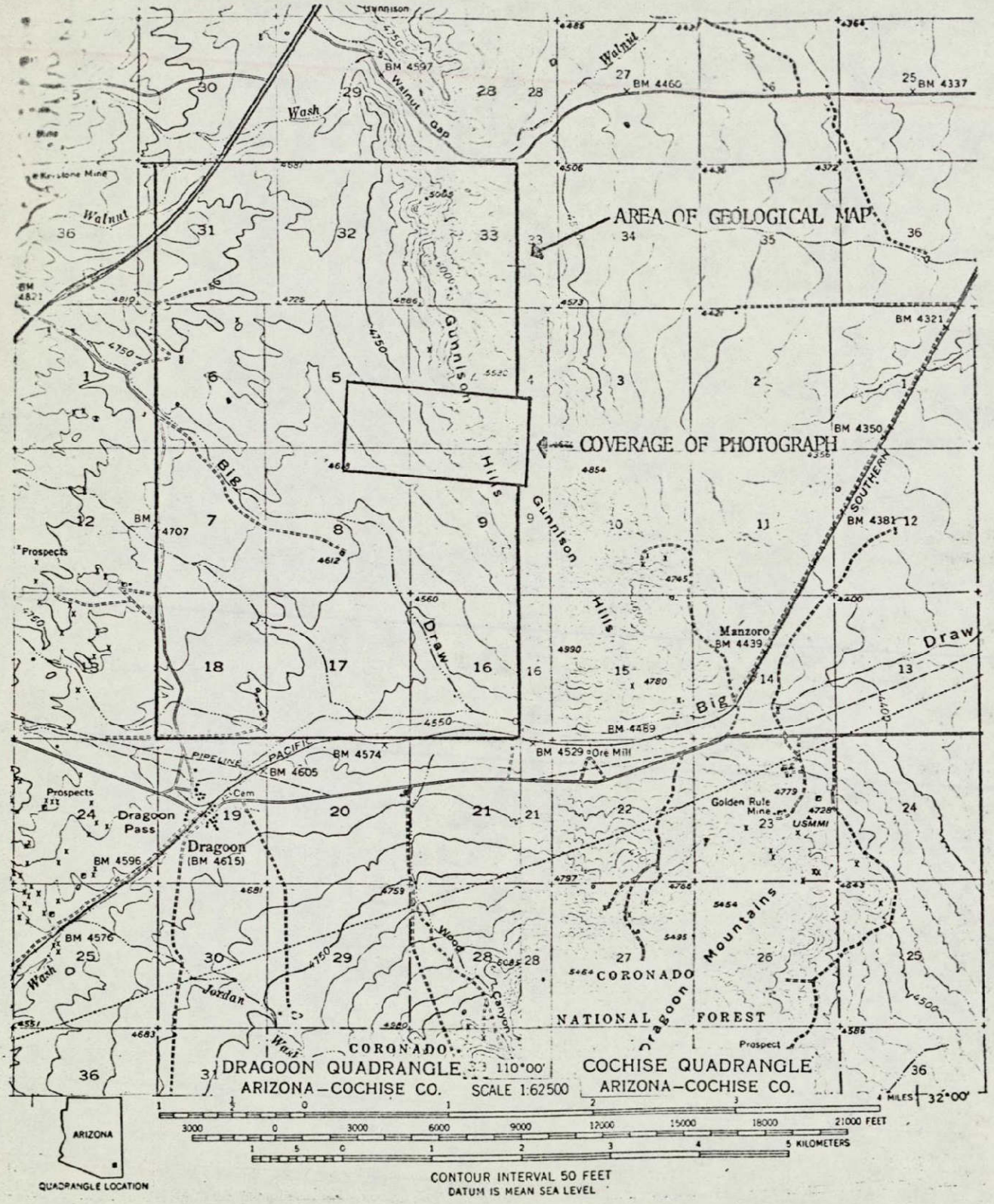

FIGURE 105: TOPOGRAPHIC MAP SHOWING THE COVERAGE OF APOLLO 9 UNDERFLIGHT ISO-LUMINOUS MULTISPECTRAL COLOR PHOTOGRAPH OBTAINED USING THE LONG ISLAND MULTISPECTRAL CAMERA.

LOW BRIGHTNESS AREA

CLOUD

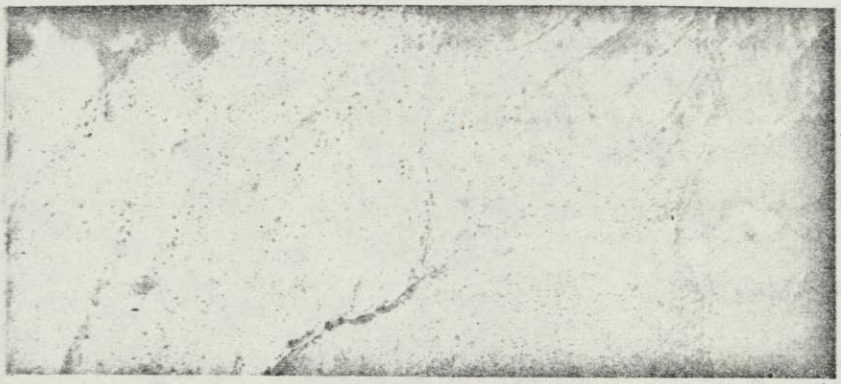

STEEP SLOPE

FIGURE 106: ADDITIVE COLOR RENDITION OF MULTISPECTRAL PHOTOGRAPHS. GREEN BAND IMAGED AS BLUE, RED BAND AS GREEN AND INFRARED AS RED. NOTE BRIGHTNESS CHANGES CORRELATED WITH SLOPES AND CLOUDS.

FIGURE 107: ISOLUMINOUS RENDITION OF THE ABOVE IMAGE SHOWING COLORS AT THE SAME BRIGHTNESS LEVEL. NOTE UNIFORM COLOR IN BOTH LOW BRIGHTNESS SLOPES AND HIGH BRIGHTNESS PLAIN.

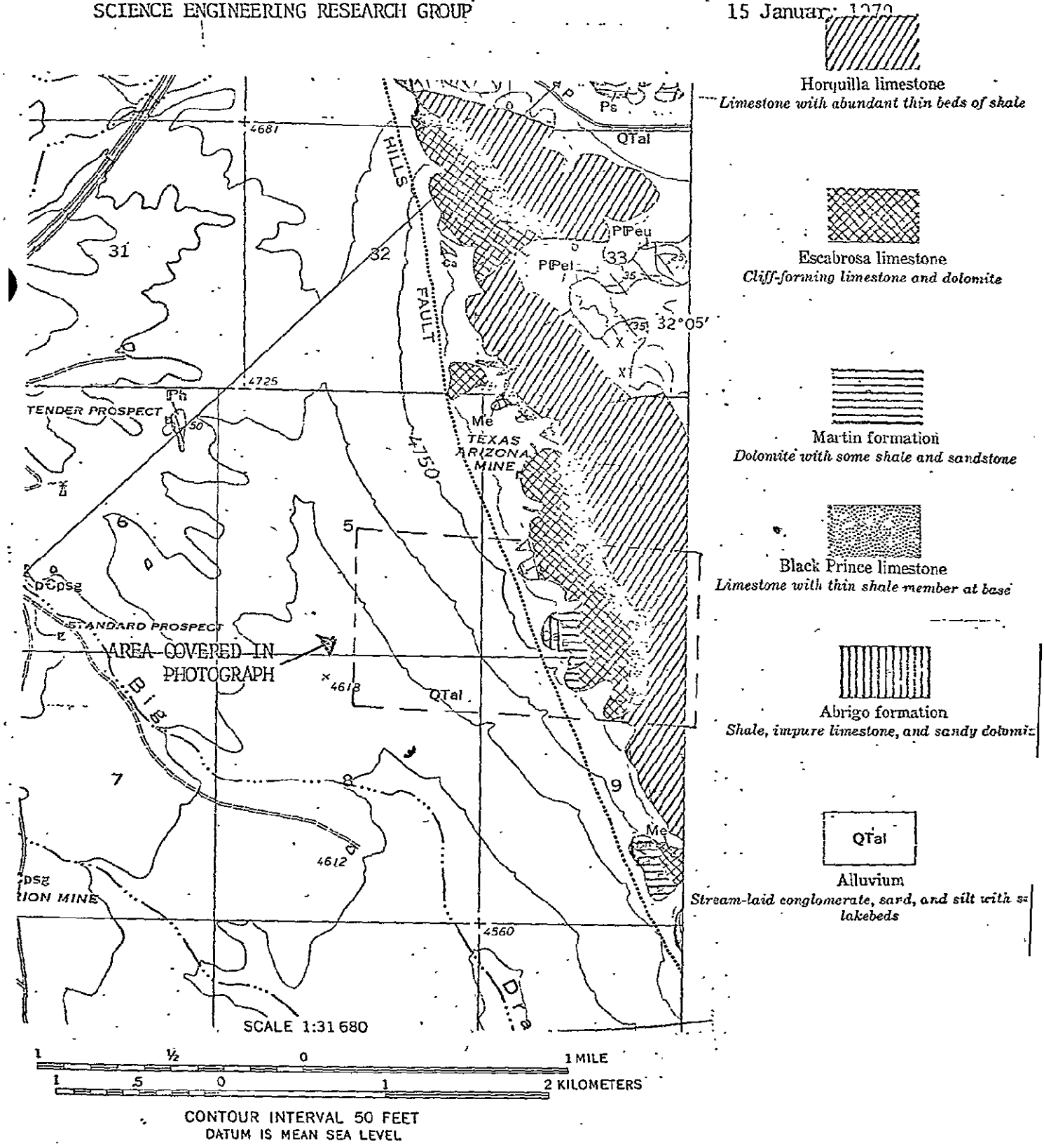

FIGURE 108: THE GEOLOGY OF THE WEST SLOPE OF THE GUNNISON HILLS AREA OF COCHISE COUNTY ARIZONA SHOWING THE COVERAGE OF LONG ISLAND UNIVERSITY MULTI-SPECTRAL PHOTOGRAPHY, APOLLO 9 UNDERFLIGHT.

general, aluvium lies to the left and center of the photographs while at the higher elevations to the right shale, sandstone, dolomite and limestone predominate. The Figures appearing on page 208 vividly show the comparison between the characteristics of images produced by an additive color multispectral presentation (Figure 106) and the isoluminous rendition of the multispectral imagery (Figure 107).

The conventional multispectral presentation, a reproduction of which is shown in Figure 106, clearly shows the effect of varying terrain brightness on image color. In this case, the variation is caused by a change in slope. In this multispectral color analogue to color infrared film (green band created as the blue image, red band as the green image, and infrared band as blue). It would not be unusual for an interpreter to have difficulty in classifying the soil-vegetation units on the left and right of Figure 106. Shadows due to clouds and terrain relief clearly cause difficulties.

In the isoluminous renditions shown in Figure 107, note how uniform the image color is independent of all variations in brightness. Only the very deepest shadows, such as in the center of the cloud, cause a variation in image color. The vegetation growing between Big Draw and the Gunnison Hills, which is barely detectable in conventional multispectral color, is clearly depicted in the isoluminous rendition.

Photographic Techniques

In obtaining isoluminous color renditions from positives, all

brightness differences are controlled by differential masking. All grey levels targets are produced at a fixed level of neutral density and all colors are represented at approximately equal brightness with variations in only hue and saturation. Making isoluminous renditions of multispectral photography requires excellent image registration, which in turn requires a minimum of differential distortion between spectral photographs. Due to the relative spatial variations in image position with respect to the principal point on the three S065 multiband, isoluminous masking was not attempted. Removal of the differential scale by projection printing of these three photographs will be required before attempting the precise image registration which is necessary.

Although the masking process used in preparing the proceeding figures was devised in previous work (Yost and Wenderoth 1967), the research reported herein has produced a more accurate and precise result which it is anticipated will find application in quantitative remote sensing studies. The masking technique which is required to produce the isoluminous image is diagrammed in Figure 109. The sequence is as follows:

1. For a given frame, three spectral photos are selected for additive color viewing.
2. From each of the three spectral negatives, a 50% positive mask is made by contact printing. The density range of a 50% mask is 50% of the density range of the negative which produced it.
3. Each negative, in turn, is mounted in register with the two

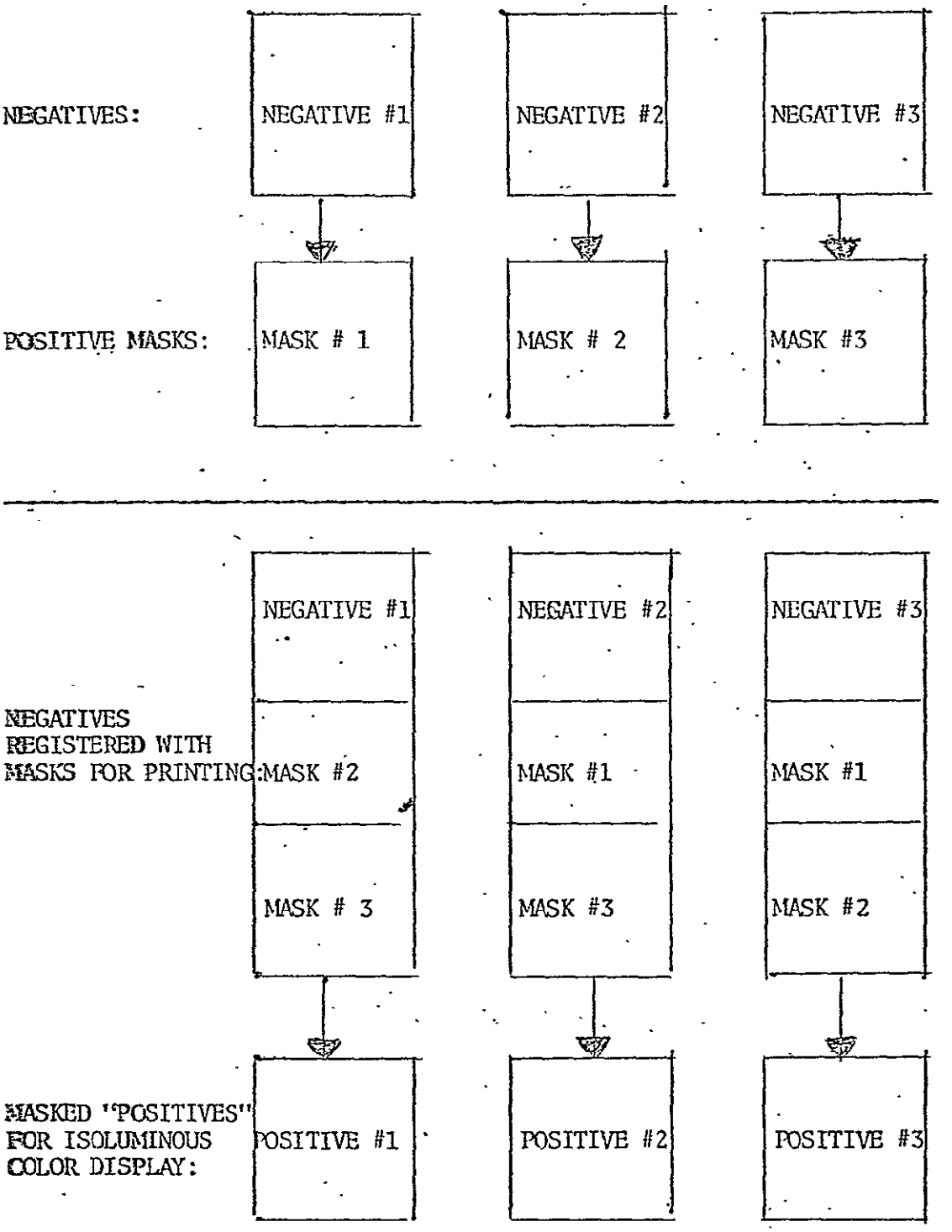

FIGURE 109: MASKING PROCEDURE FOR ISOLUMINOUS MULTISPECTRAL ADDITIVE COLOR DISPLAYS.

SECTION 12

INCIDENT SOLAR RADIATION, TERRAIN REFLECTANCE AND EXPOSURE OF S065 MULTIBAND IMAGES

During the Apollo 9 mission, when weather permitted, periodic measurements were made of the incident solar spectra at the test site west of the Willcox Playa, Arizona. Simultaneous spectroradiometric measurements were obtained of solar radiation reflected by the Playa, large plowed fields and grass areas. These data were computer processed to provide per cent directional reflectance data of homogeneous terrain objects large enough to be imaged on the space photographs.

Density measurements were made of images of the Willcox Playa that appeared on the green, red and infrared positives on S065 frames #3781, #3752, and 3753. These multiband photographs were obtained almost simultaneously with the spectroradiometric measurements of solar radiation reflected by the Willcox Playa.

These closely associated spectra and image measurements indicate that an approximate relationship of the "spectral brightness" of objects in the green, red, and infrared bands can be obtained and associated with all S065 images. This data should be helpful in attempts to quantify the relative energy reflected by terrestrial objects in the green, red, and infrared portion of the spectrum.

Instrumentation

The quantitative analysis of soils. vegetation, and rocks in situ

requires that simultaneous and accurate measurements of incident and reflected radiation be made. Since the quantity of the energy reflected by an object varies with that which is incident upon it, the spectro-radiometric measurements must be made at the same instant of time. This is particularly imperative when cloudy conditions exist as in the case of this experiment.

The arrangement of the instrumentation for simultaneous measurement of both incident and reflected radiation is shown in Figure 110. Two instruments were required to read reflected radiation due to photomultiplier sensitivity limitations.

Instrument Used to Measure Incident Sunlight

A spectroradiometer using a wedge interference filter system enabling the spectrum from 380 to 1250 nanometers to be continuously scanned was used to determine the spectral distribution of the incident solar radiation. The instrument was equipped with a diffusing screen so that its directional response was proportional to Lambert's cosine law. This method of measuring sunlight is very important becuase the incident radiation falls upon the earth's surface and is reflected into an entire hemisphere regardless of its original direction of propagation. True cosine response also eliminates the need for precise aiming of the instrument.

Whereas a radiometer measures in units of energy rate intensity

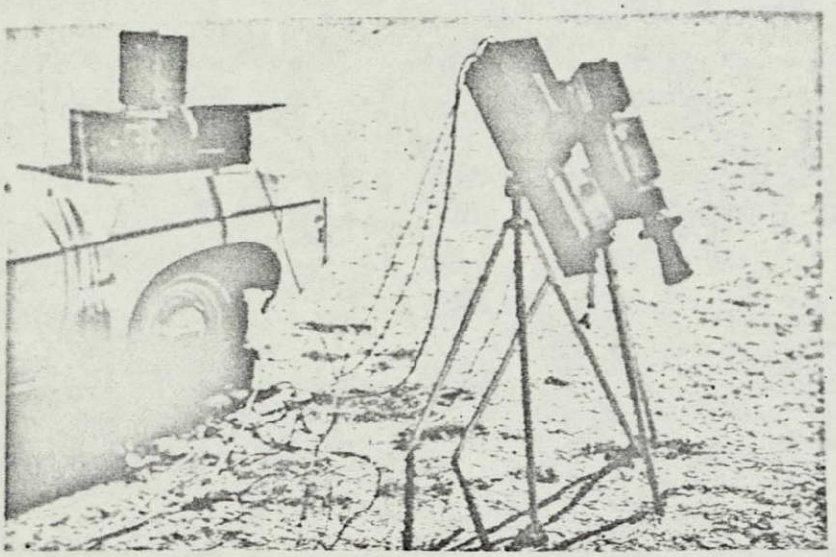

FIGURE 11b: ARRANGEMENT OF INSTRUMENTS FOR MEASURING THE SPECTRAL DISTRIBUTION OF INCIDENT AND REFLECTED SOLAR RADIATION IN THE 380 TO 1250NM REGION OF THE SPECTRUM.

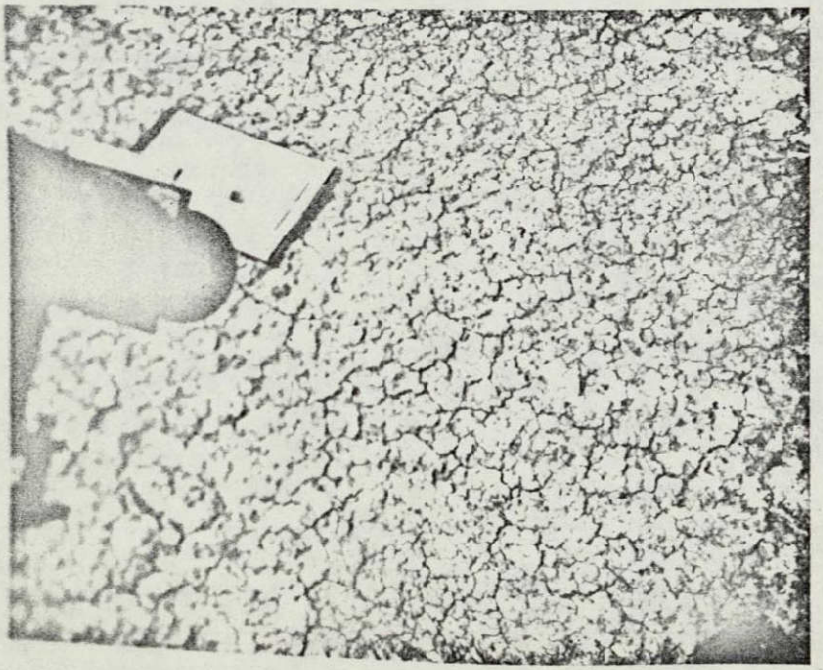

FIGURE 11c: TYPICAL REFLECTANCE SPECTRA OF THE WILLCOX PLAYA.

such as microwatts per centimeter square, a spectroradiometer measures in units of energy rate intensity per bandwidth such as microwatts per centimeter square per nanometer. This latter system of units is most meaningful for measurements of radiation since a graph of spectral distribution of radiant intensity versus wavelength can be obtained. The area under such a curve can be made numercially and dimensionally equal to energy available in the spectral bands of the S065 cameras. The spectroradiometer used was capable of measuring from .01 to 1000 microwatts per centimeter square per nanometer. These values correspond roughly to illumination levels of .03 to 30,000 foot candles.

The calibration of the spectroradiometer was verified before and after the experiment. A spectral standard lamp, serially numbered and individually calibrated against the National Bureau of Standards was used. The lamp was of the ribbon filament tungsten type and had a nominal accuracy of plus or minus five per cent relative to the NBS standard.

The half bandwidth of the spectroradiometer used to measure the incident illumination is approximately 15 nanometers in the 380 to 750 range and 30 nanometers in the 750 to 1250 nanometer range. Stray light response to unwanted wavelengths of 15 nanometer bandwidth and far from the wavelength of interest is usually in the order of .01 per cent.

The periodic calibration of the spectroradiometer used for measuring incident sunlight allowed an accuracy of plus or minus seven per cent in the long wavelength of the spectrum and plus or minus ten per

cent in the short wavelength of the spectrum. Most of this error, of course, comes from uncertainty in the secondary standard used. The relative accuracy of all points with respect to each other throughout the wavelength measured is approximately plus or minus three per cent.

Instrumentation Used to Make Reflectance Measurements

The reflectance spectroradiometer system allowed absolute measurements of the average power of the solar radiation reflected by soils and vegetation in the Willcox Playa area. By means of a grating monochromator, these energy and power readings can be made at a selected wavelength over a bandwidth determined by the grating and slits. This instrument basically consists of an optical system which limits the entrance of energy to a twelve degree field, a monochromator grating to spectrally isolate the visible energy to a five nanometer halfband pass, and the infrared energy to a ten nanometer halfband pass as well as detector heads to sense the magnitude of the incident energy.

The reflectance spectroradiometer is designed so that light reflected from an object passes through a diffuser system and is directed by the collective lens into the monochromator housing via the entrance slit. Calibration accuracy is obtained when the light incident on the diffuser is imaged on the entrance slit, completely filling the slit area with light. A collective lens in the beam input optics in front of the monochromator entrance slit, collects the incident light which is properly matched with the diffuser to create a uniform illuminating

bundle inside the monochromator housing. This bundle of light is then incident on a plane diffraction grating where it is angularly dispersed according to wavelength. Each wavelength present in the source bundle reflects off the diffraction grating at a different angle. The grating can be rotated to direct any selected wavelength bundle onto the center of a concave mirror. The mirror collects the light and, with the help of a quartz corrector lens, forms an image of the entrance slit on the exit slit.

The visible range grating is a 1350 groove per millimeter grating covering from 350 to 800 nanometers in the first order and is blazed at 500 nanometers. The reciprocal linear dispersion is 6.4 nanometers per millimeter. The combination of grating and slits determines the dispersion of the system. The effective widths of the visible grating was 20 nanometers as determined by the entrance and exit slit widths of 5.36 and 3.0 millimeters respectively.

The infrared grating is a 675 groove per millimeter grating. covering the range from 0.7 to 1.6 microns in the first order blazed at 900 nanometers. The reciprocal linear dispersion for this grating assembly is 10 nanometers per millimeter. When the effective width of the grating is 40 nanometers and the entrance and exit slit widths are 2.68 and 1.5 millimeters respectively. These particular grating widths were selected in order to obtain sufficient photomultiplier response when measuring targets of low reflected brightness.

The visible spectroradiometer utilizes a photo diode detector to produce a signal proportional to the intensity of the light which strikes it. However, in order to obtain sufficient sensitivity in the infrared, a cooled photomultiplier detector must be used to produce an output signal which is of sufficient amplitude to allow significant results to be obtained.

Readout is accomplished using a self-ranging picoammeter. This device has the advantage of displaying digitally the detector current output of the spectroradiometers. Thus calibration and dark current values can be readily obtained and monitored. In addition, no scale switching is required and readings can be obtained rapidly.

In order to obtain accurate data, the spectroradiometers were calibrated before and after the experiment. The calibration of the instrument can shift due to such factors as the collection of dust on the optical surfaces or a variety of other random factors. The electronic circuitry of the instrument is very stable and maintains uniform response, but nevertheless, the accuracy of the instrument was verified.

Data Analysis Techniques

If a sufficient number of sets of independent measurements of incident and reflected radiation (at 27 points in the spectrum from 350-1100nm) are made and the readings averaged at each wavelength, it

DATE:3/6/69
TIME:1140-1210 MST
WEATHER + LOCATION:CLR. WILL ARI
TARGET:GRASS

WAVE LENGTH (NM)	SUN READING (UW)	ACT. SUN SPECTRA (UW)	REFLECT READING (W*E-10)	ACT. REF SPECTRA (UW*E-2)	PERCENT DIR. REF. (E-1)	DENSITY SPECTRA	STD. SUN REFLECT (UW)
380	15.5	72.912	1.633	6.225	.853768	3.06866	1.40872
400	66	105.336	3.69	11.929	1.13247	2.94597	9.51278
425	127	131.699	6.27	19.1724	1.45577	2.8369	21.8366
450	179	151.255	10.41	27.8316	1.78716	2.74783	37.5303
475	205	160.105	12.08	30.4029	1.89394	2.72149	44.625
500	204	153	13.3	30.7696	2.01108	2.69657	48.266
525	195	139.815	21.7	47.2322	3.37819	2.47131	79.3876
550	160	133.92	23.1	57.1494	4.26743	2.36933	85.3486
575	160	132	16.89	47.5724	3.60397	2.44322	72.0794
600	178	124.778	12.2	40.4064	3.23826	2.48969	72.8609
625	169	117.793	7.88	33.6515	2.85684	2.54411	61.422
650	167	111.222	4.43	27.715	2.49186	2.60347	52.3291
675	176	113.344	2.09	22.3945	1.96786	2.706	44.2763
700	145	97.73	1.677	35.5271	3.63523	2.43947	67.2517
725	147	88.641	1.648	77.3462	8.72579	2.05919	161.427
750	125	81.75	.917	115.791	14.1641	1.84881	226.625
750	* 93	88.9735	5145.46	119.481	13.4841	1.87073	167.09
750	61	96.197	10290.	123.171	12.8041	1.89265	107.554
800	58	79.228	12650.	121.946	15.3918	1.81271	123.134
850	53	71.338	12670.	111.876	15.6825	1.80458	109.778
900	44	58.872	9490.	81.7089	13.8791	1.85764	77.7228
950	32	41.824	4550.	47.6385	11.3902	1.94347	43.2829
1000	36.5	45.8075	3230.	55.879	12.1987	1.91369	59.7734
1050	34.5	39.675	1150.	54.2915	13.6841	1.86378	64.3151
1100	30	29.91	218.	42.51	14.2126	1.84732	55.4293
1150	16.5	15.9225	28.8	24.9955	15.6982	1.80415	29.0417
1200	19	15.485	10.7	34.4487	22.2465	1.65274	36.7067

* = AVERAGE OF TWO INSTRUMENT READINGS

FIGURE 112:TYPICAL COMPUTER PRINTOUT OF SPECTRAL MEASUREMENTS SHOWING PER CENT DIRECTIONAL REFLECTANCE (6th COLUMN) AT EACH WAVELENGTH (1st COLUMN).

is possible to make the Central Limit Theorem apply to the distribution of average reflectance values. Thus,

$$\gamma_{ij} \equiv \left[\frac{x_{ij1}}{y_{ij1}} + \frac{x_{ij2}}{y_{ij2}} + \frac{x_{ij3}}{y_{ij3}} \right] \frac{100}{n}$$

where; $x_{ijk} \equiv$ the k th measurement of reflected radiation at wavelength i, object j

$y_{ijk} \equiv$ the k th measurement of incident solar radiation at wavelength i, object j.

$\gamma_{ij} \equiv$ the average per cent directional reflectance at wavelength i, object j

$n \equiv$ number of readings.

By the Central Limit Theorem the distribution of γ_{ij} will be approximately normal regardless of the distribution of the individual values of x_{ijk} and y_{ijk}. This of course assumes that measurement errors are independent and randomly distributed.

At each wavelength, for each object, the density spectra is also computed:

$$d_{ij} = \log \frac{100}{\gamma_{ij}}$$

The power which would be reflected if the object had incident upon it radiation emitted by a Standard Sun is also calculated as follows:

$$\delta_{ij} = \gamma_{ij} \quad X \quad \text{(Standard value for each i)}$$

Both d_{ij} and δ_{ij} have been developed to estimate the density of the image on multispectral photography. These estimates are currently

in the process of refinement and are auxillary to the spectral analysis which is contained in this section.

A flow diagram of this computer program is shown in the following diagram:

Note: computed for: (1) each wavelength
(2) each object

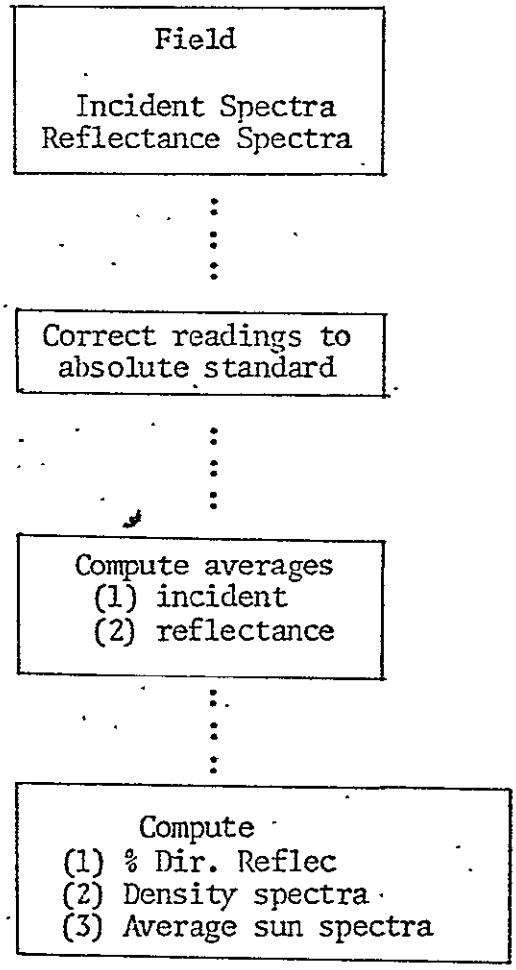

FIGURE 113: FLOW DIAGRAM OF PER CENT DIRECTIONAL REFLECTANCE READINGS

Computer Output

The computer output format of the computations performed on the incidence and reflectance spectra is shown in Figure 112. Associated with each wavelength (first column) is the instrument reading (second column) and corrected value of incident sunlight (third column) in microwatts per square centimeter. The reflectance measurements and associated corrected readings (which are determined by the standard lamp calibration) are shown in the fourth and fifth columns.

The per cent directional reflectance value shown in the sixth column is the ratio of the value in the fifth column divided by that in the third column. The last column is the value of a standard illuminant times the per cent reflectance. Thus, the actual power reflected by an object can be computed by knowing the incident radiation and the data in the sixth column of this output.

Figure 114 shows the associated computer plot of per cent directional reflectance as a function of wavelength. This is an example of the per cent directional reflectance of grass obtained in situ. The chlorophyll reflection band at 550nm and chlorophyll absorption band at 675nm are clearly evident as is the mesophyl reflection above 725nm.

Incident Solar Radiation

The intensity ans spectral distribution of solar radiation falling upon the earth's surface varies with solar angle and atmospheric con-

FIGURE 114: COMPUTER PLOT OF PER CENT DIRECTIONAL REFLECTANCE AS A FUNCTION OF WAVELENGTH

ditions. Measurement of the absolute amount of solar energy which strikes the terrain is important since all ground objects reflect different amounts of radiation in each spectral band which is in direct proportion to that which is incident.

Theoretical analysis of solar illumination based upon air mass calculations and Raleigh scattering are of little practical value in predicitng the spectral distribution of solar energy which actually reaches the ground. This is primarily due to the existance of unknown amounts of Mie scattering and absorption in the atmosphere due to particles which are large compared to the wavelength of the radiation.

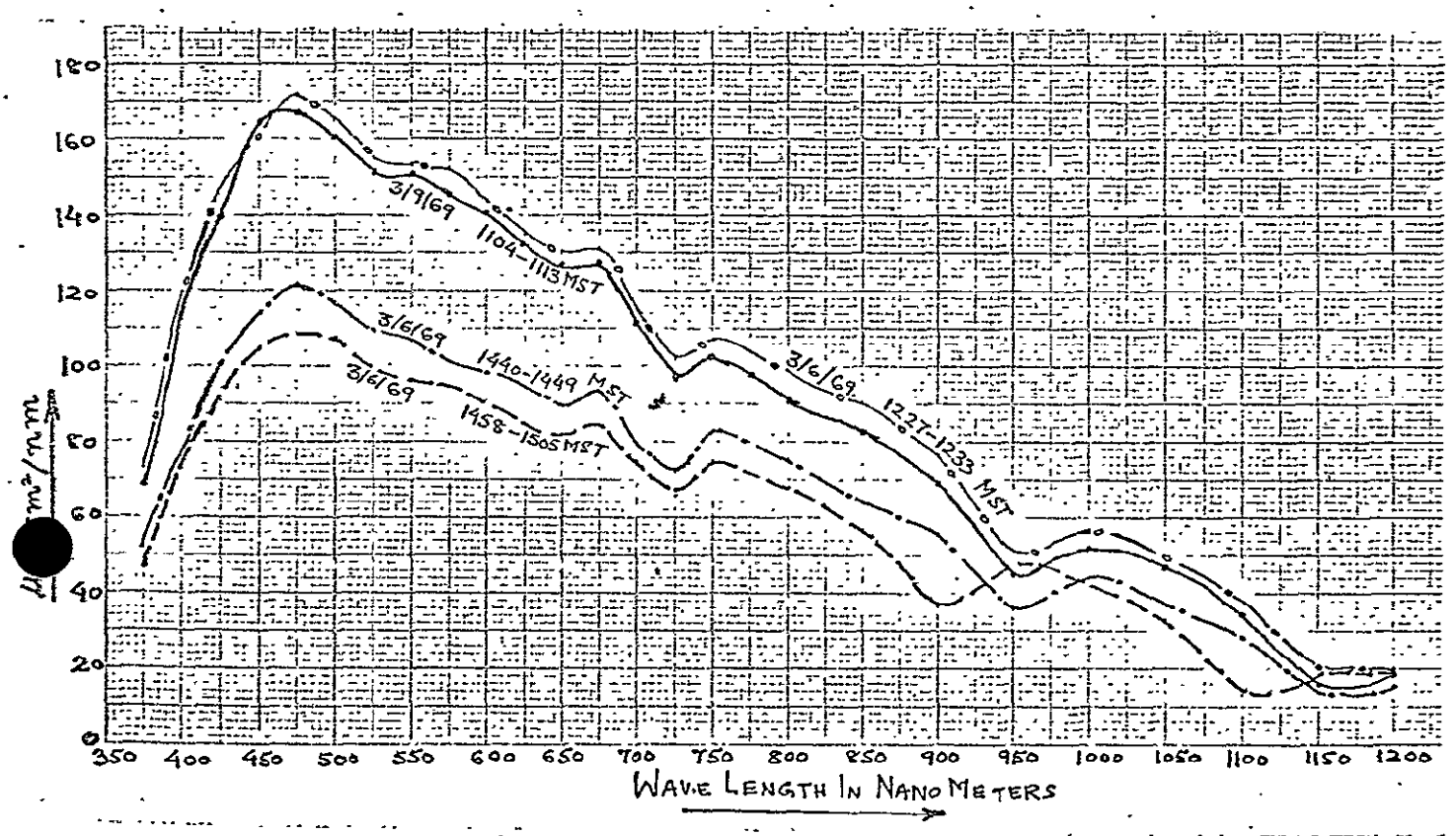

FIGURE 115: SPECTRAL DISTRIBUTION OF SOLAR RADIATION INCIDENT AT THE WILLCOX PLAYA TEST SITE AT DIFFERENT TIMES DURING THE DAY. MARCH 1969.

Figure 115 demonstrates this condition. Spectroradiometric readings of solar energy (both sunlight and diffuse skylight) using a lambertian detector were measured between 5 and 9 March 1969 at Willcox, Arizona. Spectral intensity in microwatts per centimeter squared per nanometer from 380 to 1200 nanometers is shown for four of these measurements between 1104 and 1515MST.

The first feature clearly evident from this data is the large variation in intensity with wavelength as a function of time (solar angle). The characteristic absorption band below 380 nanometers at 725 and 950 nanometers is also clearly evident.

The power incident upon the terrain in each of the nominal S065 bands is shown in Table 13 below. It is noteworthy that the ratio of green to infrared radiation decreased as the sun angle decreases in the afternoon. Thus, a slight change in the relative photometric exposure of the green and infrared images can result from variation in the relative distribution of incident energy during the day and between days.

BAND	3/9/69 1109-1113	3/6/69 1227-1233	3/6/69 1440-1449	3/6/69 1458-1505
Green 475-600	914.97	939.64	655.35	600.21
Red 575-700	783.55	806.12	556.48	512.85
Infrared 700-900	553.43	590.59	431.18	379.39
Ratio Green/Red	1.65	1.59	1.52	1.58

TABLE 13

INCIDENT SOLAR POWER UPON THE WILLCOX PLAYA DURING APOLLO 9 FLIGHT

The effects of variation in the solar radiation striking the terrain, if known, can be compensated in multispectral photography since the exposure in each spectral band can be independently adjusted. Color infrared film on the other hand has fixed spectral sensitivity of the individual dye layers and consequently the images of ground objects taken under these conditions appear more red in the afternoon than in the morning.

Figure 116 shows the relative distribution of incident power upon the terrain ten minutes after three S065 photographs of the Willcox Playa were obtained (frame #3751, #3752 and #3753). The incident solar energy in each S065 band in microwatts per square centimeter is as follows:

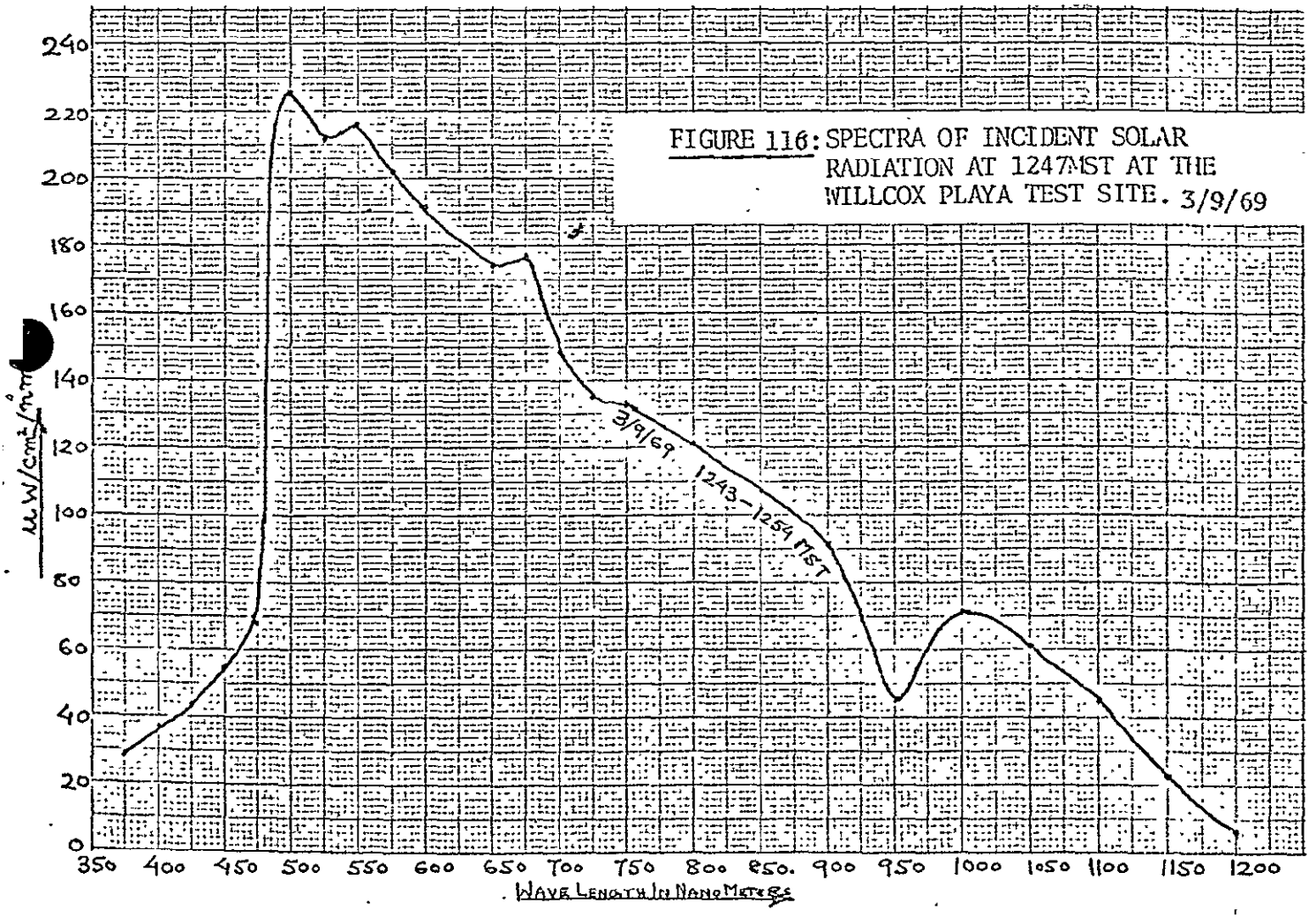

FIGURE 116: SPECTRA OF INCIDENT SOLAR RADIATION AT 1247 MST AT THE WILLCOX PLAYA TEST SITE. 3/9/69

Green	475-600nm	1117	uw/cm^2
Red	575-700nm	1075	uw/cm^2
Infrared	700-900nm	740	uw/cm^2

This data is quite useful in subsequent analysis. When the per cent directional reflectance of objects is known, and multiplied by the above data, the absolute energy reflected by the object is obtained at almost the time the three previously mentioned S065 photographs were obtained.

The Reflectance Spectra of the Willcox Playa and Surrounding Area

The per cent directional reflectance of the Willcox Playa, Arizona was obtained for two adjacent areas at the location shown in Figure 117. Simultaneous spectroradiometric measurements of incident global solar radiation were made along with measurements of the radiation reflected by the Playa.

The reflectance spectroradiometers were oriented so as to prevent any specular reflection from the Playa surface from entering the input optics of the instrument. The partly cloudy atmospheric conditions that existed required that extreme care and patience be used in making these measurements. The incident and reflected spectroradiometric data were corrected and the per cent directional reflectance calculated using the computer program discussed previously.

The per cent directional reflectance data presented in Figure 118 indicated a surprising degree of uniformity in the reflectivity of the Playa surface. Although there appears to be slight brightness differences between the two areas, the shape of the reflectance curves is quite similar.

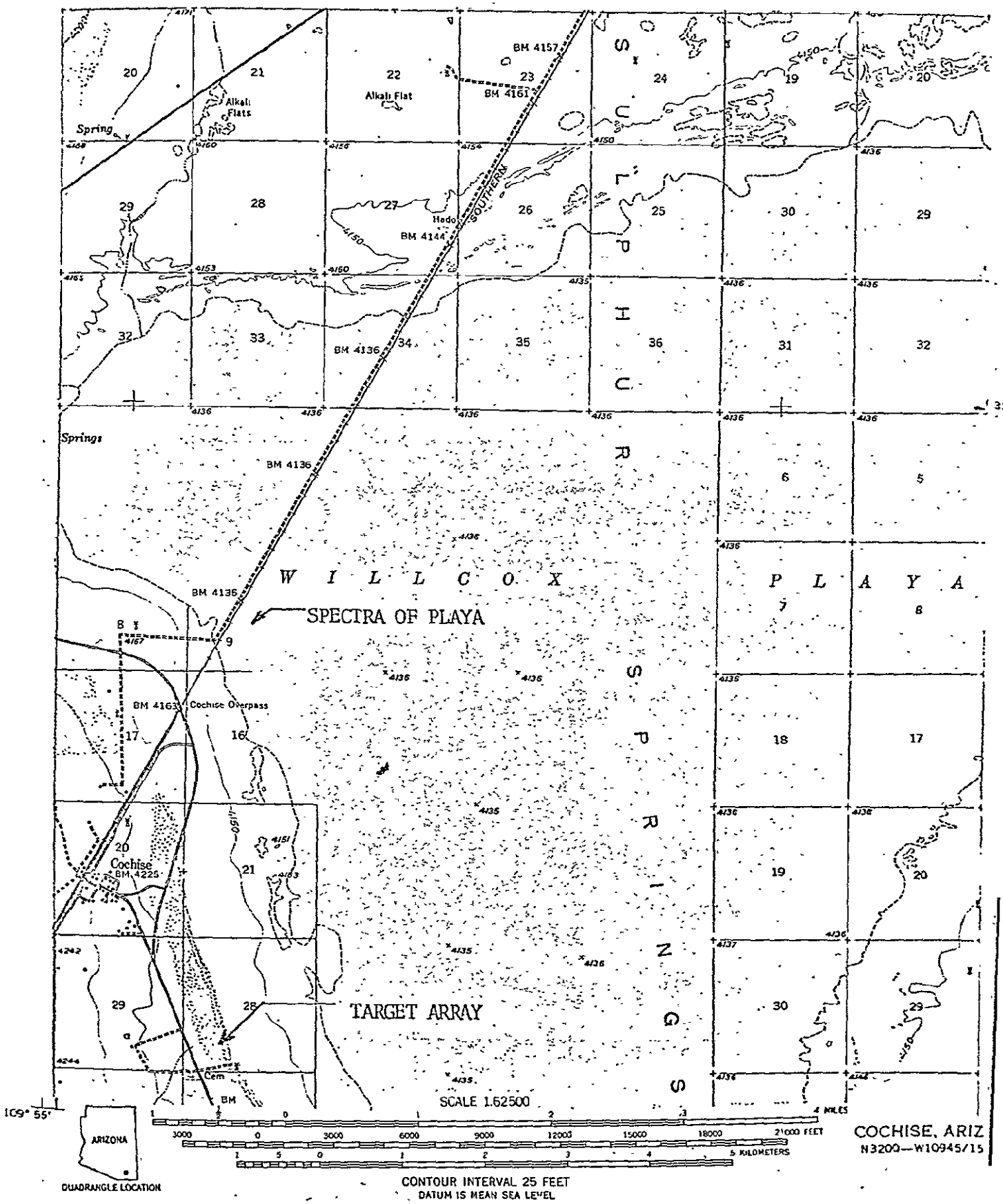

FIGURE 117: LOCATION AT WHICH INCIDENT AND REFLECTANCE SPECTRA WERE MEASURED

FIGURE 118: PER CENT DIRECTIONAL REFLECTANCE OF TWO LOCATIONS ON THE WILLCOX PLAYA, ARIZONA OBTAINED IN MARCH 1969 DURING APOLLO 9 FLIGHT.

A comparison of the spectra of plowed fields and grass with the Playa is shown in Figure 119. The area from which these readings were obtained was adjacent to the target array at the locations shown in Figure 117. The characteristic chlorophyll absorption band (675nm), chlorophyll reflection band (550nm), and mesophyl reflection (above 700nm) are shown in the spectra of the grass.

A relative comparison of the per cent directional reflectance of the Willcox Playa and the plowed and grass fields to the west are shown in the following table. Since in all cases the Playa is the brightest object, all objects have been shown as a percentage of Playa reflectance.

BAND	PLAYA	GRASS	PLOWED FIELD
Green (475-600nm)	100.00	24.39	29.46
Red (575-700nm)	100.00	21.24	35.33
Infrared (700-900nm)	100.00	99.49	86.72

RELATIVE REFLECTANCE OF THE WILLCOX PLAYA, GRASS AND PLOWED FIELDS IN EACH OF THE THREE SO65 NOMINAL SPECTRAL BANDS

TABLE 14

Photographic Density and Solar Energy Reflected from the Willcox Playa

Figure120 shows a schematic representation of the relationship between incident energy on the Playa, the energy reflected by the sur-

FIGURE 119: PER CENT DIRECTIONAL REFLECTANCE OF BARE SOIL, GRASS AND THE WILLCOX PLAYA. NOTE THE COMPARATIVE SPECTRAL UNIFORMITY OF THE PLAYA COMPARED TO HIGHER INFRA-RED REFLECTANCE OF GRASS AND BARE SOIL.

face and that "sensed" by the camera from space. Rather than attempting a theoretical analysis of atmospheric effects, it is possible to directly relate energy reflected by ground objects to image characteristics.

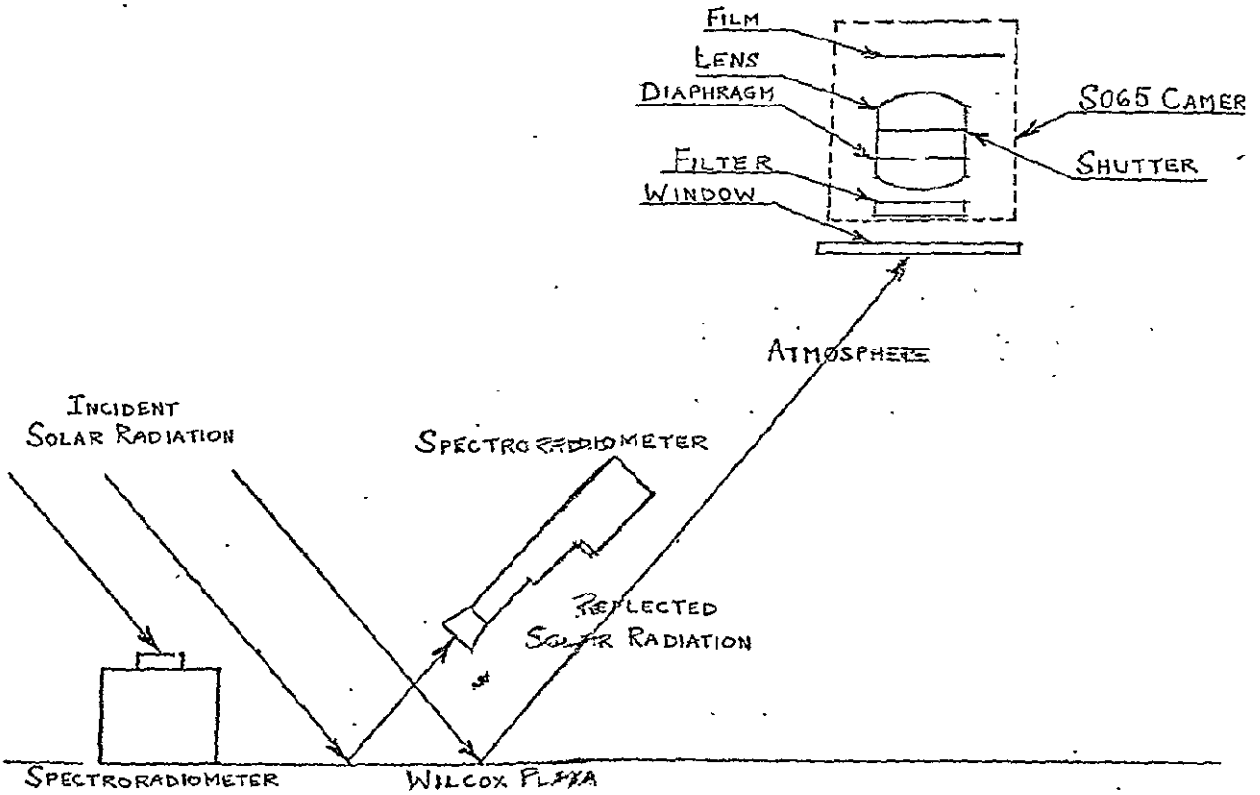

FIGURE 120: SCHEMATIC OF THE RELATIONSHIP BETWEEN SPECTRORADIOMETRIC MEASUREMENT OF SOLAR RADIATION AND IMAGE FORMING ENERGY STRIKING FILM IN S065 CAMERA

Figure 121 shows the distribution of absolute power reflected by the Willcox Playa between 1243 and 1254MST. The data were determined by spectroradiometric reflectance instruments discussed previously.

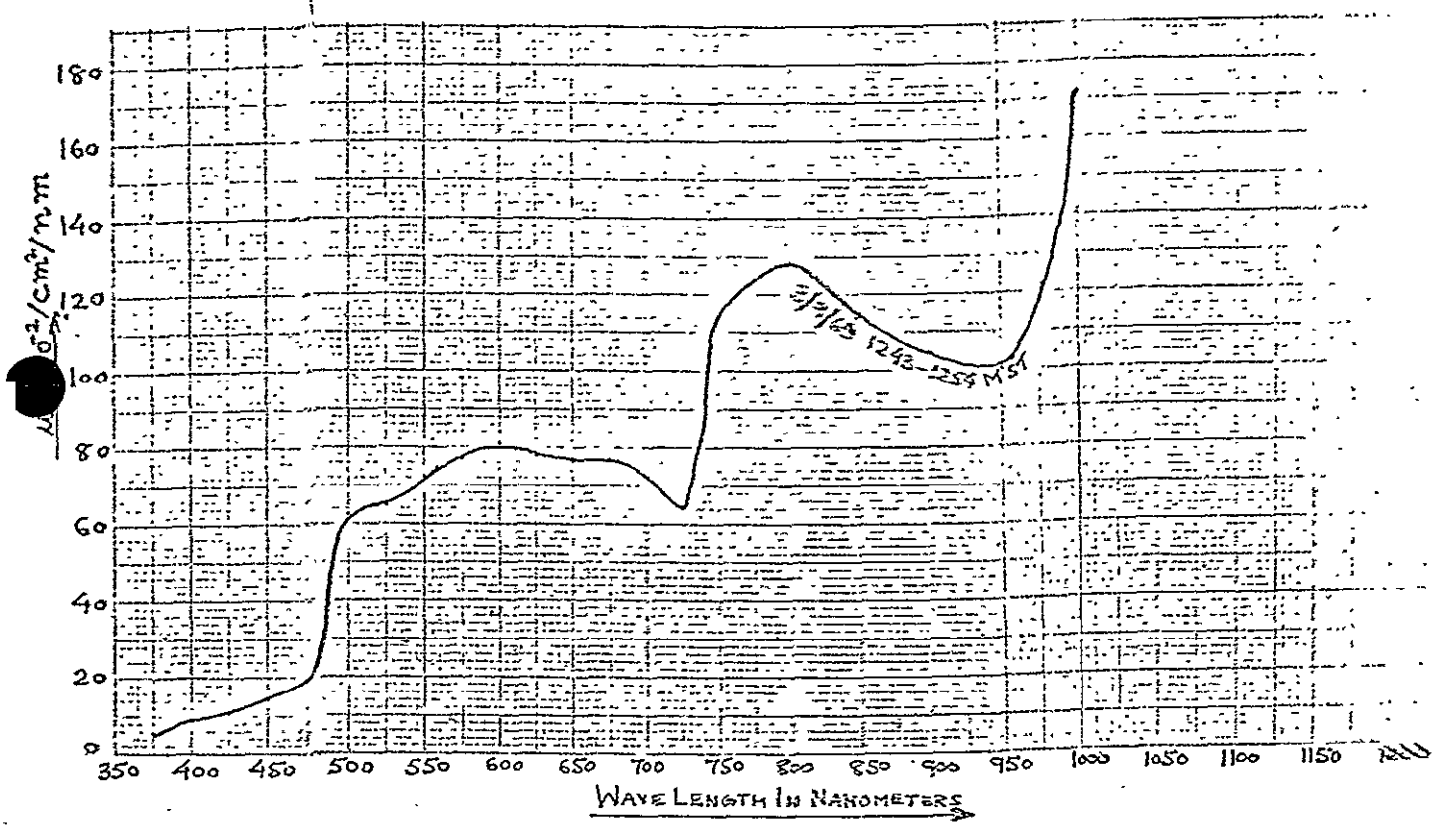

FIGURE 121: SOLAR POWER REFLECTED BY THE WILLCOX PLAYA AT APPROXIMATELY THE TIME THREE S065 PHOTOGRAPHS WERE OBTAINED.

The table below shows the power in microwatts reflected in each of the nominal S065 bands. The reader should particularly note that no spectral

WAVELENGTH BAND	REFLECTED POWER $uw/cm^2 \times 10^{-2}$	RELATIVE PER CENT
475-600	375.8	100
575-700	464.0	123
700-900	601.2	160

POWER REFLECTED BY EACH SQUARE CENTIMETER OF THE WILLCOX PLAYA BETWEEN 1243 AND 1254MST ON 9 MARCH 1969

TABLE 15

The data in the two preceeding tables show the relationship between the power ($\mu W/cm^2$) reflected by the Willcox Playa and the density of the S065 multispectral positive images. The reader should note that no attempt has been made to compute any of the effects of the components which intervene between the developed film image and the power reflected by the terrain. By relating such simultaneous ground and space measurements, a resonably accurate empirical correspondance between image density and the reflected power of an object in each band can be established as is done below for the Willcox Playa.

BAND	REFLECTED POWER $\mu W/cm^2$	POSITIVE IMAGE DENS.
GREEN	3.76	.94
RED	4.64	.78
INFRARED	6.01	.62

The careful reader will note that by obtaining an additional power reading of a second image, a functional relationship can be constructed between reflected power and image density (rather than only relating these two variables at a single point). The images of plowed and grass fields, the images of which were obtained during the S065 experiment, proved to be too small to measure using conventional densitometric techniques. A microdensitometric analysis will be required to contruct this relationship.

The Role of Calibration Targets in Multispectral Photography

The quantitative analysis of the chromatic characteristics of multiband and conventional color photography is greatly facilitated by measurement of the color and spectral characteristics of "standard" objects or targets embedded in the envrionment. In order to maximize the accuracy of these time dependent data, it is essential that these ground measurements be made as close as possible to the time the photography is taken.

This data has three important purposes.

-It allows an independent check to be made on exposure calculations and film processing characteristics.

-It permits compensation of the effects of incident solar radiation and the spectral attenuation of the atmosphere on the characteristics of the color image.

-The chromatic characteristics of images of othere "natural" objects in the environment (e.g., soils, vegetation, etc.) can be related to a standard system of color measurement.

At the Willcox Playa test site, the standard target array consisted of an array of four color panels: blue, green, yellow and red with three tri-density grey targets which had nominal reflectance values of 4, 37

and 88 per cent.

The intensity and spectral distribution of incident solar radiation was obtained each time the reflectance spectra of the panels was measured. In this way it was possible to measure the effect of variations in the incident radiation on both the spectral reflectance characteristics and color of the panels.

Spectroradiometric measurement of incident solar energy was obtained using a battery operated spectroradiometer covering a range of 380 to 1250 nanometers. The instrument incorporated a lambertian detector surface which resulted in measurement of the total energy (sun plus skylight) falling on the earth's surface. The sensitivity of the device ranged from 0.01 to 1000 microwatts per centimeter squared per nanometer with a half power bandpss of 13 nanometers in the visible range an a 30 nanometer bandpass in the infrared portion of the spectrum. The relative accuracy of the data obtained (not the absolute accuracy) was plus or minus three per cent.

Reflectance measurements were made using two narrow angle (12 degree total field) spectroradiometers, one covering 350 to 750 nanometers and the other; 750 to 1350 nanometers. The bandpass of the instruments was 20 nanometers in the visible spectrum and 40 nanometers in the infrared. The relative point to point accuracy of the reflectance spectra data obtained with these instruments was plus or minus three per cent.

Figure 122 shows the percentage directional reflectance of the

four targets placed at the Willcox Playa test site during the Apollo 9 mission. These four percentage reflectance curves were derived from spectroradiometric measurements of incident and reflected solar radiation discussed previously in this section.

The chromaticity coordinates of the targets were computed using these reflectance data along with spectroradiometric measurements of incident solar radiation. This transformation is accomplished by taking the actual sun spectra at the time of photography and computing the actual radiation reflected by each of the targets. These actual spectral radiance values are multiplied by the CIE standard observer functions shown in Table 17 to produce chromaticity coordinates by the weighted ordinate method (Hardy 1936). Table 18 shows the calculations for the yellow target. The chromaticity coordinates of the other targets at the time underflight multispectral photography was obtained on 9 March 1969 have been computed in the same fashion.

The chromaticity coordinates of the ground targets computed from the reflectance spectra by the aforementioned weighted ordinate method is shown plotted in Figure 123. Also shown in that figure are the chromaticity coordinates of the true color rendition of the multispectral photograph which was taken by the Long Island University four lens multispectral camera on 9 March 1969 (shown in Figure 13).

FIGURE 122: THE PERCENT DIRECTIONAL REFLECTANCE OF FOUR COLOR PANELS AT THE WILLCOX TEST SITE.

TABLE 17

FUNCTIONS AND ACTUAL SUN SPECTRA AT TIME UNDERFLIGHT PHOTOGRAPHS OF THE TEST PANELS WERE TAKEN

	CIE STANDARD OBSERVER FUNCTIONS FOR RED($\bar{x}$), GREEN($\bar{y}$), AND BLUE($\bar{z}$)			ACTUAL SUN SPEC. 1104-1113MST
WAVELENGTH	$\bar{x}$	$\bar{y}$	$\bar{z}$	S
380	.0013928	.00004	.0065672	69.15
400	.0144416	.00004	.0684916	113.32
425	.2132420	.0072625	1.0316506	139.99
450	.3362033	.038	1.7726892	164.77
475	.1422085	.112625	1.0426895	167.91
500	.0049194	.323	.2720063	161.25
525	.1096372	.79319	.0572187	150.57
550	.433471	.995	.0087671	150.66
575	.8424972	.91538	.0017244	144.37
600	1.0619702	.631	.0007621	140.2
625	.7514705	.321	.0001394	132.43
650	.2835212	.107	.0000039	126.54
675	.0637035	.02324		128.8
700	.0113525	.0041		111.21
725	.0020386	.00073625		96.98

TABLE IX

WEIGHTED ORDINATE CALCULATIONS FOR DETERMINING CIE CHROMATICITY COORDINATES OF YELLOW TARGET UNDER NATURAL ILLUMINATION

WAVELENGTH	% DIRECT. REFLEC. (R)	RxS S = Actual Sun Spect.	RS$\bar{x}$	RS$\bar{y}$	RS$\bar{z}$
380	2.8	193.6	.269	.007	1.271
400	3.59	406.8	5.874	.016	27.862
425	3.27	457.7	97.60	3.324	472.1
450	3.83	631.1	212.17	23.98	1118.7
475	3.62	607.8	86.43	68.45	633.74
500	3.90	628.8	3.09	203.1	171.03
525	10.13	1525.3	167.23	1209.85	87.27
550	1.67	251.6	109.06	250.34	2.28
575	1.94	280.1	235.98	256.39	.433
600	16.86	2363.7	2510.2	1491.5	1.80
625	19.62	2598.2	1952.4	834.0	.361
650	19.03	2408.0	682.7	257.6	.019
675	18.23	2348.0	149.6	54.56	--
700	20.33	2260.9	25.66	9.27	--
725	19.85	1915.1	3.90	1.41	—
		$\sum_{380}^{725}$	X=6242.16	Y=4663.8	Z=2516.8

$$x = \frac{X}{X + Y + Z} = 0.465$$

$$y = \frac{Y}{X + Y + Z} = 0.347$$

FIGURE 123: CHROMATICITY COORDINATE OF COLOR TARGET PANELS APPEARING SIMULTANEOUSLY ON THE GROUND AND ON MULTISPECTRAL COLOR PHOTOGRAPH TAKEN ON 9 MARCH 1969.

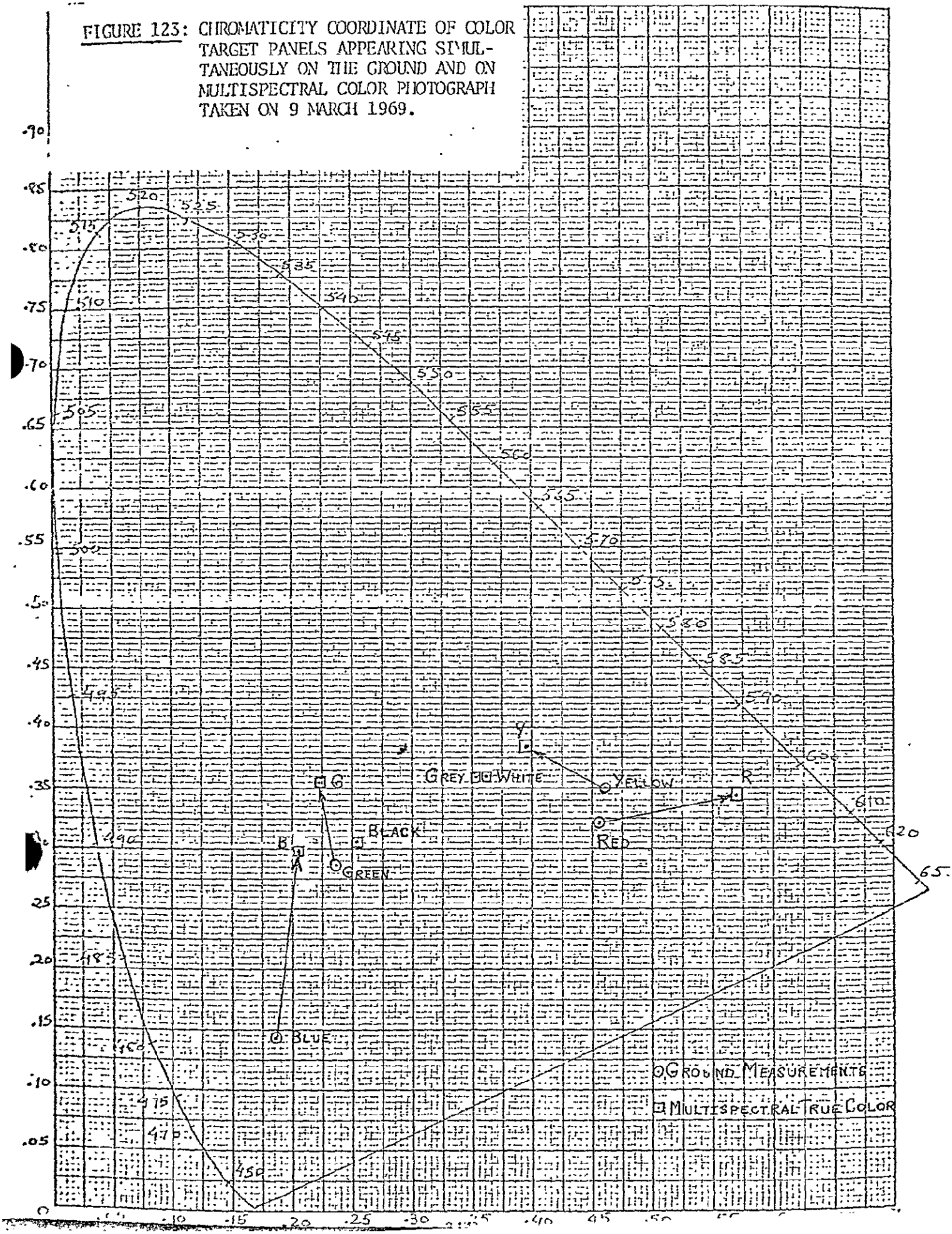

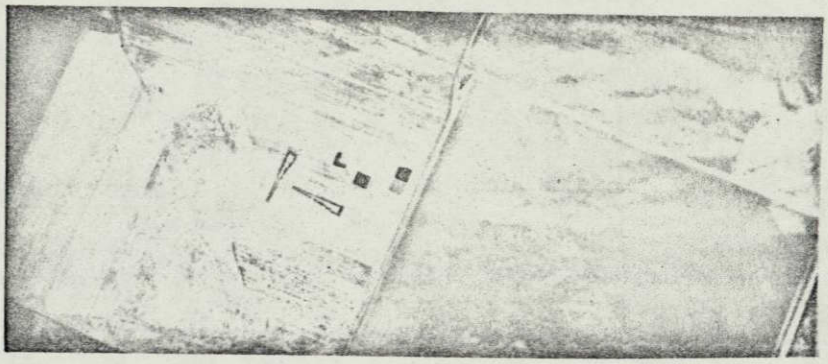

FIGURE 124: TRUE COLOR COMPOSITE OF LONG ISLAND UNIVERSITY MULTISPECTRAL APOLLO 9 UNDERFLIGHT PHOTOGRAPHY. BLUE BAND PROJECTED AS BLUE, GREEN BAND AS GREEN, AND RED BAND AS RED.

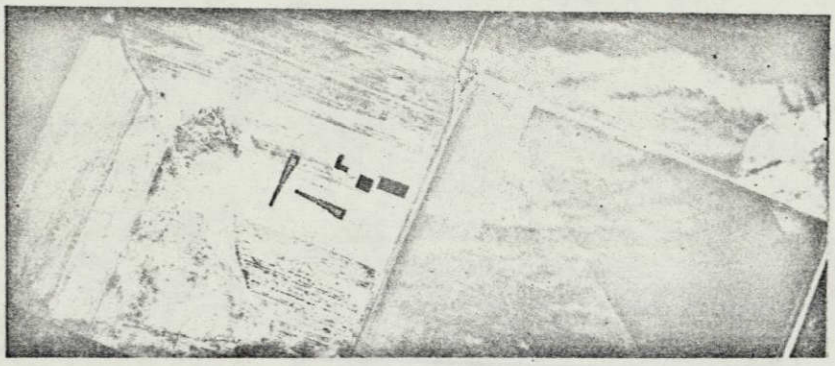

FIGURE 125: FALSE COLOR RENDITION OF APOLLO 9 UNDERFLIGHT MULTISPECTRAL PHOTOGRAPHY TAKEN USING THE LONG ISLAND UNIVERSITY MULTISPECTRAL CAMERA. GREEN BAND PROJECTED AS BLUE, RED BAND AS GREEN, AND INFRARED BAND AS RED.

precision processing is essential. This was clearly brought to the fore by the poor characteristics of the green band compared with the red and the infrared bands. Accurate spectroradiometric calibration of window, cameras, and film is essential in terms of the spectral response of the system if quantitative data are to be obtained. It is clear that newer systems will in great measure eliminate many of these difficulties but procedures for calibration and absolute reference to quantitative standards must not be ignored.

It is important to recognize the importance of obtaining spectral measurements of significant environmental variables at the same time that underflight and space imagery is obtained. Each of these has its place in sorting out just what phenomena exhibit spectral signatures and which, in face of atmospheric and illumination variables, can actually be detected from space. The longer orbits associated with SKY LAB and ERTS will provide time to collect supporting spectra and relate these to environmental variables.

Clearly, there is much more information that can yet be extracted from the S065 imagery. In the author's opinion, since a relatively low gamma processing technique must be used to process the original negatives, special attention should be given to preparing release multispectral positives. These positives should have photographic characteristics especially suited to both the resource discipline to which they are applied and the equipment used for analysis. The data presented herein unequivocally show that additive color analysis of agricultural areas requires different

processing than analysis of individual frames of estuarine hydrological areas. It may very well be that the conclusions reached to date would require modification if such optimally processed imagery is reexamined.

APPENDIX A

REFERENCES

The following references have been cited in this report:

1. Colwell, Robert, etal, "Analysis of Earth Resources on Apollo 9 Photography" Forestry Remote Sensing Lab, University of California.

2. Data Corporation,(1969) "Flight Film Control Friskits Apollo IX", Report DTN-69-4.

3. Data Corporation,(1969) "Apollo IX Corn Analysis", Report DTR-69-8.

4. Data Corporation,(1969) "Apollo IX Corn Analysis" (Supplement), Report DTR-69-14.

5. Data Corporation, private letter, 3 December 1969 from David J. Kelch.

6. Dornbach, J.(1969), private communication.

7. Hadley, (1964), Linear Programming, (Addison Wesley).

8. Hardy, A.(1936), Handbook of Colorimetry, (MIT Press).

9. Jerlov, N.(1968), Optical Oceanography, (Elsevier).

10. Judd, D and G. Wyszecki, Color in Business, Science and Industry, (Wiley).

11. Lowman, P.(1969), "Apollo 9 Multispectral Photography: Geologic Analysis", NASA Goddard Space Flight Center Report X-644-69-423.

12. Kaltenbach, J.(etal)(1970), "Apollo 9 Multispectral Photographic Information" NASA Technical Memorandum TM-X-1957.

13. Mac Adam(1967), "Color Science and Color Photography" Physics Today, January 1967, American Institute of Physics.

14. NASA/MSC (1969), "Preflight Calibration /Performance Data for Apollo 9 Experiment SO65 Assembly", MSC-TF-SO65-118.

15. Nickerson, D and S Newhall (1943), "A Psychological Color Solid", Journal of the Optical Society of America, Vol.33, pp419-422.

16. Sharkov and Kurditsk (1956), "Application of Aerial Method for Geological Investigation of Sea Bottom" Moscow Academy of Science, Aeromethod Lab, Moscow, USSR.

17. Sherman, J. (1970), private communication, Project SPOC, US Naval Oceanography Office, Washington, D.C.

18. Slater, P and P. Keenan (1969), "Preliminary Post-Flight Calibration Report on Apollo 9 Multiband Photography Experiment S065", Optical Science Center Technical Memo #1.

19. Slater, P (1970), private communication.

20. Spansail, N. (1969) "Imperial Valley Ground Truth for Apollo 9 Underflight of March 1969" Report No. 2264-7-X, Willowrun Lab., University of Michigan.

21. Yost, E. and S. Wenderoth (1967), "Multispectral Color Aerial Photography", Photogrammetric Engineering, Vol. 33, No.9.

22. Yost, E. and S.Wenderoth (1968), "Additive Color Aerial Photography" in Manual of Color Aerial Photography, J. Smith, Editor, American Society of Photogrammetry.

23. Yost, E.and S. Wenderoth (1968), "Coastal Water Penetration Using Multispectral Photographic Techniques", Proceedings of The Fifth Symposium on Remote Sensing of Environment, University of Michigan.

24. Yost, E. and S. Wenderoth (1969), "Ecological Application of Multispectral Color Aerial Photography" in Remote Sensing in Ecology, P. Johnson, Editor, University of Georgia Press.

25. Yost, E. and S. Wenderoth (1970), "Remote Sensing of Coastal Waters Using Multispectral Photographic Techniques", Science Engineering Research Group Report TR-10, Long Island University, New York.